DECENTRALIZED COORDINATION OF MULTIPLE AUTONOMOUS VEHICLES

by

Yongcan Cao

A dissertation submitted in partial fulfillment
of the requirements for the degree

of

DOCTOR OF PHILOSOPHY

in

Electrical Engineering

Approved:

Dr. Wei Ren Major Professor	Dr. YangQuan Chen Committee Member
Dr. Todd Moon Committee Member	Dr. Jacob Gunther Committee Member
Dr. Rees Fullmer Committee Member	Dr. Byron R. Burnham Dean of Graduate Studies

UTAH STATE UNIVERSITY
Logan, Utah

2010

Abstract

Decentralized Coordination of Multiple Autonomous Vehicles

by

Yongcan Cao, Doctor of Philosophy

Utah State University, 2010

Major Professor: Dr. Wei Ren
Department: Electrical and Computer Engineering

This dissertation focuses on the study of decentralized coordination algorithms of multiple autonomous vehicles. Here, the term *decentralized coordination* is used to refer to the behavior that a group of vehicles reaches the desired group behavior via local interaction. Research is conducted towards designing and analyzing distributed coordination algorithms to achieve desired group behavior in the presence of none, one, and multiple group reference states.

Decentralized coordination in the absence of any group reference state is a very active research topic in the systems and controls society. We first focus on studying decentralized coordination problems for both single-integrator kinematics and double-integrator dynamics in a sampled-data setting because real systems are more appropriate to be modeled in a sampled-data setting rather than a continuous setting. Two sampled-data consensus algorithms are proposed and the conditions to guarantee consensus are presented for both fixed and switching network topologies. Because a number of coordination algorithms can be employed to guarantee coordination, it is important to study the optimal coordination problems. We further study the optimal consensus problems in both continuous-time and discrete-time settings via an linear-quadratic regulator (LQR)-based approach. Noting that fractional-order dynamics can better represent the dynamics of certain systems, especially when the systems evolve under complicated environment, the existing integer-order coordination algorithms are extended to the fractional-order case.

Decentralized coordination in the presence of one group reference state is also called *coordinated tracking*, including both consensus tracking and swarm tracking. Consensus tracking refers to the behavior that the followers track the group reference state. Swarm tracking refers to the behavior that the followers move cohesively with the external leader while avoiding inter-vehicle collisions. In this part, consensus tracking is studied in both discrete-time setting and continuous-time settings while swarm tracking is studied in a continuous-time setting.

Decentralized coordination in the presence of multiple group reference states is also called *containment control*, where the followers will converge to the convex hull, i.e., the minimal geometric space, formed by the group references states via local interaction. In this part, the containment control problem is studied for both single-integrator kinematics and double-integrator dynamics. In addition, experimental results are provided to validate some theoretical results.

(208 pages)

Acknowledgments

I gratefully acknowledge my advisor, Professor Wei Ren, for the great opportunities to work with him. I thank Professor Wei Ren for his encouraging guidance, painstaking attention to our manuscripts, and extraordinary patience to the mistakes I made during the past several years. His critical thinking, rigorous theoretical analyses, superlative scientific writing, and his commitment to his career always inspires me.

I am deeply indebted to Professor YangQuan Chen for his help in developing the theoretical framework described in this dissertation, especially the fractional-order coordination algorithms. Professor YangQuan Chen is a very thoughtful and generous mentor. I also express my sincere gratitude to my committee members: Professor Todd Moon, Professor Jacob Gunther, and Professor Rees Fullmer. They not only spent a lot of time reading my proposal and thesis, but also provided very insightful comments and suggestions of my research. I also want to thank Mary Lee Anderson, the ECE graduate advisor, for her patience and help during my PhD program.

Collaboration is always very important when conducting research. I thank my colleagues and friends Daniel Stuart, Larry Ballard, Fei Chen, Haiyang Chao, Dr. Yan Li, and Dr. Zhen Song. I greatly acknowledge Daniel and Larry for their time and help in the experimental preparation and results. Special thanks go to Dr. Yan Li for both the fruitful discussion and his kind help. Dr. Zhen Song has been a great friend and inspired me a lot. I want to thank Fei and Haiyang for their help in many theoretical problems and their encouragement and support. I also thank past, present, and visiting lab members for their contributions and comradery, including Nathan Sorenson, Ziyang Meng, Jie Mei, Qiuyan Xing, Yunshu Liu, Vaibhav Ghadiok, and Hanshuo Sun.

My family has provided the foundation of my support. I thank my parents for their encouragement and support to me. I often think of the words that my parents told me when I was a kid: “It takes many small steps to climb a mountain.” I thank my parents-in-law for always treating me like their own son. Also to my sister and friends, your support is always important to me.

I dedicate this dissertation to my wife, Yuman Wei, whose love, patience, and understanding always keep me going. Although she is not familiar with the engineering problems I have been

working on, she always inspires me in various different ways. She is a much more talented, yet more considerate, person than I am, but she has sacrificed everything for me.

Yongcan Cao

Contents

List of Figures

Chapter 1

Introduction

Agent-based system has received more and more research attention because many real-world systems, such as flocks of birds, honey bee swarms, and even human society, can be considered examples of agent-based systems. Agent-based system is studied extensively in biology science, where the behavior of animals is shown to be closely related to the group in which they are involved.

A prominent phenomenon in agent-based system is that each agent's behavior is based on its local (time-varying) neighbors. For example, in Fig. 1.1, flock of birds fly in a regular formation. Here each bird can be considered an agent. For a large population of birds, it is impossible for them to have a leader which has the capability to control the formation of the whole group by determining the movement of each individual bird. Instead, each bird determines its movement via a local mechanism. That is, each individual bird has to act based on its local neighbors.

Fig. 1.1: Flock of birds. A large population of birds fly in a regular formation. Photo courtesy of Prof. A. Menges, A. Ziliken.

Recently, the collective motions of a group of autonomous vehicles have been investigated by researchers and engineers from various perspectives, where the autonomous vehicles can be considered agents. An emerging topic in the study of collective motions is decentralized coordination, which can be roughly categorized as formation control, rendezvous, flocking, and sensor networks based on the applications. In addition, numerous experiments were also conducted to either validate the proposed coordination schemes or apply the coordination schemes into different scenarios.

In this dissertation, we mainly focus on the mathematical study of coordination algorithms under none, one, and multiple group reference states. We also investigate the optimization problem and extend the study of integer-order dynamics to fractional-order dynamics. The main framework of this dissertation is to first propose the coordination algorithm, then analyze the stability condition, at last present simulation and/or experimental validations.

1.1 Problem Statement

Decentralized coordination among multiple autonomous vehicles, including unmanned aerial vehicles (UAVs), unmanned ground vehicles (UGVs), and unmanned underwater vehicles (UUVs) has received significant research attention in the systems and controls community. Although individual vehicles can be employed to finish various tasks, great benefits, including high adaptability, easy maintenance, and low complexity, can be achieved by having a group of vehicles work cooperatively. The cooperative behavior of a group of autonomous vehicles is called *coordination*. Coordination of multiple autonomous vehicles has numerous potential applications. Examples include rendezvous [1–3], flocking [4–6], formation control [7, 8], and sensor networks [9–11].

There are mainly two approaches used to achieve coordination of multiple autonomous vehicles: centralized and decentralized approaches. In the centralized approach, it is assumed that there exists a central vehicle which can send and receive the information from all other vehicles. Therefore, the coordination of all vehicles can be achieved if the central vehicle has the capability to process the information and inform each individual vehicle the desired localization or command frequently enough. Although the complexity of the centralized approach is essentially the same as the traditional leader-follower approach, the stringent requirement of the stable communication

among the vehicles is vulnerable because of inevitable disturbances, limited bandwidth, and unreliable communication channels. In addition, the centralized approach is not scalable since a more powerful central station is required with the increasing number of vehicles in the group.

Considering the aforementioned disadvantages of the centralized approach, decentralized approach has been proposed and studied in the past decades. An important problem in decentralized coordination is to study the effect of communication patterns on the system stability. Recently, decentralized coordination of multi-vehicle systems has been investigated under different communication patterns, including undirected/directed fixed, switching, and stochastic networks. Along this direction, we try to solve the following several decentralized coordination problems.

First, we study the decentralized coordination algorithms when there exists no group reference state. We mainly focus on the study of sampled-data coordination algorithms where a group of vehicles with double-integrator dynamics reach a desired geometric formation via local interaction. The main problem involved is to find the conditions on the network topology as well as the control gains such that coordination can be achieved.

Second, we study the decentralized coordination algorithms when there exists one group reference state. We consider two different scenarios: consensus tracking and swarm tracking. In the continuous-time setting, the objective of consensus tracking is to propose control algorithms and study the corresponding conditions such that all followers ultimately track the leaders accurately. In the discrete-time setting, the objective of consensus tracking is to propose control algorithms, show the boundedness of the tracking errors between the followers and the leader using the proposed algorithms, and quantitatively characterize the bound. For swarm tracking problem, the objective is to propose control algorithms and study the corresponding conditions such that the followers move cohesively with the leaders while avoiding collision.

Third, we study decentralized coordination algorithms when there exist multiple group reference states. In this case, the control objective is to guarantee that the vehicles stay within the convex hull, i.e., the minimum geometric space, formed by the leaders. Note that this problem is much more challenging because the desired state is not a unique point, but a set.

Lastly, two other important problems are considered, which are the optimal linear consensus

problem in the presence of global cost functions and the extension from the study of integer-order dynamics to that of fractional-order dynamics. The objective of the optimal linear consensus problem is to either find the optimal Laplacian matrix or the optimal coupling factor under certain global cost functions. The objective of fractional-order coordination algorithms is to guarantee coordination for multiple fractional-order systems.

1.2 Overview of Related Work

Due to the abundance of existing literature on decentralized coordination, we provide here an overview that is incomplete. We summarize the related work according to the following logic. As the first step, we briefly introduce the general approaches used to achieve coordination. Then we focus on introducing those papers which are closely related to the dissertation: coordination without any group reference state, coordination with one group reference state, and coordination with multiple group reference states.

1.2.1 General Coordination Approaches

The main objective of group coordination is to guarantee that a group of autonomous vehicles maintain a geometric configuration. The main application of group coordination is formation control (see [12, 13] and references therein). The objective of formation control is to guarantee that a group of autonomous vehicles can form certain desired (possibly dynamic) geometric behavior. In the absence of any external reference state, the objective of formation control is to design controllers such that certain desired geometric formation can be achieved for a group of autonomous vehicles. Differently, when there exists an external reference state, the objective of formation control is to design controllers for the vehicles such that they can form certain geometric formation and track the external reference state as a group. The approaches used to solve formation control can be roughly categorized as leader-follower [14–18], behavior [7, 19, 20], potential function [4, 5, 21–23], virtual leader/virtual structure [12, 24–30], graph rigidity [31–35], and consensus [36–41]. In the leader-follower approach, the vehicles who are designated as leaders can be designed to track the desired trajectory while the vehicles who are designated as the followers can be designed to track certain state determined by their local neighbors. Note that the leader-follower approach can be

considered a two-level control approach where the top level is responsible for the leaders while the low level is responsible for the followers. In the behavioral approach, the behavior of the vehicles can be categorized into several types, such as obstacle avoidance, formation maintenance, and target tracking. Accordingly, the control input for each vehicle at certain time is determined by the desired behavior of the vehicle at this time. In the potential function approach, the different behaviors used in behavioral approach are implemented via some potential function. In particular, the potential function for each vehicle is defined based on its state and the states of its local neighbors. The virtual leader/virtual structure approach is quite similar to the leader-follower approach except that the leader in the virtual leader/virtual structure approach which is used to represent the desired trajectory does not exist. In the rigidity approach, the formation (or shape) of a group of vehicles is determined by the edges. By changing the edges properly, the desired geometric formation can be guaranteed. In the consensus approach, the group geometric formation is achieved by properly choosing the information states on which consensus is reached.

In addition to the aforementioned approaches, consensus approach was also applied in formation control problems from different perspectives [4–6, 11, 29, 42–49]. We will overview the approach in detail in the following several subsection.

1.2.2 Coordination Without any Group Reference State

When there exists no group reference state, the control objective is to guarantee that the vehicles reach desired inter-vehicle deviation, i.e., formation stabilization. A fundamental approach used in formation stabilization is consensus (also called rendezvous or synchronization in different settings), which means that the vehicles will reach agreement on their final states. Accordingly, group coordination can be easily obtained by introducing the state deviations into the consensus algorithms. Consensus has been investigated extensively from different perspectives. In the following, we will review the existing consensus algorithms.

Consensus has an old history [50–52]. In the literature, consensus means agreement of a group faced with decision making situations. As for a group behavior, sharing information with each other, or consulting more than one expert makes the decision makers more confident [50]. Inspired

by Vicsek et al. [52], it is shown that consensus can be achieved if the undirected communication graph is jointly connected [36]. Consensus is further studied when the communication graph may be unidirectional/directed [37–39, 53]. In particular, average consensus is shown to be achieved if the communication graph is strongly connected and balanced at each time [37], while consensus can be achieved if the communication graph has a directed spanning tree jointly by using the properties of infinity products of stochastic matrices [39]. By using the set-valued Lyapunov function, Moreau [38] provided a similar condition on the communication graph as that in Ren and Beard [39] to guarantee consensus.

Given the aforementioned literature on the study of consensus problem, several directions have also been discussed recently. The first direction is the study of consensus problems over stochastic networks. The motivation here is the unstable communication among the vehicles. Consensus over stochastic networks was first studied where the communication topology is assumed to be undirected and modeled in a probabilistic setting and consensus is shown to be achieved in probability [54]. Consensus was further studied over directed stochastic networks [55–57]. In particular, necessary and sufficient conditions on the stochastic network topology were presented such that consensus can be achieved in probability [57].

The second direction is the study of asynchronous consensus algorithms, which is motivated by the fact that the agents may update their states asynchronously because the embedded clocks are not necessarily synchronized. Asynchronous consensus was studied from different perspectives using different approaches [41, 58, 59]. In particular, Cao et al. [41] used the properties of "compositions" of directed graphs and the concept of "analytic synchronization." Xiao and Wang [58] used the properties of infinite products of stochastic matrices. Differently, Fang and Antsaklis [59] used the paracontracting theorem. Note that the approaches used in Cao et al. [41] and Xiao and Wang [58] are generally used for linear systems while the approach used in Fang and Antsaklis [59] can be used for nonlinear systems.

The third direction is to study consensus for general systems, including systems with double-integrator dynamics, fractional-order dynamics, etc. For systems with double-integrator dynamics, two consensus algorithms were proposed which can guarantee the convergence of the states with, re-

spectively, (generally) nonzero final velocity and zero final velocity [60, 61]. Then the sampled-data case of the consensus algorithms was also studied [62–64]. In particular, Hayakawa et al. [62] focused on the undirected network topology case while Cao and Ren [63, 64] focused on, respectively, the fixed and switching directed network topology case. Necessary and sufficient conditions on the network topology and the control gains were presented to guarantee consensus [63]. However, only sufficient conditions on the network topology and the control gains were presented to guarantee consensus because the switching topology case is much more complicated than the fixed topology case [64]. Considering the fact that the system dynamics in reality may be fractional (nonintegral), the existing study of integer-order consensus algorithms was extended to fractional-order consensus algorithms [65]. Two survey papers provide more detailed information [46, 66].

1.2.3 Coordination With a Group Reference State

Coordination with a group reference state is also called *coordinated tracking*. Here, coordinated tracking refers to both consensus tracking and swarm tracking. The objective of consensus tracking is that a group of followers tracks the group reference state with local interaction. The unique group reference state is also called "leader." A consensus tracking algorithm was proposed and analyzed under a variable undirected network topology [67, 68]. In particular, the algorithm requires the availability of the leader's acceleration input to all followers and/or the design of distributed observers. A proportional-and-derivative-like consensus tracking algorithm under a directed network topology was proposed and studied in both continuous-time and discrete-time settings [69–71]. In particular, the algorithm requires either the availability of the leader's velocity and the followers' velocities or their estimates, or a small sampling period. A leader-follower consensus tracking problem was further studied in the presence of time-varying delays [72]. In particular, the algorithm requires the velocity measurements of the followers and an estimator to estimate the leader's velocity.

In addition to the consensus tracking algorithms, various flocking and swarm tracking algorithms were also studied when there exists a leader. The objective of flocking or swarm tracking with a leader is that a group of followers tracks the leader while the followers and the leader main-

tain a desired geometrical configuration. A flocking algorithm was proposed and studied under the assumption that the leader's velocity is constant and is available to all followers [4]. Su et al. [73] extended the results in two aspects. When the leader has a constant velocity, accurate position and velocity measurements of the leader are required [73]. When the leader has a varying velocity, the leader's position, velocity, and acceleration should be available to all followers [73]. Flocking of a group of autonomous vehicles with a dynamic leader was solved by using a set of switching control laws [74]. In particular, the algorithm requires the availability of the acceleration of the leader. A swarm tracking algorithm was proposed and studied via a variable structure approach using artificial potentials and the sliding mode control technique [23]. In particular, the algorithm requires the availability of the leader's position to all followers and an all-to-all communication pattern among all followers. Both consensus tracking and swarm tracking are solved via a variable structure approach under the following three assumptions [75]: 1) The virtual leader is a neighbor of only a subset of a group of followers; 2) There exists only local interaction among all followers; 3) The velocity measurements of the virtual leader and all followers in the case of first-order kinematics or the accelerations of the virtual leader and all followers in the case of second-order dynamics are not required.

1.2.4 Coordination With Multiple Group Reference States

Coordination with multiple group reference states is also called *containment control*. The objective of containment control is to guarantee that the followers move into the convex hull, i.e., the minimal geometric space, formed by the group references states. Sometimes, the group reference states are also called "leaders." Multiple leaders were introduced to solve the containment control problem [76], where a team of followers is guided by multiple leaders. In particular, a stop-and-go strategy was proposed to drive a collection of mobile agents to the convex polytope spanned by multiple stationary/moving leaders [76]. Note that Ji et al. [76] focused on the fixed undirected interaction case. Note that the interaction among different agents in physical systems may be directed and/or switching due to heterogeneity, nonuniform communication/sensing powers, unreliable communication/sensing, limited communication/sensing range, and/or sensing with

a limited field of view. Further study was conducted to solve decentralized containment control of a group of mobile autonomous agents with multiple stationary or dynamic leaders under fixed and switching directed network topologies [77].

1.3 Contributions of Dissertation

In this dissertation, we focus on the study of decentralized coordination of multiple autonomous vehicles in the presence of none, one, and multiple group reference states. Some materials from this dissertation have been previously published or accepted for publication in international journals and/or conferences [63–65, 70, 75, 77–82]. Some results have not yet appeared elsewhere.

Decentralized coordination in the absence of any group reference state is a very active research topic in the systems and controls society. This dissertation focuses on studied coordination problems for double-integrator dynamics in a sampled-data setting because the control inputs are generally sampled instead of being continuous. Two sampled-data coordination algorithms are proposed and the conditions to guarantee coordination are presented accordingly. Note that a number of coordination algorithms can be employed to guarantee coordination. Without loss of generality, the optimal linear consensus problems are studied in both continuous-time and discrete-time settings via an linear-quadratic regulator (LQR) based approach. Noting that fractional-order dynamics can better represent the dynamics of certain systems, the existing integer-order coordination algorithms are extended to the fractional-order case.

Decentralized coordination in the presence of one group reference state is also called *coordinated tracking*, including consensus tracking and swarm tracking. Consensus tracking refers to the behavior that the followers track the external leader ultimately. Swarm tracking refers to the behavior that the followers move cohesively with the external leader while avoiding collisions. Consensus tracking is studied in both discrete-time setting and continuous-time settings. In continuous-time setting, the followers can track the group reference state accurately. In discrete-time setting, the followers can track the group reference state with bounded errors. Swarm tracking is studied in a continuous-time setting.

Decentralized coordination in the presence of multiple group reference states is also called

containment control, where the followers will converge to the convex hull formed by the group reference states via local interaction. Containment control is studied for both single-integrator kinematics and double-integrator dynamics. In addition, experimental results are provided to validate some theoretical results.

1.4 Dissertation Outline

The remainder of the dissertation is organized as follows.

In Chapter 2, we investigate coordination problems for systems with double-integrator dynamics in a sampled-data setting without any group reference state. Two sampled-data coordination algorithms are proposed and the conditions to guarantee coordination are presented accordingly. In addition, the final equilibria are also presented if applicable. In particular, when the network topology is fixed, we present the necessary and sufficient conditions to guarantee coordination. When the network topology is switching, we present sufficient conditions to guarantee coordination.

In Chapter 3, we investigate coordinated tracking problem in both continuous-time and discrete-time setting. In the continuous-time setting, the coordination tracking problem is solved via a variable structure approach. Compared with related work, our approach requires much less state information and the availability of the leader's states to all followers is not required. Then, we investigate consensus tracking in a discrete-time setting and show the boundedness of the proposed algorithm. In particular, the requirement on the sampling period and the bounds of the tracking errors are provided.

In Chapter 4, we investigate containment control problem under fixed/switching directed network topologies. We present the necessary and/or sufficient conditions to guarantee containment control. In addition, the equilibria are given if applicable. Some experimental results are also presented to show the effectiveness of some results.

In Chapter 5, we investigate optimal linear consensus problems under fixed undirected network topologies. We propose two global cost functions, namely, interaction-free and interaction-related cost functions. With the interaction-free cost function, we derive the optimal Laplacian matrix by using a LQR-based method in both continuous-time and discrete-time settings and shown that the

optimal Laplacian matrix corresponds to a complete directed graph. With the interaction-related cost function, we derive the optimal scaling factor for a prespecified symmetric Laplacian matrix associated with the interaction graph. Both problems are studied in both continuous-time and discrete-time settings.

In Chapter 6, we investigate coordination problems for systems with fractional-order dynamics. We first introduce a general fractional-order coordination model. Then we show sufficient conditions on the interaction graph and the fractional order such that coordination can be achieved using the general model. The coordination equilibrium is also explicitly given when applicable. In addition, we characterize the relationship between the number of agents and the fractional order to ensure coordination. Furthermore, we compare the convergence speed of coordination for fractional-order systems with that for integer-order systems. It is shown that the convergence speed of the fractional-order coordination algorithms can be improved by varying the fractional orders with time. Lastly, we study coordination algorithms for fractional-order dynamics in the presence of damping terms.

In Chapter 7, we conclude the dissertation and discuss the future research directions.

Appendices include two parts: graph theory notions (see Appendix A) and Caputo fractional operator (see Appendix B). Graph theory notions serve as the basis of the dissertation which will be used throughout the dissertation. Caputo fractional operator is used in Chapter 6.

Chapter 2

Decentralized Coordination Algorithms Without a Group Reference State

Decentralized coordination algorithms have been investigated extensively for single-integrator kinematics in both continuous-time and discrete-time settings when there exists no group reference state [46, 66]. Taking into account the fact that equations of motion of a broad class of vehicles require a double-integrator dynamic model, the decentralized coordination algorithms for double-integrator dynamics have been studied recently [60, 61]. Note that decentralized coordination algorithms for double-integrator dynamics are mainly studied in a continuous-time setting. However, the control inputs in really are generally sampled rather than being continuous. In this chapter, we focus on the study of decentralized coordination algorithms for double-integrator dynamics in a sampled-data setting. We first review the existing continuous-time coordination algorithms for double-integrator dynamics and propose two sampled-data coordination algorithms, namely, coordination algorithm with, respectively, absolute damping and relative damping. The main part is to investigate the convergence condition of the two coordination algorithms in both fixed and switching network topologies. Finally, we present several simulation results to validate the theoretical results.

2.1 Continuous-time Coordination Algorithms for Double-integrator Dynamics

Consider vehicles with double-integrator dynamics given by

$$\dot{r}_i = v_i, \qquad \dot{v}_i = u_i, \quad i = 1, \ldots, n, \tag{2.1}$$

where $r_i \in \mathbb{R}^m$ and $v_i \in \mathbb{R}^m$ are, respectively, the position and velocity of the ith vehicle, and $u_i \in \mathbb{R}^m$ is the control input.

A coordination algorithm for (3.14) is studied as [61, 71]

$$u_i = -\sum_{j=1}^{n} a_{ij}(r_i - \delta_i - r_j + \delta_j) - \alpha v_i, \quad i = 1, \ldots, n, \tag{2.2}$$

where $\delta_i,\ i = 1, \cdots, n$, are real constants, a_{ij} is the (i, j)th entry of weighted adjacency matrix $\mathcal{A}$ associated with graph $\mathcal{G}$, and α is a positive gain introducing absolute damping. Define $\Delta_{ij} \triangleq \delta_i - \delta_j$. Coordination is reached for (2.2) if for all $r_i(0)$ and $v_i(0)$, $r_i(t) - r_j(t) \to \Delta_{ij}$ and $v_i(t) \to 0$ as $t \to \infty$.

A coordination algorithm for (3.14) is studied as [60]

$$u_i = -\sum_{j=1}^{n} a_{ij}[(r_i - \delta_i - r_j + \delta_j) + \alpha(v_i - v_j)], \quad i = 1, \ldots, n, \tag{2.3}$$

where δ_i and a_{ij} are defined as in (2.2) and α is a positive gain introducing relative damping. Coordination is reached for (2.3) if for all $r_i(0)$ and $v_i(0)$, $r_i(t) - r_j(t) \to \Delta_{ij}$ and $v_i(t) \to v_j(t)$ as $t \to \infty$.

2.2 Sampled-data Coordination Algorithms for Double-integrator Dynamics

We consider a sampled-data setting where the vehicles have continuous-time dynamics while the measurements are made at discrete sampling times and the control inputs are based on zero-order hold as

$$u_i(t) = u_i[k], \quad kT \le t < (k+1)T, \tag{2.4}$$

where k denotes the discrete-time index, T denotes the sampling period, and $u_i[k]$ is the control input at $t = kT$. By using direct discretization [83], the continuous-time system (3.14) can be discretized as

$$\begin{aligned} r_i[k+1] &= r_i[k] + Tv_i[k] + \frac{T^2}{2}u_i[k] \\ v_i[k+1] &= v_i[k] + Tu_i[k], \end{aligned} \tag{2.5}$$

where $r_i[k]$ and $v_i[k]$ denote, respectively, the position and velocity of the ith vehicle at $t = kT$.

Note that (2.5) is the exact discrete-time dynamics for (3.14) based on zero-order hold in a sampled-data setting.

We study the following two coordination algorithms

$$u_i[k] = -\sum_{j=1}^{n} a_{ij}(r_i[k] - \delta_i - r_j[k] + \delta_j) - \alpha v_i[k], \tag{2.6}$$

which corresponds to continuous-time algorithm (2.2) and

$$u_i[k] = -\sum_{j=1}^{n} a_{ij}[(r_i[k] - \delta_i - r_j[k] + \delta_j) + \alpha(v_i[k] - v_j[k])], \tag{2.7}$$

which corresponds to continuous-time algorithm (2.3). It is assumed in (2.7) that the topologies for both relative position and relative velocity are identical and the following analysis also focuses on the case when the topologies for both relative position and relative velocity are identical. Note that Hayakawa et al. [62] shows conditions for (2.7) under an undirected interaction topology through average-energy-like Lyapunov functions. Relying on algebraic graph theory and matrix theory, we will show necessary and sufficient conditions for convergence of both (2.6) and (2.7) under fixed undirected/directed interaction.

In the remainder of the chapter, for simplicity, we suppose that $r_i \in \mathbb{R}$, $v_i \in \mathbb{R}$, and $u_i \in \mathbb{R}$. However, all results still hold for $r_i \in \mathbb{R}^m$, $v_i \in \mathbb{R}^m$, and $u_i \in \mathbb{R}^m$ by use of the properties of the Kronecker product.

2.3 Fixed Interaction Case

In this section, we assume that the network topology is fixed, i.e., a_{ij} is constant. We use $\mathcal{G}$ and $\mathcal{A}$ to represent, respectively, the communication graph and the corresponding adjacency matrix.

2.3.1 Convergence Analysis of Sampled-data Coordination Algorithm with Absolute Damping

In this section, we analyze algorithm (2.6) under, respectively, an undirected and a directed interaction topology. Before moving on, we need the following lemmas:

Lemma 2.3.1 (Schur's formula) [84] *Let* $A, B, C, D \in \mathbb{R}^{n\times n}$. *Let* $M = \begin{bmatrix} A & B \\ C & D \end{bmatrix}$. *Then* $\det(M) = \det(AD - BC)$, *where* $\det(\cdot)$ *denotes the determinant of a matrix, if* A, B, C, *and* D *commute pairwise.*

Lemma 2.3.2 *Let* $\mathcal{L}$ *be the nonsymmetric Laplacian matrix (respectively, Laplacian matrix) associated with directed graph* $\mathcal{G}$ *(respectively, undirected graph* $\mathcal{G}$*). Then* $\mathcal{L}$ *has a simple zero eigenvalue and all other eigenvalues have positive real parts (respectively, are positive) if and only if* $\mathcal{G}$ *has a directed spanning tree (respectively, is connected). In addition, there exist* $\mathbf{1}_n$ *satisfying* $\mathcal{L}\mathbf{1}_n = 0$ *and* $\mathbf{p} \in \mathbb{R}^n$ *satisfying* $\mathbf{p} \geq 0$, $\mathbf{p}^T\mathcal{L} = 0$, *and* $\mathbf{p}^T\mathbf{1}_n = 1$, *where* $\mathbf{1}_n \in \mathbb{R}^n$ *is* $n \times 1$ *column vector of all zeros.*[1]

Proof: See Merris [85] for the case of undirected graphs and Ren and Beard [39] for the case of directed graphs. ■

Lemma 2.3.3 [86, Lemma 8.2.7 part(i), p. 498] *Let* $A \in \mathbb{R}^{n\times n}$ *be given, let* $\lambda \in \mathbb{C}$ *be given, and suppose* x *and* y *are vectors such that (i)* $Ax = \lambda x$, *(ii)* $A^Ty = \lambda y$, *and (iii)* $x^Ty = 1$. *If* $|\lambda| = \rho(A) > 0$, *where* $\rho(A)$ *denotes the spectral radius of* A, *and* λ *is the only eigenvalue of* A *with modulus* $\rho(A)$, *then* $\lim_{m\to\infty}(\lambda^{-1}A)^m \to xy^T$.

Using (2.6), (2.5) can be written in matrix form as

$$\begin{bmatrix} \tilde{r}[k+1] \\ v[k+1] \end{bmatrix} = \underbrace{\begin{bmatrix} I_n - \frac{T^2}{2}\mathcal{L} & (T - \frac{\alpha T^2}{2})I_n \\ -T\mathcal{L} & (1-\alpha T)I_n \end{bmatrix}}_{F} \begin{bmatrix} \tilde{r}[k] \\ v[k] \end{bmatrix}, \tag{2.8}$$

where $\tilde{r} = [\tilde{r}_1, \ldots, \tilde{r}_n]^T$, $\tilde{r}_i = r_i - \delta_i$, $v = [v_1, \ldots, v_n]^T$, and I_n denote the $n \times n$ identity matrix. Therefore, coordination is achieved if for any $r_i[0]$ and $v_i[0]$, $\tilde{r}_i[k] \to \tilde{r}_j[k]$ and $v_i[k] \to 0$

[1] That is, $\mathbf{1}_n$ and $\mathbf{p}$ are, respectively, the right and left eigenvectors of $\mathcal{L}$ associated with the zero eigenvalue.

as $k \to \infty$. To analyze (2.34), we first study the properties of F. Note that the characteristic polynomial of F, is given by

$$\begin{aligned}
&\det(sI_{2n} - F) \\
=&\det\left(\begin{bmatrix} sI_n - (I_n - \frac{T^2}{2}\mathcal{L}) & -(T - \frac{\alpha T^2}{2})I_n \\ T\mathcal{L} & sI_n - (1-\alpha T)I_n \end{bmatrix}\right) \\
=&\det\big([sI_n - (I_n - \frac{T^2}{2}\mathcal{L})][sI_n - (1-\alpha T)I_n] \\
&- (T\mathcal{L}[-(T - \frac{\alpha T^2}{2})I_n])\big) \\
=&\det\left((s^2 - 2s + \alpha T s + 1 - \alpha T)I_n + \frac{T^2}{2}(1+s)\mathcal{L}\right)
\end{aligned}$$

where we have used Lemma 2.3.1 to obtain the second to the last equality.

Letting μ_i be the ith eigenvalue of $-\mathcal{L}$, we get $\det(sI_n + \mathcal{L}) = \prod_{i=1}^n (s - \mu_i)$. It thus follows that $\det(sI_{2n} - F) = \prod_{i=1}^n \left(s^2 - 2s + \alpha T s + 1 - \alpha T - \frac{T^2}{2}(1+s)\mu_i\right)$. Therefore, the roots of $\det(sI_{2n} - F) = 0$, i.e., the eigenvalues of F, satisfy

$$s^2 + (\alpha T - 2 - \frac{T^2}{2}\mu_i)s + 1 - \alpha T - \frac{T^2}{2}\mu_i = 0. \tag{2.9}$$

Note that each eigenvalue of $-\mathcal{L}$, μ_i, corresponds to two eigenvalues of F, denoted by λ_{2i-1} and λ_{2i}.

Without loss of generality, let $\mu_1 = 0$. It follows from (2.9) that $\lambda_1 = 1$ and $\lambda_2 = 1 - \alpha T$. Therefore, F has at least one eigenvalue equal to one. Let $[p^T, q^T]^T$, where $p, q \in \mathbb{R}^n$, be the right eigenvector of F associated with eigenvalue $\lambda_1 = 1$. It follows that

$$\begin{bmatrix} I_n - \frac{T^2}{2}\mathcal{L} & (T - \frac{\alpha T^2}{2})I_n \\ -T\mathcal{L} & (1-\alpha T)I_n \end{bmatrix} \begin{bmatrix} p \\ q \end{bmatrix} = \begin{bmatrix} p \\ q \end{bmatrix}.$$

After some manipulation, it follows from Lemma 2.3.2 that we can choose $p = \mathbf{1}_n$ and $q = \mathbf{0}_{n\times 1}$, where $\mathbf{0}_{n\times 1}$ is the $n \times 1$ column vector of all zeros. For simplicity, we sometimes use $\mathbf{0}_n$ to replace $\mathbf{0}_{n\times 1}$ without ambiguity. Similarly, it can be shown that $[\mathbf{p}^T, (\frac{1}{\alpha} - \frac{T}{2})\mathbf{p}^T]^T$ is a left eigenvector of

F associated with eigenvalue $\lambda_1 = 1$.

Lemma 2.3.4 *Using* (2.6) *for* (2.5), $\tilde{r}_i[k] \to \mathbf{p}^T\tilde{r}[0] + (\frac{1}{\alpha} - \frac{T}{2})\mathbf{p}^T v[0]$ *and* $v_i[k] \to 0$ *as* $k \to \infty$ *if and only if one is the unique eigenvalue of* F *with maximum modulus, where* $\mathbf{p}$ *is defined in Lemma 2.3.2.*

Proof: (Sufficiency.) Note that $x = [\mathbf{1}_n^T, \mathbf{0}_n^T]^T$ and $y = [\mathbf{p}^T, (\frac{1}{\alpha} - \frac{T}{2})\mathbf{p}^T]^T$ are, respectively, a right and left eigenvector of F associated with eigenvalue one. Also note that $x^T y = 1$. If one is the unique eigenvalue with maximum modulus, then it follows from Lemma 2.3.3 that $\lim_{k\to\infty} F^k \to \begin{bmatrix} \mathbf{1}_n \\ \mathbf{0}_n \end{bmatrix} [\mathbf{p}^T, (\frac{1}{\alpha} - \frac{T}{2})\mathbf{p}^T]$. Therefore, it follows that $\lim_{k\to\infty} \begin{bmatrix} \tilde{r}[k] \\ v[k] \end{bmatrix} = \lim_{k\to\infty} F^k \begin{bmatrix} \tilde{r}[0] \\ v[0] \end{bmatrix} = \begin{bmatrix} \tilde{r}[0] + (\frac{1}{\alpha} - \frac{T}{2})\mathbf{p}^T v[0] \\ \mathbf{0}_n \end{bmatrix}$.

(Necessity.) Note that F can be written in Jordan canonical form as $F = PJP^{-1}$, where J is the Jordan block matrix. If $\tilde{r}_i[k] \to \mathbf{p}^T\tilde{r}[0] + (\frac{1}{\alpha} - \frac{T}{2})\mathbf{p}^T v[0]$ and $v_i[k] \to 0$ as $k \to \infty$, it follows that $\lim_{k\to\infty} F^k \to \begin{bmatrix} \mathbf{1}_n \\ \mathbf{0}_n \end{bmatrix} [\mathbf{p}^T, (\frac{1}{\alpha} - \frac{T}{2})\mathbf{p}^T]$, which has rank one. It thus follows that $\lim_{k\to\infty} J^k$ has rank one, which implies that all but one eigenvalue are within the unit circle. Noting that F has at least one eigenvalue equal to one, it follows that one is the unique eigenvalue of F with maximum modulus. ■

Undirected Interaction

In this subsection, we show necessary and sufficient conditions on α and T such that coordination is reached using (2.6) under an undirected interaction topology. Note that all eigenvalues of $\mathcal{L}$ are real for undirected graphs.

Lemma 2.3.5 *The polynomial*

$$s^2 + as + b = 0, \tag{2.10}$$

where $a, b \in \mathbb{C}$*, has all roots within the unit circle if and only if all roots of*

$$(1 + a + b)t^2 + 2(1 - b)t + b - a + 1 = 0 \tag{2.11}$$

are in the open left half plane (LHP).

Proof: By applying bilinear transformation $s = \frac{t+1}{t-1}$ [87], polynomial (2.10) can be rewritten as

$$(t+1)^2 + a(t+1)(t-1) + b(t-1)^2 = 0,$$

which implies (2.11). Note that the bilinear transformation maps the open LHP one-to-one onto the interior of the unit circle. The lemma follows directly. ■

Lemma 2.3.6 *Suppose that the undirected graph $\mathcal{G}$ is connected. All eigenvalues of F, where F is defined in* (2.34)*, are within the unit circle except one eigenvalue equal to one if and only if α and T are chosen from the set*

$$S_r = \left\{ (\alpha, T) | -\frac{T^2}{2} \min_i \mu_i < \alpha T < 2 \right\}.^2 \tag{2.12}$$

Proof: When undirected graph $\mathcal{G}$ is connected, it follows from Lemma 2.3.2 that $\mu_1 = 0$ and $\mu_i < 0$, $i = 2, \ldots, n$. Because $\mu_1 = 0$, it follows that $\lambda_1 = 1$ and $\lambda_2 = 1 - \alpha T$. To ensure $|\lambda_2| < 1$, it is required that $0 < \alpha T < 2$.

Let $a = \alpha T - 2 - \frac{T^2}{2}\mu_i$ and $b = 1 - \alpha T - \frac{T^2}{2}\mu_i$. It follows from Lemma 2.3.5 that for $\mu_i < 0, i = 2, \cdots, n$, the roots of (2.9) are within the unit circle if and only if all roots of

$$-T^2\mu_i t^2 + (T^2\mu_i + 2\alpha T)t + 4 - 2\alpha T = 0 \tag{2.13}$$

are in the open LHP. Because $-T^2\mu_i > 0$, the roots of (2.13) are always in the open LHP if and only if $T^2\mu_i + 2\alpha T > 0$ and $4 - 2\alpha T > 0$, which implies that $-\frac{T^2}{2}\mu_i < \alpha T < 2$, $i = 2, \ldots, n$. Combining the above arguments proves the lemma. ■

Theorem 2.3.1 *Suppose that undirected graph $\mathcal{G}$ is connected. Let $\mathbf{p}$ be defined in Lemma 2.3.2. Using* (2.6) *for* (2.5)*, $\tilde{r}_i[k] \to \mathbf{p}^T\tilde{r}[0] + (\frac{1}{\alpha} - \frac{T}{2})\mathbf{p}^T v[0]$ and $v_i[k] \to 0$ as $k \to \infty$ if and only if α and T are chosen from S_r, where S_r is defined by* (2.12)*.*

[2] Note that S_r is nonempty.

Proof: The statement follows directly from Lemmas 2.3.4 and 2.3.6. ■

Remark 2.3.2 *From Lemma 2.3.6, we can get* $T < \frac{2}{\sqrt{-\mu_i}}$. *From the Gershgorin circle theorem, we know that* $|\mu_i| \leq 2\max_i \ell_{ii}$. *Therefore, if* $T < \sqrt{\frac{2}{\max_i \ell_{ii}}}$, *then we have* $T < \frac{2}{\sqrt{-\mu_i}}$. *Note that* $\max_i \ell_{ii}$ *represents the maximal in-degree of a graph. Therefore, the sufficient bound of the sampling period is related to the maximal in-degree of a graph.*

Directed Interaction

In this subsection, we first show necessary and sufficient conditions on α and T such that coordination is reached using (2.6) under a directed interaction topology. Because it is not easy to find the explicit bounds for α and T such that the necessary and sufficient conditions are satisfied, we present sufficient conditions that can be used to compute the explicit bounds for α and T. Note that the eigenvalues of $\mathcal{L}$ may be complex for directed graphs, which makes the analysis more challenging.

Lemma 2.3.7 *Suppose that the directed graph* $\mathcal{G}$ *has a directed spanning tree. Let* $\mathrm{Re}(\cdot)$ *and* $\mathrm{Im}(\cdot)$ *denote, respectively, the real and imaginary part of a number. There exist* α *and* T *such that the following three conditions are satisfied:*

1) $0 < \alpha T < 2$*;*

2) When $\mathrm{Re}(\mu_i) < 0$ *and* $\mathrm{Im}(\mu_i) = 0$, $(\alpha, T) \in S_r$, *where* S_r *is defined in* (2.12)*;*

3) When $\mathrm{Re}(\mu_i) < 0$ *and* $\mathrm{Im}(\mu_i) \neq 0$, α *and* T *satisfy* $\frac{\alpha}{T} > -\frac{|\mu_i|^2}{2\mathrm{Re}(\mu_i)}$ *and*

i) $T < \overline{T}_{i1}$ *if* $\frac{|\mathrm{Im}(\mu_i)|}{\sqrt{-\mathrm{Re}(\mu_i)}} \leq \alpha \leq \frac{|\mu_i|}{\sqrt{-\mathrm{Re}(\mu_i)}}$, *where*

$$\overline{T}_{i1} = \frac{-2\alpha[\mathrm{Re}(\mu_i)]^2 - 2\sqrt{-\mathrm{Re}(\mu_i)[\mathrm{Im}(\mu_i)]^2[\alpha^2\mathrm{Re}(\mu_i) + |\mu_i|^2]}}{\mathrm{Re}(\mu_i)|\mu_i|^2}; \tag{2.14}$$

ii) $T < \overline{T}_{i2}$ *if* $\alpha < \frac{|\mathrm{Im}(\mu_i)|}{\sqrt{-\mathrm{Re}(\mu_i)}}$, *where*

$$\overline{T}_{i2} = \frac{-2\alpha[\mathrm{Re}(\mu_i)]^2 + 2\sqrt{-\mathrm{Re}(\mu_i)[\mathrm{Im}(\mu_i)]^2[\alpha^2\mathrm{Re}(\mu_i) + |\mu_i|^2]}}{\mathrm{Re}(\mu_i)|\mu_i|^2}. \tag{2.15}$$

In addition, all eigenvalues of F, where F is defined in (2.34)*, are within the unit circle except one eigenvalue equal to one if and only if the previous three conditions are satisfied.*

Proof: For the first statement, when T is sufficiently small, there always exists α such that conditions 1), 2), and 3) are satisfied.

For the second statement, when $\mu_1 = 0$, it follows that $\lambda_1 = 1$ and $\lambda_2 = 1 - \alpha T$. Therefore, condition 1) guarantees that λ_2 is within the unit circle. When $\mathrm{Re}(\mu_i) < 0$ and $\mathrm{Im}(\mu_i) = 0$, it follows from Lemma 2.3.6 that all roots of F corresponding to μ_i are within the unit circle if and only if condition 2) is satisfied.

We next consider the case when $\mathrm{Re}(\mu_i) < 0$ and $\mathrm{Im}(\mu_i) \neq 0$. Letting t_1 and t_2 be the two roots of (2.13), it follows that $\mathrm{Re}(t_1) + \mathrm{Re}(t_2) = 1 + 2\frac{\alpha}{T}\frac{\mathrm{Re}(\mu_i)}{|\mu_i|^2}$. Therefore, both t_1 and t_2 are in the open LHP only if $1 + 2\frac{\alpha}{T}\frac{\mathrm{Re}(\mu_i)}{|\mu_i|^2} < 0$, i.e., $\frac{\alpha}{T} > -\frac{|\mu_i|^2}{2\mathrm{Re}(\mu_i)}$. To find the bound on T, we assume that one root of (2.13) is on the imaginary axis. Without loss of generality, let $t_1 = \chi\mathbf{j}$, where χ is a real constant and $\mathbf{j}$ is the imaginary unit. Substituting $t_1 = \chi\mathbf{j}$ into (2.13) and separating the corresponding real and imaginary parts give that

$$T^2\mathrm{Re}(\mu_i)\chi^2 - T^2\mathrm{Im}(\mu_i)\chi + 4 - 2\alpha T = 0 \tag{2.16}$$

$$T^2\mathrm{Im}(\mu_i)\chi^2 + [T^2\mathrm{Re}(\mu_i) + 2\alpha T]\chi = 0. \tag{2.17}$$

It follows from (2.17) that

$$\chi = -\frac{T\mathrm{Re}(\mu_i) + 2\alpha}{T\mathrm{Im}(\mu_i)}. \tag{2.18}$$

By substituting (2.18) into (2.16) gives that

$$\frac{\mathrm{Re}(\mu_i)[T\mathrm{Re}(\mu_i) + 2\alpha]^2}{[\mathrm{Im}(\mu_i)]^2} + T[T\mathrm{Re}(\mu_i) + 2\alpha] + 4 - 2\alpha T = 0.$$

After some simplifications, we get that

$$\mathrm{Re}(\mu_i)|\mu_i|^2T^2 + 4\alpha[\mathrm{Re}(\mu_i)]^2T + 4\alpha^2\mathrm{Re}(\mu_i) + 4[\mathrm{Im}(\mu_i)]^2 = 0. \tag{2.19}$$

When $\alpha > \frac{|\mu_i|}{\sqrt{-\mathrm{Re}(\mu_i)}}$, it can be computed that

$$\begin{aligned}
&\left\{4\alpha[\mathrm{Re}(\mu_i)]^2\right\}^2 - 4\mathrm{Re}(\mu_i)|\mu_i|^2(4\alpha^2\mathrm{Re}(\mu_i) + 4[\mathrm{Im}(\mu_i)]^2) \\
=& -16\left\{\alpha^2[\mathrm{Re}(\mu_i)]^2[\mathrm{Im}(\mu_i)]^2 + \mathrm{Re}(\mu_i)|\mu_i|^2[\mathrm{Im}(\mu_i)]^2\right\} \\
=& -16\mathrm{Re}(\mu_i)[\mathrm{Im}(\mu_i)]^2[\alpha^2\mathrm{Re}(\mu_i) + |\mu_i|^2] \\
<& 0.
\end{aligned}$$

Therefore, there does not exists positive T such that t_1 (respectively, t_2) is on the imaginary axis, which implies that t_1 (respectively, t_2) is always on the left or right hand side. When $\frac{|\mathrm{Im}(\mu_i)|}{\sqrt{-\mathrm{Re}(\mu_i)}} \leq \alpha \leq \frac{|\mu_i|}{\sqrt{-\mathrm{Re}(\mu_i)}}$, it follows that $4\alpha^2\mathrm{Re}(\mu_i) + 4[\mathrm{Im}(\mu_i)]^2 \geq 0$. Noting that $\mathrm{Re}(\mu_i)|\mu_i|^2 < 0$, it follows that there exists a unique positive $\overline{T}_{i1}$ such that (2.19) holds when $T = \overline{T}_{i1}$, where $\overline{T}_{i1}$ is given by (2.14). Similarly, when $\alpha < \frac{|\mathrm{Im}(\mu_i)|}{\sqrt{-\mathrm{Re}(\mu_i)}}$, it follows that $4\alpha^2\mathrm{Re}(\mu_i) + 4[\mathrm{Im}(\mu_i)]^2 < 0$. Noting also that $\mathrm{Re}(\mu_i)|\mu_i|^2 < 0$, it follows that there are two positive solutions with the smaller one given by $\overline{T}_{i2}$. This completes the proof.

Combining the previous arguments completes the proof. ■

Theorem 2.3.3 *Suppose that directed graph $\mathcal{G}$ has a directed spanning tree. Let $\mathbf{p}$ be defined in Lemma 2.3.2. Using* (2.6) *for* (2.5)*, $\tilde{r}_i[k] \to \mathbf{p}^T\tilde{r}[0] + (\frac{1}{\alpha} - \frac{T}{2})\mathbf{p}^T v[0]$ and $v_i[k] \to 0$ as $k \to \infty$ if and only if α and T are chosen satisfying the conditions in Lemma 2.3.7.*

Proof: The statement follows directly from Lemma 2.3.4 and Lemma 2.3.7. ■

From Lemma 2.3.7, it is not easy to find α and T explicitly such that the conditions in Lemma 2.3.7 are satisfied. We next present a sufficient condition in which α and T can be easily determined. Before moving on, we need the following lemmas.

Lemma 2.3.8 [88, 89] *All the zeros of the complex polynomial*

$$P(z) = z^n + \alpha_1 z^{n-1} + \ldots + \alpha_{n-1}z + \alpha_n$$

satisfy $|z| \leq r_0$*, where* r_0 *is the unique nonnegative solution of the equation*

$$r^n - |\alpha_1| r^{n-1} - \ldots - |\alpha_{n-1}| r - |\alpha_n| = 0.$$

The bound r_0 *is attained if* $\alpha_i = -|\alpha_i|$.

Corollary 2.3.4 *All roots of polynomial* (2.10) *are within the unit circle if* $|a| + |b| < 1$*. Moreover, if* $|a+b| + |a-b| < 1$*, all roots of* (2.10) *are still within the unit circle.*

Proof: According to Lemma 2.3.8, the roots of (2.10) are within the unit circle if the unique nonnegative solution s_0 of $s^2 - |a|s - |b| = 0$ satisfies $s_0 < 1$. It is straightforward to show that $s_0 = \frac{|a|+\sqrt{|a|^2+4|b|}}{2}$. Therefore, the roots of (2.10) are within the unit circle if

$$|a| + \sqrt{|a|^2 + 4|b|} < 2. \tag{2.20}$$

We next discuss the condition under which (2.20) holds. If $b = 0$, then the statements of the corollary hold trivially. If $|b| \neq 0$, we have

$$\frac{(|a| + \sqrt{|a|^2 + 4|b|})(-|a| + \sqrt{|a|^2 + 4|b|})}{-|a| + \sqrt{|a|^2 + 4|b|}} < 2.$$

After some computation, it follows that condition (2.20) is equivalent to $|a|+|b| < 1$. Therefore, the first statement of the corollary holds. For the second statement, because $|a|+|b| \leq |a+b|+|a-b|$, if $|a+b|+|a-b| < 1$, then $|a|+|b| < 1$, which implies that the second statement of the corollary also holds. ■

Lemma 2.3.9 *Suppose that directed graph* $\mathcal{G}$ *has a directed spanning tree. There exist positive* α *and* T *such that* $S_c \cap S_r$ *is nonempty, where*

$$S_c = \bigcap_{\forall \mathrm{Re}(\mu_i)<0 \text{ and } \mathrm{Im}(\mu_i)\neq 0} \{(\alpha, T) | |1 + T^2\mu_i| + |3 - 2\alpha T| < 1\}, \tag{2.21}$$

and S_r *is defined by* (2.12)*. If* α *and* T *are chosen from* $S_c \cap S_r$*, then all eigenvalues of* F *are within the unit circle except one eigenvalue equal to one.*

Proof: For the first statement, we let $\alpha T = \frac{3}{2}$. When $\mathrm{Re}(\mu_i) < 0$ and $\mathrm{Im}(\mu_i) \neq 0$, $|1 + T^2\mu_i| + |3 - 2\alpha T| < 1$ implies $|1 + T^2\mu_i| < 1$ because $\alpha T = \frac{3}{2}$. It thus follows that $0 < T < \frac{\sqrt{-2\mathrm{Re}(\mu_i)}}{|\mu_i|}$, $\forall \mathrm{Re}(\mu_i) < 0$ and $\mathrm{Im}(\mu_i) \neq 0$. When $\mu_i \leq 0$, $-\frac{T^2}{2}\mu_i < \alpha T < 2$ can be simplified as $-T^2\mu_i < \frac{3}{2}$ because $\alpha T = \frac{3}{2}$. It thus follows that $0 < T < \sqrt{\frac{3}{-\mu_i}}$, $\forall \mu_i \leq 0$. Let $T_c = \bigcap_{\forall \mathrm{Re}(\mu_i)<0 \text{ and } \mathrm{Im}(\mu_i)\neq 0} \left\{ T | 0 < T < \frac{\sqrt{-2\mathrm{Re}(\mu_i)}}{|\mu_i|} \right\}$ and $T_r = \bigcap_{\forall \mu_i \leq 0} \left\{ T | 0 < T < \sqrt{\frac{3}{-\mu_i}} \right\}$.[3] It is straightforward to see that $T_c \cap T_r$ is nonempty. Recalling that $\alpha T = \frac{3}{2}$, it follows that $S_c \cap S_r$ is nonempty as well.

For the second statement, note that if directed graph $\mathcal{G}$ has a directed spanning tree, then it follows from Lemma 2.3.2 that $\mu_1 = 0$ and $\mathrm{Re}(\mu_i) < 0$, $i = 2, \ldots, n$. Note that $\mu_1 = 0$ implies that $\lambda_1 = 1$ and $\lambda_2 = 1 - \alpha T$. To ensure that $|\lambda_2| < 1$, it is required that $0 < \alpha T < 2$. When $\mathrm{Re}(\mu_i) < 0$ and $\mathrm{Im}(\mu_i) \neq 0$, it follows from Corollary 2.3.4 that the roots of (2.9) are within the unit circle if $|1+T^2\mu_i|+|3-2\alpha T| < 1$, where we have used the second statement of Corollary 2.3.4 by letting $a = \alpha T - 2 - \frac{T^2}{2}\mu_i$ and $b = 1 - \frac{T^2}{2}\mu_i - \alpha T$. When $\mu_i < 0$, it follows from the proof of Lemma 2.3.6 that the roots of (2.9) are within the unit circle if $-\frac{T^2}{2}\mu_i < \alpha T < 2$. Combining the above arguments proves the second statement. ■

Remark 2.3.5 *According to Lemmas 2.3.4 and 2.3.9, if α and T are chosen from $S_c \bigcap S_r$ and directed graph $\mathcal{G}$ has a directed spanning tree, coordination can be achieved ultimately. An easy way to choose α and T is to let $\alpha T = \frac{3}{2}$. It then follows that T can be chosen satisfying $T < \min_{\forall \mathrm{Re}(\mu_i)<0 \text{ and } \mathrm{Im}(\mu_i)\neq 0} \frac{|\mu_i|}{\sqrt{-\mathrm{Re}(\mu_i)}}$ and $T < \min_{\forall \mathrm{Re}(\mu_i)<0 \text{ and } \mathrm{Im}(\mu_i)=0} \sqrt{\frac{3}{-\mu_i}}$.*

2.3.2 Convergence Analysis of Sampled-data Coordination Algorithm with Relative Damping

In this section, we analyze algorithm (2.7) under, respectively, an undirected and an directed interaction topology.

[3] When $\mu_i = 0$, $T > 0$ can be chosen arbitrarily.

Using (2.7), (2.5) can be written in matrix form as

$$\begin{bmatrix} \tilde{r}[k+1] \\ v[k+1] \end{bmatrix} = \underbrace{\begin{bmatrix} I_n - \frac{T^2}{2}\mathcal{L} & TI_n - \frac{T^2}{2}\mathcal{L} \\ -T\mathcal{L} & I_n - \alpha T\mathcal{L} \end{bmatrix}}_{G} \begin{bmatrix} \tilde{r}[k] \\ v[k] \end{bmatrix}. \tag{2.22}$$

Coordination is achieved if for any $r_i[0]$ and $v_i[0]$, $\tilde{r}_i[k] \to \tilde{r}_j[k]$ and $v_i[k] \to v_j[k]$ as $k \to \infty$.

A similar analysis to that for (2.34) shows that the roots of $\det(sI_{2n} - G) = 0$, i.e., the eigenvalues of G, satisfy

$$s^2 - (2 + \alpha T\mu_i + \frac{1}{2}T^2\mu_i)s + 1 + \alpha T\mu_i - \frac{1}{2}T^2\mu_i = 0. \tag{2.23}$$

Similarly, each eigenvalue of $-\mathcal{L}$, μ_i, corresponds to two eigenvalues of G, denoted by ρ_{2i-1} and ρ_{2i}. Without loss of generality, let $\mu_1 = 0$, which implies that $\rho_1 = \rho_2 = 1$. Therefore, G has at least two eigenvalues equal to one.

Lemma 2.3.10 *Using* (2.7) *for* (2.5), $\tilde{r}_i[k] \to \mathbf{p}^T\tilde{r}[0] + kT\mathbf{p}^T v[0]$ *and* $v_i[k] \to \mathbf{p}^T v[0]$ *for large* k *if and only if* G *has exactly two eigenvalues equal to one and all other eigenvalues have modulus smaller than one.*

Proof: (Sufficiency.) Note from (2.23) that if G has exactly two eigenvalues equal to one, i.e., $\rho_1 = \rho_2 = 1$, then $-\mathcal{L}$ has exactly one eigenvalue equal to zero. Let $[p^T, q^T]^T$, where $p, q \in \mathbb{R}^n$, be the right eigenvector of G associated with eigenvalue one. It follows that

$$\begin{bmatrix} I_n - \frac{T^2}{2}\mathcal{L} & TI_n - \frac{T^2}{2}\mathcal{L} \\ -T\mathcal{L} & I_n - \alpha T\mathcal{L} \end{bmatrix} \begin{bmatrix} p \\ q \end{bmatrix} = \begin{bmatrix} p \\ q \end{bmatrix}.$$

After some computation, it follows that eigenvalue one has geometric multiplicity equal to one even if it has algebraic multiplicity equal to two. It also follows from Lemma 2.3.2 that we can choose $p = \mathbf{1}_n$ and $q = \mathbf{0}_n$. In addition, a generalized right eigenvector associated with eigenvalue one can be chosen as $[\mathbf{0}_n^T, \frac{1}{T}\mathbf{1}_n^T]^T$. Similarly, it can be shown that $[\mathbf{0}_n^T, T\mathbf{p}_n^T]^T$ and $[\mathbf{p}^T, \mathbf{0}_n^T]^T$ are, respectively, a left eigenvector and generalized left eigenvector associated with eigenvalue one.

Note that G can be written in Jordan canonical form as $G = PJP^{-1}$, where the columns of P, denoted by p_k, $k = 1, \ldots, 2n$, can be chosen to be the right eigenvectors or generalized right eigenvectors of G, the rows of P^{-1}, denoted by q_k^T, $k = 1, \ldots, 2n$, can be chosen to be the left eigenvectors or generalized left eigenvectors of G such that $p_k^T q_k = 1$ and $p_k^T q_\ell = 0$, $k \neq \ell$, and J is the Jordan block diagonal matrix with the eigenvalues of G being the diagonal entries. Note that $\rho_1 = \rho_2 = 1$ and $\mathrm{Re}(\rho_k) < 0$, $k = 3, \ldots, 2n$. Also note that we can choose $p_1 = [\mathbf{1}_n^T, \mathbf{0}_n^T]^T$, $p_2 = [\mathbf{0}_n^T, \frac{1}{T}\mathbf{1}_n^T]^T$, $q_1 = [\mathbf{p}^T, \mathbf{0}_n^T]^T$, and $q_2 = [\mathbf{0}_n^T, T\mathbf{p}_n^T]^T$. It follows that $G^k \to PJ^kP^{-1} \to \begin{bmatrix} \mathbf{1}_n & \mathbf{0}_n \\ \mathbf{0}_n & \frac{1}{T}\mathbf{1}_n \end{bmatrix} \begin{bmatrix} 1 & k \\ 0 & 1 \end{bmatrix} \begin{bmatrix} \mathbf{p}^T & \mathbf{0}_n^T \\ \mathbf{0}_n^T & T\mathbf{p}^T \end{bmatrix} = \begin{bmatrix} \mathbf{1}_n\mathbf{p}^T & kT\mathbf{1}_n\mathbf{p}^T \\ \mathbf{0}_n & \mathbf{1}_n\mathbf{p}^T \end{bmatrix}$. Therefore, it follows that $\tilde{r}_i[k] \to \mathbf{p}^T\tilde{r}[0] + kT\mathbf{p}^T v[0]$ and $v_i[k] \to \mathbf{p}^T v[0]$ for large k.

(Necessity.) Note that G has at least two eigenvalues equal to one. If $\tilde{r}_i[k] \to \mathbf{p}^T\tilde{r}[0] + kT\mathbf{p}^T v[0]$ and $v_i[k] \to \mathbf{p}^T v[0]$ for large k, it follows that F^k has rank two for large t, which in turn implies that J^k has rank two for large k. It follows that G has exactly two eigenvalues equal to one and all other eigenvalues have modulus smaller than one. ■

Undirected Interaction

In this subsection, we show necessary and sufficient conditions on α and T such that coordination is reached using (2.7) under an undirected interaction topology.

Lemma 2.3.11 *Suppose that undirected graph $\mathcal{G}$ is connected. All eigenvalues of G are within the unit circle except two eigenvalues equal to one if and only if α and T are chosen from the set*

$$Q_r = \{(\alpha, T) | \frac{T^2}{2} < \alpha T < -\frac{2}{\min_i \mu_i}\}.^4 \tag{2.24}$$

Proof: Because undirected graph $\mathcal{G}$ is connected, it follows that $\mu_1 = 0$ and $\mu_i < 0$, $i = 2, \cdots, n$. Note that $\rho_1 = \rho_2 = 1$ because $\mu_1 = 0$. Let $a = -(2 + \alpha T\mu_i + \frac{1}{2}T^2\mu_i)$ and $b = 1 + \alpha T\mu_i - \frac{1}{2}T^2\mu_i$. It follows from Lemma 2.3.5 that for $\mu_i < 0$, $i = 2, \ldots, n$, the roots of (2.23) are within the unit

[4] Note that Q_r is nonempty.

circle if and only if all roots of

$$-T^2\mu_i t^2 + (T^2\mu_i - 2\alpha T\mu_i)t + 4 + 2\alpha T\mu_i = 0, \tag{2.25}$$

are in the open LHP. Because $-T^2\mu_i > 0$, the roots of (2.25) are always in the open LHP if and only if $4 + 2\alpha T\mu_i > 0$ and $T^2\mu_i - 2\alpha T\mu_i > 0$, which implies that $\frac{T^2}{2} < \alpha T < -\frac{2}{\mu_i}$, $i = 2, \ldots, n$. Combining the above arguments proves the lemma. ■

Theorem 2.3.6 *Suppose that undirected graph $\mathcal{G}$ is connected. Let $\mathbf{p}$ be defined in Lemma 2.3.2. Using* (2.7)*, $\tilde{r}_i[k] \to \mathbf{p}^T\tilde{r}[0] + kT\mathbf{p}^T v[0]$ and $v_i[k] \to \mathbf{p}^T v[0]$ for large k if and only if α and T are chosen from Q_r, where Q_r is defined by* (2.24)*.*

Proof: The statement follows directly from Lemmas 2.3.10 and 2.3.11. ■

Directed Interaction

In this subsection, we show necessary and sufficient conditions on α and T such that coordination is reached using (2.7) under a directed interaction topology. Note again that the eigenvalues of $\mathcal{L}$ may be complex for directed graphs, which makes the analysis more challenging.

Lemma 2.3.12 *Suppose that $\mathrm{Re}(\mu_i) < 0$ and $\mathrm{Im}(\mu_i) \neq 0$. All roots of* (2.23) *are within the unit circle if and only if $\frac{\alpha}{T} > \frac{1}{2}$ and $B_i < 0$, where*

$$B_i \triangleq (\frac{4\mathrm{Re}(\mu_i)}{|\mu_i|^2T^2} + 2\frac{\alpha}{T})(1 - 2\frac{\alpha}{T})^2 + \frac{16\mathrm{Im}(\mu_i)^2}{|\mu_i|^4T^4}. \tag{2.26}$$

Proof: As in the proof of Lemma 2.3.11, all roots of (2.23) are within the unit circle if and only if all roots of (2.25) are in the open LHP. Letting s_1 and s_2 denote the roots of (2.25), it follows that

$$s_1 + s_2 = 1 - 2\frac{\alpha}{T} \tag{2.27}$$

and

$$s_1 s_2 = -\frac{4}{\mu_i T^2} - 2\frac{\alpha}{T}. \tag{2.28}$$

Noting that (2.27) implies that $\mathrm{Im}(s_1) + \mathrm{Im}(s_2) = 0$, we define $s_1 = a_1 + jb$ and $s_2 = a_2 - jb$, where j is the imaginary unit. Note that s_1 and s_2 have negative real parts if and only if $a_1 + a_2 < 0$ and $a_1 a_2 > 0$. Note from (2.27) that $a_1 + a_2 < 0$ is equivalent to $\frac{\alpha}{T} > \frac{1}{2}$. We next show conditions on α and T such that $a_1 a_2 > 0$ holds. Substituting the definitions of s_1 and s_2 into (2.28), gives $a_1 a_2 + b^2 + j(a_2 - a_1)b = -\frac{4}{\mu_i T^2} - 2\frac{\alpha}{T}$, which implies that

$$(a_2 - a_1)b = \frac{4\mathrm{Im}(\mu_i)}{|\mu_i|^2 T^2} \tag{2.29}$$

$$a_1 a_2 + b^2 = \frac{-4\mathrm{Re}(\mu_i)}{|\mu_i|^2 T^2} - 2\frac{\alpha}{T}. \tag{2.30}$$

It follows from (3.51) that $b = \frac{4\mathrm{Im}(\mu_i)}{|\mu_i|^2 T^2 (a_2 - a_1)}$. Consider also the fact that $(a_2 - a_1)^2 = (a_2 + a_1)^2 - 4a_1 a_2 = (1 - 2\frac{\alpha}{T})^2 - 4a_1 a_2$. After some manipulation, (3.52) can be written as

$$4(a_1 a_2)^2 + A_i a_1 a_2 - B_i = 0, \tag{2.31}$$

where $A_i \stackrel{\triangle}{=} 4(\frac{4\mathrm{Re}(\mu_i)}{|\mu_i|^2 T^2} + 2\frac{\alpha}{T}) - (1 - 2\frac{\alpha}{T})^2$ and B_i is defined in (2.26). It follows that $A_i^2 + 16B_i = [4(\frac{4\mathrm{Re}(\mu_i)}{|\mu_i|^2 T^2} + 2\frac{\alpha}{T}) + (1 - 2\frac{\alpha}{T})^2]^2 + \frac{16\mathrm{Im}(\mu_i)^2}{|\mu_i|^4 T^4} \geq 0$, which implies that (2.31) has two real roots. Therefore, necessary and sufficient conditions for $a_1 a_2 > 0$ are $B_i < 0$ and $A_i < 0$. Because $\frac{16\mathrm{Im}(\mu_i)^2}{|\mu_i|^4 T^4} > 0$, if $B_i < 0$, then $4(\frac{4\mathrm{Re}(\mu_i)}{|\mu_i|^2 T^2} + 2\frac{\alpha}{T}) < 0$, which implies $A_i < 0$ as well. Combining the previous arguments proves the lemma. ■

Lemma 2.3.13 *Suppose that directed graph $\mathcal{G}$ has a directed spanning tree. There exist positive α and T such that $Q_c \cap Q_r$ is nonempty, where*

$$Q_c = \bigcap_{\forall \mathrm{Re}(\mu_i)<0 \text{ and } \mathrm{Im}(\mu_i)\neq 0} \left\{ (\alpha, T) | \frac{1}{2} < \frac{\alpha}{T},\ B_i < 0 \right\}, \tag{2.32}$$

where B_i is defined by (2.26) *and Q_r is defined by* (2.24)*. All eigenvalues of G are within the unit circle except two eigenvalues equal to one if and only if α and T are chosen from $Q_r \cap Q_c$.*

Proof: For the first statement, we let $\alpha > T > 0$. When $\mathrm{Re}(\mu_i) < 0$ and $\mathrm{Im}(\mu_i) \neq 0$, it follows that $\frac{\alpha}{T} > \frac{1}{2}$ holds apparently. Note that $\alpha > T$ implies $(T - 2\alpha)^2 > \alpha^2$. Therefore, a sufficient

condition for $B_i < 0$ is

$$\alpha T < -\frac{8\mathrm{Im}(\mu_i)^2}{|\mu_i|^4\alpha^2} - \frac{2\mathrm{Re}(\mu_i)}{|\mu_i|^2}. \tag{2.33}$$

To ensure that there are feasible $\alpha > 0$ and $T > 0$ satisfying (2.33), we first need to ensure that the right side of (2.33) is positive, which requires $\alpha > \frac{2|\mathrm{Im}(\mu_i)|}{|\mu_i|\sqrt{-\mathrm{Re}(\mu_i)}}$. It also follows from (2.33) that $T < -\frac{8\mathrm{Im}(\mu_i)^2}{|\mu_i|^4\alpha^3} - \frac{2\mathrm{Re}(\mu_i)}{|\mu_i|^2\alpha}$, $\forall \mathrm{Re}(\mu_i) < 0$ and $\mathrm{Im}(\mu_i) \neq 0$. Therefore, (2.32) is ensured to be nonempty if α and T are chosen from, respectively, $\alpha_c = \bigcap_{\forall \mathrm{Re}(\mu_i)<0 \text{ and } \mathrm{Im}(\mu_i)\neq 0}\{\alpha|\alpha > \frac{2|\mathrm{Im}(\mu_i)|}{|\mu_i|\sqrt{-\mathrm{Re}(\mu_i)}}\}$ and $T_c = \bigcap_{\forall \mathrm{Re}(\mu_i)<0 \text{ and } \mathrm{Im}(\mu_i)\neq 0}\{T|T < -\frac{8\mathrm{Im}(\mu_i)^2}{|\mu_i|^4\alpha^3} - \frac{2\mathrm{Re}(\mu_i)}{|\mu_i|^2\alpha} \text{ and } 0 < T < \alpha\}$. Note that (2.24) is ensured to be nonempty if α and T are chosen from, respectively, $\alpha_r = \{\alpha|\alpha > 0\}$ and $T_r = \bigcap_{\forall \mu_i<0}\{T|0 < T < 2\alpha \text{ and } T < -\frac{2}{\mu_i\alpha}\}$. It is straightforward to see that both $\alpha_c \cap \alpha_r$ and $T_c \cap T_r$ are nonempty. Combining the above arguments shows that $Q_c \cap Q_r$ is nonempty.

For the second statement, note that if directed graph $\mathcal{G}$ has a directed spanning tree, it follows from Lemma 2.3.2 that $\mu_1 = 0$ and $\mathrm{Re}(\mu_i) < 0$, $i = 2, \ldots, n$. Note that $\mu_1 = 0$ implies that $\rho_1 = 1$ and $\rho_2 = 1$. When $\mathrm{Re}(\mu_i) < 0$ and $\mathrm{Im}(\mu_i) \neq 0$, it follows from Lemma 2.3.12 that the roots of (2.23) are within unit circle if and only if $\frac{\alpha}{T} > \frac{1}{2}$ and $B_i < 0$. When $\mu_i < 0$, it follows from Lemma 2.3.11 that the roots of (2.23) are within unit circle if and only if $\frac{T^2}{2} < \alpha T < -\frac{2}{\mu_i}$. Combining the above arguments shows that all eigenvalues of G are within the unit circle except two eigenvalues equal to one if and only if α and T are chosen from $Q_c \cap Q_r$. ■

Remark 2.3.7 *From the proof of the first statement of Lemma 2.3.13, an easy way to choose α and T is to let $\alpha > T$. Then α is chosen from α_c and T is chosen from $T_c \bigcap T_r$, where α_c, T_c, and T_r are defined in the proof of Lemma 2.3.13.*

Theorem 2.3.8 *Suppose that directed graph $\mathcal{G}$ has a directed spanning tree. Using* (2.7)*, $\tilde{r}_i[k] \to \mathbf{p}^T\tilde{r}[0] + kT\mathbf{p}^T v[0]$ and $v_i[k] \to \mathbf{p}^T v[0]$ for large k if and only if α and T are chosen from $Q_c \cap Q_r$, where Q_c and Q_r are defined in* (2.32) *and* (2.24)*, respectively.*

Proof: The proof follows directly from Lemma 2.3.11 and Theorem 2.3.13. ■

Remark 2.3.9 *Note that it is required in Theorems 2.3.3 and 2.4.3 that the communication graph has a directed spanning tree in order to guarantee coordination. The connectivity requirement in*

Theorems 2.3.3 and 2.4.3 can be interpreted as follows. For a group of vehicles, if the communication graph does not have a directed spanning tree, then the group of vehicles can be divided into at least two disconnected subgroups. Because there is no communication among these subgroups, the final states of the subgroups in general cannot reach coordination.

2.3.3 Simulation

In this section, we present simulation results to validate the theoretical results derived in Sections 2.4.1 and 2.4.2. We consider a team of four vehicles with directed graph $\mathcal{G}$ shown by Fig. 2.1. Note that $\mathcal{G}$ has a directed spanning tree. The nonsymmetric Laplacian matrix associated with $\mathcal{G}$ is chosen as

$$\mathcal{L} = \begin{bmatrix} 1 & -1 & 0 & 0 \\ 0 & 1.5 & -1.5 & 0 \\ -2 & 0 & 2 & 0 \\ -2.5 & 0 & 0 & 2.5 \end{bmatrix}.$$

It can be computed that for $\mathcal{L}$, $\mathbf{p} = [0.4615, 0.3077, 0.2308, 0]^T$. Here for simplicity, we have chosen $\delta_i = 0,\ i = 1, \cdots, 4$.

For coordination algorithm (2.6), let $r[0] = [0.5, 1, 1.5, 2]^T$ and $v[0] = [-0.1, 0, 0.1, 0]^T$. Fig. 2.2(a) shows the convergence result using (2.6) with $\alpha = 4$ and $T = 0.4$ sec. Note that the conditions in Theorem 2.3.3 are satisfied. It can be seen that coordination is reached with the final equilibrium for $r_i[k]$ being 0.8835, which is equal to $\mathbf{p}^T\tilde{r}[0] + (\frac{1}{\alpha} - \frac{T}{2})\mathbf{p}^T v[0]$ as argued in Theorem 2.3.3. Figure 2.2(b) shows the convergence result using (2.6) with $\alpha = 1.2$ and $T = 0.5$ sec. Note that coordination is not reached in this case.

For coordination algorithm (2.7), let $r[0] = [0, 1, 2, 3]^T$ and $v[0] = [0, 0.2, 0.4, 0.6]^T$. Figure 2.2(c) shows the convergence result using (2.7) with $\alpha = 0.6$ and $T = 0.02$ sec. Note that the conditions in Theorem 2.4.3 are satisfied. It can be seen that coordination is reached with the final equilibrium for $v_i[k]$ being 0.1538, which is equal to $\mathbf{p}^T v[0]$ as argued in Theorem 2.4.3. Figure 2.2(d) shows the convergence result using (2.7) with $\alpha = 0.6$ and $T = 0.5$ sec. Note that coordination is not reached in this case.

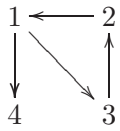

Fig. 2.1: Directed graph $\mathcal{G}$ for four vehicles. An arrow from j to i denotes that vehicle i can receive information from vehicle j.

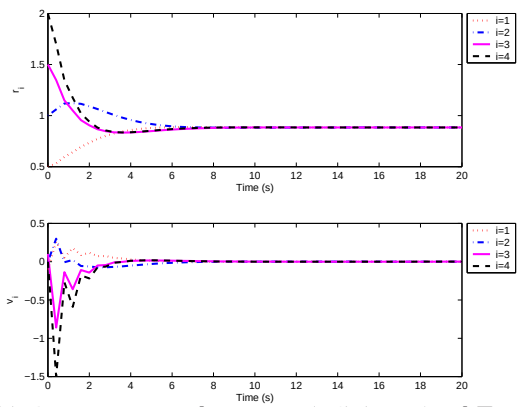

(a) Convergence resulting using (2.6) ($\alpha = 4$ and $T = 0.4$ sec).

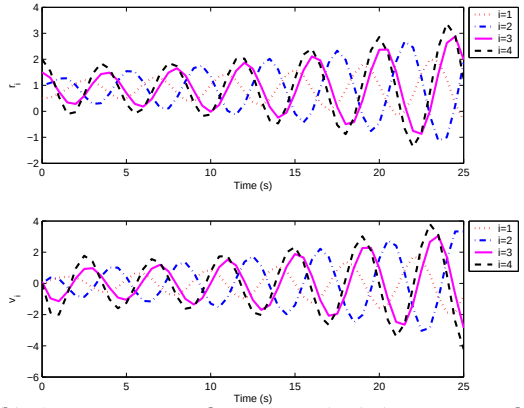

(b) Convergence resulting using (2.6) ($\alpha = 1.2$ and $T = 0.5$ sec).

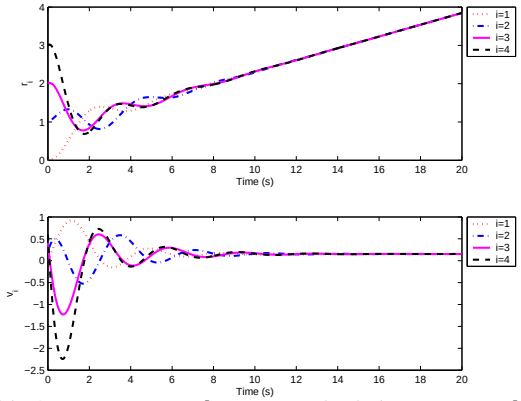

(c) Convergence resulting using (2.7) ($\alpha = 0.6$ and $T = 0.02$ sec).

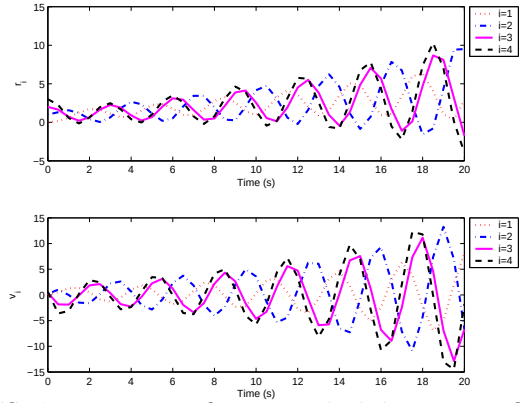

(d) Convergence resulting using (2.7) ($\alpha = 0.6$ and $T = 0.5$ sec).

Fig. 2.2: Convergence results using (2.6) and (2.7) with different α and T values. Note that coordination is reached in (a) and (c) but not in (b) and (d) depending on different choices of α and T.

2.4 Dynamic Interaction Case

In this section, we assume that the network topology switches at each sampling point and remains constant at each sampling period. Let directed graph $\mathcal{G}_k$ denote the interaction graph for the n vehicles for $t \in [kT; (k+1)T), k = 0, 1, \cdots$. We use $\mathcal{A}_k$ to represent the corresponding

adjacency matrix associated with $\mathcal{G}_k$.

2.4.1 Convergence Analysis of Sampled-data Algorithm with Absolute Damping under Dynamic Directed Interaction

In this section, we show sufficient conditions on α, T, and directed graph $\mathcal{G}_k$ such that coordination is achieved using (2.6) under dynamic directed interaction.

Using (2.6), (2.5) can be written in matrix form as

$$\begin{bmatrix} \tilde{r}[k+1] \\ v[k+1] \end{bmatrix} = \underbrace{\begin{bmatrix} I_n - \frac{T^2}{2}\mathcal{L}_k & (T - \frac{\alpha T^2}{2})I_n \\ -T\mathcal{L}_k & (1-\alpha T)I_n \end{bmatrix}}_{F_k} \begin{bmatrix} \tilde{r}[k] \\ v[k] \end{bmatrix}, \tag{2.34}$$

where $\tilde{r} = [\tilde{r}_1, \ldots, \tilde{r}_n]^T$ with $\tilde{r}_i = r_i - \delta_i$, $v = [v_1, \ldots, v_n]^T$, and $\mathcal{L}_k$ is the (nonsymmetric) Laplacian matrix associated with $\mathcal{A}_k$ for $t \in [kT, (k+1)T)$. Note that the solution of (2.34) can be written as

$$\begin{bmatrix} \tilde{r}[k+1] \\ v[k+1] \end{bmatrix} = \begin{bmatrix} B_k & C_k \\ D_k & E_k \end{bmatrix} \begin{bmatrix} \tilde{r}[0] \\ v[0] \end{bmatrix}, \tag{2.35}$$

where $\begin{bmatrix} B_k & C_k \\ D_k & E_k \end{bmatrix} \triangleq F_k F_{k-1} \cdots F_0$. Therefore, B_k, C_k, D_k, and E_k satisfy

$$\begin{bmatrix} B_k \\ D_k \end{bmatrix} = \begin{bmatrix} I_n - \frac{T^2}{2}\mathcal{L}_k & (T - \frac{\alpha T^2}{2})I_n \\ -T\mathcal{L}_k & (1-\alpha T)I_n \end{bmatrix} \begin{bmatrix} B_{k-1} \\ D_{k-1} \end{bmatrix}, \tag{2.36}$$

and

$$\begin{bmatrix} C_k \\ E_k \end{bmatrix} = \begin{bmatrix} I_n - \frac{T^2}{2}\mathcal{L}_k & (T - \frac{\alpha T^2}{2})I_n \\ -T\mathcal{L}_k & (1-\alpha T)I_n \end{bmatrix} \begin{bmatrix} C_{k-1} \\ E_{k-1} \end{bmatrix}. \tag{2.37}$$

Lemma 2.4.1 *Assume that $\alpha T \neq 2$. Using* (2.6) *for* (2.5), $r_i[k] - r_j[k] \to \Delta_{ij}$ *and* $v_i[k] \to 0$ *as* $k \to \infty$ *if* $\lim_{k\to\infty} B_k$ *exists and all rows of* $\lim_{k\to\infty} B_k$ *are the same for any initial matrices* B_0 *and* D_0.

Proof: When $\lim_{k\to\infty} B_k$ exists and all rows of $\lim_{k\to\infty} B_k$ are the same for any initial matrices B_0 and D_0, it follows that $\lim_{k\to\infty} C_k$ exists and all rows of $\lim_{k\to\infty} C_k$ are the same for any initial matrices C_0 and E_0 as well because (2.36) and (2.37) have the same structure. It then follows from (2.36) that

$$B_k = B_{k-1} - \frac{T^2}{2}\mathcal{L}_k B_{k-1} + (T - \frac{\alpha T^2}{2})D_{k-1}.$$

Because $\mathcal{L}_k \mathbf{1}_n = \mathbf{0}_{n\times 1}$ and all rows of $\lim_{k\to\infty} B_{k-1}$ are the same, it follows that $\lim_{k\to\infty} \mathcal{L}_k B_{k-1} = \mathbf{0}_{n\times n}$. It thus follows that

$$\lim_{k\to\infty} (T - \frac{\alpha T^2}{2})D_{k-1} = \lim_{k\to\infty} (B_k - B_{k-1}) = \mathbf{0}_{n\times n}.$$

Because $\alpha T \neq 2$, i.e., $T - \frac{\alpha T^2}{2} \neq 0$, it follows that $\lim_{k\to\infty} D_k = \mathbf{0}_{n\times n}$ for any initial matrices B_0 and D_0. Similarly, it follows that $\lim_{k\to\infty} E_k = \mathbf{0}_{n\times n}$ for any initial matrices C_0 and E_0 because (2.36) and (2.37) have the same structure. Combining the previous arguments with (2.35) shows that $\tilde{r}_i[k] \to \tilde{r}_j[k]$ and $v_i[k] \to 0$ as $k \to \infty$, which implies that $r_i[k] - r_j[k] \to \Delta_{ij}$ and $v_i[k] \to 0$ as $k \to \infty$. ■

We next study the conditions on α, T, and the directed graph $\mathcal{G}_k$ such that all rows of $\lim_{k\to\infty} B_k$ are the same for any initial matrices B_0 and D_0. Before moving on, we need the following lemmas and corollary.

Lemma 2.4.2 [36] *Let $m \geq 2$ be a positive integer and let $P_1, P_2, \cdots, P_m$ be nonnegative $n \times n$ matrices with positive diagonal entries, then $P_1 P_2 \cdots P_m \geq \gamma(P_1 + P_2 + \cdots + P_m$, where $\gamma > 0$ can be specified from matrices $P_i, i = 1, \cdots, m$.*

Lemma 2.4.3 *Assume that the directed graph of a row stochastic matrix $A \in \mathbb{R}^{n\times n}$ has a directed spanning tree. Then the directed graph of $\begin{bmatrix} A & A \\ A & A \end{bmatrix}$ also has a directed spanning tree.*

Proof: Note that $\frac{1}{2}\begin{bmatrix} A & A \\ A & A \end{bmatrix}$ can be written as

$$\frac{1}{2}\begin{bmatrix} A & A \\ A & A \end{bmatrix} = \begin{bmatrix} \frac{1}{2} & \frac{1}{2} \\ \frac{1}{2} & \frac{1}{2} \end{bmatrix} \otimes A,$$

where $\otimes$ denotes the Kronecker product. It can be computed that the eigenvalues of $\begin{bmatrix} \frac{1}{2} & \frac{1}{2} \\ \frac{1}{2} & \frac{1}{2} \end{bmatrix}$ are 0 and 1. Assume that the eigenvalues of A are $\lambda_1, \cdots, \lambda_n$. It follows that the eigenvalues of $\frac{1}{2}\begin{bmatrix} A & A \\ A & A \end{bmatrix}$ are $0, \lambda_1, \cdots, 0, \lambda_n$ by using the properties of the Kronecker product. Because the directed graph of A has a directed spanning tree, it follows from Corollary 3.5 [39] that A has one simple eigenvalue equal to one, which implies that $\frac{1}{2}\begin{bmatrix} A & A \\ A & A \end{bmatrix}$ also has one simple eigenvalue equal to one. Because $\frac{1}{2}\begin{bmatrix} A & A \\ A & A \end{bmatrix}$ is a row stochastic matrix, it then follows from Corollary 3.5 [39] that the directed graph of $\frac{1}{2}\begin{bmatrix} A & A \\ A & A \end{bmatrix}$ has a directed spanning tree, which in turn implies that the directed graph of $\begin{bmatrix} A & A \\ A & A \end{bmatrix}$ also has a directed spanning tree. ■

Corollary 2.4.1 *Assume that every row of a nonnegative matrix $A \in \mathbb{R}^{n\times n}$ has the same sum. If the directed graph of A has a directed spanning tree, the directed graph of $\begin{bmatrix} A & A \\ A & A \end{bmatrix}$ also has a directed spanning tree.*

Lemma 2.4.4 *Suppose that $A \in \mathbb{R}^{n\times n}$ is a row stochastic matrix with positive diagonal entries. If the directed graph of A has a directed spanning tree, then A is SIA.*

Proof: See Corollary 3.5 and Lemma 3.7 [39]. ■

Lemma 2.4.5 [90] *Let $S_1, S_2, \cdots, S_k \in \mathbb{R}^{n\times n}$ be a finite set of SIA matrices with the property that for each sequence $S_{i_1}, S_{i_2}, \cdots, S_{i_j}$ of positive length, the matrix product $S_{i_j} S_{i_{j-1}} \cdots S_{i_1}$ is SIA. Then, for each infinite sequence $S_{i_1}, S_{i_2}, \cdots$, there exists a column vector y such that*

$$\lim_{j\to\infty} S_{i_j} S_{i_{j-1}} \cdots S_{i_1} = \mathbf{1}_n y^T.$$

Based on the previous lemmas and corollary, we have the following lemma regarding the conditions on α, T and the directed graph $\mathcal{G}_k$ such that all rows of $\lim_{k\to\infty} B_k$ are the same.

Lemma 2.4.6 *Let $\Phi_{k1} = (2-\alpha T)I_n - \frac{T^2}{2}\mathcal{L}_k$ and $\Phi_{k2} = (\alpha T - 1)I_n - \frac{T^2}{2}\mathcal{L}_{k-1}$, where $\mathcal{L}_k, k = 0, 1, \cdots$, are the (nonsymmetric) Laplacian matrices associated with $\mathcal{A}_k$ for $t \in [kT, (k+1)T)$. There exist positive α and T such that both Φ_{k1} and Φ_{k2} are nonnegative matrices with positive diagonal entries. If positive α and T are chosen such that both Φ_{k1} and Φ_{k2} are nonnegative with positive diagonal entries, and there exists a positive integer κ such that for any nonnegative integer k_0, the union of $\mathcal{G}_k$ across $k \in [k_0, k_0+\kappa]$ has a directed spanning tree, the iteration*

$$B_k = \Phi_{k1} B_{k-1} + \Phi_{k2} B_{k-2} \tag{2.38}$$

is stable for any initial matrices B_0 and B_1 and all rows of $\lim_{k\to\infty} B_k$ are the same.

Proof: For the first statement, consider $\alpha T = \frac{3}{2}$. It follows that if $T^2 < \min_i \frac{1}{\ell_{ii}[k]}, k = 0, 1, \cdots$, where $\ell_{ii}[k]$ is the ith diagonal entry of $\mathcal{L}_k$, then both Φ_{k1} and Φ_{k2} are nonnegative matrices with positive diagonal entries.

For the second statement, rewrite (2.38) as

$$\begin{bmatrix} B_k \\ B_{k-1} \end{bmatrix} = \underbrace{\begin{bmatrix} \Phi_{k1} & \Phi_{k2} \\ I_n & \mathbf{0}_{n\times n} \end{bmatrix}}_{H_k} \begin{bmatrix} B_{k-1} \\ B_{k-2} \end{bmatrix}. \tag{2.39}$$

When positive α and T are chosen such that both Φ_{k1} and Φ_{k2} are nonnegative matrices with positive diagonal entries, it follows that H_k is a row stochastic matrix. It then follows that $H_{k+1}H_k =$

$\begin{bmatrix} \Phi_{(k+1)1}\Phi_{k1} + \Phi_{(k+1)2} & \Phi_{(k+1)1}\Phi_{k2} \\ \Phi_{k1} & \Phi_{k2} \end{bmatrix}$ is also a row stochastic matrix because the product of row stochastic matrices is also a row stochastic matrix. In addition, the diagonal entries of $H_{k+1}H_k$ are positive because both Φ_{k1} and Φ_{k2} are nonnegative matrices with positive diagonal entries. Similarly, for any positive integer m and nonnegative integer ℓ_0, matrix product $H_{m+\ell_0} \cdots H_{\ell_0}$ is also a row stochastic matrix with positive diagonal entries. From Lemma 2.4.2, we have that

$$\begin{aligned} & H_{k+1}H_k \\ & \geq \begin{bmatrix} \gamma_1(\Phi_{(k+1)1} + \Phi_{k1}) + \Phi_{(k+1)2} & \gamma_2(\Phi_{(k+1)1} + \Phi_{k2}) \\ \Phi_{k1} & \Phi_{k2} \end{bmatrix} \\ & \geq \gamma \begin{bmatrix} \Phi_{(k+1)1} + \Phi_{k1} + \Phi_{(k+1)2} & \Phi_{(k+1)1} + \Phi_{k2} \\ \Phi_{k1} & \Phi_{k2} \end{bmatrix} \end{aligned}$$

for some positive γ that is determined by γ_1, γ_2, Φ_{k1}, Φ_{k2}, $\Phi_{(k+1)1}$, and $\Phi_{(k+1)2}$, where γ_1 is determined by $\Phi_{(k+1)1}$ and Φ_{k1}, and γ_2 is determined by $\Phi_{(k+1)1}$ and Φ_{k2}. Note also that the directed graph of Φ_{k1} is the same as that of $\Phi_{(k+1)2}$. We can thus replace Φ_{k1} with $\Phi_{(k+1)2}$ without changing the directed graph of H_k and vice versa. Therefore, it follows that $H_{k+1}H_k \geq \hat{\gamma} \begin{bmatrix} \Phi_{(k+1)1} + \Phi_{k1} & \Phi_{(k+1)1} + \Phi_{(k-1)1} \\ \Phi_{k1} & \Phi_{(k-1)1} \end{bmatrix}$ for some positive $\hat{\gamma}$ that is determined by Φ_{k1}, Φ_{k2}, $\Phi_{(k+1)1}$, $\Phi_{(k+1)2}$, and γ. Similarly, $H_{m+\ell_0} \cdots H_{\ell_0}$ can also be written as

$$\begin{aligned} H_{\ell_0+m} \cdots H_{\ell_0} & \geq \tilde{\gamma} \begin{bmatrix} \sum_{i=\ell_0}^{\ell_0+m} \Phi_{i1} & \sum_{i=\ell_0+1}^{\ell_0+m} \Phi_{i1} + \Phi_{(\ell_0-1)1} \\ \sum_{i=\ell_0}^{\ell_0+m-1} \Phi_{i1} & \sum_{i=\ell_0+1}^{\ell_0+m-1} \Phi_{i1} + \Phi_{(\ell_0-1)1} \end{bmatrix} \\ & \geq \tilde{\gamma} \begin{bmatrix} \sum_{i=\ell_0+1}^{\ell_0+m-1} \Phi_{i1} & \sum_{i=\ell_0+1}^{\ell_0+m-1} \Phi_{i1} \\ \sum_{i=\ell_0+1}^{\ell_0+m-1} \Phi_{i1} & \sum_{i=\ell_0+1}^{\ell_0+m-1} \Phi_{i1} \end{bmatrix} \end{aligned} \tag{2.40}$$

for some positive $\tilde{\gamma}$.

Because there exists a positive integer κ such that for any nonnegative integer k_0, the union of $\mathcal{G}_k$ across $k \in [k_0, k_0 + \kappa]$ has a directed spanning tree, it follows that the directed graph of

$\sum_{i=k_0}^{k_0+\kappa}\Phi_{i1}$ also has a directed spanning tree. It thus follows from (2.40) and Corollary 2.4.1 that the directed graph of $H_{k_0+\kappa+1}\cdots H_{k_0-1}$ also has a directed spanning tree because $H_{k_0+\kappa+1}\cdots H_{k_0-1}\geq \tilde{\gamma}\begin{bmatrix}\sum_{i=k_0}^{k_0+\kappa}\Phi_{i1} & \sum_{i=k_0}^{k_0+\kappa}\Phi_{i1}\\ \sum_{i=k_0}^{k_0+\kappa}\Phi_{i1} & \sum_{i=k_0}^{k_0+\kappa}\Phi_{i1}\end{bmatrix}$. Because $H_{k_0+\kappa+1}\cdots H_{k_0-1}$ is a row stochastic matrix with positive diagonal entries and the directed graph of $H_{k_0+\kappa+1}\cdots H_{k_0-1}$ has a directed spanning tree, it follows from Lemma 2.4.4 that $H_{k_0+\kappa+1}\cdots H_{k_0-1}$ is SIA. It then follows from Lemma 2.4.5 that $\lim_{k\to\infty}H_k\cdots H_0=\mathbf{1}_{2n}y^T$ for some column vector $y\in\mathbb{R}^{2n}$. Therefore, it follows from (2.39) that $\lim_{k\to\infty}B_k$ exists and all rows of $\lim_{k\to\infty}B_k$ are the same. ■

Theorem 2.4.2 *Assume that there exists a positive integer κ such that for any nonnegative integer k_0, the union of $\mathcal{G}_k$ across $k\in[k_0,k_0+\kappa]$ has a directed spanning tree. Let $\Phi_{k1}=(2-\alpha T)I_n-\frac{T^2}{2}\mathcal{L}_k$ and $\Phi_{k2}=(\alpha T-1)I_n-\frac{T^2}{2}\mathcal{L}_{k-1}$, where $\mathcal{L}_k, k=0,1,\cdots$, are (nonsymmetric) Laplacian matrices associated with $\mathcal{A}_k$ for $t\in[kT,(k+1)T)$. If positive α and T are chosen such that both Φ_{k1} and Φ_{k2} are nonnegative with positive diagonal entries, $r_i[k]-r_j[k]\to\Delta_{ij}$ and $v_i[k]\to 0$ as $k\to\infty$.*

Proof: It follows from (2.36) that

$$B_k=(I_n-\frac{T^2}{2}\mathcal{L}_k)B_{k-1}+(T-\frac{\alpha T^2}{2})D_{k-1}, \tag{2.41}$$

$$B_{k-1}=(I_n-\frac{T^2}{2}\mathcal{L}_{k-1})B_{k-2}+(T-\frac{\alpha T^2}{2})D_{k-2}, \tag{2.42}$$

and

$$D_{k-1}=-T\mathcal{L}_{k-1}B_{k-2}+(1-\alpha T)D_{k-2}. \tag{2.43}$$

Therefore, it follows from (2.41) and (2.42) that

$$\begin{aligned}&B_k-(1-\alpha T)B_{k-1}\\ &=(I_n-\frac{T^2}{2}\mathcal{L}_k)B_{k-1}-(1-\alpha T)(I_n-\frac{T^2}{2}\mathcal{L}_{k-1})B_{k-2}\\ &\quad+(T-\frac{\alpha T^2}{2})[D_{k-1}-(1-\alpha T)D_{k-2}].\end{aligned} \tag{2.44}$$

By substituting (2.43) into (2.44), (2.44) can be simplified as (5.26). It then follows from Lemma 2.4.6 that $\lim_{k\to\infty} B_k$ exists and all rows of $\lim_{k\to\infty} B_k$ are the same under the condition of the theorem. Because Φ_{k1} is nonnegative with positive diagonal entries, it follows that $\alpha T < 2$. It then follows from Lemma 2.4.1 that $r_i[k] - r_j[k] \to \Delta_{ij}$ and $v_i[k] \to 0$ as $k \to \infty$ under the condition of the theorem. ■

2.4.2 Convergence Analysis of Sampled-data Algorithm with Relative Damping under Dynamic Directed Interaction

In this section, we show sufficient conditions on α, T, and directed graph $\mathcal{G}_k$ such that coordination is achieved using (2.7) under dynamic directed interaction.

Using (2.7), (2.5) can be written in matrix form as

$$\begin{bmatrix} \tilde{r}[k+1] \\ v[k+1] \end{bmatrix} = \underbrace{\begin{bmatrix} I_n - \frac{T^2}{2}\mathcal{L}_k & TI_n - \frac{T^2}{2}\mathcal{L}_k \\ -T\mathcal{L}_k & I_n - \alpha T\mathcal{L}_k \end{bmatrix}}_{G_k} \begin{bmatrix} \tilde{r}[k] \\ v[k] \end{bmatrix}, \tag{2.45}$$

where $\tilde{r}$, v, and $\mathcal{L}_k$ are defined as in (2.34). Note that G_k can be written as

$$G_k = \underbrace{\begin{bmatrix} (1-T)I_n - \frac{T^2}{2}\mathcal{L}_k & TI_n - \frac{T^2}{2}\mathcal{L}_k \\ \sqrt{T}I_n - T\mathcal{L}_k & (1-\sqrt{T})I_n - \alpha T\mathcal{L}_k \end{bmatrix}}_{R_k} + \underbrace{\begin{bmatrix} TI_n & \mathbf{0}_{n\times n} \\ -\sqrt{T}I_n & \sqrt{T}I_n \end{bmatrix}}_{S}. \tag{2.46}$$

In the following, we study the property of matrix product $G_k \cdots G_0$ defined as

$$G_k \cdots G_0 \triangleq \begin{bmatrix} \tilde{G}_{k1} & \tilde{G}_{k2} \\ \tilde{G}_{k3} & \tilde{G}_{k4} \end{bmatrix}, \tag{2.47}$$

where $\tilde{G}_{ki} \in \mathbb{R}^{n\times n}, i = 1, 2, 3, 4$.

Lemma 2.4.7 *Assume that directed graph $\mathcal{G}_k, k = 0, 1, \cdots$, has a directed spanning tree. There exist positive α and T such that the following two conditions are satisfied:*

1) $(1-T)I_n - \frac{T^2}{2}\mathcal{L}_k$ and $(1-\sqrt{T})I_n - \alpha T\mathcal{L}_k$, $k = 0, 1, \cdots$, are nonnegative matrices with positive diagonal entries, and $TI_n - \frac{T^2}{2}\mathcal{L}_k$ and $\sqrt{T}I_n - T\mathcal{L}_k$, $k = 0, 1, \cdots$, are nonnegative matrices.

2) $\|S\|_\infty < 1$, where S is defined in (2.46).

In addition, if α and T are chosen such that conditions 1) and 2) are satisfied, matrix product $G_k \cdots G_0$ has the property that all rows of each $\tilde{G}_{ki}, i = 1, 2, 3, 4$, are the same as $k \to \infty$, where $\tilde{G}_{ki}, i = 1, 2, 3, 4$ are defined in (2.47).

Proof: For the first statement, it can be noted that when T is sufficiently small, condition 1) is satisfied. Similarly, when $T < \frac{1}{4}$, it follows that $\|S\| < 1$. Therefore, there exist positive α and T such that conditions 1) and 2) are satisfied.

For the second statement, it is assumed that α and T are chosen such that conditions 1) and 2) are satisfied. It can be computed that $R_k, k = 0, 1, \cdots$, are row stochastic matrices with positive diagonal entries when condition 1) is satisfied. Note that product $G_k \cdots G_0$ can be written as

$$G_k \cdots G_0 = (R_k + S) \cdots (R_0 + S). \tag{2.48}$$

It follows from the binomial expansion that $G_k \cdots G_0 = \sum_{j=1}^{2^{k+1}} \widehat{G_j}$, where $\widehat{G_j}$ is the product of $k+1$ matrices by choosing either R_i or S in $(R_i + S)$ for $i = 0, \cdots, k$. As $k \to \infty$, $\widehat{G_j}$ takes the form of the following three cases:

Case I: $\widehat{G_j}$ is constructed from an infinite number of S and a finite number of R_i as $k \to \infty$. In this case, it follows that as $k \to \infty$, $\left\|\widehat{G_j}\right\|_\infty \leq \|R_{k_0}\|_\infty \|R_{k_1}\|_\infty \cdots \|S\|_\infty^\infty = \|S\|_\infty^\infty = 0$, where we have used the fact that $\|R_{k_i}\|_\infty = 1$ because R_{k_i} is a row stochastic matrix and $\|S\|_\infty < 1$ as shown in condition 2). Therefore $\widehat{G_j}$ approaches $\mathbf{0}_{2n\times 2n}$ as $k \to \infty$.

Case II: $\widehat{G_j}$ is constructed from an infinite number of S and an infinite number of R_i as $k \to \infty$. A similar analysis to that in Case I shows that $\widehat{G_j}$ approaches $\mathbf{0}_{2n\times 2n}$ as $k \to \infty$.

Case III: $\widehat{G_j}$ is constructed from a finite number of S and an infinite number of R_i as $k \to \infty$. In

this case, as $k \to \infty$, $\widehat{G_j}$ can be written as

$$\widehat{G_j} = M \underbrace{\prod_j R_{k_j}}_{J} N,$$

where both M and N are the product of a finite number of matrices by choosing either $R_i, i \neq k_j, j = 0, 1, \cdots$, or S from $(R_i + S)$ and J is the product of an infinite number of R_{k_j}.[5] Note that the directed graph of R_k is the same as that of $\begin{bmatrix} (1-T)I_n - \frac{T^2}{2}\mathcal{L}_k & (1-T)I_n - \frac{T^2}{2}\mathcal{L}_k \\ (1-T)I_n - \frac{T^2}{2}\mathcal{L}_k & (1-T)I_n - \frac{T^2}{2}\mathcal{L}_k \end{bmatrix}$ because the directed graphs of all four matrices in condition 1) are the same. It then follows from Corollary 2.4.1 that $\begin{bmatrix} (1-T)I_n - \frac{T^2}{2}\mathcal{L}_k & (1-T)I_n - \frac{T^2}{2}\mathcal{L}_k \\ (1-T)I_n - \frac{T^2}{2}\mathcal{L}_k & (1-T)I_n - \frac{T^2}{2}\mathcal{L}_k \end{bmatrix}$ has a directed spanning tree if the directed graph of $(1-T)I_n - \frac{T^2}{2}\mathcal{L}_k$, i.e., directed graph $\mathcal{G}_k$, has a directed spanning tree. Therefore, the directed graph of R_k also has a directed spanning tree. Also note that $R_k, k = 0, 1, \cdots$, are row stochastic matrices with positive diagonal entries. It then follows from Lemma 2.4.4 that R_{k_j} is SIA. Therefore, it follows from Lemma 2.4.5 that all rows of J are the same as $k \to \infty$. By writing

$$J = \begin{bmatrix} J_1 & J_2 \\ J_3 & J_4 \end{bmatrix}, \tag{2.49}$$

where $J_i \in \mathbb{R}^{n \times n}, i = 1, 2, 3, 4$, it follows from the fact that all rows of J are the same that all rows of $J_i, i = 1, 2, 3, 4$, are also the same. It then follows that

$$\begin{aligned} R_i J &= \begin{bmatrix} (1-T)I_n - \frac{T^2}{2}\mathcal{L}_i & TI_n - \frac{T^2}{2}\mathcal{L}_i \\ \sqrt{T}I_n - T\mathcal{L}_i & (1-\sqrt{T})I_n - \alpha T\mathcal{L}_i \end{bmatrix} J \\ &= \begin{bmatrix} (1-T)I_n & TI_n \\ \sqrt{T}I_n & (1-\sqrt{T})I_n \end{bmatrix} J, \end{aligned}$$

where we have used the fact that $\mathcal{L}_i J_i = \mathbf{0}_{n \times n}, i = 1, 2, 3, 4$. By separating $R_i J$ into four $n \times n$ submatrices as that of J in (2.49), all rows of every one of the four $n \times n$ submatrices are the same.

[5] Here M and N are I_{2n} if neither R_i nor S is chosen.

The same property also applies to matrix products JR_i, SJ, and JS. A similar analysis shows that the same property also holds for matrix product formed by pre-multiplying or post-multiplying J by a finite number of R_i and/or S. Therefore, by separating $\widehat{G_j}$ into four $n \times n$ submatrices as that of J in (2.49), it follows that all rows of every one of the four $n \times n$ submatrices are the same. Combining the previous arguments shows that as $k \to \infty$, all rows of $\tilde{G}_{ki}, i = 1, 2, 3, 4$, are the same. ■

Theorem 2.4.3 *Suppose that directed graph $\mathcal{G}_k, k = 0, 1, \cdots$, has a directed spanning tree. Using* (2.7) *for* (2.5), *$r_i[k] - r_j[k] \to \Delta_{ij}[k]$ and $v_i[k] \to v_j[k]$ as $k \to \infty$ when positive α and T are chosen such that conditions $1)$ and $2)$ in Lemma 2.4.7 are satisfied.*

Proof: Note that the solution of (2.45) can be written as

$$\begin{bmatrix} \tilde{r}[k+1] \\ v[k+1] \end{bmatrix} = G_k \cdots G_0 \begin{bmatrix} \tilde{r}[0] \\ v[0] \end{bmatrix}. \tag{2.50}$$

When directed graph $\mathcal{G}_k, k = 0, 1, \cdots$, has a directed spanning tree, and conditions $1)$ and $2)$ in Lemma 2.4.7 are satisfied, it follows that all rows of $\tilde{G}_{ki}, i = 1, 2, 3, 4$, are the same as $k \to \infty$, where $\tilde{G}_{ki}, i = 1, 2, 3, 4$, are defined in (2.47). Combining with (2.50) shows that $\tilde{r}_i[k] \to \tilde{r}_j[k]$ and $v_i[k] \to v_j[k]$ as $k \to \infty$, which implies that $r_i[k] - r_j[k] \to \Delta_{ij}$ and $v_i[k] \to v_j[k]$ as $k \to \infty$. ■

Remark 2.4.4 *Note that Theorem 2.4.2 requires that the communication graph has a directed spanning tree jointly to guarantee coordination while Theorem 2.4.3 requires that the communication graph has a directed spanning tree at each time interval to guarantee coordination. The different connectivity requirement for Theorems 2.4.2 and 2.4.3 is caused by different damping terms. For the coordination algorithm with an absolute damping term, when the damping gain and the sampling period are chosen properly, all vehicles always have a zero final velocity disregard of the communication graph. However, for the coordination algorithm with a relative damping term, the vehicles in general do not have a zero final velocity. From this point of view, it is not surprising to see that the connectivity requirement in Theorem 2.4.3 corresponding to the relative damping case is more stringent than that in Theorem 2.4.2 corresponding to the absolute damping case.*

Remark 2.4.5 *In Theorem 2.4.2 (respectively, Theorem 2.4.3), it is assumed that the sampling period is uniform. When the sampling periods are nonuniform, we can always find corresponding damping gains such that the conditions in Theorem 2.4.2 (respectively, Theorem 2.4.3) are satisfied. Therefore, similar results can be obtained in the presence of nonuniform sampling periods if the conditions in Theorem 2.4.2 (respectively, Theorem 2.4.3) are satisfied.*

2.4.3 Simulation

In this section, we present simulation results to illustrate the theoretical results derived in Sections 2.4.1 and 2.4.2. For both coordination algorithms (2.6) and (2.7), we consider a team of four vehicles. Here for simplicity, we have chosen $\delta_i = 0, i = 1, \cdots, 4$.

For coordination algorithm (2.6), let $r[0] = [0.5, 1, 1.5, 2]^T$ and $v[0] = [-1, 0, 1, 0]^T$. The interaction graph switches from a set $\{\mathcal{G}_{(1)}, \mathcal{G}_{(2)}, \mathcal{G}_{(3)}\}$ as shown in Fig. 2.3 with the corresponding (nonsymmetric) Laplacian matrices chosen as

$$\mathcal{L}_{(1)} = \begin{bmatrix} 1 & -1 & 0 & 0 \\ 0 & 0 & 0 & 0 \\ 0 & 0 & 0 & 0 \\ 0 & 0 & 0 & 0 \end{bmatrix},$$

$$\mathcal{L}_{(2)} = \begin{bmatrix} 0 & 0 & 0 & 0 \\ 0 & 1 & -1 & 0 \\ 0 & 0 & 0 & 0 \\ 0 & 0 & 0 & 0 \end{bmatrix},$$

and

$$\mathcal{L}_{(3)} = \begin{bmatrix} 0 & 0 & 0 & 0 \\ 0 & 0 & 0 & 0 \\ 0 & 0 & 1 & -1 \\ -1 & 0 & 0 & 1 \end{bmatrix}.$$

From subfigure (d) in Fig 2.3, it can be noted that the union of $\mathcal{G}_{(1)}$, $\mathcal{G}_{(2)}$, and $\mathcal{G}_{(3)}$ has a directed

spanning tree. We choose sampling period $T = 0.2$ sec and $\alpha = 6$. It can be computed that the condition in Theorem 2.4.2 is satisfied. Figs. 2.4(a) and 2.4(b) show, respectively, the positions and velocities of the four vehicles using (2.6) when the interaction graph switches from $\mathcal{G}_{(1)}$ to $\mathcal{G}_{(2)}$ and then to $\mathcal{G}_{(3)}$ every T sec. The same process then repeats. It can be seen that coordination is achieved on positions with a zero final velocity as urged in Theorem 2.4.2. Note that the velocities of the four vehicles demonstrate large oscillation as shown in Fig. 2.4(b) because the interaction graph does not have a directed spanning tree at each time interval and switches very fast.

For coordination algorithm (2.7), let $r[0] = [0.5, 1, 1.5, 2]^T$ and $v[0] = [-1, 0, 1, 0]^T$. The interaction graph switches from a set $\{\mathcal{G}_{(4)}, \mathcal{G}_{(5)}, \mathcal{G}_{(6)}\}$ as shown in Fig. 2.5 with the corresponding (nonsymmetric) Laplacian matrices chosen as

$$\mathcal{L}_{(4)} = \begin{bmatrix} 1 & -1 & 0 & 0 \\ 0 & 1 & -1 & 0 \\ 0 & -1 & 1 & 0 \\ -1 & 0 & 0 & 1 \end{bmatrix},$$

$$\mathcal{L}_{(5)} = \begin{bmatrix} 2 & -1 & -1 & 0 \\ -1 & 1 & 0 & 0 \\ -1 & 0 & 2 & -1 \\ -1 & -1 & 0 & 2 \end{bmatrix},$$

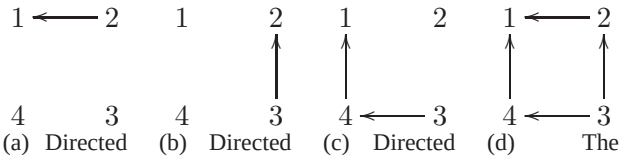

(a) Directed graph $\mathcal{G}_{(1)}$. (b) Directed graph $\mathcal{G}_{(2)}$. (c) Directed graph $\mathcal{G}_{(3)}$. (d) The union of $\mathcal{G}_{(1)}, \mathcal{G}_{(2)}, \mathcal{G}_{(3)}$.

Fig. 2.3: Interaction graphs for four vehicles. An arrow from j to i denotes that vehicle i can receive information from vehicle j.

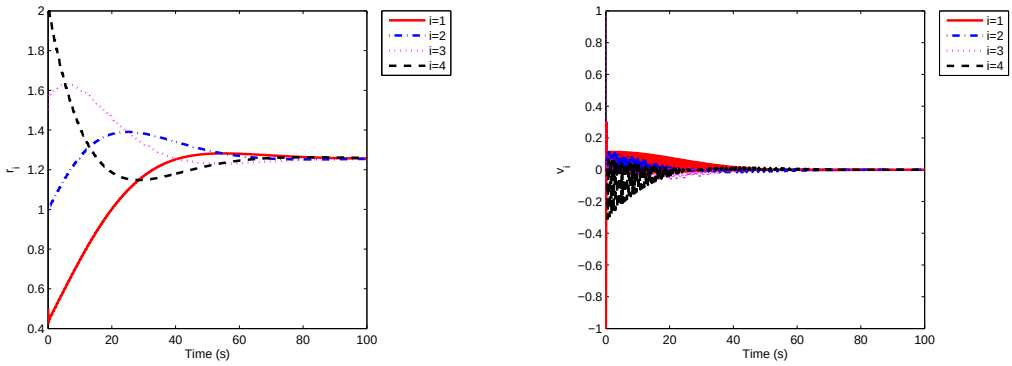

(a) Positions. (b) Velocities.

Fig. 2.4: Convergence results using (2.6) with a switching interaction.

and

$$\mathcal{L}_{(6)} = \begin{bmatrix} 1 & -1 & 0 & 0 \\ -1 & 2 & -1 & 0 \\ 0 & 0 & 1 & -1 \\ 0 & -1 & 0 & 1 \end{bmatrix}.$$

Note that directed graphs $\mathcal{G}_{(i)}, i = 4, 5, 6$, all have a directed spanning tree. We choose sampling period $T = 0.1$ sec and $\alpha = 1$. It can be computed that the condition in Theorem 2.4.3 is satisfied. Figs. 2.6(a) and 2.6(b) show, respectively, the positions and velocities of the four vehicles using (2.7) when the interaction graph switches from $\mathcal{G}_{(4)}$ to $\mathcal{G}_{(5)}$ and then to $\mathcal{G}_{(6)}$ every T sec. The same process then repeats. It can be seen that coordination is achieved on positions with a constant final velocity as urged in Theorem 2.4.3.

We also show an example to illustrate that using (2.7) for (2.5), coordination is not necessarily achieved even if the interaction graph has a directed spanning tree jointly, and α and T satisfy

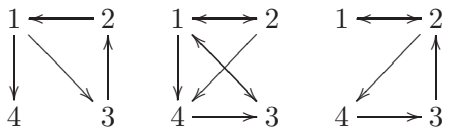

(a) Directed graph $\mathcal{G}_{(4)}$. (b) Directed graph $\mathcal{G}_{(5)}$. (c) Directed graph $\mathcal{G}_{(6)}$.

Fig. 2.5: Interaction graphs for four vehicles. An arrow from j to i denotes that vehicle i can receive information from vehicle j.

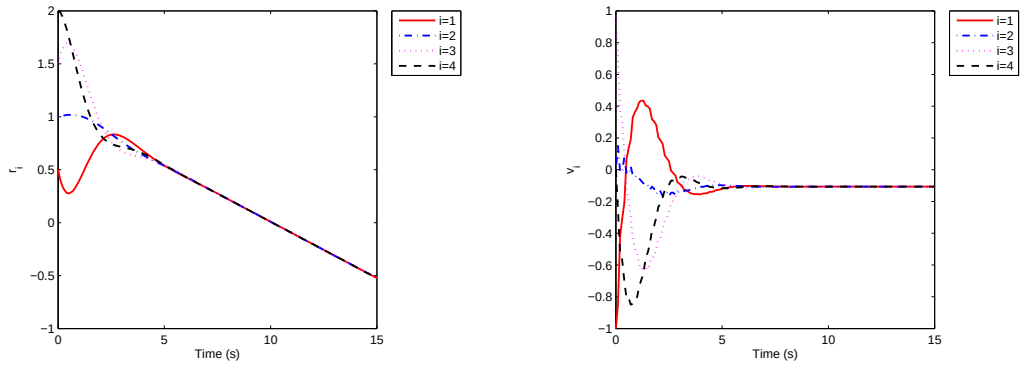

(a) Positions. (b) Velocities.

Fig. 2.6: Convergence results using (2.7) with $\alpha = 1$, $T = 0.1$ sec, and the interaction graph switches from a set $\{\mathcal{G}_{(4)}, \mathcal{G}_{(5)}, \mathcal{G}_{(6)}\}$.

conditions 1) and 2) in Lemma 2.4.7. The initial positions and velocities, α, and T are chosen to be the same as those for Figs. 2.6(a) and 2.6(b). Figs. 2.7(a) and 2.7(b) show, respectively, the positions and velocities of the four vehicles using (2.7) when the interaction graph switches from $\mathcal{G}_{(1)}$ to $\mathcal{G}_{(2)}$ then to $\mathcal{G}_{(3)}$ every T sec. The same process then repeats. It can be seen that coordination is not achieved even when the interaction graph has a directed spanning tree jointly and α and T satisfy conditions 1) and 2) in Lemma 2.4.7.

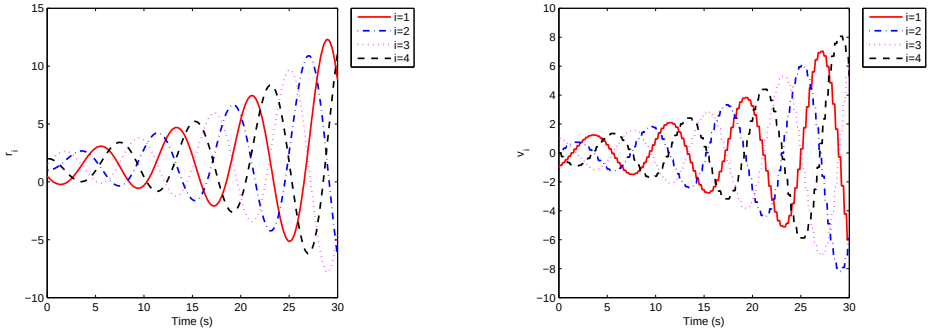

(a) Positions. (b) Velocities.

Fig. 2.7: Convergence results using (2.7) with $\alpha = 1$, $T = 0.1$ sec, and the interaction graph switches from a set $\{\mathcal{G}_{(1)}, \mathcal{G}_{(2)}, \mathcal{G}_{(3)}\}$.

Chapter 3

Decentralized Coordination Algorithms with a Group Reference State

In Chapter 2, we studied decentralized coordination algorithms without a group reference state. Although the study of decentralized coordination in the absence of any group reference state is interesting, it is of great importance to study decentralized coordination algorithms in the presence of a group reference which usually represents the interest of the group. In this chapter, we focus on the study of decentralized coordination algorithms with a group reference state. The unique group reference state is also called "leader." Decentralized coordination with a group reference state is also called "coordinated tracking." When the leader's state is constant, the leader can be considered one agent which has no local neighbors. Therefore, the decentralized coordination problem is a special case of decentralized coordination without a group reference state. In the following, we assume that the group references is time-varying for generality. The existing literature [67–69, 72, 73] focuses on the study of coordinated tracking algorithms for continuous-time systems requiring the availability of the velocity and/or acceleration measurements or the design of distributed observers. In this following, we will study three problems in this chapter: decentralized consensus tracking, decentralized swarm tracking, and PD-like (proportional and derivative like) consensus tracking. In particular, the first two problems are studied in a continuous-time setting. Compared with the aforementioned references, the proposed approaches require milder condition on the information transmission between the leader and the followers and less information from the leader and/or the followers. The last is investigated in a discrete-time setting and the proposed algorithms can be easily implemented in real systems.

3.1 Continuous-time Setting

In this section, we will study decentralized coordinated tracking, including consensus tracking

and swarm tracking, in a continuous-time setting. Both single-integrator kinematics and double-integrator dynamics will be considered accordingly.

3.1.1 Decentralized Coordinated Tracking for Single-integrator Kinematics

In this section, we study decentralized coordinated tracking for first-order kinematics. Suppose that in addition to the n vehicles, labeled as vehicles 1 to n, called *followers* hereafter, there exists a virtual leader, labeled as vehicle 0, with a (time-varying) position r_0 and velocity $\dot{r}_0$. We assume that $|\dot{r}_0| \leq \gamma_\ell$, where γ_ℓ is a positive constant.

Consider followers with first-order kinematics given by

$$\dot{r}_i = u_i, \quad i = 1, \ldots, n, \tag{3.1}$$

where $r_i \in \mathbb{R}$ is the position and $u_i \in \mathbb{R}$ is the control input associated with the ith vehicle. Here we have assumed that all vehicles are in a one-dimensional space for the simplicity of presentation. However, all results hereafter are still valid for any high-dimensional case by introduction of the Kronecker product.

Decentralized Consensus Tracking under Fixed and Switching Network Topologies

In this subsection, we design u_i for (3.1) such that all followers track the virtual leader with local interaction in the absence of velocity measurements. We propose the decentralized consensus tracking algorithm for (3.1) as

$$u_i = -\alpha \sum_{j=0}^{n} a_{ij}(r_i - r_j) - \beta \text{sgn}[\sum_{j=0}^{n} a_{ij}(r_i - r_j)], \tag{3.2}$$

where a_{ij}, $i, j = 1, \ldots, n$, is the (i, j)th entry of the adjacency matrix $\mathcal{A}$, a_{i0}, $i = 1, \ldots, n$, is a positive constant if the virtual leader's position is available to follower i and $a_{i0} = 0$, otherwise, α is a nonnegative constant, β is a positive constant, and $\text{sgn}(\cdot)$ is the signum function. We first consider the case of a fixed network topology.

Theorem 3.1.1 *Suppose that the fixed undirected graph $\mathcal{G}$ is connected and at least one a_{i0} is nonzero (and hence positive). Using* (3.2) *for* (3.1)*, if $\beta > \gamma_\ell$, then $r_i(t) \to r_0(t)$ in finite time. In particular, $r_i(t) = r_0(t)$ for any $t \geq \bar{t}$, where*

$$\bar{t} = \frac{\sqrt{\tilde{r}^T(0) M \tilde{r}(0)}\sqrt{\lambda_{\max}(M)}}{(\beta - \gamma_\ell)\lambda_{\min}(M)}, \tag{3.3}$$

where $\tilde{r}$ is the column stack vector of $\tilde{r}_i, i = 1, \cdots, n$, with $\tilde{r}_i = r_i - r_0$, $M = \mathcal{L} + diag(a_{10}, \cdots, a_{n0})$ with $\mathcal{L}$ being the Laplacian matrix, and $\lambda_{\min}(\cdot)$ and $\lambda_{\max}(\cdot)$ denote, respectively, the smallest and the largest eigenvalue of a symmetric matrix.

Proof: Noting that $\tilde{r}_i = r_i - r_0$, we can rewrite the closed-loop system of (3.1) using (3.2) as

$$\dot{\tilde{r}}_i = -\alpha \sum_{j=0}^{n} a_{ij}(\tilde{r}_i - \tilde{r}_j) - \beta \text{sgn}[\sum_{j=0}^{n} a_{ij}(\tilde{r}_i - \tilde{r}_j)] - \dot{r}_0. \tag{3.4}$$

Equation (3.4) can be written in matrix form as

$$\dot{\tilde{r}} = -\alpha M \tilde{r} - \beta \text{sgn}(M\tilde{r}) - \mathbf{1}\dot{r}_0,$$

where $\tilde{r}$ and M are defined in (3.3), and $\text{sgn}(\cdot)$ is defined componentwise. Because the fixed undirected graph $\mathcal{G}$ is connected and at least one a_{i0} is nonzero (and hence positive), M is symmetric positive definite.

Consider the Lyapunov function candidate $V = \frac{1}{2}\tilde{r}^T M \tilde{r}$. The derivative of V is

$$\begin{aligned}
\dot{V} &= \tilde{r}^T M[-\alpha M\tilde{r} - \beta \text{sgn}(M\tilde{r}) - \mathbf{1}\dot{r}_0] \\
&\leq -\alpha \tilde{r}^T M^2 \tilde{r} - \beta \left\| M\tilde{r} \right\|_1 + |\dot{r}_0| \left\| M\tilde{r} \right\|_1 \\
&\leq -\alpha \tilde{r}^T M^2 \tilde{r} - (\beta - \gamma_\ell) \left\| M\tilde{r} \right\|_1,
\end{aligned} \tag{3.5}$$

where we have used the Hölder's inequality to obtain the first inequality and $|\dot{r}_0| \leq \gamma_\ell$ to obtain the second inequality. Note that M^2 is symmetric positive definite, α is nonnegative, and $\beta > \gamma_\ell$. Therefore, it follows that $\dot{V}$ is negative definite.

We next show that V will decrease to zero in finite time, i.e., $\tilde{r}_i(t) \to 0$ in finite time. Note that $V \leq \frac{1}{2}\lambda_{\max}(M)\,\|\tilde{r}\|_2^2$. It then follows from (3.5) that the derivative of V satisfies

$$\begin{aligned}
\dot{V} &\leq -(\beta-\gamma_\ell)\,\|M\tilde{r}\|_2 \\
&= -(\beta-\gamma_\ell)\sqrt{\tilde{r}^T M^2 \tilde{r}} \\
&\leq -(\beta-\gamma_\ell)\sqrt{\lambda_{\min}^2(M)\,\|\tilde{r}\|_2^2} \\
&= -(\beta-\gamma_\ell)\lambda_{\min}(M)\,\|\tilde{r}\|_2 \\
&\leq -(\beta-\gamma_\ell)\frac{\sqrt{2}\lambda_{\min}(M)}{\sqrt{\lambda_{\max}(M)}}\sqrt{V}.
\end{aligned}$$

After some manipulation, we can get that

$$2\sqrt{V(t)} \leq 2\sqrt{V(0)} - (\beta-\gamma_\ell)\frac{\sqrt{2}\lambda_{\min}(M)}{\sqrt{\lambda_{\max}(M)}}t.$$

Therefore, we have $V(t) = 0$ when $t \geq \overline{t}$, where $\overline{t}$ is given by (3.3). This completes the proof. ■

Let $\overline{\mathcal{N}}_i \subseteq \{0, 1, \ldots, n\}$ denote the neighbor set of follower i in the team consisting of the n followers and the virtual leader. We next consider the case of a switching network topology by assuming that $j \in \overline{\mathcal{N}}_i(t), i = 1, \cdots, n, j = 0, \cdots, n$, if $|r_i - r_j| \leq R$ at time t and $j \notin \overline{\mathcal{N}}_i(t)$ otherwise, where R denotes the communication/sensing radius of the vehicles. In this case, we consider the decentralized consensus tracking algorithm for (3.1) as

$$u_i = -\alpha \sum_{j \in \overline{\mathcal{N}}_i(t)} b_{ij}(r_i - r_j) - \beta \text{sgn}[\sum_{j \in \overline{\mathcal{N}}_i(t)} b_{ij}(r_i - r_j)], \tag{3.6}$$

where b_{ij}, $i = 1, \ldots, n$, $j = 0, \ldots, n$, are positive constants, and α, β, and sgn$(\cdot)$ are defined as in (3.2).

Theorem 3.1.2 *Suppose that the undirected graph $\mathcal{G}(t)$ is connected and the virtual leader is a neighbor of at least one follower, i.e., $0 \in \overline{\mathcal{N}}_i(t)$ for some i, at each time instant. Using* (3.2) *for* (3.1)*, if $\beta > \gamma_\ell$, then $r_i(t) \to r_0(t)$ as $t \to \infty$.*

Proof: Let $V_{ij} = \frac{1}{2}b_{ij}(r_i - r_j)^2$, $i, j = 1, \ldots, n$, when $|r_i - r_j| \leq R$ and $V_{ij} = \frac{1}{2}b_{ij}R^2$ when

$|r_i - r_j| > R$. Also let $V_{i0} = \frac{1}{2} b_{i0}(r_i - r_0)^2$, $i = 1, \ldots, n$, when $|r_i - r_0| \leq R$ and $V_{i0} = \frac{1}{2} b_{i0} R^2$ when $|r_i - r_0| > R$. Consider the Lyapunov function candidate $V = \frac{1}{2} \sum_{i=1}^{n} \sum_{j=1}^{n} V_{ij} + \sum_{i=1}^{n} V_{i0}$. Note that V is not smooth but is regular. We use differential inclusions [91, 92] and nonsmooth analysis [5, 93] to analyze the stability of (3.1) using (3.6). Therefore, the closed-loop system of (3.1) using (3.6) can be written as

$$\dot{r}_i \in^{a.e.} - K\left[\alpha \sum_{j \in \overline{\mathcal{N}}_i(t)} b_{ij}(r_i - r_j) + \beta \text{sgn}[\sum_{j \in \overline{\mathcal{N}}_i(t)} b_{ij}(r_i - r_j)]\right], \tag{3.7}$$

where $K[\cdot]$ is the differential inclusion [92] and a.e. stands for "almost everywhere."

The generalized derivative of V is given by

$$\begin{aligned}
V^o &= \frac{1}{2} \sum_{i=1}^{n} \sum_{j=1}^{n} b_{ij} \left[\frac{\partial V_{ij}}{\partial r_i} \dot{r}_i + \frac{\partial V_{ij}}{\partial r_j} \dot{r}_j\right] + \sum_{i=1}^{n} b_{i0} \left[\frac{\partial V_{ij}}{\partial r_i} \dot{r}_i + \frac{\partial V_{ij}}{\partial r_0} \dot{r}_0\right] \\
&= \frac{1}{2} \sum_{i=1}^{n} \sum_{j \in \overline{\mathcal{N}}_i(t), j \neq 0} b_{ij} \left[(r_i - r_j)\dot{r}_i + (r_j - r_i)\dot{r}_j\right] + \sum_{0 \in \overline{\mathcal{N}}_i(t)} b_{i0} \left[(r_i - r_0)\dot{r}_i + (r_0 - r_i)\dot{r}_0\right] \\
&= -\alpha \sum_{i=1}^{n} \left[\sum_{j \in \overline{\mathcal{N}}_i(t)} b_{ij}(r_i - r_j)\right]^2 - \beta \sum_{i=1}^{n} \left|\sum_{j \in \overline{\mathcal{N}}_i(t)} b_{ij}(r_i - r_j)\right| + \sum_{0 \in \overline{\mathcal{N}}_i(t)} b_{i0}(r_0 - r_i)\dot{r}_0 \\
&= -\alpha \tilde{r}^T [\hat{M}(t)]^2 \tilde{r} - \beta \left\|\hat{M}(t)\tilde{r}\right\|_1 + \dot{r}_0 \sum_{0 \in \overline{\mathcal{N}}_i(t)} b_{i0}(r_0 - r_i) + \dot{r}_0 \sum_{i=1}^{n} \sum_{j \in \overline{\mathcal{N}}_i(t), j \neq 0} b_{ij}(r_i - r_j)
\end{aligned} \tag{3.8}$$

$$\begin{aligned}
&= -\alpha \tilde{r}^T [\hat{M}(t)]^2 \tilde{r} - \beta \left\|\hat{M}(t)\tilde{r}\right\|_1 + \dot{r}_0 \sum_{i=1}^{n} \sum_{j \in \overline{\mathcal{N}}_i(t)} b_{ij}(r_i - r_j) \\
&\leq -\alpha \tilde{r}^T [\hat{M}(t)]^2 \tilde{r} - \beta \left\|\hat{M}(t)\tilde{r}\right\|_1 + \dot{r}_0 \left\|\hat{M}(t)\tilde{r}\right\|_1 \\
&\leq -\alpha \tilde{r}^T [\hat{M}(t)]^2 \tilde{r} - (\beta - \gamma_\ell) \left\|\hat{M}(t)\tilde{r}\right\|_1,
\end{aligned} \tag{3.9}$$

where we have used the fact $\sum_{i=1}^{n} \sum_{j \in \overline{\mathcal{N}}_i(t), j \neq 0} b_{ij}(r_i - r_j) = 0$ to derive (3.8) and $|\dot{r}_0| \leq \gamma_\ell$ to derive (3.9), $\tilde{r}$ is the column stack vector of $\tilde{r}_i, i = 1, \cdots, n$, with $\tilde{r}_i = r_i - r_0$, and $\hat{M}(t) =$

$[\hat{m}_{ij}(t)] \in \mathbb{R}^{n\times n}$ is defined as

$$\hat{m}_{ij}(t) = \begin{cases} -b_{ij}, & j \in \overline{\mathcal{N}}_i(t),\ j \neq i, \\ 0, & j \notin \overline{\mathcal{N}}_i(t),\ j \neq i, \\ \sum_{k\in\overline{\mathcal{N}}_i(t)} b_{ik}, & j = i. \end{cases} \tag{3.10}$$

Note that $\hat{M}(t)$ is symmetric positive definite at each time instant under the condition of the theorem. Because $\beta > \gamma_\ell$, it then follows that the generalized derivative of V is negative definite under the condition of the theorem, which implies that $V(t) \to 0$ as $t \to \infty$. Therefore, we can get that $r_i(t) \to r_0(t)$ as $t \to \infty$. ■

Remark 3.1.3 *Under the condition of Theorem 3.1.2, decentralized consensus tracking can be achieved in finite time under a switching network topology. However, in contrast to the result in Theorem 3.1.1, it is not easy to explicitly compute the bound of the time, i.e., $\overline{t}$ in Theorem 3.1.1, because the switching pattern of the network topology also plays an important role in determining the bound of the time.*

Decentralized Swarm Tracking under a Switching Network Topology

In this subsection, we extend the decentralized consensus tracking algorithm in Section 3.1.1 to achieve decentralized swarm tracking. The objective here is to design u_i for (3.1) such that all followers move cohesively with the virtual leader while avoiding inter-vehicle collision with local interaction in the absence of velocity measurements. Before moving on, we need to define potential functions which will be used in the decentralized swarm tracking algorithms.

Definition 3.1.4 *The potential function V_{ij} is a differentiable, nonnegative function of $||r_i - r_j||$[1] satisfying the following conditions:*

1) V_{ij} achieves its unique minimum when $||r_i - r_j||$ is equal to its desired value d_{ij}.

2) $V_{ij} \to \infty$ if $||r_i - r_j|| \to 0$.

3) $\frac{\partial V_{ij}}{\partial(\|r_i - r_j\|)} = 0$ if $||r_i - r_j|| > R$, where $R > \max_{i,j} d_{ij}$ is a positive constant.

4) $V_{ii} = c, i = 1, \cdots, n$, where c is a positive constant.

[1] In this definition, r_i can be m-dimensional.

Lemma 3.1.1 *Let V_{ij} be defined in Definition 3.1.4. The following equality holds*

$$\frac{1}{2}\sum_{i=1}^{n}\sum_{j=1}^{n}\left(\frac{\partial V_{ij}}{\partial r_i}\dot{r}_i+\frac{\partial V_{ij}}{\partial r_j}\dot{r}_j\right)=\sum_{i=1}^{n}\sum_{j=1}^{n}\frac{\partial V_{ij}}{\partial r_i}\dot{r}_i.$$

Proof: Note that

$$\begin{aligned}
&\frac{1}{2}\sum_{i=1}^{n}\sum_{j=1}^{n}\left(\frac{\partial V_{ij}}{\partial r_i}\dot{r}_i+\frac{\partial V_{ij}}{\partial r_j}\dot{r}_j\right)\\
=&\frac{1}{2}\sum_{i=1}^{n}\sum_{j=1}^{n}\frac{\partial V_{ij}}{\partial r_i}\dot{r}_i-\frac{1}{2}\sum_{i=1}^{n}\sum_{j=1}^{n}\frac{\partial V_{ij}}{\partial r_i}\dot{r}_j\\
=&\frac{1}{2}\sum_{i=1}^{n}\sum_{j=1}^{n}\frac{\partial V_{ij}}{\partial r_i}\dot{r}_i-\frac{1}{2}\sum_{j=1}^{n}\sum_{i=1}^{n}\frac{\partial V_{ji}}{\partial r_j}\dot{r}_i\\
=&\frac{1}{2}\sum_{i=1}^{n}\sum_{j=1}^{n}\frac{\partial V_{ij}}{\partial r_i}\dot{r}_i+\frac{1}{2}\sum_{j=1}^{n}\sum_{i=1}^{n}\frac{\partial V_{ij}}{\partial r_i}\dot{r}_i\\
=&\sum_{i=1}^{n}\sum_{j=1}^{n}\frac{\partial V_{ij}}{\partial r_i}\dot{r}_i,
\end{aligned}$$

where we have used the fact that $\frac{\partial V_{ij}}{\partial r_i}=-\frac{\partial V_{ij}}{\partial r_j}$ from Definition 3.1.4. Therefore, the lemma holds. ■

We propose the decentralized swarm tracking algorithm for (3.1) as

$$u_i=-\alpha\sum_{j\in\overline{\mathcal{N}}_i(t)}\frac{\partial V_{ij}}{\partial r_i}-\beta\text{sgn}\left(\sum_{j\in\overline{\mathcal{N}}_i(t)}\frac{\partial V_{ij}}{\partial r_i}\right),\tag{3.11}$$

where α, β, and $\overline{\mathcal{N}}_i(t)$ are defined as in Section 3.1.1, and V_{ij} is defined in Definition 3.1.4.

Theorem 3.1.5 *Suppose that the undirected graph $\mathcal{G}(t)$ is connected and the virtual leader is a neighbor of at least one follower, i.e., $0\in\overline{\mathcal{N}}_i(t)$ for some i, at each time instant. Using* (3.11) *for* (3.1)*, if $\beta>\gamma_\ell$, the relative distances of all followers and the virtual leader will move closely with the virtual leader and the inter-vehicle collision is avoided.*

Proof: Consider the Lyapunov function candidate

$$V = \frac{1}{2}\sum_{i=1}^{n}\sum_{j=1}^{n} V_{ij} + \sum_{i=1}^{n} V_{i0}.$$

Taking derivative of V gives that

$$\begin{aligned}
\dot{V} =& \frac{1}{2}\sum_{i=1}^{n}\sum_{j=1}^{n}\left(\frac{\partial V_{ij}}{\partial r_i}\dot{r}_i + \frac{\partial V_{ij}}{\partial r_j}\dot{r}_j\right) + \sum_{i=1}^{n}\left(\frac{\partial V_{i0}}{\partial r_i}\dot{r}_i + \frac{\partial V_{i0}}{\partial r_0}\dot{r}_0\right) \\
=& \sum_{i=1}^{n}\sum_{j=1}^{n}\frac{\partial V_{ij}}{\partial r_i}\dot{r}_i + \sum_{i=1}^{n}\left(\frac{\partial V_{i0}}{\partial r_i}\dot{r}_i + \frac{\partial V_{i0}}{\partial r_0}\dot{r}_0\right) \qquad (3.12) \\
=& \sum_{i=1}^{n}\sum_{j=1}^{n}\frac{\partial V_{ij}}{\partial r_i}\left[-\alpha\sum_{j=0}^{n}\frac{\partial V_{ij}}{\partial r_i} - \beta\,\mathrm{sgn}\left(\sum_{j=0}^{n}\frac{\partial V_{ij}}{\partial r_i}\right)\right] \\
&+ \sum_{i=1}^{n}\frac{\partial V_{i0}}{\partial r_i}\left[-\alpha\sum_{j=0}^{n}\frac{\partial V_{ij}}{\partial r_i} - \beta\,\mathrm{sgn}\left(\sum_{j=0}^{n}\frac{\partial V_{ij}}{\partial r_i}\right)\right] + \sum_{i=1}^{n}\frac{\partial V_{i0}}{\partial r_0}\dot{r}_0 \\
=& -\alpha\sum_{i=1}^{n}\left(\sum_{j=0}^{n}\frac{\partial V_{ij}}{\partial r_i}\right)^2 - \beta\sum_{i=1}^{n}\left|\sum_{j=0}^{n}\frac{\partial V_{ij}}{\partial r_i}\right| + \sum_{i=1}^{n}\frac{\partial V_{i0}}{\partial r_0}\dot{r}_0 \\
=& -\alpha\sum_{i=1}^{n}\left(\sum_{j=0}^{n}\frac{\partial V_{ij}}{\partial r_i}\right)^2 - \beta\sum_{i=1}^{n}\left|\sum_{j=0}^{n}\frac{\partial V_{ij}}{\partial r_i}\right| + \sum_{i=1}^{n}\frac{\partial V_{i0}}{\partial r_0}\dot{r}_0 + \sum_{i=1}^{n}\sum_{j=1}^{n}\frac{\partial V_{ij}}{\partial r_i}\dot{r}_0 \qquad (3.13) \\
\leq& -\alpha\sum_{i=1}^{n}\left(\sum_{j=0}^{n}\frac{\partial V_{ij}}{\partial r_i}\right)^2 - \beta\sum_{i=1}^{n}\left|\sum_{j=0}^{n}\frac{\partial V_{ij}}{\partial r_i}\right| + \dot{r}_0\sum_{i=1}^{n}\left|\sum_{j=0}^{n}\frac{\partial V_{ij}}{\partial r_i}\right|,
\end{aligned}$$

where we have used Lemma 3.1.1 to derive (3.12) and the fact that $\sum_{i=1}^{n}\sum_{j=1}^{n}\frac{\partial V_{ij}}{\partial r_i} = 0$ to derive (3.13). Because $\beta > \gamma_\ell$, we get that $\dot{V} \leq 0$, which in turn proves the theorem. ■

3.1.2 Decentralized Coordinated Tracking for Second-order Dynamics

In this section, we study decentralized coordinated tracking for second-order dynamics. Suppose that there exists a virtual leader, labeled as vehicle 0, with a (time-varying) position r_0 and velocity v_0. We consider four different cases.

Decentralized Consensus Tracking with a Varying Virtual Leader's Velocity

Consider followers with second-order dynamics given by

$$\dot{r}_i = v_i, \qquad \dot{v}_i = u_i, \quad i = 1, \ldots, n, \tag{3.14}$$

where $r_i \in \mathbb{R}$ and $v_i \in \mathbb{R}$ are, respectively, the position and velocity of follower i, and $u_i \in \mathbb{R}$ is the control input. We assume that $|\dot{v}_0| \leq \varphi_\ell$, where φ_ℓ is a positive constant. Again we only consider the case when all vehicles are in a one-dimensional space. All results hereafter are still valid for the m-dimensional ($m > 1$) case by introduction of the Kronecker product.

In this subsection, we assume that the virtual leader has a varying velocity, i.e., v_0 is time-varying. The objective here is to design u_i for (3.14) such that all followers track the virtual leader with local interaction in the absence of acceleration measurements. We propose the decentralized consensus tracking algorithm for (3.14) as

$$\begin{aligned} u_i = &-\sum_{j=0}^{n} a_{ij}[(r_i - r_j) + \alpha(v_i - v_j)] \\ &- \beta \text{sgn}\{\sum_{j=0}^{n} a_{ij}[\gamma(r_i - r_j) + (v_i - v_j)]\}, \end{aligned} \tag{3.15}$$

where a_{ij}, $i, j = 1, \ldots, n$, is the (i, j)th entry of the adjacency matrix $\mathcal{A}$, a_{i0}, $i = 1, \ldots, n$, is a positive constant if the virtual leader's position and velocity are available to follower i and $a_{i0} = 0$ otherwise, and α, β, and γ are positive constants. We first consider the case of a fixed network topology. Before moving on, we need the following lemma.

Lemma 3.1.2 *Suppose that the fixed undirected graph $\mathcal{G}$ is connected and at least one a_{i0} is nonzero (and hence positive). Let $P = \begin{bmatrix} \frac{1}{2}M^2 & \frac{\gamma}{2}M \\ \frac{\gamma}{2}M & \frac{1}{2}M \end{bmatrix}$ and $Q = \begin{bmatrix} \gamma M^2 & \frac{\alpha\gamma}{2}M^2 \\ \frac{\alpha\gamma}{2}M^2 & \alpha M^2 - \gamma M \end{bmatrix}$, where γ and α are positive constants and $M = \mathcal{L} + diag(a_{10}, \ldots, a_{n0})$. If γ satisfies*

$$0 < \gamma < \min\{\sqrt{\lambda_{\min}(M)}, \frac{4\alpha\lambda_{\min}(M)}{4 + \alpha^2\lambda_{\min}(M)}\}, \tag{3.16}$$

then both P and Q are symmetric positive definite.

Proof: When the fixed undirected graph $\mathcal{G}$ is connected and at least one a_{i0} is nonzero (and hence positive), M is symmetric positive definite. It follows that M can be diagonalized as $M = \Gamma^{-1}\Lambda\Gamma$, where $\Lambda = \text{diag}\{\lambda_1, \cdots, \lambda_n\}$ with λ_i being the ith eigenvalue of M. It then follows that P can be written as

$$P = \begin{bmatrix} \Gamma^{-1} & \mathbf{0}_{n\times n} \\ \mathbf{0}_{n\times n} & \Gamma^{-1} \end{bmatrix} \underbrace{\begin{bmatrix} \frac{1}{2}\Lambda^2 & \frac{\gamma}{2}\Lambda \\ \frac{\gamma}{2}\Lambda & \frac{1}{2}\Lambda \end{bmatrix}}_{F} \begin{bmatrix} \Gamma & \mathbf{0}_{n\times n} \\ \mathbf{0}_{n\times n} & \Gamma \end{bmatrix}, \tag{3.17}$$

where $\mathbf{0}_{n\times n}$ is the $n \times n$ zero matrix. Let μ be an eigenvalue of F. Because Λ is a diagonal matrix, it follows from (3.17) that μ satisfies $(\mu - \frac{1}{2}\lambda_i^2)(\mu - \frac{1}{2}\lambda_i) - \frac{\gamma^2}{4}\lambda_i^2 = 0$, which can be simplified as

$$\mu^2 - \frac{1}{2}(\lambda_i^2 + \lambda_i)\mu + \frac{1}{4}(\lambda_i^3 - \gamma^2\lambda_i^2) = 0. \tag{3.18}$$

Because F is symmetric, the roots of (3.18) are real. Therefore, all roots of (3.18) are positive if and only if $\frac{1}{2}(\lambda_i^2 + \lambda_i) > 0$ and $\frac{1}{4}(\lambda_i^3 - \gamma^2\lambda_i^2) > 0$. Because $\lambda_i > 0$, it follows that $\frac{1}{2}(\lambda_i^2 + \lambda_i) > 0$. When $\gamma^2 < \lambda_i$, it follows that $\frac{1}{4}(\lambda_i^3 - \gamma^2\lambda_i^2) > 0$. It thus follows that when $\gamma^2 < \lambda_i$, the roots of (3.18) are positive. Noting that P has the same eigenvalues as F, we can get that P is positive definite if $0 < \gamma < \sqrt{\lambda_{\min}(M)}$.

By following a similar analysis, we can get that Q is positive definite if $0 < \gamma < \frac{4\alpha\lambda_{\min}(M)}{4+\alpha^2\lambda_{\min}(M)}$. Combining the above arguments proves the lemma. ■

Theorem 3.1.6 *Suppose that the fixed undirected graph $\mathcal{G}$ is connected and at least one a_{i0} is nonzero (and hence positive). Using* (3.15) *for* (3.14)*, if $\beta > \varphi_\ell$ and γ satisfies* (3.16)*, then $r_i(t) \to r_0(t)$ and $v_i(t) \to v_0(t)$ globally exponentially as $t \to \infty$. In particular, it follows that*

$$\left\| \begin{bmatrix} \tilde{r}^T(t) & \tilde{v}^T(t) \end{bmatrix}^T \right\|_2 \leq \kappa_1 e^{-\kappa_2 t}, \tag{3.19}$$

where $\tilde{r}$ and $\tilde{v}$ are, respectively, the column stack vectors of $\tilde{r}_i$ and $\tilde{v}_i$, $i = 1, \ldots, n$, with $\tilde{r}_i = r_i - r_0$ and $\tilde{v}_i = v_i - v_0$, P and Q are defined in Lemma 3.1.2, $\kappa_1 = \sqrt{\frac{\begin{bmatrix} \tilde{r}^T(0) & \tilde{v}^T(0) \end{bmatrix} P \begin{bmatrix} \tilde{r}^T(0) & \tilde{v}^T(0) \end{bmatrix}^T}{\lambda_{\min}(P)}}$, and $\kappa_2 = \frac{\lambda_{\min}(Q)}{2\lambda_{\max}(P)}$.

Proof: Noting that $\tilde{r}_i = r_i - r_0$ and $\tilde{v}_i = v_i - v_0$, we rewrite the closed-loop system of (3.14) using (3.15) as

$$\begin{aligned}
\dot{\tilde{r}}_i &= \tilde{v}_i \\
\dot{\tilde{v}}_i &= -\sum_{j=0}^{n} a_{ij}[(\tilde{r}_i - \tilde{r}_j) + \alpha(\tilde{v}_i - \tilde{v}_j)] \\
&\quad - \beta \text{sgn}\left\{\sum_{j=0}^{n} a_{ij}[\gamma(\tilde{r}_i - \tilde{r}_j) + (\tilde{v}_i - \tilde{v}_j)]\right\} - \dot{v}_0.
\end{aligned} \tag{3.20}$$

Equation (3.20) can be written in matrix form as

$$\begin{aligned}
\dot{\tilde{r}} &= \tilde{v} \\
\dot{\tilde{v}} &= -M\tilde{r} - \alpha M\tilde{v} - \beta \text{sgn}[M(\gamma\tilde{r} + \tilde{v})] - \mathbf{1}\dot{v}_0,
\end{aligned}$$

where $\tilde{r}$ and $\tilde{v}$ are defined in (3.19) and $M = \mathcal{L} + \text{diag}(a_{10}, \ldots, a_{n0})$.

Consider the Lyapunov function candidate

$$\begin{aligned}
V &= \begin{bmatrix} \tilde{r}^T & \tilde{v}^T \end{bmatrix} P \begin{bmatrix} \tilde{r} \\ \tilde{v} \end{bmatrix} \\
&= \frac{1}{2}\tilde{r}^T M^2 \tilde{r} + \frac{1}{2}\tilde{v}^T M\tilde{v} + \gamma\tilde{r}^T M\tilde{v}.
\end{aligned} \tag{3.21}$$

Note that according to Lemma 3.1.2, P is symmetric positive definite when γ satisfies (3.16). The derivative of V is

$$\begin{aligned}
\dot{V} =& \tilde{r}^T M^2\tilde{v} + \tilde{v}^T M\dot{\tilde{v}} + \gamma\tilde{v}^T M\tilde{v} + \gamma\tilde{r}^T M\dot{\tilde{v}} \\
=& -\begin{bmatrix} \tilde{r}^T & \tilde{v}^T \end{bmatrix} Q \begin{bmatrix} \tilde{r} \\ \tilde{v} \end{bmatrix} - (\gamma\tilde{r}^T + \tilde{v}^T)M\{\beta \text{sgn}[M(\gamma\tilde{r} + \tilde{v})] + \mathbf{1}\dot{v}_0\} \\
\leq& -\begin{bmatrix} \tilde{r}^T & \tilde{v}^T \end{bmatrix} Q \begin{bmatrix} \tilde{r} \\ \tilde{v} \end{bmatrix} - (\beta - \varphi_\ell) \left\| M(\gamma\tilde{r} + \tilde{v}) \right\|_1,
\end{aligned} \tag{3.22}$$

where the last inequality follows from the fact that $|\dot{v}_0| \leq \varphi_\ell$. Note that according to Lemma 3.1.2, Q is symmetric positive definite when γ satisfies (3.16). Also note that $\beta > \varphi_\ell$. It follows that $\dot{V}$ is negative definite. Therefore, it follows that $\tilde{r}(t) \to \mathbf{0}_n$ and $\tilde{v}(t) \to \mathbf{0}_n$ as $t \to \infty$, where $\mathbf{0}_n$ is the $n \times 1$ zero vector. Equivalently, it follows that $r_i(t) \to r_0(t)$ and $v_i(t) \to v_0(t)$ as $t \to \infty$.

We next show that decentralized consensus tracking is achieved at least globally exponentially. Note that $V \leq \lambda_{\max}(P) \left\| \begin{bmatrix} \tilde{r}^T & \tilde{v}^T \end{bmatrix}^T \right\|_2^2$. It then follows from (3.22) that

$$\begin{aligned} \dot{V} &\leq - \begin{bmatrix} \tilde{r}^T & \tilde{v}^T \end{bmatrix} Q \begin{bmatrix} \tilde{r} \\ \tilde{v} \end{bmatrix} \\ &\leq -\lambda_{\min}(Q) \left\| \begin{bmatrix} \tilde{r}^T & \tilde{v}^T \end{bmatrix}^T \right\|_2^2 \leq -\frac{\lambda_{\min}(Q)}{\lambda_{\max}(P)} V. \end{aligned}$$

Therefore, we can get that $V(t) \leq V(0) e^{-\frac{\lambda_{\min}(Q)}{\lambda_{\max}(P)} t}$. Note also that $V \geq \lambda_{\min}(P) \left\| \begin{bmatrix} \tilde{r}^T & \tilde{v}^T \end{bmatrix}^T \right\|_2^2$. After some manipulation, we can get (3.19). ■

Remark 3.1.7 *In the proof of Theorem 3.1.6, the Lyapunov function is chosen as* (3.21). *Here P can also be chosen as $P = \begin{bmatrix} \frac{1}{2}M & \frac{\gamma}{2}M \\ \frac{\gamma}{2}M & \frac{1}{2}M \end{bmatrix}$ and the derivative of V also satisfies* (3.22) *with $Q = \begin{bmatrix} \gamma M^2 & \frac{\alpha\gamma}{2}M^2 + \frac{M^2 - \gamma M}{2} \\ \frac{\alpha\gamma}{2}M^2 + \frac{M^2 - \gamma M}{2} & \alpha M^2 - \gamma M \end{bmatrix}$. By following a similar analysis to that of Lemma 3.1.2, we can show that there always exist positive α and γ such that both P and Q are symmetric positive definite and derive proper conditions for α and γ. In particular, one special choice for α and γ is $\alpha\gamma = 1$ and $\gamma < \frac{4\lambda_{\min}(M)}{4\lambda_{\min}(M)+1}$.*

We next consider the case of a switching network topology. We assume that the network topology switches according to the same model as described right before (3.6). In this case, we

propose the decentralized consensus tracking algorithm for (3.14) as

$$\begin{aligned} u_i = &- \sum_{j\in\overline{\mathcal{N}}_i(t)} b_{ij}[(r_i - r_j) + \alpha(v_i - v_j)] \\ &- \beta \sum_{j\in\overline{\mathcal{N}}_i(t)} b_{ij}\Bigg(\text{sgn}\left\{\sum_{k\in\overline{\mathcal{N}}_i(t)} b_{ik}[\gamma(r_i - r_k) + (v_i - v_k)]\right\} \\ &- \text{sgn}\left\{\sum_{k\in\overline{\mathcal{N}}_j(t)} b_{jk}[\gamma(r_j - r_k) + (v_j - v_k)]\right\}\Bigg), \end{aligned} \tag{3.23}$$

where $\overline{\mathcal{N}}_i(t)$ is defined as in Section 3.1.1, b_{ij}, $i = 1, \cdots, n, j = 0, \cdots, n$, are positive constants, and α, β, and γ are positive constants.[2] Before moving on, we need the following lemma.

Lemma 3.1.3 *Suppose that the undirected graph $\mathcal{G}(t)$ is connected and the virtual leader is a neighbor of at least one follower, i.e., $0 \in \overline{\mathcal{N}}_i(t)$ for some i, at each time instant. Let $\hat{M}(t)$ be defined as in* (3.10)*. Let $\hat{P}(t) = \begin{bmatrix} \frac{1}{2}\hat{M}(t) & \frac{\gamma}{2}I_n \\ \frac{\gamma}{2}I_n & \frac{1}{2}I_n \end{bmatrix}$ and $\hat{Q}(t) = \begin{bmatrix} \gamma\hat{M}(t) & \frac{\alpha\gamma}{2}\hat{M}(t) \\ \frac{\alpha\gamma}{2}\hat{M}(t) & \alpha\hat{M}(t) - \gamma I_n \end{bmatrix}$, where γ and α are positive constants. If γ satisfies*

$$0 < \gamma < \min_t\{\sqrt{\lambda_{\min}(\hat{M}(t))}, \frac{4\alpha\lambda_{\min}(\hat{M}(t))}{4 + \alpha^2\lambda_{\min}(\hat{M}(t))}\}, \tag{3.24}$$

then both $\hat{P}(t)$ and $\hat{Q}(t)$ are symmetric positive definite at each time instant.

Proof: The proof is similar to that of Lemma 3.1.2 and is therefore omitted here. ■

Theorem 3.1.8 *Suppose that the undirected graph $\mathcal{G}(t)$ is connected and the virtual leader is a neighbor of at least one follower, i.e., $0 \in \overline{\mathcal{N}}_i(t)$ for some i, at each time instant. Using* (3.23) *for* (3.14)*, if $\beta > \varphi_\ell$ and* (3.24) *is satisfied, then $r_i(t) \to r_0(t)$ and $v_i(t) \to v_0(t)$ as $t \to \infty$.*

Proof: Let $V_{ij} = \frac{1}{2}b_{ij}(r_i - r_j)^2$, $i, j = 1, \ldots, n$, when $|r_i - r_j| \le R$ and $V_{ij} = \frac{1}{2}b_{ij}R^2$ when $|r_i - r_j| > R$. Also let $V_{i0} = \frac{1}{2}b_{i0}(r_i - r_0)^2$, $i = 1, \ldots, n$, when $|r_i - r_0| \le R$ and $V_{i0} = \frac{1}{2}b_{i0}R^2$ when $|r_i - r_0| > R$. Consider the Lyapunov function candidate $V = \frac{1}{2}\sum_{i=1}^n \sum_{j=1}^n V_{ij} + \sum_{i=1}^n V_{i0} +$

[2] Because the virtual leader has no neighbor, we let $\text{sgn}\left\{\sum_{k\in\overline{\mathcal{N}}_0(t)} b_{0k}[\gamma(r_0 - r_k) + (v_0 - v_k)]\right\} = 0$.

$\frac{1}{2}\tilde{v}^T\tilde{v}+\gamma\tilde{r}^T\tilde{v}$, where $\tilde{r}=[\tilde{r}_1,\cdots,\tilde{r}_n]^T$ with $\tilde{r}_i=r_i-r_0$ and $\tilde{v}=[\tilde{v}_1,\cdots,\tilde{v}_n]^T$ with $\tilde{v}_i=v_i-v_0$. Note that V can be written as

$$V=\begin{bmatrix}\tilde{r}^T & \tilde{v}^T\end{bmatrix}\hat{P}(t)\begin{bmatrix}\tilde{r}\\ \tilde{v}\end{bmatrix}+\frac{1}{4}\sum_{i=1}^{n}\sum_{j\notin\overline{\mathcal{N}}_i(t),j\neq 0}b_{ij}R^2+\frac{1}{2}\sum_{0\in\overline{\mathcal{N}}_i(t)}b_{i0}R^2. \tag{3.25}$$

Note also that according to Lemma 3.1.3, $\hat{P}(t)$ is symmetric positive definite when (3.24) is satisfied. By following a similar line to the proof of Theorem 3.1.6 and using nonsmooth analysis, we can obtain that the generalized derivative of V is negative definite under the condition of the theorem. Therefore, we have that $r_i(t)\to r_0(t)$ and $v_i(t)\to v_0(t)$ as $t\to\infty$. ■

Remark 3.1.9 *It can be noted that* (3.23) *requires the availability of the information from both the neighbors, i.e., one-hop neighbors, and the neighbors' neighbors, i.e., two-hop neighbors. However,* accurate *measurements of the two-hop neighbors' information are not necessary because only the signs, i.e., '+' or '-', are required in* (3.23). *In fact,* (3.23) *can be easily implemented in real systems in the sense that follower $i, i=1,\cdots,n$, shares both its own state, i.e., position and velocity, and the sign of $\sum_{j\in\overline{\mathcal{N}}_i(t)}b_{ij}[\gamma(r_i-r_j)+(v_i-v_j)]$ with its neighbors. Note that follower i also has to compute $\sum_{j\in\overline{\mathcal{N}}_i(t)}b_{ij}(r_i-r_j)$ and $\sum_{j\in\overline{\mathcal{N}}_i(t)}b_{ij}(v_i-v_j)$ in* (3.23) *(correspondingly, $\sum_{j=0}^{n}a_{ij}(r_i-r_j)$ and $\sum_{j=0}^{n}a_{ij}(v_i-v_j)$ in* (3.15)*) in order to derive the corresponding control input for itself.*

Remark 3.1.10 *Under the condition of Theorem 3.1.8, the decentralized consensus tracking algorithm* (3.23) *guarantees at least global exponential tracking under a switching network topology. However, in contrast to the result in Theorem 3.1.6, it might not be easy to explicitly compute the decay rate, i.e., κ_2 in Theorem 3.1.8, because the switching pattern of the network topology will play an important role in determining the decay rate.*

Remark 3.1.11 *Similar to the analysis in Remark 3.1.7, in Lyapunov function* (3.25)*, we can choose $\hat{P}(t)=\begin{bmatrix}\frac{1}{2}I_n & \frac{\gamma}{2}I_n\\ \frac{\gamma}{2}I_n & \frac{1}{2}I_n\end{bmatrix}$. It then follows that $\hat{Q}(t)=\begin{bmatrix}\gamma\hat{M}(t) & \frac{\alpha\gamma}{2}\hat{M}(t)+\frac{\hat{M}(t)-\gamma I_n}{2}\\ \frac{\alpha\gamma}{2}\hat{M}(t)+\frac{\hat{M}(t)-\gamma I_n}{2} & \alpha\hat{M}(t)-\gamma I_n\end{bmatrix}$. We can show that there always exist positive α and γ such that both $\hat{P}(t)$ and $\hat{Q}(t)$ are symmetric*

positive definite and derive proper conditions for α and γ. In particular, one special choice for α and γ is $\alpha\gamma = 1$ and $\gamma < \min_t \frac{4\lambda_{\min}[\hat{M}(t)]}{4\lambda_{\min}[\hat{M}(t)]+1}$.

Remark 3.1.12 *In Theorems 3.1.2 and 3.1.8, it is assumed that the undirected graph $\mathcal{G}(t)$ is connected and the virtual leader is a neighbor of at least one follower at each time instant. However, this poses an obvious constraint in real applications because the connectivity requirement is not necessarily always satisfied. Next, we propose an adaptive connectivity maintenance mechanism in which the adjacency matrix with entries b_{ij} in* (3.6) *and* (3.23) *is redefined as follows:*
1) When $||r_i(0) - r_j(0)|| > R$, $b_{ij}(t) = 1$ if $||r_i(t) - r_j(t)|| \leq R$ and $b_{ij}(t) = 0$, otherwise.
2) When $||r_i(0) - r_j(0)|| \leq R$, $b_{ij}(t)$ is defined such that: 1) $b_{ij}(0) > 0$; 2) $b_{ij}(t)$ is nondecreasing; 3) $b_{ij}(t)$ is differentiable (or differentiable almost everywhere); 4) $b_{ij}(t)$ goes to infinity if $||r_i(t) - r_j(t)||$ goes to R.

The motivation here is to maintain the initially existing connectivity patterns. That is, if two followers are neighbors of each other (correspondingly, the virtual leader is a neighbor of a follower) at $t = 0$, the two followers are guaranteed to be neighbors of each other (correspondingly, the virtual leader is guaranteed to be a neighbor of this follower) at $t > 0$. However, if two followers are not neighbors of each other (correspondingly, the virtual leader is not a neighbor of a follower) at $t = 0$, the two followers are not necessarily guaranteed to be neighbors of each other (correspondingly, the virtual leader is not necessarily guaranteed to be a neighbor of this follower) at $t > 0$.

Using the proposed adaptive adjacency matrix, the consensus tracking algorithm for (3.1) *can be chosen as*

$$u_i = -\alpha \sum_{j\in\overline{\mathcal{N}}_i(t)} b_{ij}(t)(r_i - r_j) - \beta \sum_{j\in\overline{\mathcal{N}}_i(t)} b_{ij}(t)$$
$$\left\{ sgn[\sum_{k\in\overline{\mathcal{N}}_i(t)} b_{ik}(t)(r_i - r_k)] - sgn[\sum_{k\in\overline{\mathcal{N}}_j(t)} b_{jk}(t)(r_j - r_k)] \right\} \tag{3.26}$$

with the Lyapunov function chosen as $V = \frac{1}{2}\tilde{r}^T\tilde{r}$ while the consensus tracking algorithm for (3.14)

can be chosen as (3.23) *with the Lyapunov function chosen as* $V = \begin{bmatrix} \tilde{r}^T & \tilde{v}^T \end{bmatrix} \hat{P}(t) \begin{bmatrix} \tilde{r} \\ \tilde{v} \end{bmatrix}$ *with* $\hat{P}(t)$ *chosen as in Remark 3.1.11. Note that there always exist* α *and* γ *satisfying the conditions in Remark 3.1.11 because* $\lambda_{\min}[\hat{M}(t)]$ *is nondecreasing under the connectivity maintenance mechanism. When the control gains are chosen properly, i.e.,* $\alpha > 0$ *and* $\beta > \gamma_\ell$ *for single-integrator kinematics and* α *and* γ *satisfies Remark 3.1.11 and* $\beta > \varphi_\ell$ *for double-integrator dynamics, it can be shown that decentralized consensus tracking can be guaranteed for both first-order kinematics and second-order dynamics if the undirected graph* $\mathcal{G}(t)$ *is initially connected and the virtual leader is initially a neighbor of at least one follower, i.e., at* $t = 0$*. The proof follows a similar analysis to that of the corresponding algorithm in the absence of connectivity maintenance mechanism except that the initially existing connectivity patterns can be maintained because otherwise* $\dot{V} \to -\infty$ *as* $||r_i(t) - r_j(t)|| \to R$ *by noting that* $\dot{V} = -\alpha \tilde{r} \hat{M}(t) \tilde{r} - (\beta - \gamma_\ell) \left\| \hat{M}(t) \tilde{r} \right\|$ *for single-integrator kinematics and* $\dot{V} = -\begin{bmatrix} \tilde{r}^T & \tilde{v}^T \end{bmatrix} \hat{Q}(t) \begin{bmatrix} \tilde{r} \\ \tilde{v} \end{bmatrix}$ *for double-integrator dynamics, where* $\hat{Q}(t)$ *is defined in Remark 3.1.11.*

Decentralized Consensus Tracking with a Constant Virtual Leader's Velocity

In this subsection, we assume that the virtual leader has a constant velocity, i.e., v_0 is constant. We propose the decentralized consensus tracking algorithm for (3.14) as

$$u_i = -\sum_{j=0}^{n} a_{ij}(r_i - r_j) - \beta \text{sgn}\left[\sum_{j=0}^{n} a_{ij}(v_i - v_j)\right], \tag{3.27}$$

where a_{ij} is defined as in (3.15) and β is a positive constant. We first consider a fixed network topology.

Theorem 3.1.13 *Suppose that the fixed undirected graph* $\mathcal{G}$ *is connected and at least one* a_{i0} *is nonzero (and hence positive). Using* (3.27) *for* (3.14)*,* $r_i(t) \to r_0(t)$ *and* $v_i(t) \to v_0$ *as* $t \to \infty$*.*

Proof: Letting $\tilde{r}_i = r_i - r_0$ and $\tilde{v}_i = v_i - v_0$, we can rewrite the closed-loop system of (3.14) using (3.27) as

$$\begin{aligned}\dot{\tilde{r}}_i &= \tilde{v}_i \\ \dot{\tilde{v}}_i &= -\sum_{j=0}^{n} a_{ij}(\tilde{r}_i - \tilde{r}_j) - \beta \text{sgn}\left[\sum_{j=0}^{n} a_{ij}(\tilde{v}_i - \tilde{v}_j)\right].\end{aligned} \tag{3.28}$$

Equation (3.28) can be written in matrix form as

$$\dot{\tilde{r}} = \tilde{v}, \quad \dot{\tilde{v}} = -M\tilde{r} - \beta \text{sgn}(M\tilde{v}), \tag{3.29}$$

where $\tilde{r}$ and $\tilde{v}$ are, respectively, the column stack vectors of $\tilde{r}_i$ and $\tilde{v}_i$, $i = 1, \ldots, n$, and $M = \mathcal{L} + \text{diag}(a_{10}, \ldots, a_{n0})$.

Consider the Lyapunov function candidate $V = \frac{1}{2}\tilde{r}^T M^2 \tilde{r} + \frac{1}{2}\tilde{v}^T M\tilde{v}$. The derivative of V is given by

$$\begin{aligned}\dot{V} &= \tilde{r}^T M^2 \tilde{v} + \tilde{v}^T M\dot{\tilde{v}} \\ &= \tilde{r}^T M^2 \tilde{v} + \tilde{v}^T M[-M\tilde{r} - \beta \text{sgn}(M\tilde{v})] \\ &= -\beta \left\| M\tilde{v} \right\|_1 .\end{aligned}$$

Because M is symmetric positive definite, it follows that $\dot{V}$ is negative semidefinite. Note that $\dot{V} \equiv 0$ implies that $\tilde{v} \equiv \mathbf{0}_n$, which in turn implies that $\tilde{r} \equiv \mathbf{0}_n$ from (3.29). By using the LaSalle's invariance principle for nonsmooth systems [94], it follows that $\tilde{r}(t) \to \mathbf{0}_n$ and $\tilde{v}(t) \to \mathbf{0}_n$ as $t \to \infty$. Equivalently, it follows that $r_i(t) \to r_0(t)$ and $v_i(t) \to v_0(t)$ as $t \to \infty$. ■

Remark 3.1.14 *When the network topology is switching according to the model described right before* (3.6)*, we propose the decentralized consensus tracking algorithm for* (3.14) *as*

$$\begin{aligned} u_i = & -\sum_{j\in\overline{\mathcal{N}}_i(t)} b_{ij}(r_i - r_j) \\ & -\beta \sum_{j\in\overline{\mathcal{N}}_i(t)} b_{ij}\Bigg\{ sgn\left[\sum_{k\in\overline{\mathcal{N}}_i(t)} b_{ik}(v_i - v_k)\right] \\ & - sgn\left[\sum_{k\in\overline{\mathcal{N}}_j(t)} b_{jk}(v_j - v_k)\right]\Bigg\}, \end{aligned} \tag{3.30}$$

where $\overline{\mathcal{N}}_i(t)$ is defined as in Section 3.1.1, $b_{ij},\ b_{ik},\ b_{jk}$ are defined as in (3.23)*, and β is a positive constant. For any positive β, the algorithm* (3.30) *guarantees decentralized consensus tracking under the conditions of Theorem 3.1.8. The proof follows a similar line to that of Theorem 3.1.8 by using the Lyapunov function candidate $V = \frac{1}{2}\tilde{r}^T\hat{M}(t)\tilde{r} + \frac{1}{2}\tilde{v}^T\tilde{v}$ and is omitted here. Meanwhile, the adaptive connectivity maintenance mechanism proposed in Remark 3.1.12 can also be applied here by noting that $V \to \infty$ when $||r_i(t) - r_j(t)|| \to R$, which then contradicts the fact that $\dot{V} \leq 0$.*

Remark 3.1.15 *In contrast to* (3.15) *and* (3.23)*, which require both accurate position and velocity measurements,* (3.27) *and* (3.30) *do not necessarily require* accurate *velocity measurements because the velocity measurements are only used to calculate the sign, i.e., '+' or '-'. Therefore,* (3.27) *and* (3.30) *are more robust to measurement inaccuracy.*

Decentralized Swarm Tracking with a Constant Virtual Leader's Velocity

In this subsection, we study decentralized swarm tracking under switching network topologies when the velocity of the virtual leader is constant. We again assume that the network topology switches according to the model described right before (3.6). We propose the decentralized swarm

tracking algorithm for (3.14) as

$$\begin{aligned} u_i = & - \sum_{j\in\overline{\mathcal{N}}_i(t)} \frac{\partial V_{ij}}{\partial r_i} \\ & - \beta \sum_{j\in\overline{\mathcal{N}}_i(t)} b_{ij}\Bigg\{ \text{sgn}\left[\sum_{k\in\overline{\mathcal{N}}_i(t)} b_{ik}(v_i - v_k)\right] \\ & - \text{sgn}\left[\sum_{k\in\overline{\mathcal{N}}_j(t)} b_{jk}(v_j - v_k)\right]\Bigg\}, \end{aligned} \tag{3.31}$$

where V_{ij} is the potential function defined in Definition 3.1.4, $\overline{\mathcal{N}}_i(t)$ is defined as in Section 3.1.1, β is a positive constant, and b_{ij}, b_{ik}, and b_{jk} are defined as in (3.23). Note that (3.31) requires both the one-hop and two-hop neighbors' information.

Theorem 3.1.16 *Suppose that the undirected graph $\mathcal{G}(t)$ is connected and the virtual leader is a neighbor of at least one follower, i.e., $0 \in \overline{\mathcal{N}}_i(t)$ for some i, at each time instant. Using* (3.31) *for* (3.14)*, the velocity differences of all followers and the virtual leader will ultimately converge to zero, the relative distances of all followers and the virtual leader will ultimately converge to local minima, i.e., $\lim_{t\to\infty} \sum_{j\in\overline{\mathcal{N}}_i(t)} \frac{\partial V_{ij}}{\partial r_i} = 0, i = 1, \cdots, n$, and the inter-vehicle collision is avoided.*

Proof: Letting $\tilde{r}_i = r_i - r_0$ and $\tilde{v}_i = v_i - v_0$, it follows that (3.31) can be written as

$$\begin{aligned} u_i = & - \sum_{j\in\overline{\mathcal{N}}_i(t)} \frac{\partial V_{ij}}{\partial \tilde{r}_i} \\ & - \beta \sum_{j\in\overline{\mathcal{N}}_i(t)} b_{ij}\Bigg\{ \text{sgn}\left[\sum_{k\in\overline{\mathcal{N}}_i(t)} b_{ik}(\tilde{v}_i - \tilde{v}_k)\right] \\ & - \text{sgn}\left[\sum_{k\in\overline{\mathcal{N}}_j(t)} b_{jk}(\tilde{v}_j - \tilde{v}_k)\right]\Bigg\}. \end{aligned}$$

Consider the Lyapunov function candidate

$$V = \frac{1}{2}\sum_{i=1}^{n}\sum_{j=1}^{n} V_{ij} + \sum_{i=1}^{n} V_{i0} + \frac{1}{2}\tilde{v}^T\tilde{v},$$

where $\tilde{v}$ is a column stack vector of $\tilde{v}_i$. Taking derivative of V gives that

$$\begin{aligned}
\dot{V} =& \frac{1}{2}\sum_{i=1}^{n}\sum_{j=1}^{n}\left(\frac{\partial V_{ij}}{\partial \tilde{r}_i}\dot{\tilde{r}}_i + \frac{\partial V_{ij}}{\partial \tilde{r}_j}\dot{\tilde{r}}_j\right) \\
&+ \sum_{i=1}^{n}\left(\frac{\partial V_{i0}}{\partial \tilde{r}_i}\dot{\tilde{r}}_i + \frac{\partial V_{i0}}{\partial \tilde{r}_0}\dot{\tilde{r}}_0\right) + \tilde{v}^T\dot{\tilde{v}} \\
=& \sum_{i=1}^{n}\sum_{j=1}^{n}\frac{\partial V_{ij}}{\partial \tilde{r}_i}\dot{\tilde{r}}_i + \sum_{i=1}^{n}\frac{\partial V_{i0}}{\partial \tilde{r}_i}\dot{\tilde{r}}_i - \sum_{i=1}^{n}\tilde{v}_i\sum_{j=0}^{n}\frac{\partial V_{ij}}{\partial \tilde{r}_i} \\
&- \beta\tilde{v}^T\hat{M}(t)\text{sgn}\left[\hat{M}(t)\tilde{v}\right] \qquad (3.32) \\
=& -\beta\left\|\hat{M}(t)\tilde{v}\right\|_1, \qquad (3.33)
\end{aligned}$$

where $\hat{M}(t)$ is defined in (3.10), (3.32) is derived by using Lemma 3.1.1 and the fact that $\dot{\tilde{r}}_0 = 0$, and (3.33) is derived by using the fact that $\hat{M}(t)$ is symmetric. By following a similar analysis to that in the proof of Theorem 3.1.13, it follows from the LaSalle's invariance principle for nonsmooth systems [94] that $v_i(t) \to v_0$ and $\sum_{j=0}^{n}\frac{\partial V_{ij}}{\partial r_i} \to 0$ as $t \to \infty$, which in turn proves the theorem. ■

Decentralized Swarm Tracking with a Varying Virtual Leader's Velocity

In this subsection, we assume that the virtual leader's velocity is varying, i.e., the virtual leader's acceleration is, in general, nonzero. We propose the following decentralized swarm tracking algorithm with a distributed estimator for (3.14) as

$$\begin{aligned}
u_i =& -\gamma\text{sgn}\left\{\sum_{j\in\overline{\mathcal{N}}_i(t)} b_{ij}[\hat{v}_{i0} - \hat{v}_{j0}]\right\} - \sum_{j\in\overline{\mathcal{N}}_i(t)}\frac{\partial V_{ij}}{\partial r_i} \\
&- \beta\sum_{j\in\overline{\mathcal{N}}_i(t)} b_{ij}\Bigg\{\text{sgn}\left[\sum_{k\in\overline{\mathcal{N}}_i(t)} b_{ik}(v_i - v_k)\right] \\
&- \text{sgn}\left[\sum_{k\in\overline{\mathcal{N}}_j(t)} b_{jk}(v_j - v_k)\right]\Bigg\}, \qquad (3.34)
\end{aligned}$$

where γ and β are positive constants, V_{ij}, $\overline{\mathcal{N}}_i(t)$, b_{ij}, b_{ik}, and b_{kj} are defined in (3.31), and

$$\dot{\hat{v}}_{i0} = -\gamma \text{sgn}\left\{\sum_{j\in\overline{\mathcal{N}}_i(t)} b_{ij}[\hat{v}_{i0} - \hat{v}_{j0}]\right\},\ i = 1, \cdots, n, \tag{3.35}$$

with $\hat{v}_{i0}$ being the ith vehicle's estimate of the virtual leader's velocity and $\hat{v}_{00} = v_0$. Here (3.35) is a distributed estimator motivated by the results in Section 3.1.1.

Theorem 3.1.17 *Suppose that the undirected graph $\mathcal{G}(t)$ is connected and the virtual leader is a neighbor of at least one follower, i.e., $0 \in \overline{\mathcal{N}}_i(t)$ for some i, at each time instant. Using* (3.34) *for* (3.14)*, if $\gamma > \varphi_\ell$, the velocity differences of all followers and the virtual leader will ultimately converge to zero, the relative distances of all followers, the virtual leader will ultimately converge to local minima, i.e., $\lim_{t\to\infty}\sum_{j\in\overline{\mathcal{N}}_i(t)}\frac{\partial V_{ij}}{\partial r_i} = 0, i = 1, \cdots, n$, and the inter-vehicle collision is avoided.*

Proof: For (3.35), it follows from Theorem 3.1.2 that there exists positive $\overline{t}$ such that $\hat{v}_{i0}(t) = v_0(t)$ for any $t \geq \overline{t}$. Note that $\dot{\hat{v}}_{i0}$ in (3.35) is a switching signal, which is different from $\dot{v}_0(t)$ at each time instant. However, for $t_2 \geq t_1 \geq \overline{t}$, we have that $\int_{t_1}^{t_2}\dot{\hat{v}}_{i0}(t)dt = \int_{t_1}^{t_2}\dot{v}_0(t)dt$ by noting that $\hat{v}_{i0}(t) = v_0(t)$ for any $t \geq \overline{t}$. Therefore, r_i will be unchanged when replacing $\dot{\hat{v}}_{i0}$ with $\dot{v}_0$ for $t \geq \overline{t}$. For $t \geq \overline{t}$, by replacing $\dot{\hat{v}}_{i0}$ with $\dot{v}_0$ and choosing the same Lyapunov function candidate as in the proof of Theorem 3.1.16, it follows from a similar analysis to that in the proof of Theorem 3.1.16 and the LaSalle's invariance principle for nonsmooth systems [94] that $v_i(t) \to v_0(t)$ and $\sum_{j=0}^{n}\frac{\partial V_{ij}}{\partial r_i} \to 0$ as $t \to \infty$. This completes the proof. ■

Remark 3.1.18 *Note that* (3.31) *and* (3.34) *require the availability of both the one-hop and two-hop neighbors' information. In contrast to some flocking algorithms* [4, 73]*, the availability of the virtual leader's information, i.e., the position, velocity, and acceleration, to all followers is not required in* (3.34) *due to the introduction of the distributed estimator. In addition, in contrast to the flocking algorithms* [4, 5, 73], (3.31) *does not require* accurate *velocity measurements because the velocity measurements are only used to calculate the sign, i.e., '+' or '-', in* (3.31) *and* (3.34)*. Therefore,* (3.31) *and* (3.34) *are more robust to measurement inaccuracy.*

Remark 3.1.19 *In Theorems 3.1.5, 3.1.16, and 3.1.17, it is assumed that the undirected graph $\mathcal{G}(t)$ is connected and the virtual leader is a neighbor of at least one follower at each time instant. However, this poses an obvious constraint in real applications because the connectivity requirement is not necessarily always satisfied. In the following, a mild connectivity requirement is proposed for decentralized swarm tracking by adopting a connectivity maintenance mechanism in which the potential function in Definition 3.1.4 is redefined as follows:*

1) When $||r_i - r_j|| \geq R$ at the initial time, i.e., $t = 0$, V_{ij} is defined as in Definition 3.1.4.

2) When $||r_i - r_j|| < R$ at the initial time, i.e., $t = 0$, V_{ij} is defined satisfying conditions 1), 2), and 4) in Definition 3.1.4 and condition 3) in Definition 3.1.4 is replaced with the condition that $V_{ij} \to \infty$ as $||r_i - r_j|| \to R$. The motivation here is also to maintain the initially existing connectivity patterns as in Remark 3.1.12.

Using the potential function defined above, decentralized swarm tracking can be guaranteed for both first-order kinematics (cf. Theorem 3.1.5) and second-order dynamics (cf. Theorems 3.1.16 and 3.1.17) if the undirected graph $\mathcal{G}(t)$ is initially connected, i.e., $t = 0$, the virtual leader is initially a neighbor of at least one follower, and the other conditions for the control gains are satisfied. The proof follows directly from those of Theorems 3.1.5, 3.1.16, and 3.1.17 except that a pair of followers who are neighbors of each other initially will always be the neighbors of each other (correspondingly, if the virtual leader is initially a neighbor of a follower, the virtual leader will always be a neighbor of this follower) because otherwise the potential function will go to infinity. This contradicts the fact that $\dot{V} \leq 0$ in Theorems 3.1.5 and 3.1.16 and the facts that

$$\begin{aligned}\dot{V} &\leq -\beta \left\| \hat{M}(t)\tilde{v} \right\|_1 + (\gamma + \varphi_\ell) \left\| \tilde{v} \right\|_1 \\ &\leq (\gamma + \varphi_\ell)\sqrt{n} \left\| \tilde{v} \right\|_2 \\ &\leq (\gamma + \varphi_\ell)\sqrt{n}\sqrt{2V}\end{aligned}$$

for $0 \leq t < \overline{t}$, which implies that $V(t) \leq (\sqrt{V(0)} + \frac{(\gamma+\varphi_\ell)\sqrt{n}}{\sqrt{2}}\overline{t})^2$, and $\dot{V} \leq 0$ for $t \geq \overline{t}$ in Theorem 3.1.17. Note that the connectivity maintenance strategy in Zalvanos et al. [95] *requires that the number of edges be always nondecreasing. That is, if a pair of followers are neighbors of each other*

(respectively, the virtual leader is a neighbor of a follower) at some time instant T,[3] *then the pair of followers are always neighbors of each other (respectively, the virtual leader is always a neighbor of this follower) at any time $t > T$. This requirement might not be applicable in reality, especially in large-scale systems where the size of the vehicles cannot be ignored because the group of vehicles will become very compact with the increasing number of edges. Meanwhile, the computation burden will increase significantly as well. In contrast, the connectivity maintenance mechanism with the corresponding potential function proposed in Remark 3.1.19 takes these practical issues into consideration. In addition,* hysteresis *is introduced to the connectivity maintenance strategy* [95] *to avoid the singularity of the Lyapunov function. However, the hysteresis is not required in the potential function proposed in Remark 3.1.19.*

To illustrate the connectivity maintenance mechanism as proposed in Remark 3.1.19, we compare two different potential functions V_{ij}^1 and V_{ij}^2 whose derivatives satisfy, respectively,

$$\frac{\partial V_{ij}^1}{\partial r_i} = \begin{cases} 0, & ||r_i - r_j|| > R, \\ \frac{2\pi(r_i - r_j)\sin[2\pi(||r_i - r_j|| - d_{ij})]}{||r_i - r_j||}, & d_{ij} < ||r_i - r_j|| \leq R, \\ \frac{20(r_i - r_j)}{||r_i - r_j||}\frac{||r_i - r_j|| - d_{ij}}{||r_i - r_j||}, & ||r_i - r_j|| \leq d_{ij}, \end{cases} \tag{3.36}$$

and

$$\frac{\partial V_{ij}^2}{\partial r_i} = \begin{cases} \frac{r_i - r_j}{||r_i - r_j||}\frac{||r_i - r_j|| - d_{ij}}{(||r_i - r_j|| - R)^2}, & d_{ij} < ||r_i - r_j|| < R, \\ 20\frac{r_i - r_j}{||r_i - r_j||}\frac{||r_i - r_j|| - d_{ij}}{||r_i - r_j||}, & ||r_i - r_j|| \leq d_{ij}, \end{cases} \tag{3.37}$$

where $R = 2.5$ and $d_{ij} = 2$. Figure 3.1 shows the plot of the potential functions V_{ij}^1 and V_{ij}^2.[4] It can be seen from Fig. 3.1(b) that V_{ij}^2 approaches infinity as the distance $||r_i - r_j||$ approaches R. However, V_{ij}^1 does not have the property (cf. Fig. 3.1(a)). In particular, V_{ij}^1 satisfies condition 3) in Definition 3.1.4 as shown in Fig. 3.1(a). In addition, both V_{ij}^1 and V_{ij}^2 satisfy conditions 1), 2), and 4) in Definition 3.1.4. According to Remark 3.1.19, we can choose the potential function as V_{ij}^2 when $||r_i(0) - r_j(0)|| < R$ and V_{ij}^1 otherwise.

[3] Equivalently, a pair of followers are within the communication range of each other (respectively, the virtual leader is within the communication range of a follower).

[4] Note that neither V_{ij}^1 nor V_{ij}^2 is unique because for positive constant C, $V_{ij}^1 + C$ and $V_{ij}^2 + C$ are also potential functions satisfying, respectively, (3.36) and (3.37). We only plot one possible choice for them.

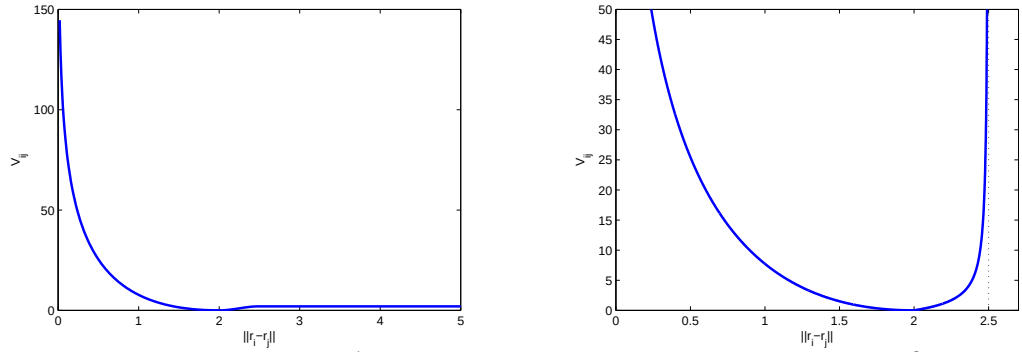

(a) Potential function V_{ij}^1. (b) Potential function V_{ij}^2.

Fig. 3.1: Potential functions V_{ij}^1 and V_{ij}^2 with $R = 2.5$ and $d_{ij} = 2$.

Simulation

In this section, we present several simulation examples to validate some theoretical results in the previous sections. We consider a group of six followers with a virtual leader. We let $a_{ij} = 1$ if vehicle j is a neighbor of vehicle i, where $j = 0, 1, \cdots, 6$ and $i = 1, \cdots, 6$, and $a_{ij} = 0$, otherwise.

In the case of first-order kinematics, the network topology is chosen as in Fig. 3.2(a). It can be noted that the undirected graph $\mathcal{G}$ for all followers 1 to 6 is connected and the virtual leader is a neighbor of follower 4. Using (3.2) in 2D, we choose $r_0(t) = [t-5, -5+10\sin(\frac{\pi t}{25})]^T$, $\alpha = 1$, and $\beta = 1.5$. The trajectories of the followers and the virtual leader are shown in Fig. 3.3. The tracking errors of the x and y positions are shown in, respectively, Fig. 3.4(a) and Fig. 3.4(b). It can be seen from Fig. 3.4 that the tracking errors converge to zero in finite time. That is, all followers track the virtual leader accurately after a finite period of time as also shown in Fig. 3.3.

For decentralized swarm tracking in the case of first-order kinematics, we choose $R = 2.5$, $d_{ij} = 2$, $\alpha = 1$, $\beta = 3$, and $a_{ij} = 1$ if $d_{ij} \leq R$ and $a_{ij} = 0$ otherwise. The partial derivative

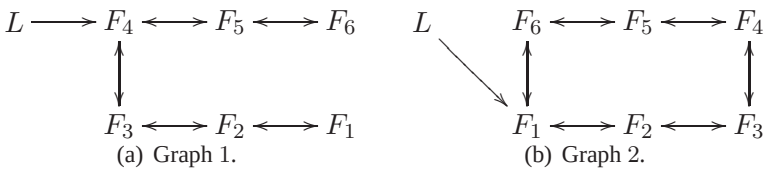

(a) Graph 1. (b) Graph 2.

Fig. 3.2: Network topology for a group of six followers with a virtual leader. Here L denotes the virtual leader while $F_i, i = 1, \cdots, 6$, denote the followers.

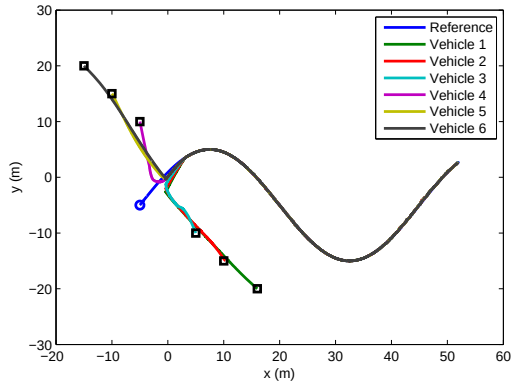

Fig. 3.3: Trajectories of the followers and the virtual leader using (3.2) in 2D. The circle denotes the starting position of the virtual leader while the squares denote the starting positions of the follwers.

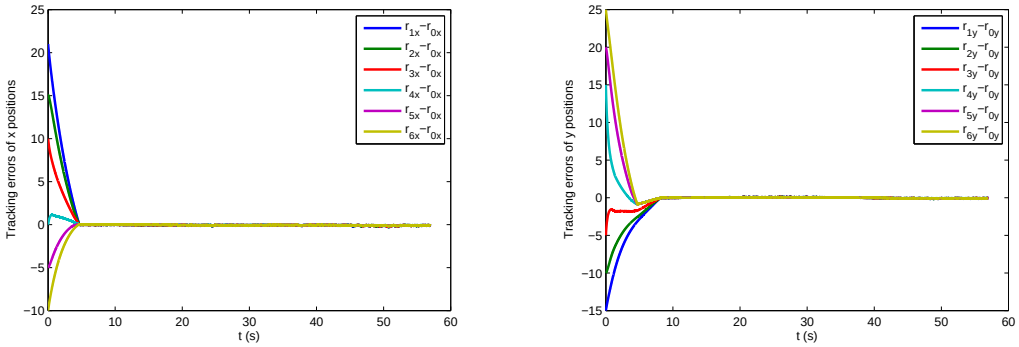

(a) x position. (b) y position.

Fig. 3.4: Position tracking errors using (3.2) in 2D.

of the potential function is chosen as in (3.36). Using (3.11) for (3.1) in 2D, Fig. 3.5 shows the consecutive snapshots of decentralized swarm tracking for 48 followers with a virtual leader. The initial states of the followers are randomly chosen from the square box $[-5, 15]^2$ and $r_0(t)$ is chosen as $[t, 5+10\sin(\frac{\pi T}{25})]^T$. It can be seen that the relative distances of the followers and the virtual leader ultimately converge to local minima.

In the case of second-order dynamics, the network topology is chosen as in Fig. 3.2(b). It can be noted that the undirected graph $\mathcal{G}$ for all followers 1 to 6 is connected as well and the virtual leader is a neighbor of follower 1. Using (3.15) in 2D, we choose $r_0(t) = [t, t + \sin(t)]^T$, $\alpha = 1$, $\beta = 5$, and $\gamma = 0.1$. The trajectories of the followers and the virtual leader are shown in Fig. 3.6. The tracking errors of the x and y positions are shown in Figs. 3.7(a) and 3.7(b). The tracking errors of the x and y velocities are shown in Figs. 3.7(c) and 3.7(d). It can be seen from Fig. 3.7 that the tracking errors ultimately converge to zero. That is, all followers ultimately track the virtual leader as also shown in Fig. 3.6.

For decentralized swarm tracking in the case of second-order dynamics, R, d_{ij}, α, β, a_{ij}, and the partial derivative of the potential function is chosen as in the case of single-integrator kinematics. In the case of a constant virtual leader's velocity, the initial states of the followers are randomly chosen from the square box $[-5, 10]^2$ and $r_0(t)$ is chosen as $[t, 2t + 5]^T$. Using (3.31) for (3.14) in 2D, Fig. 3.8 shows the consecutive snapshots of decentralized swarm tracking for 49 followers with a virtual leader. In the case of a dynamic virtual leader's velocity, the initial states of the followers are randomly chosen from the square box $[-5, 15]^2$ and $r_0(t)$ is chosen as $[t, 5 + t + 2\sin(t)]^T$. Using (3.34) for (3.14) in 2D, Fig. 3.9 shows the consecutive snapshots of decentralized swarm tracking for 50 followers with a virtual leader. Due to the random choice of the initial states, the vehicles form separated subgroups initially. As a result, fragmentation appears in this case. However, for each subgroup, the relative distances of the followers and the virtual leader if the virtual leader is in the subgroup reach local minima.

For decentralized consensus tracking with the connectivity maintenance mechanism in Remark 3.1.12, we choose $R = 3$, α and β the same as those without connectivity maintenance, and $b_{ij}(t)$ according to Remark 3.1.12 with $\frac{d}{dt}b_{ij}(t) = \frac{100||r_i(t)-r_j(t)||}{R^2-||r_i(t)-r_j(t)||^2}$ and $b_{ij}(0) = 1$ when

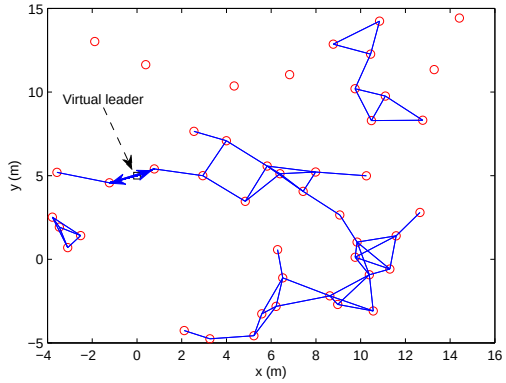

(a) t=0 s.

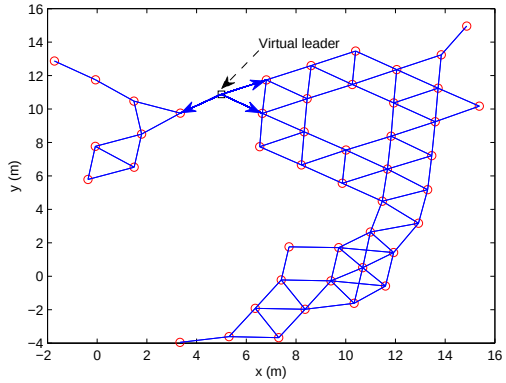

(b) t=5 s.

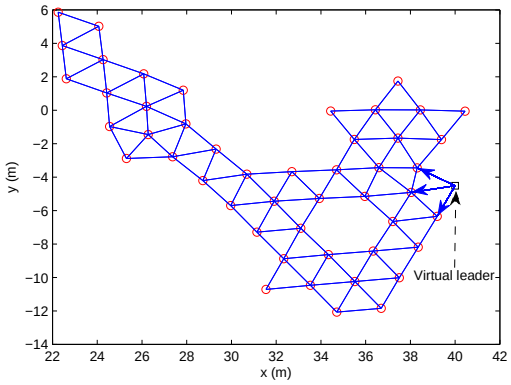

(c) t=40 s.

Fig. 3.5: Decentralized swarm tracking for 48 followers using (3.11) in 2D in the presence of a virtual leader. The circles denote the positions of the followers while the square denotes the position of the virtual leader. An undirected edge connecting two followers means that the two followers are neighbors of each other while a directed edge from the virtual leader to a follower means that the virtual leader is a neighbor of the follower.

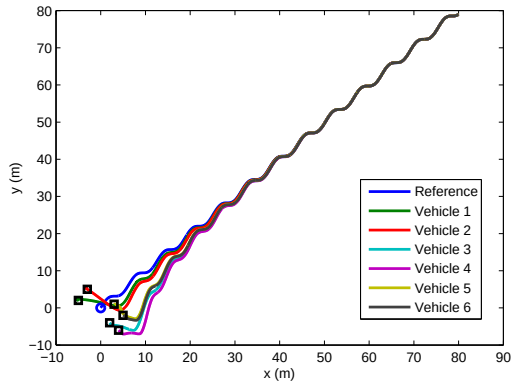

Fig. 3.6: Trajectories of the followers and the virtual leader using (3.15) in 2D. The circle denotes the starting position of the virtual leader while the squares denote the starting positions of the followers.

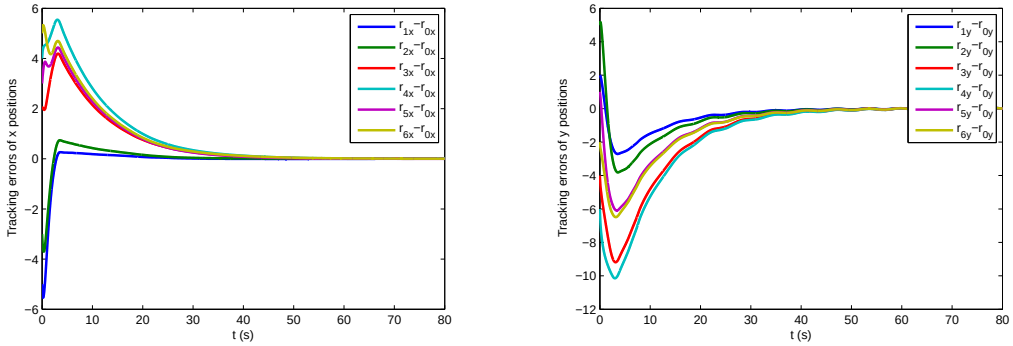

(a) x position.

(b) y position.

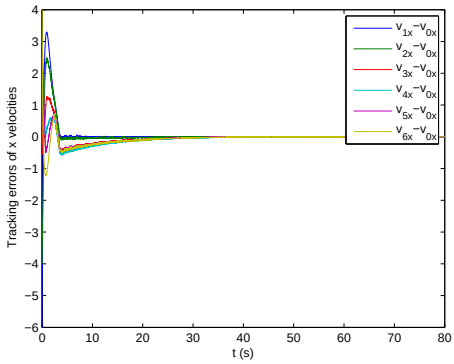

(c) x velocity.

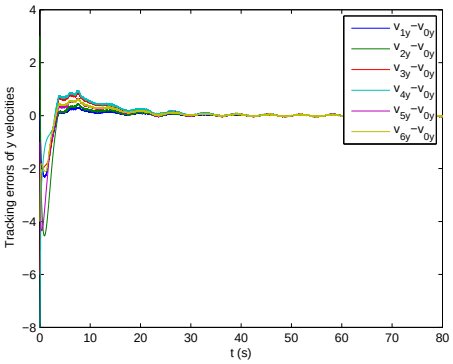

(d) y velocity.

Fig. 3.7: Position and velocity tracking errors using (3.15) in 2D.

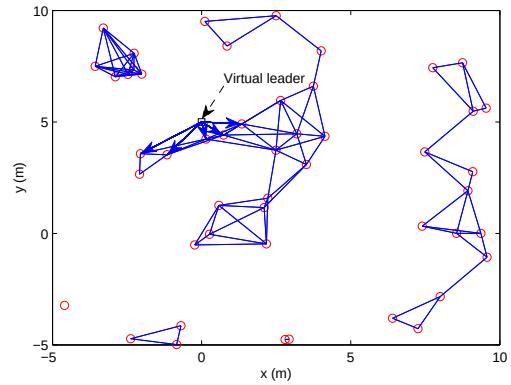

(a) t=0 s.

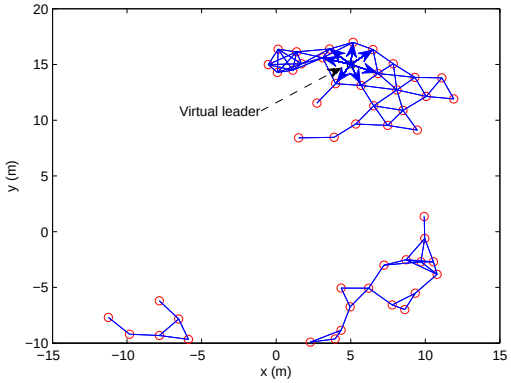

(b) t=5 s.

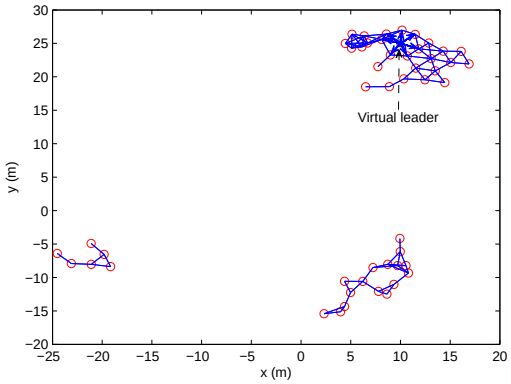

(c) t=10 s.

Fig. 3.8: Decentralized swarm tracking for 49 followers using (3.31) in 2D in the presence of a virtual leader. The circles denote the positions of the followers while the square denotes the position of the virtual leader. An undirected edge connecting two followers means that the two followers are neighbors of each other while a directed edge from the virtual leader to a follower means that the virtual leader is a neighbor of the follower.

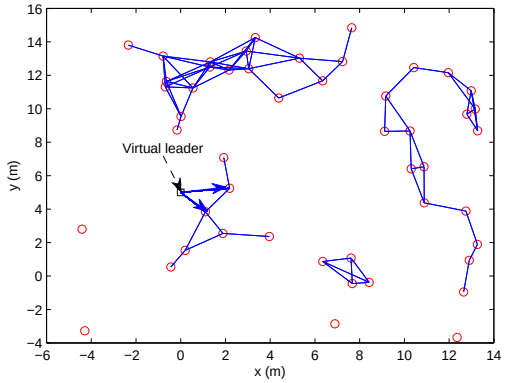

(a) t=0 s.

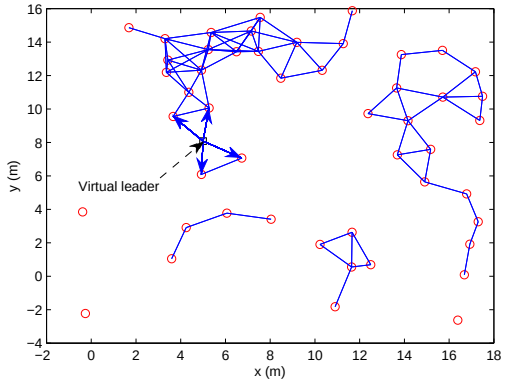

(b) t=5 s.

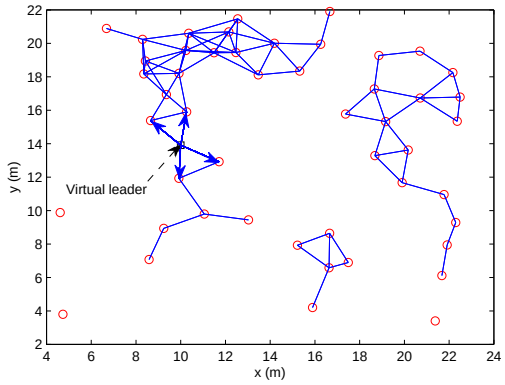

(c) t=10 s.

Fig. 3.9: Decentralized swarm tracking for 50 followers using (3.34) in 2D in the presence of a virtual leader. The circles denote the positions of the followers while the square denotes the position of the virtual leader. An undirected edge connecting two followers means that the two followers are neighbors of each other while a directed edge from the virtual leader to a follower means that the virtual leader is a neighbor of the follower.

$||r_i(0) - r_j(0)|| \leq R$, and $b_{ij}(t) = 1$ if $||r_i(t) - r_j(t)|| \leq R$ and $b_{ij}(t) = 0$ if $||r_i(t) - r_j(t)|| > R$ when $||r_i(0) - r_j(0)|| > R$. Using (3.26) for (3.1) in 2D with the connectivity maintenance mechanism in Remark 3.1.12, Fig. 3.10 shows the trajectories of the followers and the virtual leader. The initial positions of the followers are randomly chosen from the square box $[-2, 2]^2$ and $r_0(t)$ is chosen as $[t, 3\sin(\frac{\pi t}{10})]^T$. The tracking errors of the x and y positions are shown in Figs. 3.11(a) and 3.11(b). It can be seen that the tracking errors ultimately converge to zero. That is, all followers ultimately track the virtual leader as also shown in Fig. 3.10. Using (3.23) for (3.14) in 2D with the connectivity maintenance mechanism in Remark 3.1.12, Fig. 3.12 shows the trajectories of the followers and the virtual leader. The initial positions of the followers are randomly chosen from the square box $[-2, 2]^2$ and $r_0(t)$ is chosen as $[t, t + \sin(t)]^T$. The tracking errors of the x and y positions are shown in Figs. 3.13(a) and 3.13(b). It can be seen from Fig. 3.13 that the tracking errors ultimately converge to zero. That is, all followers ultimately track the virtual leader as also shown in Fig. 3.12.

For decentralized swarm tracking with the connectivity maintenance mechanism as in Remark 3.1.19, R, d_{ij}, α, β, and a_{ij} are chosen the same as those for decentralized swarm tracking without connectivity maintenance. When two followers are initially neighbors of each other or the virtual leader is initially a neighbor of some follower(s), the partial derivative of the corresponding potential function is chosen as (3.37). Otherwise, the partial derivative of the potential function is chosen as (3.36). The initial positions of the followers are randomly chosen from the square box $[-6, 4]^2$ and $r_0(t)$ is chosen the same as the corresponding simulation in the absence of connectivity maintenance mechanism. In the case of single-integrator kinematics, Fig. 3.14 shows the consecutive snapshots of decentralized swarm tracking for 50 followers with a virtual leader in 2D with the connectivity maintenance mechanism in Remark 3.1.19. In the case of double-integrator dynamics with a constant virtual leader's velocity, Fig. 3.15 shows the consecutive snapshots of decentralized swarm tracking for 50 followers with a virtual leader in 2D with the connectivity maintenance mechanism in Remark 3.1.19. In the case of double-integrator dynamics with a varying virtual leader's velocity, Fig. 3.16 shows the consecutive snapshots of decentralized swarm tracking for 50 followers with a virtual leader in 2D with the connectivity maintenance mechanism in Remark 3.1.19. It can

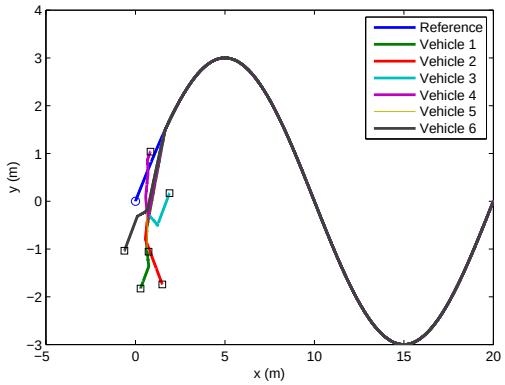

Fig. 3.10: Trajectories of the followers and the virtual leader using (3.26) in 2D with connectivity maintenance mechanism. The circle denotes the starting position of the virtual leader while the squares denote the starting positions of the followers.

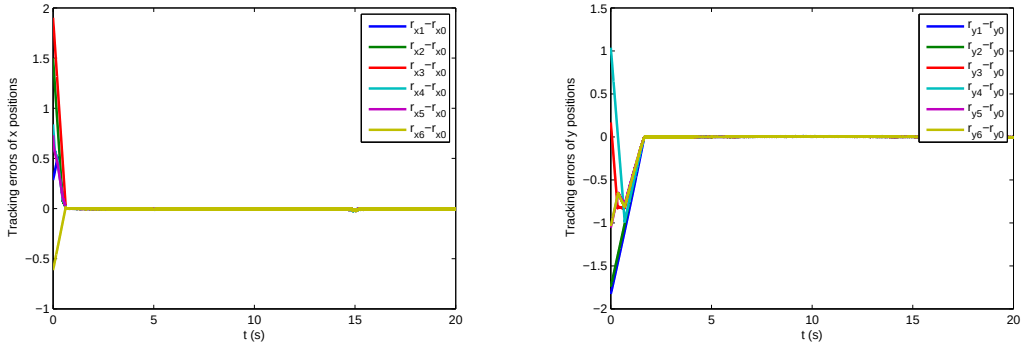

(a) x position. (b) y position.

Fig. 3.11: Position tracking errors using (3.26) in 2D in the presence of connectivity maintenance mechanism.

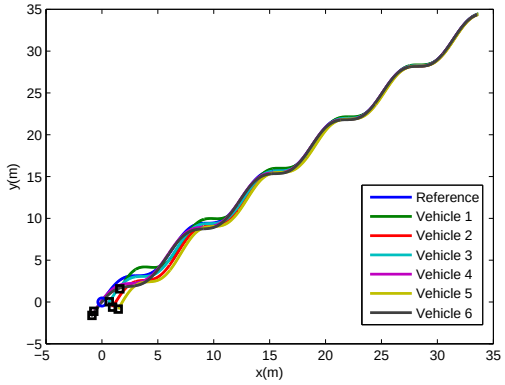

Fig. 3.12: Trajectories of the followers and the virtual leader using (3.23) in 2D with connectivity maintenance mechanism. The circle denotes the starting position of the virtual leader while the squares denote the starting positions of the followers.

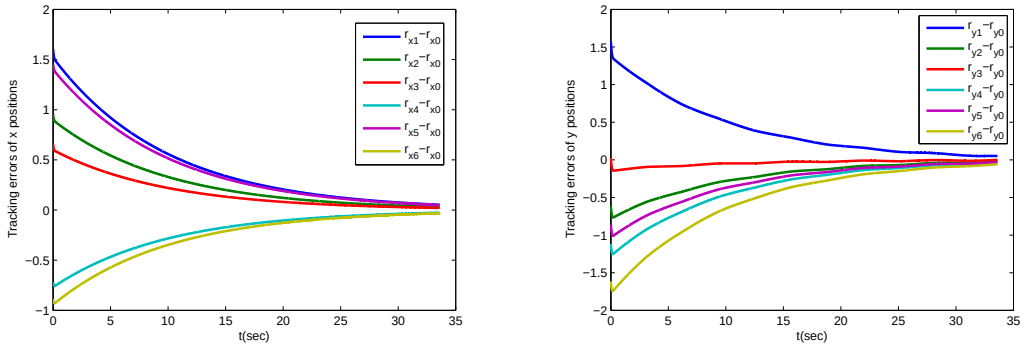

(a) x position. (b) y position.

Fig. 3.13: Position tracking errors using (3.23) in 2D in the presence of connectivity maintenance mechanism.

be seen that at each snapshot the network topology for the 50 followers is connected and the virtual leader is a neighbor of at least one follower because of the initial connectivity and the existence of the connectivity maintenance mechanism. Meanwhile, the relative distances of the followers and the virtual leader ultimately converge to local minima. In contrast to Figs. 3.5, 3.8, and 3.9 where the initially existing connectivity patterns might not always exist, the initially existing connectivity patterns in Fig. 3.14, 3.15, and 3.16 always exist due to the existence of connectivity maintenance mechanism.

3.2 PD-like Discrete-time Consensus Tracking Algorithms with a Reference State

In this section, we propose and study a PD-like discrete-time consensus tracking algorithm in the presence of a group reference state. The comparison between the proposed PD-like discrete-time consensus tracking algorithm and the P-like (proportional like) discrete-time consensus tracking algorithm is also studied.

3.2.1 Existing PD-like Continuous-time Consensus Algorithm

Consider vehicles with single-integrator dynamics given by

$$\dot{r}_i(t) = u_i(t), \quad i = 1, \cdots, n \tag{3.38}$$

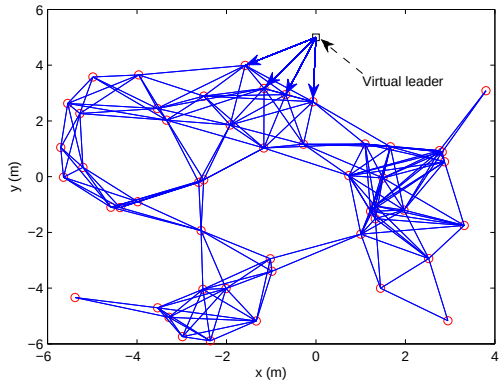

(a) t=0 s.

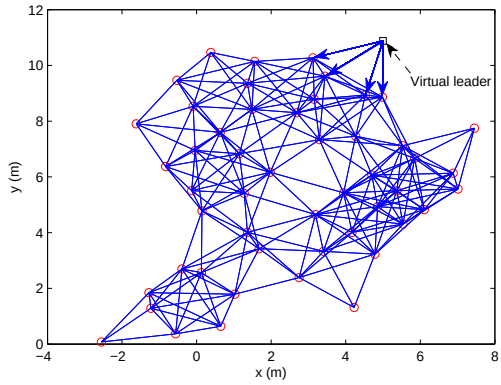

(b) t=5 s.

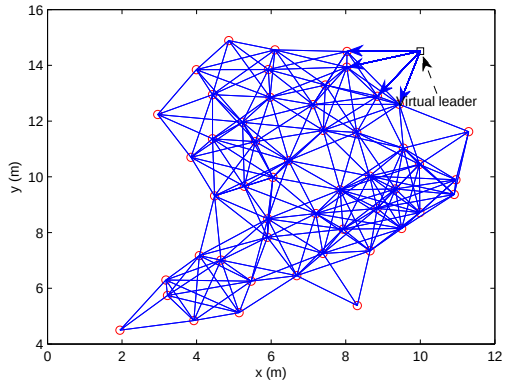

(c) t=10 s.

Fig. 3.14: Decentralized swarm tracking for 50 followers with a virtual leader using (3.11) in 2D in the presence of the connectivity maintenance mechanism in Remark 3.1.19. The circles denote the positions of the followers while the square denotes the position of the virtual leader. An undirected edge connecting two followers means that the two followers are neighbors of each other while a directed edge from the virtual leader to a follower means that the virtual leader is a neighbor of the follower.

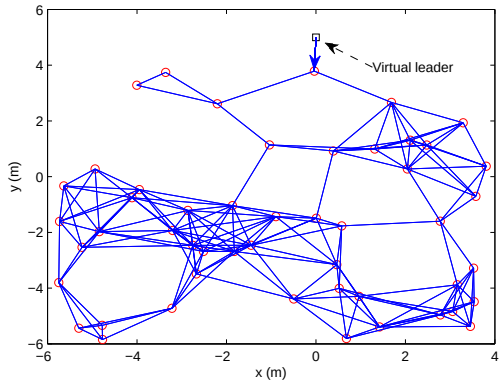

(a) t=0 s.

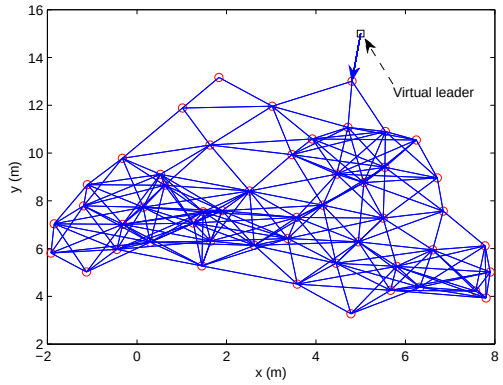

(b) t=5 s.

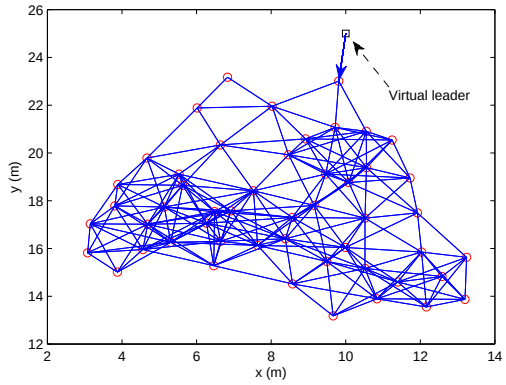

(c) t=10 s.

Fig. 3.15: Decentralized swarm tracking for 50 followers with a virtual leader using (3.31) in 2D in the presence of the connectivity maintenance mechanism in Remark 3.1.19. The circles denote the positions of the followers while the square denotes the position of the virtual leader. An undirected edge connecting two followers means that the two followers are neighbors of each other while a directed edge from the virtual leader to a follower means that the virtual leader is a neighbor of the follower.

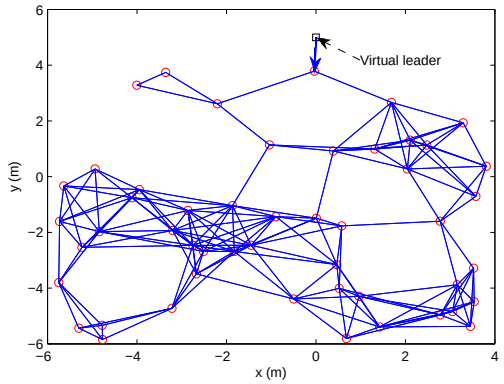

(a) t=0 s.

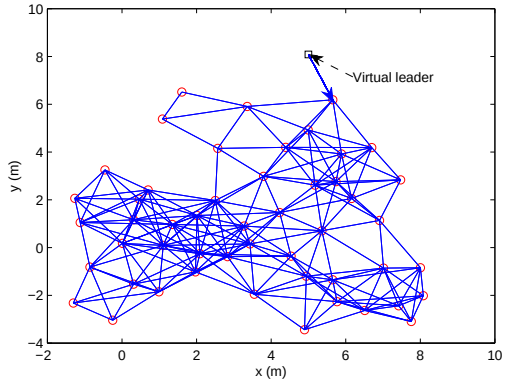

(b) t=5 s.

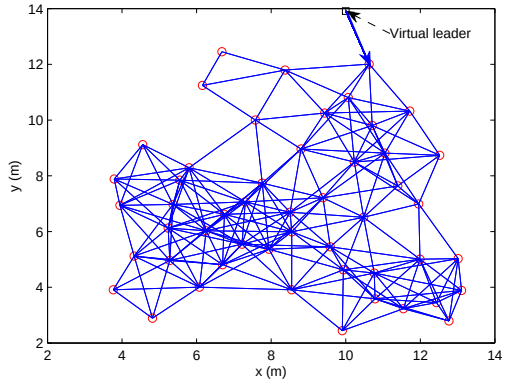

(c) t=10 s.

Fig. 3.16: Decentralized swarm tracking for 50 followers with a virtual leader using (3.34) in 2D in the presence of the connectivity maintenance mechanism in Remark 3.1.19. The circles denote the positions of the followers while the square denotes the position of the virtual leader. An undirected edge connecting two followers means that the two followers are neighbors of each other while a directed edge from the virtual leader to a follower means that the virtual leader is a neighbor of the follower.

where $r_i(t)$ and $u_i(t)$ represent, respectively, the state and control input of the ith vehicle. Suppose that there exists a virtual leader, labeled as vehicle $n+1$, whose state is $r^c(t)$. A PD-like continuous-time consensus algorithm with a time-varying reference state is proposed as [69]

$$\begin{aligned} u_i(t) =& \frac{1}{\eta_i}\sum_{j=1}^{n} a_{ij}\left\{\dot{r}_j(t) - \gamma[r_i(t) - r_j(t)]\right\} \\ &+ \frac{1}{\eta_i} a_{i(n+1)}\left\{\dot{r}^c(t) - \gamma[r_i(t) - r^c(t)]\right\}, \end{aligned} \tag{3.39}$$

where a_{ij} is the (i,j)th entry of adjacency matrix A, $i,j = 1, 2, \cdots, n$, γ is a positive gain, $r^c(t)$ is the time-varying reference state, $a_{i(n+1)} > 0$ if the ith vehicle can access the virtual leader's state[5] and $a_{i(n+1)} = 0$ otherwise, and $\eta_i \triangleq \sum_{j=1}^{n+1} a_{ij}$.

3.2.2 PD-like Discrete-time Consensus Algorithm

Note that (3.39) requires each vehicle to obtain measurements of the derivatives of its neighbors' states and the reference state. This requirement may not be realistic in real applications. We next propose a PD-like discrete-time consensus algorithm with a time-varying reference state. In discrete-time formulation, the single-integrator dynamics (3.38) can be approximated by

$$\frac{r_i[k+1] - r_i[k]}{T} = u_i[k], \tag{3.40}$$

where T is the sampling period, and $r_i[k]$ and $u_i[k]$ represent, respectively, the state and control input of the ith vehicle at $t = kT$. We sample (3.39) to obtain

$$\begin{aligned} u_i[k] =& \frac{1}{\eta_i}\sum_{j=1}^{n} a_{ij}\left(\frac{r_j[k] - r_j[k-1]}{T} - \gamma\{r_i[k] - r_j[k]\}\right) \\ &+ \frac{1}{\eta_i} a_{i(n+1)}\left(\frac{r^c[k] - r^c[k-1]}{T} - \gamma\{r_i[k] - r^c[k]\}\right), \end{aligned} \tag{3.41}$$

where $r^c[k]$ is the reference state at $t = kT$, and $\frac{r_j[k]-r_j[k-1]}{T}$ and $\frac{r^c[k]-r^c[k-1]}{T}$ are used to approximate, respectively, $\dot{r}_j[k]$ and $\dot{r}^c[k]$ in (3.39) because $r_j[k+1]$ and $r^c[k+1]$ cannot be accessed

[5] That is, the virtual leader is a neighbor of vehicle i.

at $t = kT$. Using (3.41) for (3.40), we get the PD-like discrete-time consensus algorithm with a time-varying reference state as

$$\begin{aligned} r_i[k+1] = & r_i[k] \\ & + \frac{T}{\eta_i} \sum_{j=1}^{n} a_{ij} \left(\frac{r_j[k] - r_j[k-1]}{T} - \gamma\{r_i[k] - r_j[k]\} \right) \\ & + \frac{T a_{i(n+1)}}{\eta_i} \left(\frac{r^c[k] - r^c[k-1]}{T} - \gamma\{r_i[k] - r^c[k]\} \right). \end{aligned} \tag{3.42}$$

Note that using algorithm (3.42), each vehicle essentially updates its next state based on its current state and its neighbors' current and previous states as well as the virtual leader's current and previous states if the virtual leader is a neighbor of the vehicle. As a result, (3.42) can be easily implemented in practice.

3.2.3 Convergence Analysis of the PD-like Discrete-time Consensus Algorithm with a Time-varying Reference State

In this section, we analyze algorithm (3.42). We let $\mathrm{diag}\{c_1, \cdots, c_n\}$ denote a diagonal matrix with diagonal entries c_i.

By defining $\delta_i[k] \triangleq r_i[k] - r^c[k]$, it follows that (3.42) can be written as

$$\begin{aligned} \delta_i[k+1] = & \delta_i[k] + \frac{T}{\eta_i} \sum_{j=1}^{n} a_{ij} \left(\frac{\delta_j[k] - \delta_j[k-1]}{T} - \gamma\{\delta_i[k] - \delta_j[k]\} \right) \\ & + \frac{T a_{i(n+1)}}{\eta_i} \left\{ \frac{r^c[k] - r^c[k-1]}{T} - \gamma\delta_i[k] \right\} \\ & - \{r^c[k+1] - r^c[k]\} + \frac{1}{\eta_i} \sum_{j=1}^{n} a_{ij}\{r^c[k] - r^c[k-1]\}, \end{aligned}$$

which can then be written in matrix form as

$$\Delta[k+1] = [(1 - T\gamma)I_n + (1 + T\gamma)D^{-1}A]\Delta[k] - D^{-1}A\Delta[k-1] + X^r[k], \tag{3.43}$$

where $\Delta[k] = [\delta_1[k], \cdots, \delta_n[k]]^T$, $D = \mathrm{diag}\{\eta_1, \cdots, \eta_n\}$, $X^r[k] = \{2r^c[k] - r^c[k-1] - r^c[k+$

$1]\}\mathbf{1}_n$, and A is the adjacency matrix. By defining $Y[k+1] \triangleq \begin{bmatrix} \Delta[k+1] \\ \Delta[k] \end{bmatrix}$, it follows from (3.43) that

$$Y[k+1] = \tilde{A}Y[k] + \tilde{B}X^r[k], \tag{3.44}$$

where

$$\tilde{A} = \begin{bmatrix} (1-T\gamma)I_n + (1+T\gamma)D^{-1}A & -D^{-1}A \\ I_n & \mathbf{0}_{n\times n} \end{bmatrix}, \tag{3.45}$$

and $\tilde{B} = \begin{bmatrix} I_n \\ \mathbf{0}_{n\times n} \end{bmatrix}$. It follows that the solution of (3.44) is

$$Y[k] = \sum_{i=1}^{k} \tilde{A}^{k-i}\tilde{B}X^r[i-1] + \tilde{A}^k Y[0]. \tag{3.46}$$

Note that the eigenvalues of $\tilde{A}$ play an important role in determining the value of $Y[k]$ as $k \to \infty$. In the following, we will study the eigenvalues of $\tilde{A}$. Before moving on, we first need to study the eigenvalues of $D^{-1}A$.

Lemma 3.2.1 *Suppose that the virtual leader has a directed path to all vehicles* 1 *to* n*. Then* $D^{-1}A$ *satisfies* $\left\|(D^{-1}A)^n\right\|_\infty < 1$*, where* D *is defined right after* (3.43) *and* A *is the adjacency matrix. If* $\left\|(D^{-1}A)^n\right\|_\infty < 1$*,* $D^{-1}A$ *has all eigenvalues within the unit circle.*

Proof: For the first statement, denote $\bar{i}_1$ as the set of vehicles that are the children of the virtual leader, and $\bar{i}_j$, $j = 2, 3, \cdots, m$, as the set of vehicles that are the children of $\bar{i}_{j-1}$ that are not in the set $\bar{i}_r$, $1 \le r \le j-1$. Because the virtual leader has a directed path to all vehicles 1 to n, there are at most n edges from the virtual leader to all vehicles 1 to n, which implies $m \le n$. Let p_i and q_i^T denote, respectively, the ith column and row of $D^{-1}A$. When the virtual leader has a directed path to all vehicles 1 to n, without loss of generality, assume that kth vehicle is a child of the virtual leader, i.e., $a_{k(n+1)} > 0$. It follows that $q_k\mathbf{1}_n = 1 - \frac{a_{k(n+1)}}{\sum_{j=1}^{n+1} a_{kj}} < 1$. The same property also applies to other elements in set $\bar{i}_1$. Similarly, assume that the lth vehicle (one node in set $\bar{i}_2$) is a child of the kth vehicle (one node in set $\bar{i}_1$), which implies $a_{lk} > 0$. It follows that the sum of the lth row of

$(D^{-1}A)^2$ can be written as $q_l^T \sum_{i=1}^{n} p_i \leq q_l^T \mathbf{1}_n = 1 - \frac{a_{lk}}{\sum_{j=1}^{n+1} a_{lj}} < 1$. Meanwhile, the sum of the kth row of $(D^{-1}A)^2$ is also less than 1. By following a similar analysis, every row of $(D^{-1}A)^m$ has a sum less than one when the virtual leader has a directed path to all vehicles 1 to n. Because $m \leq n$ and $D^{-1}A$ is nonnegative, $\left\|(D^{-1}A)^n\right\|_\infty < 1$ holds.

For the second statement, when $\left\|(D^{-1}A)^n\right\|_\infty < 1$, it follows that $\lim_{s\to\infty} \left\|[(D^{-1}A)^n]^s\right\|_\infty \leq \lim_{s\to\infty} \left\|(D^{-1}A)^n\right\|_\infty^s = 0$. Assume that some eigenvalues of $D^{-1}A$ are not within the unit circle. By writing $D^{-1}A$ in a canonical Jordan form, it can be computed that $\lim_{s\to\infty}[(D^{-1}A)^n]^s \neq \mathbf{0}_{n\times n}$, which contradicts the fact that $\lim_{s\to\infty} \left\|(D^{-1}A)^n\right\|_\infty^s = 0$. Therefore, $D^{-1}A$ has all eigenvalues within the unit circle. ■

It can be noted from Lemma 3.2.1 that the eigenvalues of $D^{-1}A$ are all within the unit circle if the virtual leader has a directed path to all vehicles 1 to n. We next study the eigenvalues of $\tilde{A}$. Based on Lemmas 3.2.1 and 2.3.1, we next show under what condition the eigenvalues of $\tilde{A}$ are all within the unit circle.

Lemma 3.2.2 *Assume that the virtual leader has a directed path to all vehicles* 1 *to* n*. Let* λ_i *be the* i*th eigenvalue of* $D^{-1}A$*, where* D *is defined right after* (3.43) *and* A *is the adjacency matrix. Then* $\frac{|1-\lambda_i|^2\{2[1-\mathrm{Re}(\lambda_i)]-|1-\lambda_i|^2\}}{|1-\lambda_i|^4+4[\mathrm{Im}(\lambda_i)]^2} > 0$ *holds, where* $\mathrm{Re}(\cdot)$ *and* $\mathrm{Im}(\cdot)$ *denote, respectively, the real and imaginary parts of a number. If positive scalars* T *and* γ *are chosen satisfying* $T\gamma < \min\{1, \min_{i=1,\cdots,n} \frac{2|1-\lambda_i|^2\{2[1-\mathrm{Re}(\lambda_i)]-|1-\lambda_i|^2\}}{|1-\lambda_i|^4+4[\mathrm{Im}(\lambda_i)]^2}\}$*,* $\tilde{A}$*, defined in* (3.45)*, has all eigenvalues within the unit circle.*

Proof: For the first statement, when the virtual leader has a directed path to all vehicles 1 to n, it follows from the second statement in Lemma 3.2.1 that $|\lambda_i| < 1$. It then follows that $|1-\lambda_i|^2 > 0$ and $|1-\lambda_i|^2 = 1 - 2\mathrm{Re}(\lambda_i) + [\mathrm{Re}(\lambda_i)]^2 + [\mathrm{Im}(\lambda_i)]^2 < 2[1-\mathrm{Re}(\lambda_i)]$, which implies $\frac{|1-\lambda_i|^2\{2[1-\mathrm{Re}(\lambda_i)]-|1-\lambda_i|^2\}}{|1-\lambda_i|^4+4[\mathrm{Im}(\lambda_i)]^2} > 0$.

For the second statement, note that the characteristic polynomial of $\tilde{A}$ is given by

$$\begin{aligned}
&\det(sI_{2n} - \tilde{A}) \\
&= \det\left(\begin{bmatrix} sI_n - [(1-T\gamma)I_n + (1+T\gamma)D^{-1}A] & D^{-1}A \\ -I_n & sI_n \end{bmatrix}\right) \\
&= \det\left([sI_n - (1-T\gamma)I_n - (1+T\gamma)D^{-1}A]sI_n + D^{-1}A\right) \\
&= \det\left([s^2 + (T\gamma - 1)s]I_n + [1 - (1+T\gamma)s]D^{-1}A\right),
\end{aligned}$$

where we have used Lemma 2.3.1 to obtain the last equality because $sI_n - [(1-T\gamma)I_n + (1+T\gamma)D^{-1}A]$, $D^{-1}A$, $-I_n$ and sI_n commute pairwise. Noting that λ_i is the ith eigenvalue of $D^{-1}A$, we can get $\det(sI_n + D^{-1}A) = \prod_{i=1}^{n}(s+\lambda_i)$. It thus follows that $\det(sI_{2n} - \tilde{A}) = \prod_{i=1}^{n}\{s^2 + (T\gamma - 1)s + [1-(1+T\gamma)s]\lambda_i\}$. Therefore, the roots of $\det(sI_{2n} - \tilde{A}) = 0$ satisfy

$$s^2 + s[T\gamma - 1 - (1+T\gamma)\lambda_i] + \lambda_i = 0. \tag{3.47}$$

It can be noted that each eigenvalue of $D^{-1}A$, λ_i, corresponds to two eigenvalues of $\tilde{A}$.

Instead of computing the roots of (3.47) directly, we apply the bilinear transformation $s = \frac{z+1}{z-1}$ in (3.47) to get

$$T\gamma(1-\lambda_i)z^2 + 2(1-\lambda_i)z + (2+T\gamma)\lambda_i + 2 - T\gamma = 0. \tag{3.48}$$

Because the bilinear transformation maps the left half of the complex s-plane to the interior of the unit circle in the z-plane, it follows that (3.47) has all roots within the unit circle if and only if (4.27) has all roots in the open left half plane (LHP). In the following, we will study the condition on T and γ under which (4.27) has all roots in the open LHP. Letting z_1 and z_2 denote the roots of (4.27), it follows from (4.27) that

$$z_1 + z_2 = -\frac{2}{T\gamma} \tag{3.49}$$

$$z_1 z_2 = \frac{(2+T\gamma)\lambda_i + 2 - T\gamma}{T\gamma(1-\lambda_i)}. \tag{3.50}$$

Noting that (3.49) implies that $\mathrm{Im}(z_1) + \mathrm{Im}(z_2) = 0$, we define $z_1 = a_1 + \mathbf{j}b$ and $z_2 = a_2 - \mathbf{j}b$,

where **j** is the imaginary unit. It can be noted that z_1 and z_2 have negative real parts if and only if $a_1a_2 > 0$ and $a_1 + a_2 < 0$. Note that (3.49) implies $a_1 + a_2 < 0$ because $T\gamma > 0$. We next show the sufficient condition on T and γ such that $a_1a_2 > 0$ holds. By substituting the definitions of z_1 and z_2 into (3.50), we have

$$a_1a_2 + b^2 + \mathbf{j}(a_2 - a_1)b = \frac{(2 + T\gamma)\lambda_i + 2 - T\gamma}{T\gamma(1 - \lambda_i)},$$

which implies

$$a_1a_2 + b^2 = -\frac{2 + T\gamma}{T\gamma} + \frac{4[1 - \mathrm{Re}(\lambda_i)]}{T\gamma|1 - \lambda_i|^2} \tag{3.51}$$

$$(a_2 - a_1)b = \frac{4\mathrm{Im}(\lambda_i)}{T\gamma|1 - \lambda_i|^2}. \tag{3.52}$$

It follows from (3.52) that $b = \frac{4\mathrm{Im}(\lambda_i)}{T\gamma(a_2-a_1)|1-\lambda_i|^2}$. Considering also the fact that $(a_2 - a_1)^2 = (a_1 + a_2)^2 - 4a_1a_2 = \frac{4}{T^2\gamma^2} - 4a_1a_2$. After some manipulation, (3.51) can be written as

$$K_1(a_1a_2)^2 + K_2a_1a_2 + K_3 = 0, \tag{3.53}$$

where $K_1 = T^2\gamma^2|1 - \lambda_i|^4$, $K_2 = -|1 - \lambda_i|^4 + (2 + T\gamma)T\gamma|1 - \lambda_i|^4 - 4[1 - \mathrm{Re}(\lambda_i)]T\gamma|1 - \lambda_i|^2$ and $K_3 = \frac{1}{T\gamma}\{4[1 - \mathrm{Re}(\lambda_i)]|1 - \lambda_i|^2 - (2 + T\gamma)|1 - \lambda_i|^4\} - 4[\mathrm{Im}(\lambda_i)]^2$. It can be computed that $K_2^2 - 4K_1K_3 = \{|1 - \lambda_i|^4 + (2 + T\gamma)T\gamma|1 - \lambda_i|^4 - 4[1 - \mathrm{Re}(\lambda_i)]T\gamma|1 - \lambda_i|^2\}^2 + 16T^2\gamma^2|1 - \lambda_i|^4[\mathrm{Im}(\lambda_i)]^2 \geq 0$, which implies that (3.53) has two real roots. Because $|\lambda_i| < 1$, it is straightforward to know $K_1 > 0$. Therefore, a sufficient condition for $a_1a_2 > 0$ is that $K_2 < 0$ and $K_3 > 0$. When $0 < T\gamma \leq 1$, because $|1 - \lambda_i|^2 < 2[1 - \mathrm{Re}(\lambda_i)]$ as is shown in the proof of the first statement, it follows that $K_2 < -|1 - \lambda_i|^4 + (2 + T\gamma)T\gamma|1 - \lambda_i|^4 - 2|1 - \lambda_i|^2T\gamma|1 - \lambda_i|^2 = |1 - \lambda_i|^4[-1 + (T\gamma)^2] \leq 0$. Similarly, when $0 < T\gamma < \frac{2|1-\lambda_i|^2\{2[1-\mathrm{Re}(\lambda_i)]-|1-\lambda_i|^2\}}{|1-\lambda_i|^4+4[\mathrm{Im}(\lambda_i)]^2}$, it follows that $K_3 > 0$. Therefore, if positive scalars γ and T satisfy $T\gamma < \min\{1, \min_{i=1,\cdots,n} \frac{2|1-\lambda_i|^2\{2[1-\mathrm{Re}(\lambda_i)]-|1-\lambda_i|^2\}}{|1-\lambda_i|^4+4[\mathrm{Im}(\lambda_i)]^2}\}$, all eigenvalues of $\tilde{A}$ are within the unit circle. ■

In the following, we apply Lemma 3.2.2 into (3.46) to derive the bound of the tracking errors.

Theorem 3.2.1 *Assume that the reference state $r^c[k]$ satisfies $|\frac{r^c[k-1]-r^c[k]}{T}| \leq \bar{r}$, and the virtual*

leader has a directed path to all vehicles 1 *to* n*. Let* λ_i *be the* i*th eigenvalue of* $D^{-1}A$*, where* D *is defined right after* (3.43) *and* A *is the adjacency matrix. When positive scalars* γ *and* T *satisfy* $T\gamma < \min\{1, \min_{i=1,\cdots,n} \frac{2|1-\lambda_i|^2\{2[1-\mathrm{Re}(\lambda_i)]-|1-\lambda_i|^2\}}{|1-\lambda_i|^4+4[\mathrm{Im}(\lambda_i)]^2}\}$*, using algorithm* (3.42)*,* $||Y[k]||_\infty$*, defined before* (3.44)*, is bounded by* $2T\bar{r}\left\|\tilde{A}(I_{2n}-\tilde{A})^{-1}\right\|_\infty$ *as* $k \to \infty$*, where* $\tilde{A}$ *is defined in* (3.45)*.*

Proof: When the virtual leader has a directed path to all vehicles 1 to n, it follows from Lemma 3.2.2 that $\tilde{A}$ has all eigenvalues within the unit circle if positive scalars T and γ are chosen satisfying $T\gamma < \min\{1, \min_{i=1,\cdots,n} \frac{2|1-\lambda_i|^2\{2[1-\mathrm{Re}(\lambda_i)]-|1-\lambda_i|^2\}}{|1-\lambda_i|^4+4[\mathrm{Im}(\lambda_i)]^2}\}$. Therefore, $\lim_{k\to\infty}\tilde{A}^k = \mathbf{0}_{2n\times 2n}$. It follows from (3.46) that

$$\begin{aligned}\lim_{k\to\infty}\|Y[k]\|_\infty &= \lim_{k\to\infty}\left\|\sum_{i=1}^{k-1}\tilde{A}^{k-i}\tilde{B}X^r[k]\right\|_\infty \\ &\le \lim_{k\to\infty}\left\|\sum_{i=1}^{k-1}\tilde{A}^i\right\|_\infty\left\|\tilde{B}\right\|_\infty\|X^r[k]\|_\infty .\end{aligned}$$

Similarly, we have

$$\begin{aligned}\lim_{k\to\infty}\|X^r[k]\|_\infty =& \|\{2r^c[k]-r^c[k-1]-r^c[k+1]\}\mathbf{1}_n\|_\infty \\ \le& 2T\bar{r}, \end{aligned} \tag{3.54}$$

where we have used the fact that $|\frac{r^c[k]-r^c[k-1]}{T}| \le \bar{r}$ to derive (3.54). Meanwhile, because all eigenvalues of $\tilde{A}$ are within the unit circle, it follows from Lemma $5.6.10$ [86] that there exists a matrix norm $|||\cdot|||$ such that $|||\tilde{A}||| < 1$. It then follows from Theorem 4.3 [96] that

$$\lim_{k\to\infty}\|Y[k]\|_\infty \le 2T\bar{r}\left\|\tilde{A}(I_{2n}-\tilde{A})^{-1}\right\|_\infty .$$

■

Remark 3.2.2 *From Theorem 3.2.1, it can be noted that the bound of the tracking error using PD-like discrete-time consensus algorithm with a time-varying reference state is proportional to the sampling period* T*. As* $T \to 0$*, the tracking error will go to zero ultimately when* $|\frac{r^c[k]-r^c[k-1]}{T}|$ *is bounded and the virtual leader has a directed path to all vehicles* 1 *to* n*.*

3.2.4 Comparison Between P-like and PD-like Discrete-time Consensus Algorithms with a Time-varying Reference State

A P-like continuous-time consensus algorithm without a reference state is studied for (3.38) as [36,37,39] $u_i(t) = \sum_{j=1}^{n} a_{ij}[r_j(t) - r_i(t)]$. When there exists a virtual leader whose state is the reference state $\xi^r(t)$, a P-like continuous-time consensus algorithm is given as

$$u_i(t) = \sum_{j=1}^{n} a_{ij}[r_j(t) - r_i(t)] + a_{i(n+1)}[r^c(t) - r_i(t)], \tag{3.55}$$

where a_{ij} and $a_{i(n+1)}$ are defined as in (3.39). By sampling (3.55), we obtain

$$u_i[k] = \sum_{j=1}^{n} a_{ij}\{r_j[k] - r_i[k]\} + a_{i(n+1)}\{r^c[k] - r_i[k]\}. \tag{3.56}$$

Using (3.56) for (3.40), we get the P-like discrete-time consensus algorithm with a time-varying reference state as

$$r_i[k+1] = r_i[k] + T\sum_{j=1}^{n} a_{ij}(r_j[k] - r_i[k]) + Ta_{i(n+1)}(r^c[k] - r_i[k]), \tag{3.57}$$

where T is the sampling period. By defining $\delta_i[k] \triangleq r_i[k] - r^c[k]$, we rewrite (3.57) as

$$\delta_i[k+1] = \delta_i[k] + T\sum_{j=1}^{n} a_{ij}(\delta_j[k] - \delta_i[k]) - Ta_{i(n+1)}\delta_i[k] - (r^c[k+1] - r^c[k]),$$

which can then be written in matrix form as

$$\Delta[k+1] = Q\Delta[k] - (r^c[k+1] - r^c[k])\mathbf{1}_n, \tag{3.58}$$

where $\Delta[k] = [\delta_1[k], \cdots, \delta_n[k]]^T$, $Q = I_n - T\mathcal{L} - T\mathrm{diag}\{a_{1(n+1)}, \cdots, a_{n(n+1)}\}$, and $\mathcal{L}$ is the Laplacian matrix. It follows that Q is nonnegative when $T < \min_{i=1,\cdots,n} \frac{1}{\sum_{j=1}^{n+1} a_{ij}}$.

Lemma 3.2.3 *Assume that the virtual leader has a directed path to all vehicles* 1 *to* n*. When* $T < \min_{i=1,\cdots,n} \frac{1}{\sum_{j=1}^{n+1} a_{ij}}$*,* Q *satisfies* $\|Q^n\|_\infty < 1$*, where* Q *is defined right after* (3.58)*. Furthermore, if* $\|Q^n\|_\infty < 1$*,* Q *has all eigenvalues within the unit circle.*

Proof: The proof is similar to that of Lemma 3.2.1 and is omitted here.

Theorem 3.2.3 *Assume that the reference state $r^c[k]$ satisfies $|\frac{r^c[k]-r^c[k-1]}{T}| \leq \bar{r}$, and the virtual leader has a directed path to all vehicles 1 to n. When $T < \min_{i=1,\cdots,n} \frac{1}{\sum_{j=1}^{n+1} a_{ij}}$, using algorithm* (3.57)*, $\|\Delta[k]\|_\infty$ is bounded by $\bar{r} \left\|Q(L + \mathrm{diag}\{a_{1(n+1)}, \cdots, a_{n(n+1)}\})^{-1}\right\|_\infty$ as $k \to \infty$, where Q and $\Delta[k]$ are defined after* (3.58)*.*

Proof: The solution of (3.58) is

$$\Delta[k] = Q^k \Delta[0] - \sum_{i=1}^{k-1} Q^{k-i}(r^c[k+1] - r^c[k])\mathbf{1}_n. \tag{3.59}$$

When the virtual leader has a directed path to all vehicles 1 to n, it follows from Lemma 3.2.3 that Q has all eigenvalues within the unit circle when $T < \min_{i=1,\cdots,n} \frac{1}{\sum_{j=1}^{n+1} a_{ij}}$, which implies $Q^k \to \mathbf{0}_{n\times n}$ as $k \to \infty$. It follows from (3.59) that

$$\lim_{k\to\infty} \Delta[k] = -\lim_{k\to\infty} \sum_{i=1}^{k} Q^{k-i}(r^c[k+1] - r^c[k])\mathbf{1}_n.$$

As $|\frac{r^c[k]-r^c[k-1]}{T}| \leq \bar{r}$, it follows that

$$\lim_{k\to\infty} \|\Delta[k]\|_\infty \leq \lim_{k\to\infty} \bar{r}T \left\|\sum_{i=1}^{k-1} Q^{k-i}\right\|_\infty. \tag{3.60}$$

Because Q has all eigenvalues within the unit circle, it follows from Lemma $5.6.10$ [86] that there exists a matrix norm $|||\cdot|||$ such that $|||Q||| < 1$. It then follows from (3.60) that

$$\begin{aligned}
&\lim_{k\to\infty} \|\Delta[k]\|_\infty \\
&\leq \lim_{k\to\infty} \bar{r}T \left\|(Q + Q^2 + \ldots + Q^{k-1})\right\|_\infty \\
&= \bar{r}T \left\|Q(I_n - Q)^{-1}\right\|_\infty \\
&= \bar{r} \left\|Q(\mathcal{L} + \mathrm{diag}\{a_{1(n+1)}, \cdots, a_{n(n+1)}\})^{-1}\right\|_\infty,
\end{aligned}$$

where we have used Theorem 4.3 [96] to obtain the last equality. ■

Remark 3.2.4 *In contrast to the results in Theorem 3.2.1, the bound of the tracking error using P-like discrete-time consensus algorithm* (3.57) *is not proportional to the sampling period* T*. In fact, as* $T \to 0$*, the tracking error using* (3.57) *will not go to zero* [69].

The comparison between Theorem 3.2.1 and Theorem 3.2.3 shows the benefit of the PD-like discrete-time consensus algorithm over the P-like discrete-time consensus algorithm when there exists a time-varying reference state that is available to only a subset of the team members. As a special case, when the reference state is time-invariant, i.e., $\bar{r} = 0$, it follows from Theorems 3.2.1 and 3.2.3 that the tracking error will go to zero ultimately for both P-like and PD-like discrete-time consensus algorithms.

Remark 3.2.5 *From Theorem 3.2.1, it can be noted that the product* $T\gamma$ *should be less than a positive upper bound to ensure system stability when using PD-like discrete-time consensus algorithm* (3.42)*. Accordingly, the sampling period* T *can be increased by decreasing the control gain* γ*. In contrast, when using P-like discrete-time consensus algorithm* (3.57)*, the sampling period* T *should be less than a positive upper bound to ensure system stability. In real applications, the sampling period may be large. In this case, PD-like discrete-time consensus algorithm also shows benefit over P-like discrete-time consensus algorithm.*

3.2.5 Simulation

In this section, a simulation example is presented to illustrate the PD-like discrete-time consensus algorithm. To show the benefit of the PD-like discrete-time consensus algorithm, the simulation result using the P-like discrete-time consensus algorithm is also presented. We consider a team of four vehicles with a directed graph given by Fig. 3.17 and let the first, third and fourth vehicles access the time-varying reference state. It can be noted that the virtual leader has a directed path to all four vehicles. The Laplacian matrix is chosen as $\mathcal{L} = \begin{bmatrix} 1 & -1 & 0 & 0 \\ -1 & 2 & -1 & 0 \\ -1 & 0 & 1 & 0 \\ 0 & -1 & -1 & 2 \end{bmatrix}$.

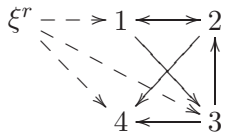

Fig. 3.17: Directed graph for four vehicles. A solid arrow from j to i denotes that vehicle i can receive information from vehicle j. A dashed arrow from ξ^r to l denotes that vehicle l can receive information from the virtual leader.

For both the P-like and PD-like discrete-time consensus algorithms with a time-varying reference state, we let the initial states of the four vehicles $[r_1[0], r_2[0], r_3[0], r_4[0]] = [3, 1, -1, -2]$ and $[r_1[-1], r_2[-1], r_3[-1], r_4[-1]] = [0, 0, 0, 0]$. The reference state is chosen as $\sin(t) + t$. Figs. 3.18(a) and 3.18(b) show, respectively, the states $r_i(t)$ and tracking errors $r^c(t) - r_i(t)$ by using PD-like discrete-time consensus algorithm (3.42) with a time-varying reference state when $T = 0.5$ sec and $\gamma = 1$. From Fig. 3.18(b), it can be seen that the four vehicles can track the reference state with large tracking errors. Figures 3.18(c) and 3.18(d) show, respectively, the states $\xi_i(t)$ and tracking errors $r^c(t) - r_i(t)$ by using PD-like discrete-time consensus algorithm (3.42) with the same reference state when $T = 0.1$ sec and $\gamma = 5$. From Fig. 3.18(d), it can be seen that the four vehicles can track the reference state with very small tracking errors. This shows that the tracking errors will be larger if the sampling period becomes larger. As a counterexample, Figs. 3.18(e) and 3.18(f) show, respectively, the state $r_i(t)$ and tracking errors $r^c(t) - r_i(t)$ when $T = 0.2$ sec and $\gamma = 5$. It can be noted that the system is unstable when the product $T\gamma$ is larger than the positive upper bound proposed in Theorem 3.2.1. Figures. 3.19(a) and 3.19(b) show, respectively, the states $r_i(t)$ and tracking errors $r^c(t) - r_i(t)$ by using P-like discrete-time consensus algorithm (3.57) with the same time-varying reference state when $T = 0.1$ sec and $\gamma = 5$. It can be seen that the tracking error using P-like discrete-time consensus algorithm (3.57) is much larger than that using PD-like discrete-time consensus algorithm (3.42) under the same condition. This shows the benefit of the PD-like discrete-time consensus algorithm over the P-like discrete-time consensus algorithm when there exists a time-varying reference state that is available to only a subset of the team members.

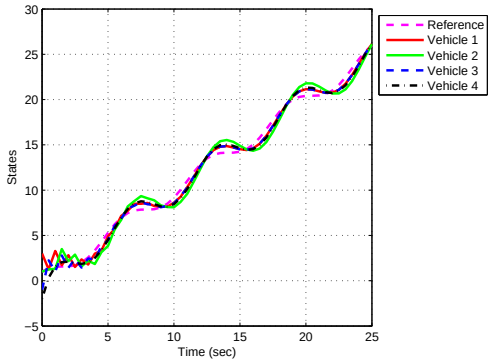

(a) States ($T = 0.5$ sec and $\gamma = 1$).

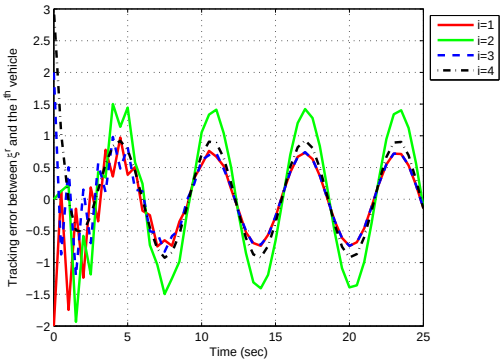

(b) Tracking errors ($T = 0.5$ sec and $\gamma = 1$).

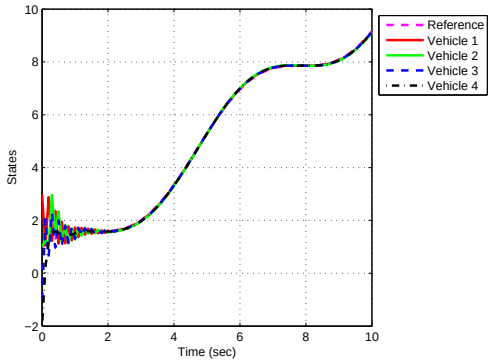

(c) States ($T = 0.1$ sec and $\gamma = 5$).

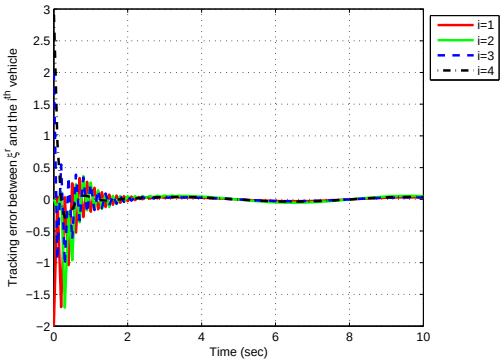

(d) Tracking errors ($T = 0.1$ sec and $\gamma = 5$).

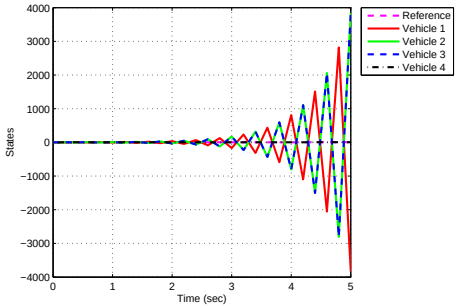

(e) States ($T = 0.2$ sec and $\gamma = 5$).

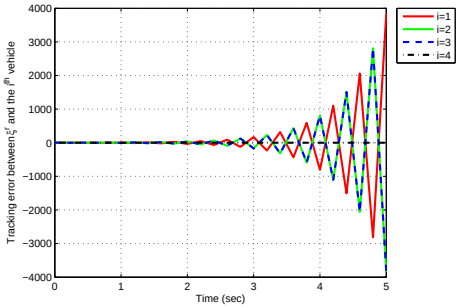

(f) Tracking errors ($T = 0.2$ sec and $\gamma = 5$).

Fig. 3.18: Consensus tracking with a time-varying reference state using PD-like discrete-time consensus algorithm (3.42) under different T and γ.

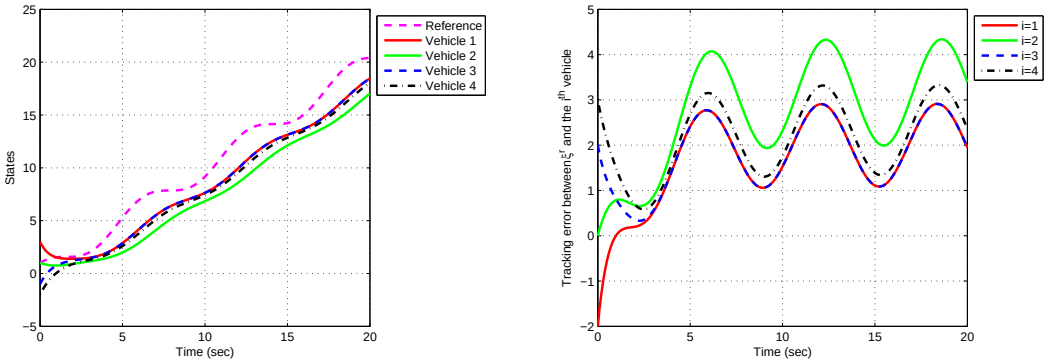

(a) States ($T = 0.1$ sec and $\gamma = 5$). (b) Tracking errors ($T = 0.1$ sec and $\gamma = 5$).

Fig. 3.19: Consensus tracking with a time-varying reference state using P-like discrete-time consensus algorithm (3.57).

Chapter 4

Decentralized Containment Control with Multiple Group Reference States

In the previous several chapters, we have investigated the coordination problems when there exists at most one group reference state. In this chapter, we study the case when there exists multiple group reference states. The group reference states are also called "leaders." We study the decentralized containment control problem in which all followers will converge to the convex hull formed by the leaders and consistently stay within the convex hull. A stop-and-go strategy was proposed to solve the problem of driving a collection of mobile agents to the convex polytope spanned by dedicated leaders under an undirected network topology [97]. This stop-and-go strategy was then used to solve the problem of driving a collection of mobile agents to the convex polytope formed by the stationary/dynamic leaders in an orderly manner [76]. Note that the study focused on fixed undirected interaction.

In this chapter, we will study containment problems for both single-integrator kinematics and double-integrator dynamics in both fixed and switching directed network topology. In addition, we will also present experimental results on a multi-robot platform to validate some theoretical results.

4.1 Definitions and Notations

Definition 4.1.1 *For a directed graph $\mathcal{G} = (\mathcal{V}, \mathcal{W})$, an agent is called a* leader *if the agent has no neighbor. An agent is called a* follower *if the agent is not a leader. Assume that there are m leaders, where $m < n$. We use $\mathcal{R}$ and $\mathcal{F}$ to denote, respectively, the leader set and the follower set. The directed graph $\mathcal{G}$ has a* united directed spanning tree *if for any one of the $n - m$ followers, there exists at least one leader which has a directed path to the follower.*

Definition 4.1.2 *Let $\mathcal{C}$ be a set in a real vector space $V \subseteq \mathbb{R}^p$. The set $\mathcal{C}$ is called* convex *if, for any x and y in $\mathcal{C}$, the point $(1-z)x + zy$ is in $\mathcal{C}$ for any $z \in [0,1]$. The convex hull for a set of points $X = \{x_1, \cdots, x_q\}$ in V is the minimal convex set containing all points in X. We use $\mathbf{Co}(X)$ to denote the convex hull of X. In particular, when $V \subseteq \mathbb{R}$, $\mathbf{Co}(X) = \{x | x \in [\min_i x_i, \max_i x_i]\}$.*

Definition 4.1.3 *The matrix $B \in \mathbb{R}^{n\times n}$ is called a (row)* stochastic matrix *if each entry of B is nonnegative and each row of B has a sum equal to one.*

4.2 Single-integrator Kinematics

4.2.1 Stability Analysis with Multiple Stationary Leaders

In this section, we study the conditions on, respectively, the fixed and switching directed network topologies such that all followers will ultimately converge to the stationary convex hull formed by the stationary leaders.

Consider a group of n autonomous agents with single-integrator kinematics given by

$$\dot{r}_i(t) = u_i(t), \quad i = 1, \ldots, n, \tag{4.1}$$

where $r_i(t) \in \mathbb{R}^p$ and $u_i(t) \in \mathbb{R}^p$ are, respectively, the state and the control input of the ith agent. A common consensus algorithm for (4.1) was studied as [36, 37, 39, 98, 99]

$$u_i(t) = -\sum_{j=1}^{n} a_{ij}(t)[r_i(t) - r_j(t)], \quad i = 1, \ldots, n, \tag{4.2}$$

where $a_{ij}(t)$ is the (i,j)th entry of the adjacency matrix $\mathcal{A}(t)$ at time t. The objective of (6.2) is to guarantee consensus, i.e., $r_i(t) \to r_j(t)$ for arbitrary initial conditions $r_i(0)$, $i = 1, \cdots, n$. Conditions on the network topology to ensure consensus were studied [36, 37, 39, 98, 99], but these references only considered the case when there exists at most one leader in the group.

Suppose that there are $m, m < n$, stationary leaders and $n - m$ followers. Equation (4.2) becomes

$$u_i(t) = 0, \quad i \in \mathcal{R}$$
$$u_i(t) = -\sum_{j \in \mathcal{F} \bigcup \mathcal{R}} a_{ij}(t)[r_i(t) - r_j(t)], \quad i \in \mathcal{F}. \tag{4.3}$$

Note that $r_j, j \in \mathcal{R}$, is constant because the leaders are stationary.

Fixed Directed Interaction

In this subsection, we assume that the directed interaction is fixed, i.e., all $a_{ij}(t)$ in (4.14) are constant. We first assume that all agents are in a one-dimensional space, i.e., $p = 1$ in (4.1).

Theorem 4.2.1 *For an n-agent system, using* (4.14) *for* (4.1)*, all followers will always converge to the stationary convex hull $\mathbf{Co}\{r_j, j \in \mathcal{R}\}$ for arbitrary initial conditions $r_i(0), i \in \mathcal{F}$, if and only if the directed graph $\mathcal{G}$ for the n agents has a united directed spanning tree.*

Proof: (Necessity) Suppose that the directed graph $\mathcal{G}$ does not have a united directed spanning tree. Then there exists a follower, labeled as k, to which all leaders do not have a directed path. It follows that the state of follower k is independent of the states of the leaders. Therefore, follower k cannot always converge to the stationary convex hull $\mathbf{Co}\{r_j, j \in \mathcal{R}\}$ for arbitrary initial conditions.

(Sufficiency) Define $r_L^+ \triangleq \max\{r_j, j \in \mathcal{R}\}$, $r_L^- \triangleq \min\{r_j, j \in \mathcal{R}\}$, $r_F^+ \triangleq \max\{x_j, j \in \mathcal{F}\}$, and $r_F^- \triangleq \min\{x_j, j \in \mathcal{F}\}$. To show that all followers will converge to the stationary convex hull $\mathbf{Co}\{r_j, j \in \mathcal{R}\}$, we study the following four cases:

Case 1. All followers are initially within the stationary convex hull $\mathbf{Co}\{r_j, j \in \mathcal{R}\}$. In this case, it follows from (4.14) that the states of the $n - m$ followers cannot be larger than r_L^+ or less than x_L^- because for any follower j, $\dot{r}_j < 0$ if $r_j > r_L^+$ and $\dot{r}_j > 0$ if $r_j < r_L^-$. Therefore, all $n - m$ followers will always be within the stationary convex hull $\mathbf{Co}\{r_j, j \in \mathcal{R}\}$.

Case 2. The initial states of some followers are larger than r_L^+ and the others are initially within the stationary convex hull $\mathbf{Co}\{r_j, j \in \mathcal{R}\}$. We next show that $r_F^+ \leq r_L^+$ as $t \to \infty$ and $r_F^- \leq r_L^-$ for all t.

Step 1: r_F^+ is a nonincreasing function if $r_F^+ > r_L^+$. From (4.14), for the follower(s) with the state r_F^+, the control input will be less than or equal to zero. Therefore, the state(s) of the follower(s) with the state r_F^+ will not increase. Meanwhile, the states of the other followers in $\mathcal{F}$ cannot be larger than the current maximal state r_F^+ according to (4.14). Therefore, r_F^+ is a nonincreasing function.

Step 2: r_F^+ will decrease after a finite period of time if $r_F^+ > r_L^+$ and the directed graph $\mathcal{G}$ has a united directed spanning tree. The proof of this part is motivated by Moreau's work [98]. Different from the analysis in Moreau's work [98], we consider the multi-leader case. By using the convexity property and following a similar analysis to that in Moreau's work [98], it can be shown that r_F^+ will decrease after a finite period of time.

Combining Steps 1 and 2, we get that $r_F^+ \leq r_L^+$ as $t \to \infty$. Note also that $r_F^- \geq r_L^-$ for all t according to (4.14). Therefore, all followers will converge to the stationary convex hull $\mathbf{Co}\{r_j, j \in \mathcal{R}\}$.

Case 3. The initial states of some followers are less than r_L^- and the others are initially within the stationary convex hull $\mathbf{Co}\{r_j, j \in \mathcal{R}\}$. The analysis of this case is similar to the analysis of Case 2 by showing that $r_F^- \geq r_L^-$ as $t \to \infty$ and $r_F^+ \leq r_L^+$ for all t.

Case 4. The initial states of some followers are larger than r_L^+, the initial states of some followers are less than r_L^-, and the others are initially within the stationary convex hull $\mathbf{Co}\{r_j, j \in \mathcal{R}\}$. The analysis of this case is a combination of Cases 2 and 3. ■

Remark 4.2.2 *In Theorem 4.2.1, the containment control problem is studied in a one-dimensional space. We next show that the same conclusion holds for any high-dimensional space. In the case of a high-dimensional space, i.e.,* $p > 1$ *in* (4.1)*, by using the decoupling technique, it follows that all followers will converge to the smallest hyperrectangle containing the stationary leaders under the conditions of Theorem 4.2.1. Note that from* (4.1) *and* (4.14)*,*

$$\begin{aligned} R\dot{r}_i(t) &= -R \sum_{j \in \mathcal{F} \bigcup \mathcal{R}} a_{ij}(t)[r_i(t) - r_j(t)] \\ &= - \sum_{j \in \mathcal{F} \bigcup \mathcal{R}} a_{ij}(t)[Rr_i(t) - Rr_j(t)], \quad i \in \mathcal{F}, \end{aligned}$$

where $R \in \mathbb{R}^{p\times p}$ represents any coordinate transformation matrix. It follows that the closed-loop system is independent of the coordinate frame. That is, all followers will converge to the smallest hyperrectangle containing the leaders under any coordinate frame. Therefore, all followers will converge to the intersection of all smallest hyperrectangles containing the leaders under various coordinate frames. Note that the intersection of all smallest hyperrectangles containing the leaders under various coordinate frames is essentially the minimal geometric space spanned by the leaders, i.e., the convex hull formed by the leaders. Therefore, all followers will converge to the convex hull formed by the leaders in any high-dimensional space. We illustrate the idea in a two-dimensional space. Assume that there are four stationary leaders whose positions are denoted by the four squares in Fig. 4.1. Under the condition of Theorem 4.2.1, it follows from the above analysis that the followers will ultimately converge to the red rectangle under the (X_1, Y_1) coordinate frame and the blue rectangle under the (X_2, Y_2) coordinate frame. Therefore, the followers will converge to the intersection of the two rectangles, i.e., the convex hull formed by the leaders.

In the following of this subsection and Section 4.2.1, we assume that $p = 1$ in (4.1) *for the simplicity of presentation. However, all the results in the following of this subsection and Section 4.2.1 are still valid for $p > 1$ in* (4.1) *by following the previous analysis.*

Remark 4.2.3 *Using* (4.14) *for* (4.1)*, the final states for the n agents are unique constants. When all $a_{ij}(t)$ in* (4.14) *are constant, using* (4.14)*,* (4.1) *can be written as*

$$\dot{X}(t) = -\mathcal{L}X(t), \tag{4.4}$$

where $X(t) = [r_1(t), \cdots, r_n(t)]^T$ and $\mathcal{L}$ is the Laplacian matrix. Note that each entry of the jth row of $\mathcal{L}$ is equal to zero for $j \in \mathcal{R}$. Because the zero eigenvalue of $\mathcal{L}$ has the same algebraic and geometric multiplicities [100] *and the other eigenvalues of $\mathcal{L}$ are on the open right half plane, by writing $-\mathcal{L}$ into a Jordan canonical form, it follows that the solution to* (4.4) *is unique and constant. In particular, let r_i^e and X^e denote, respectively, the steady state of $r_i(t)$ and $X(t)$. Under the condition of Theorem 4.2.1, the steady state of* (4.4) *obtained by solving $\mathcal{L}X^e = \mathbf{0}$, where $\mathbf{0}$ is an all-zero column vector with a compatible size, satisfies the fact that $r_i^e \in \mathbf{Co}\{r_j, j \in \mathcal{R}\}$, $i \in \mathcal{F}$.*

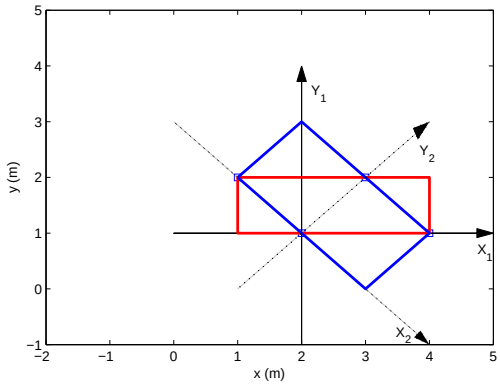

Fig. 4.1: Containment control under different coordinate frames in the two-dimensional space. The squares denote the positions of the four leaders. The blue and red rectangles represent the smallest rectangles containing the leaders under, respectively, the (X_1, Y_1) coordinate frame and the (X_2, Y_2) coordinate frame.

Remark 4.2.4 *Existing consensus algorithms primarily studied the case where the Laplacian matrix has exactly one zero eigenvalue. When there exist multiple leaders, the Laplacian matrix* $\mathcal{L}$ *in* (4.4) *has multiple zero eigenvalues* [101]. *Theorem 4.2.1 studied the case when the Laplacian matrix has multiple zero eigenvalues.*

Remark 4.2.5 *Ji et al.* [76] *focused on the case where the network topology for the followers is undirected and connected. Theorem 4.2.1 considers a general case where the network topology for the followers is directed and not necessarily connected.*

Switching Directed Interaction

In this subsection, we assume that $\mathcal{A}(t)$, i.e., the interaction among the n agents, is constant over time intervals $[\sum_{j=1}^{k}\Delta_j, \sum_{j=1}^{k+1}\Delta_j)$[1] and switches at time $t = \sum_{j=1}^{k}\Delta_j$ with $k = 0, 1, \cdots$, where $\Delta_j > 0$, $j = 1, \cdots$. Let $\mathcal{G}_k$ and $\mathcal{A}_k$ denote, respectively, the directed graph and the adjacency matrix for the n agents for $t \in [\sum_{j=1}^{k}\Delta_j, \sum_{j=1}^{k+1}\Delta_j)$. Equation (4.4) becomes

$$\dot{X}(t) = -\mathcal{L}_k X(t), \tag{4.5}$$

where $\mathcal{L}_k \in \mathbb{R}^{n\times n}$ represents the Laplacian matrix associated with $\mathcal{A}_k$.

[1] When $k = 0$, we define $\sum_{j=1}^{k}\Delta_j \triangleq 0$.

Theorem 4.2.6 *For an n-agent system, using* (4.14) *for* (4.1)*, all followers will always converge to the stationary convex hull $\mathbf{Co}\{r_j, j \in \mathcal{R}\}$ for arbitrary initial conditions $r_i(0), i \in \mathcal{F}$, if and only if there exists N_2 such that the union of $\mathcal{G}_i, i = N_1, \cdots, N_1 + N_2$, has a united directed spanning tree for any finite N_1.*

Proof: The proof is motivated by Moreau's work [38] but here we consider the multi-leader case. (Necessity) When there does not exist N_2 such that the union of $\mathcal{G}_i, i = N_1, \cdots, N_1 + N_2$, has a united directed spanning tree for any finite N_1, there exists at least one follower such that all leaders do not have a directed path to the follower for $t \in [\sum_{j=1}^{N_1} \Delta_j, \infty)$. It follows that the state of the follower is independent of the states of the leaders for $t \geq \sum_{j=1}^{N_1} \Delta_j$. A similar analysis to that in Theorem 4.2.1 shows that at least one follower cannot converge to the stationary convex hull $\mathbf{Co}\{x_j, j \in \mathcal{R}\}$ for arbitrary initial states.

(Sufficiency) Define r_L^+, r_L^-, r_F^+, and r_F^- as in the proof of Theorem 4.2.1. By considering the same four cases as in the proof of Theorem 4.2.1, using the convexity property, and following a similar analysis to that in Moreau's work [38], the theorem is proved. ■

Remark 4.2.7 *Different from the existing consensus algorithms using which the final states for all agents are fixed, when there exist multiple stationary leaders, the final states of all followers might not be constant under a switching network topology.*

Remark 4.2.8 *In Section 4.2.1, we assume that each leader has no neighbor. However, for some network topologies, it is possible to view a subgroup of agents as one leader. For example, for the network topology given by Fig. 4.2, agents* 1 *and* 2 *(respectively, agents* 5 *and* 6*) can reach consensus on a constant value independent of the states of the other agents. The results in Section 4.2.1 can also be applied to this case by viewing agents* 1 *and* 2 *(respectively, agents* 5 *and* 6*) as one leader with the state being the constant consensus equilibrium of agents* 1 *and* 2 *(respectively, agents* 5 *and* 6*).*

Remark 4.2.9 *For the discrete-time consensus algorithm, i.e., the distributed weighted averaging algorithm, with multiple stationary leaders, the convergence results are the same as those in Theorems 4.2.1 and 4.2.6 by following a similar analysis.*

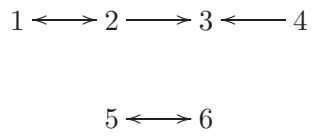

Fig. 4.2: A special network topology when a subgroup of agents can be viewed as a leader.

4.2.2 Stability Analysis with Multiple Dynamic Leaders

In this section, we propose a decentralized tracking control algorithm without velocity measurements and then analyze the stability condition under both fixed and switching network topologies.

For agents with the single-integrator kinematics (4.1), when there exist $m, m < n$, dynamic leaders and $n - m$ followers, we propose the following tracking control algorithm without velocity measurements as

$$\begin{aligned} u_i(t) =& v_i(t), \quad i \in \mathcal{R} \\ u_i(t) =& -\alpha \sum_{j \in \mathcal{F} \bigcup \mathcal{R}} a_{ij}(t)[r_i(t) - r_j(t)] \\ & - \beta \text{sgn} \left\{ \sum_{j \in \mathcal{F} \bigcup \mathcal{R}} a_{ij}(t)[r_i(t) - r_j(t)] \right\}, \quad i \in \mathcal{F}, \end{aligned} \tag{4.6}$$

where $v_i(t) \in \mathbb{R}^p$ denotes the time-varying velocity of leader i, $i \in \mathcal{R}$, $a_{ij}(t)$ is defined as in (6.2), sgn$(\cdot)$ is the signum function defined entrywise, α is a nonnegative constant scalar, and β is a positive constant scalar. We assume that $||v_i(t)||$, $i \in \mathcal{R}$, is bounded.

Fixed Directed Interaction

In this subsection, we assume that the directed interaction is fixed, i.e., all $a_{ij}(t)$ in (4.6) are constant. We first assume that all agents are in a one-dimensional space, i.e., $p = 1$ in (4.6). Before moving on, we need the following lemma.

Lemma 4.2.1 *Suppose that the directed graph $\mathcal{G}$ has a directed spanning tree. For n agents with kinematics given by* (4.1)*, using $u_i(t) = -\sum_{j=1}^{n} a_{ij} f_{i,j}[r_i(t), r_j(t), t], i = 1, \cdots, n$, consensus*

can be achieved if $f_{i,j}(\cdot,\cdot,\cdot)$ satisfies

$$f_{i,j}[x(t),y(t),t]\begin{cases} >\epsilon, & x(t)>y(t) \\ =0, & x(t)=y(t) \\ <-\epsilon, & x(t)<y(t), \end{cases} \tag{4.7}$$

or

$$f_{i,j}[x(t),y(t),t]=f_{i,j}[x(t),y(t)]\begin{cases} >0, & x(t)>y(t) \\ =0, & x(t)=y(t) \\ <0, & x(t)<y(t) \end{cases} \tag{4.8}$$

for any nonnegative t, where ϵ can be any positive constant.

Proof: The proof of this lemma is motivated by Moreau's work [98]. Consider the Lyapunov function candidate $V(t)=\max_i r_i(t)-\min_i r_i(t)$. When $f_{i,j}(x(t),y(t),t)$ satisfies (4.7) or (4.8), the convexity property [98] is also satisfied. By following a similar analysis to that in Moreau's work [98], when the directed graph $\mathcal{G}$ has a directed spanning tree, we can get that $V(t)\to 0$ as $t\to\infty$, which implies that $x_i(t)\to x_j(t)$ as $t\to\infty$. ■

Theorem 4.2.10 *For an n-agent system, suppose that $\beta>\gamma_l$, where $\gamma_l\triangleq\sup_{i\in\mathcal{R}}||v_i(t)||$. Using* (4.6) *for* (4.1)*, all followers will always converge to the dynamic convex hull $\mathbf{Co}\{r_j(t),j\in\mathcal{R}\}$ as $t\to\infty$ for arbitrary initial conditions $r_i(0),i\in\mathcal{F}$, if and only if the directed graph $\mathcal{G}$ has a united directed spanning tree.*

Proof: (Necessity) The necessity proof is similar to that in Theorem 4.2.1.

(Sufficiency) Without loss of generality, suppose that agents 1 to $n-m$ are followers and agents $n-m+1$ to n are leaders. Denote $X(t)\triangleq[r_1(t),\cdots,r_n(t)]^T$ and let $\mathcal{L}\in\mathbb{R}^{n\times n}$ be the Laplacian matrix for the n agents. It can be noted that the last m rows of $\mathcal{L}$ are all equal to zero. Using (4.6), (4.1) can be written in matrix form as

$$\dot{X}(t)=-\alpha\mathcal{L}X(t)-\beta\text{sgn}[\mathcal{L}X(t)]+V(t), \tag{4.9}$$

where $V(t) = [0, \cdots, v_{(n-m+1)}(t), \cdots, v_n(t)]^T$. Let $Z(t) = [z_1(t), \cdots, z_n(t)]^T = \mathcal{L}X(t)$. It follows

$$\dot{Z}(t) = \mathcal{L}\dot{X}(t) = -\alpha\mathcal{L}Z(t) - \beta\mathcal{L}\text{sgn}[Z(t)] + \mathcal{L}V(t). \tag{4.10}$$

Because the last m rows of $\mathcal{L}$ are equal to zero, we get that $z_i(t) \equiv 0, i = n-m+1, \cdots, n$. We can thus view agents $n-m+1$ to n as a single agent, labeled as 0, instead of m agents. It thus follows that $z_0(t) \equiv 0$. When $\mathcal{G}$ has a united directed spanning tree, it follows that agent 0 has a directed path to the $n-m$ followers.

Considering the group consisting of agents 0 to $n-m$, we know that

$$\begin{aligned}
&z_0(t) \equiv 0,\\
&\dot{z}_i(t) = -\alpha \sum_{j=1}^{n-m} a_{ij} \left([z_i(t) - z_j(t)] + \beta\{\text{sgn}[z_i(t)] - \text{sgn}[z_j(t)]\}\right)\\
&\qquad - \sum_{j=n-m+1}^{n} a_{ij}\{z_i(t) + \beta\text{sgn}[z_i(t)] - v_j(t)\}, \quad i = 1, \ldots, n-m,
\end{aligned}$$

where we have used (4.10) by noting that $z_i(t) \equiv 0$, $i = n-m+1, \cdots, n$. We next show that (4.10) satisfies the condition (4.7) or (4.8). When $\beta > 0$ and $z_i(t) > z_j(t)$, it follows that $\alpha[z_i(t) - z_j(t)] + \beta[\text{sgn}(z_i(t)) - \text{sgn}(z_j(t))] > 0, j = 1, \cdots, n-m$. Similarly, when $\beta > 0$ and $z_i(t) < z_j(t)$, it follows that $\alpha[z_i(t) - z_j(t)] + \beta[\text{sgn}(z_i(t)) - \text{sgn}(z_j(t))] < 0, j = 1, \cdots, n-m$. Therefore, $\alpha[z_i(t) - z_j(t)] + \beta[\text{sgn}(z_i(t)) - \text{sgn}(z_j(t))]$ satisfies the condition (4.7). When $\beta > \gamma_l$ and $z_i(t) > z_0(t) \equiv 0$, it follows that $\alpha z_i(t) + \beta\text{sgn}(z_i(t)) - v_j(t) > \beta - \gamma_l > 0$. When $\beta > \gamma_l$ and $z_i(t) < z_0(t) \equiv 0$, it follows that $\alpha z_i(t) + \beta\text{sgn}(z_i(t)) - v_j(t) < -(\beta - \gamma_l) < 0$. Therefore, $\alpha z_i(t) + \beta\text{sgn}(z_i(t)) - v_j(t)$ satisfies the condition (4.8). Because agent 0 has a directed path to agents 1 to $n-m$, i.e., the network topology for agents 0 to $n-m$ has a directed spanning tree, it follows from Lemma 4.2.1 that $z_i(t) \to z_0(t) \equiv 0, i = 1, \cdots, n-m$, as $t \to \infty$. Because $Z(t) \to \mathbf{0}$ as $t \to \infty$, it follows that $\mathcal{L}X(t) \to \mathbf{0}$ as $t \to \infty$. Therefore, all followers will always converge to the dynamic convex hull $\mathbf{Co}\{r_j(t), j \in \mathcal{R}\}$ as $t \to \infty$ under the condition of the theorem. ■

Remark 4.2.11 *When the agents are in a one-dimensional space, it is shown in Theorem 4.2.10 that $\mathcal{L}X(t) \to \mathbf{0}$ as $t \to \infty$. Similarly, when the agents are in a p-dimensional space ($p > 1$), by using the decoupling technique, it can be shown that $(\mathcal{L} \otimes I_p)X(t) \to \mathbf{0}$ as $t \to \infty$ under the condition of Theorem 4.2.10. Note that $(\mathcal{L} \otimes I_p)X(t) \to \mathbf{0}$ implies that $r_i(t) \in \mathbf{Co}\{r_j(t), j \in \mathcal{R}\}$ as $t \to \infty$. That is, the same conclusion in Theorem 4.2.10 holds for any high-dimensional space.*

Switching Directed Interaction

In this subsection, we assume that the adjacency matrix $\mathcal{A}(t)$ (and hence the interaction) is switching over time but remains constant for $t \in [\sum_{j=1}^{k} \Delta_j, \sum_{j=1}^{k+1} \Delta_j)$ as in Section 4.2.1. We first study the case when all agents are in a one-dimensional space.

Theorem 4.2.12 *For an n-agent system, suppose that $\beta > \gamma_l$, where γ_l is defined in Theorem 4.2.10. Using* (4.6) *for* (4.1)*, all followers will always converge to the dynamic convex hull $\mathbf{Co}\{r_j(t), j \in \mathcal{R}\}$ as $t \to \infty$ for arbitrary initial conditions $r_i(0), i \in \mathcal{F}$, if the directed graph $\mathcal{G}$ has a united directed spanning tree at each time interval $[\sum_{j=1}^{k} \Delta_j, \sum_{j=1}^{k+1} \Delta_j)$.*

Proof: Define $r_L^+(t) \stackrel{\triangle}{=} \max\{r_j(t), j \in \mathcal{R}\}$ and $\tilde{r}_i(t) \stackrel{\triangle}{=} r_i(t) - r_L^+(t)$, $i \in \mathcal{F} \bigcup \mathcal{R}$. It follows that $\tilde{r}_i(t) \leq 0$, $i \in \mathcal{R}$. Using (4.6) for (4.1), the closed-loop system can be written as

$$\begin{aligned}
&\dot{\tilde{r}}_i(t) = v_i(t) - \dot{r}_L^+(t), \quad i \in \mathcal{R} \\
&\dot{\tilde{r}}_i(t) = -\alpha \sum_{j \in \mathcal{F} \bigcup \mathcal{R}} a_{ij}[k][\tilde{r}_i(t) - \tilde{r}_j(t)] \\
&\quad - \beta \text{sgn} \left\{ \sum_{j \in \mathcal{F} \bigcup \mathcal{R}} a_{ij}[k][\tilde{r}_i(t) - \tilde{r}_j(t)] \right\} - \dot{r}_L^+(t), \quad i \in \mathcal{F},
\end{aligned} \tag{4.11}$$

where $a_{ij}[k]$ is the (i,j)th entry of the adjacency matrix $\mathcal{A}(t)$ for $t \in [\sum_{j=1}^{k} \Delta_j, \sum_{j=1}^{k+1} \Delta_j)$.

Define $\tilde{r}_+(t) \stackrel{\triangle}{=} \max\{\tilde{r}_i(t), i \in \mathcal{F} \bigcup \mathcal{R}\}$. We next study $\tilde{r}_+(t)$ in the following two cases:

Case 1: $\tilde{r}_+(t)$ is a nonincreasing function if $\tilde{r}_+(t) \geq 0$ at $t = 0$. We prove this statement by contradiction. Suppose that $\tilde{r}_+(t)$ increases over some time period $[t_1, t_2]$. It then follows that there exists at least one follower, labeled as j, with the state $\tilde{r}_+(t)$ satisfying that $\tilde{r}_j(t)$ will increase over $[t_1, t_3]$, where $t_3 \leq t_2$. From (4.11), if the states of the neighbors of agent j are less than

or equal to $\tilde{r}_+(t)$ and $\tilde{r}_j(t)$ increases for an arbitrary small amount, it follows from the analysis in Theorem 4.2.10 that $\dot{\tilde{r}}_j(t) < 0$, which implies that $\tilde{r}_j(t)$ cannot increase. This results in a contradiction.

Case 2: $\tilde{r}_+(t)$ will decrease after a finite period of time if the graph has a united directed spanning tree at each time interval and $\tilde{r}_+(t) > 0$ at $t = 0$. Suppose that the states of some followers, labeled as $k_1, \cdots, k_s$, are equal to $\tilde{r}_+(t)$. Because the directed graph at each time interval has a united directed spanning tree, followers $k_1, \cdots, k_s$ as a subgroup has at least one neighbor which is not within this subgroup at each time interval. By following a similar analysis to that in the proof of Theorem 4.2.10, it then follows from (4.11) that $\dot{\tilde{r}}_{k_i}(t) < -\tilde{\epsilon} < 0$ for some k_i and some positive constant $\tilde{\epsilon}$, which implies that $\tilde{r}_{k_i}(t)$ will decrease. By following a similar analysis to that for follower k_i, we can get that all other followers with the maximal state $\tilde{r}_+(t)$ will also decrease. Therefore, $\tilde{r}_+(t)$ will decrease after a finite period of time.

Combining the previous two cases shows that $\tilde{r}_+(t) \to 0$ as $t \to \infty$.

Similarly, define $r_L^-(t) = \min\{r_j(t), j \in \mathcal{R}\}$ and $\breve{r}_i(t) \triangleq r_i(t) - r_L^-(t)$. It follows that $\breve{r}_i(t) \geq 0$, $i \in \mathcal{R}$. Note that (4.6) can be written as

$$\dot{\breve{r}}_i(t) = -\alpha \sum_{j \in \mathcal{F} \bigcup \mathcal{R}} a_{ij}[k][\breve{r}_i(t) - \breve{r}_j(t)] - \beta \text{sgn}\left\{ \sum_{j \in \mathcal{F} \bigcup \mathcal{R}} a_{ij}[k][\breve{r}_i(t) - \breve{r}_j(t)] \right\} - \dot{r}_L^-(t), \quad i \in \mathcal{F}.$$

Define $\breve{r}_-(t) \triangleq \min\{\breve{r}_i(t), i \in \mathcal{F} \bigcup \mathcal{R}\}$. A similar analysis to that for $\tilde{r}_+(t)$ can also show that $\breve{r}_-(t) \to 0$ as $t \to \infty$. Combining the previous arguments shows that $r_i(t) \leq r_L^+(t)$ and $r_i(t) \geq r_L^-(t)$ as $t \to \infty$, which implies that all followers will converge to the dynamic convex hull $\mathbf{Co}\{r_j(t), j \in \mathcal{R}\}$ as $t \to \infty$ under the condition of the theorem. ■

Remark 4.2.13 *Unlike the case of stationary leaders, the case of dynamic leaders requires more stringent conditions on network topologies to guarantee dynamic containment control. This is due to the fact that the leaders move with time-varying velocities rather than remain still.*

Remark 4.2.14 *Theorem 4.2.12 focuses on the one-dimensional space. For any high-dimensional space, by using the decoupling technique, all followers will converge to the smallest hyperrectangle containing the dynamic leaders under the conditions of Theorem 4.2.12. Note that all followers might not converge to the dynamic convex hull formed by the dynamic leaders because the closed-loop system depends on the coordinate frame, which is different from Remark 4.2.2. To illustrate, we present the following counterexample. Consider a group of agents with four leaders and one follower where the leaders have the same velocity. The network topology switches from Fig. 4.3(a) to Fig. 4.3(b) every* 0.4 *seconds and the process repeats. Simulation results using* (4.6) *in the two-dimensional space are given in Fig. 4.4 where the red square represents the position of the follower and the blue circles represent the positions of the four leaders. From the simulation results, it can be seen that even if the follower is originally within the dynamic convex hull, it cannot always stay to the dynamic convex hull although the directed graph has a united directed spanning tree at each time interval. Instead, the follower will converge to the smallest rectangle containing the dynamic leaders.*

Remark 4.2.15 *For a high-dimensional space, the sgn*(ν) *function in* (4.6) *can also be defined as*[2]

$$sgn(\nu) = \begin{cases} \mathbf{0}, & \nu = \mathbf{0}, \\ \frac{\nu}{\|\nu\|}, & otherwise. \end{cases} \tag{4.12}$$

[2]In a one-dimensional space, sgn(ν) becomes the standard signum function.

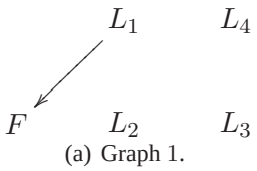

(a) Graph 1.

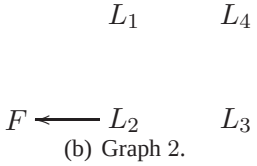

(b) Graph 2.

Fig. 4.3: Switching directed network topologies for a group of agents with four leaders and one follower. Here $L_i, i = 1, \cdots, 4$, denote the leaders while F denotes the follower.

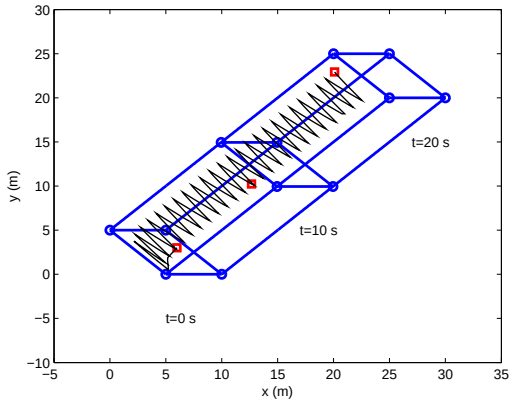

Fig. 4.4: A counterexample to illustrate that the follower cannot converge to the dynamic convex hull in the two-dimensional space. The red square represents the position of the follower and the blue circles represent the positions of the four leaders.

Under this definition, the closed-loop system is independent of the coordinate frame. However, all followers might still not converge to the dynamic convex hull formed by the dynamic leaders. We consider the same example as in Remark 4.2.14 but with $\mathrm{sgn}(\cdot)$ *defined by* (4.12)*. Simulation results are given in Fig. 4.5. It can be noted that the follower cannot converge to the dynamic convex hull formed by the dynamic leaders even if the follower is initially within the convex hull.*

Remark 4.2.16 *For decentralized containment control with multiple dynamic leaders under a switching directed network topology, it is, in general, impossible to find decentralized tracking control algorithms without velocity measurements to guarantee that all followers will converge to the dynamic convex hull formed by the dynamic leaders in a high-dimensional space. In a one-dimensional space, the degree of freedom of the dynamic leaders is* 1 *and only the minimum and maximum states of the dynamic leaders are required to determine the dynamic convex hull formed by the dynamic leaders. Therefore, the signum function can be used to drive all followers to the dynamic convex hull formed by the dynamic leaders under a switching directed network topology given that the network topology and the control gain satisfy the conditions in Theorem 4.2.12. However, in a high-dimensional space, the degree of freedom of the dynamic leaders is larger than* 1*. The dynamic convex hull formed by the dynamic leaders might depend on a number of leaders' states. Therefore, the signum function, in general, does not have the capability to drive all followers to the*

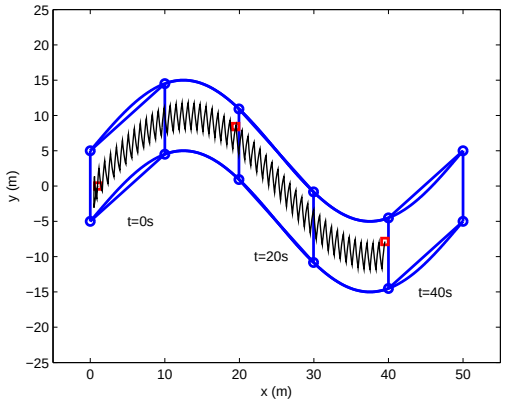

Fig. 4.5: A counterexample to illustrate that the follower cannot converge to the dynamic convex hull in the two-dimensional space when $\mathrm{sgn}(\cdot)$ is defined by (4.12). The red square represents the position of the follower and the blue circles represent the positions of the four leaders.

dynamic convex hull formed by the dynamic leaders. Similarly, without velocity measurements, the basic linear decentralized control algorithms do not have such capability either. Therefore, more information, i.e., velocity measurements, topology switching sequence, topologies, etc., is needed in order to guarantee decentralized containment control with multiple dynamic leaders under a switching directed network topology in a high-dimensional space.

4.3 Double-integrator Dynamics

4.3.1 Stability Analysis with Multiple Stationary Leaders

In this section, we study the conditions on, respectively, the fixed and switching network topologies such that all followers will converge to the stationary convex hull formed by the stationary leaders.

Consider a group of n vehicles with double-integrator dynamics given by

$$\dot{r}_i(t) = v_i(t), \quad \dot{v}_i(t) = u_i(t) \quad i = 1, \ldots, n, \tag{4.13}$$

where $r_i(t) \in \mathbb{R}^p$, $v_i(t) \in \mathbb{R}^p$, and $u_i(t) \in \mathbb{R}^p$ are, respectively, the position, the velocity, and the control input associated with the ith vehicle. We propose the following containment control

algorithm for (4.13) as

$$\begin{aligned} v_i(t) =& 0, \quad i \in \mathcal{R}, \\ u_i(t) =& -\beta v_i(t) - \sum_{j \in \mathcal{F} \bigcup \mathcal{R}} a_{ij}(t) \Big\{ \beta[r_i(t) - r_j(t)] \\ & + [v_i(t) - v_j(t)] \Big\}, \quad i \in \mathcal{F}, \end{aligned} \tag{4.14}$$

where $\mathcal{R}$ and $\mathcal{F}$ are defined in Definition 4.1.1, $a_{ij}(t)$ is the (i,j)th entry of the adjacency matrix $\mathcal{A}$ at time t, and β is a positive constant. The objective of (4.14) is to guarantee that all vehicles move into the convex hull formed by the leaders. Note that $r_j(t), j \in \mathcal{R}$, is constant because the leaders are stationary.

We assume that $\mathcal{A}(t)$, i.e., the interaction among the n vehicles, is constant over time intervals $[\sum_{j=1}^{k} \Delta_j, \sum_{j=1}^{k+1} \Delta_j)$[3] and switches randomly at time $t = \sum_{j=1}^{k} \Delta_j$ with $k = 0, 1, \cdots$, where $\Delta_j > 0, j = 1, \cdots$. Let $\mathcal{G}_k$ and $\mathcal{A}[k]$ denote, respectively, the directed graph and the adjacency matrix for the n vehicles for $t \in [\sum_{j=1}^{k} \Delta_j, \sum_{j=1}^{k+1} \Delta_j)$. We first consider the case when the vehicles are in a one-dimensional space, i.e., $p = 1$ in (4.13).

Theorem 4.3.1 *Using* (4.14) *for* (4.13)*, all followers will always converge to the stationary convex hull* $\mathbf{Co}\{r_j, j \in \mathcal{R}\}$ *for arbitrary initial conditions* $x_i(0),\ i \in \mathcal{F}$*, if and only if there exists a positive integer* N_2 *such that the union of* $\mathcal{G}_i, i = N_1, \cdots, N_1 + N_2$*, has a united directed spanning tree for any finite* N_1*.*

Proof: (Necessity) The proof follows a similar analysis to that in the proof of Theorem 3.5 [82].

(Sufficiency) Define $z_i(t) \stackrel{\triangle}{=} \beta r_i(t) + v_i(t), i = 1, \cdots, n$. Using (4.14) for (4.13), we can get that

$$\begin{aligned} \dot{z}_i(t) &= 0, i \in \mathcal{R}, \\ \dot{z}_i(t) &= -\sum_{j \in \mathcal{R} \bigcup \mathcal{F}} a_{ij}[k][z_i(t) - z_j(t)], \quad i \in \mathcal{F}. \end{aligned} \tag{4.15}$$

[3]When $k = 0$, we define $\sum_{j=1}^{k} \Delta_j \stackrel{\triangle}{=} 0$.

By following a similar analysis to that in the proof of Theorem 3.1 [82], it can be shown that $z_i(t), i \in \mathcal{F}$, will converge to the convex hull $\mathbf{Co}\{z_j, j \in \mathcal{R}\}$ under the condition of the theorem. Define $\overline{z} \stackrel{\triangle}{=} \max_{i\in\mathcal{R}} z_i$, $\overline{r} \stackrel{\triangle}{=} \max_{i\in\mathcal{R}} r_i$ and $\delta_i \stackrel{\triangle}{=} r_i - \overline{r}, i \in \mathcal{F}$. Note that $z_i(t) - \overline{z}(t)$ is bounded and $z_i(t) - \overline{z}(t) \leq 0$ as $t \to \infty$. Letting $f_i(t) = z_i(t) - \overline{z}(t)$, it then follows that

$$\dot{\delta}_i(t) + \beta\delta_i(t) = f_i(t), \tag{4.16}$$

where we have used the fact that $x_i(t), i \in \mathcal{R}$, are constant. Therefore, the solution of (4.16) is given by

$$\delta_i(t) = e^{-\beta t}\delta_i(0) + \int_0^t e^{-\beta(t-\tau)} f_i(\tau)d\tau.$$

It follows that

$$\begin{aligned}\lim_{t\to\infty} \delta_i(t) &= \lim_{t\to\infty} e^{-\beta t}\delta_i(0) + \lim_{t\to\infty} \int_0^t e^{-\beta(t-\tau)} f_i(\tau)d\tau \\ &= \lim_{t\to\infty} \frac{\int_0^t e^{\beta\tau} f_i(\tau)d\tau}{e^{\beta t}}.\end{aligned}$$

We consider two cases. In the first case, if $\int_0^t e^{\beta\tau} f_i(\tau)d\tau$ is bounded, then $\delta_i(t) \to 0$ as $t \to \infty$. If $\lim_{t\to\infty} \int_0^t e^{\beta\tau} f_i(\tau)d\tau \to \infty$, then it follows from L'Hopital's rule that

$$\lim_{t\to\infty} \frac{\int_0^t e^{\beta\tau} f_i(\tau)d\tau}{e^{\beta t}} = \frac{\frac{d}{dt}\int_0^t e^{\beta\tau} f_i(\tau)d\tau}{\frac{d}{dt}e^{\beta t}} = \lim_{t\to\infty} \frac{e^{\beta t} f_i(t)}{\beta e^{\beta t}} = \lim_{t\to\infty} \frac{f_i(t)}{\beta}.$$

Noting that $\beta > 0$ and $f_i(t) \leq 0$ as $t \to \infty$, it then follows that $\delta_i(t) \leq 0$ as $t \to \infty$, i.e., $r_i(t) \leq \overline{r}(t)$ as $t \to \infty$. This implies that $r_i(t) \leq \max_{j\in\mathcal{R}} r_j(t)$ as $t \to \infty$. By following a similar analysis, it can be shown that $r_i(t) \geq \min_{j\in\mathcal{R}} r_j(t)$ as $t \to \infty$. Therefore, all followers will converge to the convex hull formed by the leaders. ■

Remark 4.3.2 *In Theorem 4.3.1, all followers are shown to converge to the convex hull in a one-dimensional space. For any high-dimensional space, by using the decoupling technique, it is straightforward to show that all followers will converge to the smallest hyperrectangles containing the leaders. Note that the closed-loop system by using* (4.14) *for* (4.13) *is independent of the*

coordinate frame. Therefore, the followers will converge to the intersection of various smallest hyperrectangle containing the leaders under different coordinate frames. Note also that the intersection of various smallest hyperrectangles containing the leaders under different coordinate frames is essentially the convex hull formed by the leaders. Therefore, all followers will converge to the convex hull formed by the leaders in any high-dimensional space.

4.3.2 Stability Analysis with Multiple Dynamic Leaders

In this section, we study decentralized containment control for double-integrator dynamics in the presence of multiple dynamic leaders. We consider two cases: leaders with an identical velocity and leaders with nonidentical velocities.

Leaders with an Identical Velocity

In this subsection, we assume that the velocities of all leaders are the same, i.e., $v_i(t) = v_j(t)$ for $i, j \in \mathcal{R}$.

For (4.13), we propose the following containment control algorithm as

$$\begin{aligned} v_i(t) =& v^o(t), \quad i \in \mathcal{R}, \\ u_i(t) =& -\gamma \text{sgn}\Bigg(\sum_{j \in \mathcal{F} \bigcup \mathcal{R}} a_{ij}(t) \Big\{ \beta[r_i(t) - r_j(t)] \\ & + [v_i(t) - v_j(t)] \Big\} \Bigg) - \beta v_i(t), \quad i \in \mathcal{F}, \end{aligned} \tag{4.17}$$

where $v^o(t)$ is the common velocity of the leaders, β and γ are positive constants, and sgn$(\cdot)$ is the signum function defined entrywise. We first study the case when the vehicles are in a one-dimensional space.

Theorem 4.3.3 *Assume that the network topology switches according to the same model as described right before Theorem 4.3.1. Assume also that $\gamma > \gamma_\ell$, where $\gamma_\ell \stackrel{\triangle}{=} \sup_{i \in \mathcal{R}} ||\dot{v}^o(t) + \beta v^o(t)||$. All followers will always converge to the dynamic convex hull $\mathbf{Co}\{r_j, j \in \mathcal{R}\}$ for arbitrary initial*

conditions $x_i(0), i \in \mathcal{F}$, if the network topology has a united directed spanning tree at each time interval.

Proof: Define $z_i(t) \stackrel{\triangle}{=} \beta x_i(t) + v_i(t)$. Using (4.17) for (4.13) gives

$$\begin{aligned} \dot{z}_i(t) &= \dot{v}^o(t) + \beta v^o(t), \quad i \in \mathcal{R}, \\ \dot{z}_i(t) &= -\gamma \text{sgn}\left\{ \sum_{j \in \mathcal{R} \bigcup \mathcal{F}} a_{ij}[k][z_i(t) - z_j(t)] \right\}, i \in \mathcal{F}. \end{aligned} \tag{4.18}$$

We next show that $z_i(t)$ will converge to the convex hull $\mathbf{Co}\{z_j, j \in \mathcal{R}\}$ in *finite time*.

Define $\overline{z} \stackrel{\triangle}{=} \max_{i \in \mathcal{R}} z_i$, $\underline{z} \stackrel{\triangle}{=} \min_{i \in \mathcal{R}} z_i$, $\tilde{z} \stackrel{\triangle}{=} \max_{i \in \mathcal{F}} z_i - \overline{z}$, and $\breve{z} \stackrel{\triangle}{=} \min_{i \in \mathcal{F}} z_i - \underline{z}$. We will show that $\tilde{z}(t) \leq 0$ and $\breve{z}(t) \geq 0$ in finite time. Here we only consider the case when $\tilde{z}(0) > 0$ and $\breve{z}(0) \geq 0$. Similar analysis can also be applied to other cases. We next show that when $\tilde{z}(t) > 0$ for $t \leq T$ with $T > 0$, $\dot{\tilde{z}}(t) \leq -\gamma + \gamma_\ell$ for $t \leq T$ except for some isolated time instants. We prove this by contradiction. Because $\tilde{z}(t) > 0$ for $t \leq T$, it follows from (4.18) and the definition of $\tilde{z}$ that $\dot{\tilde{z}}(t) = -\dot{\overline{z}}(t)$ or $\dot{\tilde{z}}(t) < -\gamma + \gamma_\ell$ for $t \leq T$. Assume that $\dot{\tilde{z}}(t) = -\dot{\overline{z}}(t)$ for $t \in [t_1, t_2]$, where $t_1 < t_2 \leq T$. There exists some vehicle, labeled j, with the maximal state satisfying $\dot{z}_j(t) = -\dot{\overline{z}}(t)$ for $t \in [t_1, t_3]$, where $t_1 < t_3 \leq t_2$. It then follows from (4.18) that $\sum_{i \in \mathcal{R} \bigcup \mathcal{F}} a_{ji}[k][z_j(t) - z_i(t)] = 0$ for $t \in [t_1, t_3]$. Because vehicle j is with the maximal state, it then follows that $z_i(t) = z_j(t), \forall i \in \mathcal{N}_j$, for $t \in [t_1, t_3]$. By following a similar analysis, when $\mathcal{G}$ has a united directed spanning tree at each time interval, $z_\kappa(t) = z_j(t)$ for some $\kappa \in \mathcal{R}$ for $t \in [t_1, t_3]$, which results in a contradiction because $\tilde{z}(T) > 0$. Therefore, $\tilde{z}(t)$ will keep decreasing with a speed large than $\gamma - \gamma_\ell$ for $t \leq T$ except for some isolated time instants. From the proof of Theorem 4.2 [82], if $\tilde{z}(t_1) \leq 0$, then $\tilde{z}(t) \leq 0$ for $t \geq t_1$. It then follows that $\tilde{z}(t) \leq 0$ in finite time. Similarly, it can be shown that $\breve{z}(t) \geq 0$ in finite time. Therefore, $z_i(t), i \in \mathcal{F}$, will converge to the convex hull $\mathbf{Co}\{z_j, j \in \mathcal{R}\}$ in finite time.

Because $z_i(t), i \in \mathcal{F}$, will converge to the convex hull $\mathbf{Co}\{z_j, j \in \mathcal{R}\}$ in finite time, there exists positive $\overline{t}$ such that $\min_{j \in \mathcal{R}} z_j(t) \leq z_i(t) \leq \max_{j \in \mathcal{R}} z_j(t)$, $i \in \mathcal{F}$, for $t \geq \overline{t}$. Because the leaders have the same velocity, if $r_i(0) \geq r_j(0), \forall i, j \in \mathcal{R}$, then $r_i(t) \geq r_j(t)$ for any $t > 0$, which implies that $z_i(t) \geq z_j(t)$ for any $t > 0$. Without loss of generality, let $\max_{j \in \mathcal{R}} z_j(t) =$

$\beta r_p(t) + \dot{r}_p(t)$ for some $p \in \mathcal{R}$ and $\min_{j\in\mathcal{R}} z_j(t) = \beta r_q(t) + \dot{r}_q(t)$ for some $q \in \mathcal{R}$. It then follows that $\beta r_q(t) + \dot{r}_q(t) \leq \beta r_i(t) + \dot{r}_i(t) \leq \beta r_p(t) + \dot{r}_p(t)$, $i \in \mathcal{F}$, for $t \geq \overline{t}$. For $t \geq \overline{t}$ and $i \in \mathcal{F}$,

$$\dot{r}_i(t) - \dot{r}_q(t) \geq -\beta[r_i(t) - r_q(t)],$$
$$\dot{r}_i(t) - \dot{r}_p(t) \leq -\beta[r_i(t) - r_p(t)].$$

Therefore, $r_q(t) \leq r_i(t) \leq r_p(t)$, $i \in \mathcal{F}$, as $t \to \infty$. Because the leaders have the same velocity, all followers will converge to the convex hull formed by the leaders. ■

Remark 4.3.4 *When the directed network topology is fixed and the vehicles are in a one-dimensional space, by following a similar analysis to that of Theorem* 4.1 [82]*, it can be shown that* $\mathcal{L}Z(t) \to \mathbf{0}$ *as* $t \to \infty$*, where* $Z(t) = [z_1(t), \cdots, z_n(t)]^T$ *and* $\mathbf{0}$ *is an all-zero vector with a compatible size, under the condition of Theorem 4.3.3. Noting that all leaders have the same velocity, it is easy to show that* $\mathcal{L}X(t) \to \mathbf{0}$ *as* $t \to \infty$*, where* $X(t) = [r_1(t), \cdots, r_n(t)]^T$*. Similarly, when the vehicles are in any high-dimensional space, i.e.,* $p > 1$ *in* (4.13)*, by using the decoupling technique, it can be shown that* $(\mathcal{L} \otimes I_p)X(t) \to \mathbf{0}$ *as* $t \to \infty$*, where* $\otimes$ *is the Kronecker product. Therefore, all followers will converge to the convex hull formed by the leaders for any high-dimensional space under a fixed directed network topology when the conditions of Theorem 4.3.3 are satisfied. In contrary, when the directed network topology is switching and the vehicles are in a high-dimensional space, it can only be shown by using the decoupling technique that the followers will converge to the smallest hyperrectangle containing the leaders but not necessarily the convex hull formed by the leaders.*

We next propose a decentralized containment control algorithm which can guarantee that all followers converge to the convex hull formed by the leaders in finite time. In the following of this subsection and Section 4.3.2, we assume that all vehicles are in a one-dimensional space for the simplicity of presentation. However, all the results hereafter are still valid for arbitrary high-dimensional space by using the decoupling technique and the Kronecker product.

Inspired by Bhat and Bernstein's work [102], we propose the following finite-time containment control algorithm as

$$\begin{aligned} u_i(t) =& \dot{\hat{v}}_i(t) - \text{sgn}[v_i(t) - \hat{v}_i(t)]|v_i(t) - \hat{v}_i(t)|^{\kappa} \\ & - \text{sgn}[\phi(t)]|\phi(t)|^{\frac{\kappa}{2-\kappa}}, \end{aligned} \tag{4.19}$$

where $0 < \kappa < 1$, $\phi(t) = r_i(t) - \hat{r}_i(t) + \frac{1}{2-\kappa}\text{sgn}[v_i(t) - \hat{v}_i(t)]|v_i(t) - \hat{v}_i(t)|^{2-\kappa}$, and

$$\dot{\hat{r}}_i(t) = \hat{v}_i(t) - \rho_1 \text{sgn}\left\{\sum_{j \in \mathcal{R} \bigcup \mathcal{F}} a_{ij}[\hat{r}_i(t) - \hat{r}_j(t)]\right\}, \tag{4.20}$$

$$\dot{\hat{v}}_i(t) = -\rho_2 \text{sgn}\left\{\sum_{j \in \mathcal{R} \bigcup \mathcal{F}} a_{ij}[\hat{v}_i(t) - \hat{v}_j(t)]\right\},\ i \in \mathcal{F} \tag{4.21}$$

with $\hat{r}_i(t) = r_i(t)$ and $\hat{v}_i(t) = v^o(t)$ for $i \in \mathcal{R}$.

Theorem 4.3.5 *Assume that the fixed network topology has a united directed spanning tree. Using* (4.19) *for* (4.13)*, all followers will converge to the dynamic convex hull formed by the leaders in finite time if* $\rho_1 > 0$ *and* $\rho_2 > \sup_t |\dot{v}^o(t)|$.

Proof: Note that $\hat{v}_j(t) = v^o(t), \forall j \in \mathcal{R}$. When $\rho_2 > \sup_t |\dot{v}^o(t)|$, it follows from (4.21) and a similar proof to that of Theorem 4.3.3 that $\hat{v}_i(t), i \in \mathcal{F}$, will converge to $v^o(t)$ in finite time. Without loss of generality, let $\hat{v}_i(t) = v^o(t), i \in \mathcal{F} \bigcup \mathcal{R}$, for $t \geq \overline{t}_1$, where $\overline{t}_1$ is some positive constant. For $t \geq \overline{t}_1$, (4.20) can be written in matrix form as

$$\dot{\hat{r}}(t) = v^o(t)\mathbf{1} - \rho_1 \text{sgn}[\mathcal{L}\hat{r}(t)], \tag{4.22}$$

where $\hat{r}(t) = [\hat{r}_1(t), \cdots, \hat{r}_n(t)]^T$ and $\mathcal{L}$ is the Laplacian matrix of the n vehicles including both the leaders and the followers. Let $z(t) = [z_1(t), \cdots, z_n(t)]^T = \mathcal{L}\hat{r}(t)$. Because $\mathcal{L}\mathbf{1} = 0$, it follows that (4.22) can be rewritten as

$$\dot{z}(t) = -\rho_1 \mathcal{L}\text{sgn}[z(t)].$$

Note that $z_i(t) = 0, i \in \mathcal{R}$, because the ith row of $\mathcal{L}$ is zero. When the fixed graph has a united directed spanning tree, it can be shown that $z_i(t) \to 0$ in finite time by showing that both the maximal and minimal states will go to zero in finite time. This implies that $\hat{r}_i(t), i \in \mathcal{F}$, will be within the convex hull formed by the leaders in finite time. It then follows from (4.22) that $\dot{\hat{r}}_i(t) \to v^o(t)$ in finite time. Without loss of generality, let $\dot{\hat{r}}_i(t) = v^o(t)$ for $t \geq \overline{t}_2$, where $\overline{t}_2$ is some positive constant. Note also that $\dot{\hat{v}}_i(t)$ can be replaced with $\dot{v}^o(t)$ for $t \geq \overline{t}_2$ because $\int_{t_1}^{t_2} \dot{\hat{v}}_i(t)dt = \int_{t_1}^{t_2} \dot{v}_i^o(t)dt$ for any $t_2 \geq t_1 \geq \overline{t}_2$. Define $\delta_i \stackrel{\triangle}{=} r_i(t) - \hat{r}_i(t)$. For $t \geq \overline{t}_2$, by replacing $\dot{\hat{v}}_i(t)$ with $\dot{v}^o(t)$, (4.19) can be rewritten as

$$\ddot{\delta}_i(t) = -\,\mathrm{sgn}[\dot{\delta}_i(t)]|\dot{\delta}_i(t)|^{\kappa} - \mathrm{sgn}[\phi_i(t)]\,|\phi_i(t)|^{\frac{\kappa}{2-\kappa}}\,.$$

It then follows from Proposition 1 [102] that $\delta_i(t) \to 0$ in finite time.

Combining the previous statements completes the proof. ■

Leaders with Nonidentical Velocities

In this subsection, we assume that the velocities of the leaders are nonidentical. Without loss of generality, we assume that the first $n - m$ vehicles are leaders.

For (4.13), we propose the following containment control algorithm as

$$\begin{aligned} u_i(t) =& a_i(t), \quad i = 1, \cdots, n-m \\ u_i(t) =& -\sum_{j \in \mathcal{R} \bigcup \mathcal{F}} a_{ij}[(r_i - r_j) + \alpha(v_i - v_j)] \\ & - \beta \mathrm{sgn}\{\sum_{j \in \mathcal{R} \bigcup \mathcal{F}} a_{ij}[\gamma(r_i - r_j) + (v_i - v_j)]\}, \\ & i = n-m+1, \cdots, n, \end{aligned} \tag{4.23}$$

where $a_i(t)$ is the acceleration input for the ith leader, and α, β, and γ are positive constants. Using (4.23), (4.13) can be written in matrix form as

$$\ddot{X} = -\mathcal{L}X - \alpha\mathcal{L}\dot{X} - \beta \mathrm{sgn}(\gamma\mathcal{L}X + \mathcal{L}\dot{X}) - \Psi, \tag{4.24}$$

where $X = [r_1, \cdots, r_n]^T$, $\Psi(t) = [\psi_1(t), \cdots, \psi_n(t)]^T$ with $\psi_i(t) = a_i(t)$ for $i = 1, \cdots, n-m$, and $\psi_i(t) = 0$ for $i = n-m+1, \cdots, n$, and $\mathcal{L}$ is the Laplacian matrix. Note that the first $n-m$ rows of $\mathcal{L}$ are equal to zero. Define $\tilde{X} \triangleq \mathcal{L}X$. It follows that the first $n-m$ entries of $\tilde{X}$ are equal to zero. Then (4.24) can be written as

$$\ddot{\tilde{X}} = -\mathcal{L}\tilde{X} - \alpha\mathcal{L}\dot{\tilde{X}} - \beta\mathcal{L}\text{sgn}(\gamma\tilde{X} + \dot{\tilde{X}}) - \mathcal{L}\Psi. \tag{4.25}$$

Let $\tilde{X}_F$ be the vector containing only the last m entries of $\tilde{X}$ and Ψ_F be the vector containing only the last m entries of $\mathcal{L}\Psi$. Therefore, (4.26) can be rewritten as

$$\ddot{\tilde{X}}_F = -M\tilde{X}_F - \alpha M\dot{\tilde{X}}_F - \beta M\text{sgn}(\gamma\tilde{X}_F + \dot{\tilde{X}}_F) - \Psi_F, \tag{4.26}$$

where $M = [m_{ij}] \in \mathbb{R}^{m\times m}$ with $m_{ij} = \ell_{ij}$ if $i \neq j$ and $m_{ii} = \sum_{k\neq i}\ell_{ik}$.

Lemma 4.3.1 *Assume that the fixed graph has a united directed spanning tree and the communication patterns among the followers are undirected. Let* $P = \begin{bmatrix} I_n & \frac{\gamma}{2}M^{-1} \\ \frac{\gamma}{2}M^{-1} & M^{-1} \end{bmatrix}$ *and* $Q = \begin{bmatrix} \gamma I_n & \frac{\alpha\gamma}{2}I_n \\ \frac{\alpha\gamma}{2}I_n & \alpha I_n - \gamma M^{-1} \end{bmatrix}$*, where* γ *and* α *are two positive constants and* M *is defined right before this lemma. If* α *and* γ *are chosen satisfying* $\gamma < \min\{\sqrt{4\lambda_{\min}(M)}, \frac{4\alpha\lambda_{\min}(M)}{4+\alpha^2\lambda_{\min}(M)}\}$*, both* P *and* Q *are symmetric positive definite, where* $\lambda_{\min}(\cdot)$ *denotes the smallest eigenvalue of a symmetric matrix.*

Proof: When the graph has a united directed spanning tree and the communication patterns among the followers are undirected, M is symmetric positive definite. Therefore, M^{-1} is also symmetric positive definite. Then M^{-1} can be diagonalized as $M^{-1} = \Gamma^{-1}\Lambda\Gamma$, where $\Lambda = \text{diag}\{\frac{1}{\lambda_1}, \cdots, \frac{1}{\lambda_m}\}$ with λ_i being the ith eigenvalue of M. Let μ be an eigenvalue of P. It then follows that μ satisfies

$$(\mu - 1)(\mu - \frac{1}{\lambda_i}) - \frac{\gamma^2}{4\lambda_i^2} = 0, \tag{4.27}$$

which can be simplified as

$$\mu^2 - (1 + \frac{1}{\lambda_i})\mu + \frac{1}{\lambda_i} - \frac{\gamma^2}{4\lambda_i^2} = 0.$$

Because P is symmetric, the eigenvalues of P are real. Therefore, the roots of (4.27) are all positive if and only if $1 + \frac{1}{\lambda_i} > 0$ and $\frac{1}{\lambda_i} - \frac{\gamma^2}{4\lambda_i^2} > 0$. After some simplification, we can get that $\gamma < \sqrt{4\lambda_i}$. Therefore, P is symmetric positive definite if $\gamma < \sqrt{4\lambda_{\min}(M)}$.

Similarly, it can be shown that Q is symmetric positive definite if $\gamma < \frac{4\alpha\lambda_{\min}(M)}{4+\alpha^2\lambda_{\min}(M)}$. ■

Theorem 4.3.6 *Assume that the fixed graph has a united directed spanning tree and the communication patterns among the followers are undirected. Using* (4.23) *for* (4.13)*, if α and γ satisfy the conditions in Lemma 4.3.1 and $\beta > \left\|M^{-1}\Psi_F\right\|_1$, all followers will converge to the convex hull formed by the leaders, where Ψ_F is defined right before* (4.26) *and M are defined right after* (4.26)*.*

Proof: Consider the Lyapunov function candidate

$$\begin{aligned} V =& \begin{bmatrix} \tilde{X}_F^T & \dot{\tilde{X}}_F^T \end{bmatrix} P \begin{bmatrix} \tilde{X}_F \\ \dot{\tilde{X}}_F \end{bmatrix} \\ =& \tilde{X}_F^T \tilde{X}_F + \gamma \tilde{X}_F^T M^{-1} \dot{\tilde{X}}_F + \dot{\tilde{X}}_F^T M^{-1} \dot{\tilde{X}}_F. \end{aligned}$$

Note that according to Lemma 4.3.1, P is symmetric positive definite when α and γ satisfy the conditions in Lemma 4.3.1. Taking derivative of V gives that

$$\begin{aligned} \dot{V} =& \tilde{X}_F^T \tilde{X}_F + \dot{\tilde{X}}_F^T M^{-1} \ddot{\tilde{X}} + \gamma \dot{\tilde{X}}^T M^{-1} \dot{\tilde{X}} + \gamma \tilde{X}^T M \ddot{\tilde{X}} \\ =& - \begin{bmatrix} \tilde{X}_F^T & \dot{\tilde{X}}_F^T \end{bmatrix} Q \begin{bmatrix} \tilde{X}_F \\ \dot{\tilde{X}}_F \end{bmatrix} \\ & - (\gamma \tilde{X}_F^T + \dot{\tilde{X}}_F^T) M \{\beta \text{sgn}[M(\gamma \tilde{X}_F + \dot{\tilde{X}}_F)] + M^{-1}\Psi_F\} \\ \leq & - \begin{bmatrix} \tilde{X}_F^T & \dot{\tilde{X}}_F^T \end{bmatrix} Q \begin{bmatrix} \tilde{X}_F \\ \dot{\tilde{X}}_F \end{bmatrix} \\ & - (\beta - \left\|M^{-1}\Psi_F\right\|_1) \left\|M(\gamma \tilde{X}_F + \dot{\tilde{X}}_F)\right\|_1. \end{aligned}$$

Note that according to Lemma 4.3.1, Q is symmetric positive definite when α and γ satisfy conditions in Lemma 4.3.1. Noting also that $\beta > \left\|M^{-1}\Psi_F\right\|_1$, it follows that $\dot{V}$ is negative definite. It then follows that $\tilde{X}_F = \mathbf{0}$ and $\dot{\tilde{X}}_F = \mathbf{0}$. Therefore, $\mathcal{L}X = \mathbf{0}$, which implies that all followers will converge to the convex hull formed by the leaders. ■

4.3.3 Simulation

In this section, we present several simulation results to validate some theoretical results. We consider a group of vehicles with four leaders and four followers and the topology is given in Fig. 4.6.

When the leaders are stationary, the fixed directed network topology $\mathcal{G}$ is chosen as in Fig. 4.6(a). It can be noted that $\mathcal{G}$ has a united directed spanning tree. Simulation results using (4.14) are shown in Fig. 4.7(a). We can see that all followers will converge to the stationary convex hull formed by the leaders. In the case of switching network topologies, the network topology switches from Fig. 4.6(b) to Fig. 4.6(c) every 0.5 seconds. Note that neither Figs. 4.6(b) nor 4.6(c) has a united directed spanning tree while the union of Figs. 4.6(b) and 4.6(c) has a united directed spanning tree. Simulation results using (4.14) are shown in Fig. 4.7(b). We can see that all followers will converge to the stationary convex hull formed by the leaders.

For the algorithms (4.17) and (4.19), the fixed network topology is chosen as in Fig. 4.6(a). Simulation results using (4.17) are shown in Fig. 4.8. We can see that all followers will converge to the dynamic convex hull formed by the leaders. In addition, two snapshots at $t = 25\ s$ and $t = 50\ s$ show that all followers remain in the dynamic convex hull formed by the dynamic leaders. Simulation results using (4.19) are shown in Fig. 4.9. Note that all followers will converge to the dynamic convex hull formed by the leaders in finite time. In addition, two snapshots at $t = 25\ s$ and $t = 50\ s$ show that all followers remain in the dynamic convex hull formed by the dynamic leaders as well.

When the velocities of the leaders are nonidentical, the fixed network topology $\mathcal{G}$ is chosen as in Fig. 4.6(a). Note that $\mathcal{G}$ has a united directed spanning tree and the communication patterns among the followers are undirected. Simulation results using (4.23) are shown in Fig. 4.10. It can

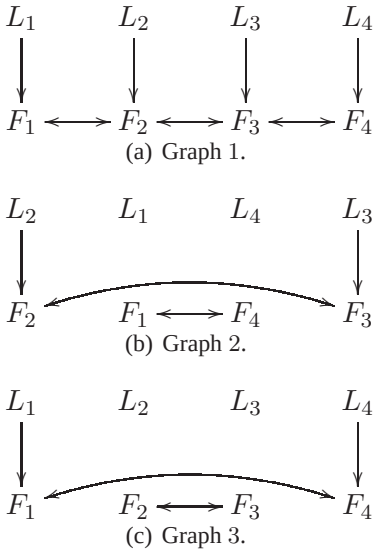

(a) Graph 1.

(b) Graph 2.

(c) Graph 3.

Fig. 4.6: Network topology for a group of vehicles with multiple leaders. $L_i, i = 1, \cdots, 4$, denote the leaders. $F_i, i = 1, \cdots, 6$, denote the followers.

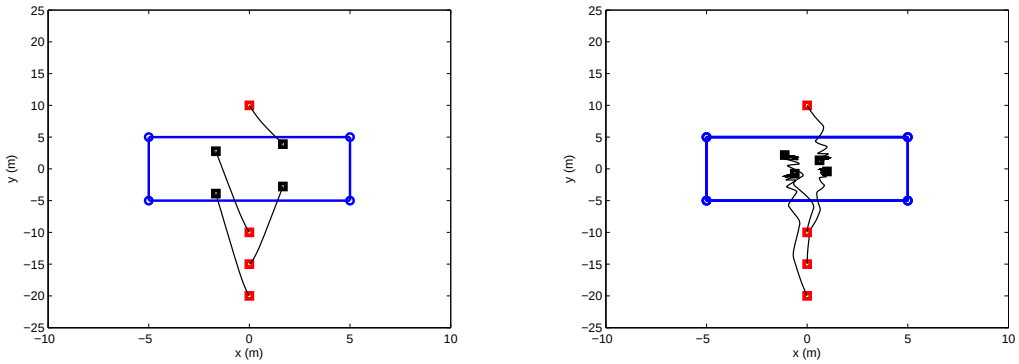

(a) Fixed directed network topology.

(b) Switching directed network topology.

Fig. 4.7: Trajectories of the agents using (4.14) under a fixed and a switching directed network topology in the two-dimensional space. Circles denote the starting positions of the stationary leaders while the red and black squares denote, respectively, the starting and ending positions of the followers.

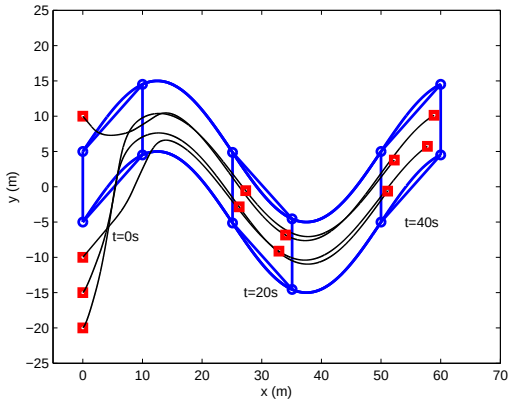

Fig. 4.8: Trajectories of the agents using (4.17) under a fixed directed network topology in the two-dimensional space. Circles denote the positions of the dynamic leaders while the squares denote the positions of the followers. Two snapshots at $t = 25s$ and $t = 50\ s$ show that all followers remain in the dynamic convex hull formed by the dynamic leaders.

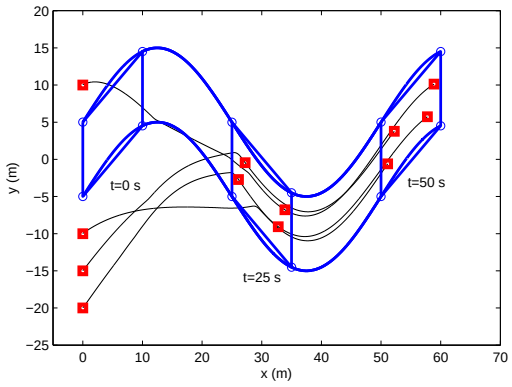

Fig. 4.9: Trajectories of the vehicles using (4.19) under a fixed directed network topology in the two-dimensional space. Circles denote the positions of the dynamic leaders while the squares denote the positions of the followers. Two snapshots at $t = 25\ s$ and $t = 50\ s$ show that all followers remain in the dynamic convex hull formed by the dynamic leaders.

be noted that all followers will converge to the dynamic convex hull formed by the dynamic leaders. In addition, two snapshots at $t = 21.47\ s$ and $t = 45.17\ s$ show that all followers remain in the dynamic convex hull formed by the dynamic leaders.

4.3.4 Experimental Validation

In this section, we experimentally validate some of the proposed containment algorithms on a multi-robot platform. In the experiments, five wheeled mobile robots are used to obtain the experimental results. In particular, three robots are designated as the leaders and the other two robots are designated as the followers. We next briefly introduce the experiment platform developed in the COoperative VEhicle Networks (COVEN) Laboratory at Utah State University.

The textbed in the COVEN Laboratory includes five Amigobots and two P3-DX from the ActivMedia Robotics as shown in Fig. 4.11. Both the Amigobots and P3-DX are similar in terms of functionalities. Each robot has a differential-drive system with rear caster, high-precision wheel encoders, and eight sonar positioned around the robot. The robots can calculate their positions and orientations based on the encoders. The eight sonar can be used for localization and detection of obstacles. The maximum speed for the AmigoBots is 1 m/s and the AmigoBots can climb a 1.5% incline.

In order to control multiple mobile robots under various network topologies, a control software was developed to emulate a limited or even changing network topology. The control platform can be divided into two layers. The top layer is responsible for network topology setting, control algorithm implementation, and bi-directional communication with the onboard micro-controller. The bottom layer is responsible for sensor data acquisition and direct PID loop control where both linear and rotational velocity commands are generated and executed.

The system dynamics of the wheeled mobile robots can be described as

$$\dot{x}_i = v_i \cos(\theta_i), \quad \dot{y}_i = v_i \sin(\theta_i), \quad \dot{\theta}_i = \omega_i, \tag{4.28}$$

where (x_i, y_i) is the position of the center of the ith robot, θ_i is the orientation of the ith robot, and v_i and w_i are the linear and angular velocities of the ith robot. To avoid using the nonlinear

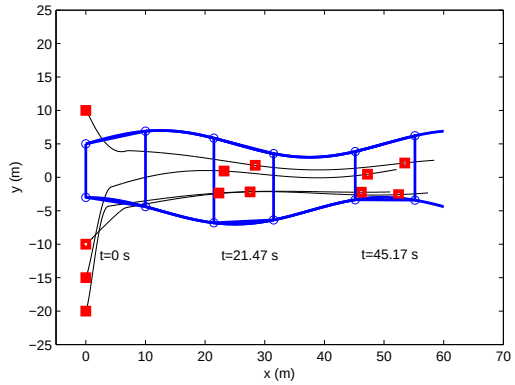

Fig. 4.10: Trajectories of the vehicles using (4.23) under a fixed directed network topology in the two-dimensional space. Circles denote the positions of the dynamic leaders while the squares denote the positions of the followers. Two snapshots at $t = 21.47\ s$ and $t = 45.17\ s$ show that all followers remain in the dynamic convex hull formed by the dynamic leaders.

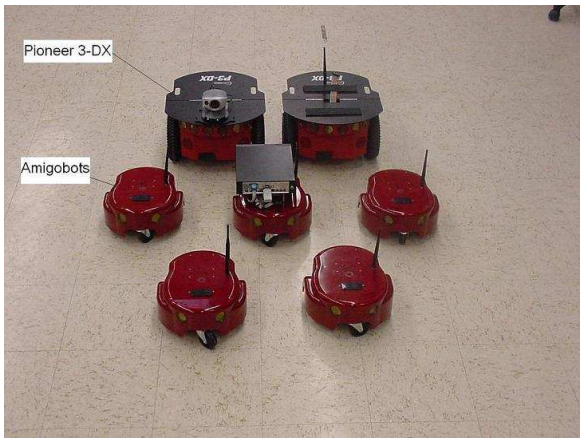

Fig. 4.11: Multi-vehicle experimental platform at Utah State University.

dynamics (4.28), we feedback linearize (4.28) for a fixed point off the center of the wheel axis denoted as (x_{hi}, y_{hi}), where $x_{hi} = x_i + d_i \cos(\theta_i)$ and $y_{hi} = y_i + d_i \cos(\theta_i)$ with $d = 0.15\ m$. By letting

$$\begin{bmatrix} v_i \\ \omega_i \end{bmatrix} = \begin{bmatrix} \cos\theta_i & \sin\theta_i \\ -\frac{1}{d_i}\sin\theta_i & \frac{1}{d_i}\cos\theta_i \end{bmatrix} \begin{bmatrix} u_{xi} \\ u_{yi} \end{bmatrix},$$

we can get that

$$\begin{bmatrix} \dot{x}_i \\ \dot{y}_i \end{bmatrix} = \begin{bmatrix} u_{xi} \\ u_{yi} \end{bmatrix}. \tag{4.29}$$

Note that (4.29) is a single-integrator kinematics model. By letting $\dot{u}_{xi} = \tau_{xi}$ and $\dot{u}_{yi} = \tau_{yi}$, a double-integrator dynamics model can be obtained by designing the control inputs τ_{xi} and τ_{yi}.

In the following, we present several experimental results to validate some theoretical results in this paper. The network topology is chosen as shown in Fig. 4.12. It can be noted from Fig. 4.12 that the network topology has a united directed spanning tree. We use triangles and circles to denote, respectively, the starting and ending positions of the leaders, and diamonds and squares to denote, respectively, the starting and ending positions of the followers.

When the velocities of leaders are identical, experimental results using (4.17) are given in Fig. 4.13 where Figs. 4.13(a) and 4.13(b) together show the trajectories of the five robots. In each subfigure, two snapshots are presented to show, respectively, the starting positions of the five robots as well as the convex hull formed by the leaders and the ending positions of the five robots as well as the convex hull formed by the leaders. It can be seen from Fig. 4.13(b) that the two followers moved into the convex hull formed by the leaders.

When the velocities of leaders are nonidentical, experimental results using (4.23) are given in Fig. 4.14 where Figs. 4.14(a) and 4.14(b) together show the trajectories of the five robots. In each

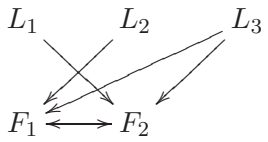

Fig. 4.12: Network topology for five mobile robots. $L_i, i = 1, \cdots, 3$, denote the leaders. $F_i, i = 1, \cdots, 2$, denote the followers.

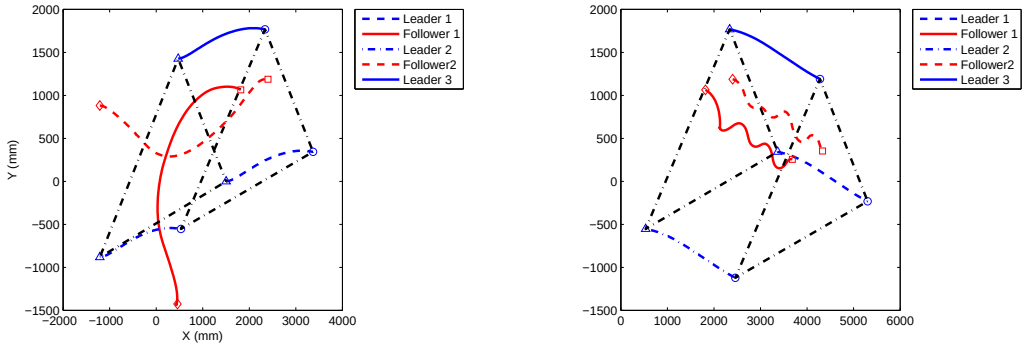

(a) Part I of the trajectories. (b) Part II of the trajectories.

Fig. 4.13: Trajectories of the five mobile robots using (4.17).

subfigure, we also use two snapshots to show, respectively, the starting positions of the five robots as well as the convex hull formed by the leaders and the ending positions of the five robots as well as the convex hull formed by the leaders. It can be seen from Fig. 4.14(b) that the two followers moved into the convex hull formed by the leaders.

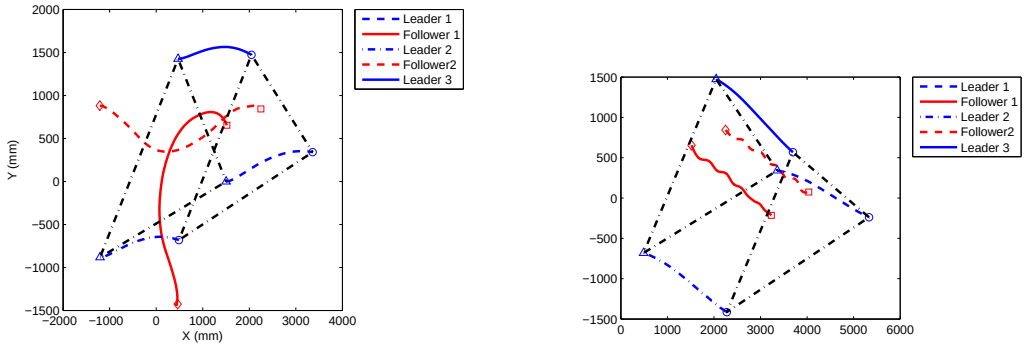

(a) Part I of the trajectories. (b) Part II of the trajectories.

Fig. 4.14: Trajectories of the five mobile robots using (4.23).

Chapter 5

LQR-based Optimal Consensus Algorithms

Among various studies of linear consensus algorithms, a noticeable phenomenon is that the algorithms with different parameters, i.e., different Laplacian matrices, can be applied to the same system to ensure consensus. It is natural to ask these questions: Is there an optimal linear consensus algorithm with the associated optimal Laplacian matrix (under a given cost function)? How may the optimal linear consensus algorithm be found?

Optimality issues in consensus algorithms have also been studied in the literature recently. A (locally) optimal nonlinear consensus strategy was proposed by imposing individual objectives [103]. An optimal interaction graph, a de Bruijn's graph, was proposed in the average consensus problem [104]. A semi-decentralized optimal control strategy was proposed by minimizing the individual cost [105]. In addition, the cooperative game theory was employed to ensure cooperation with a team cost function. An iterative algorithm was proposed to maximize the second smallest eigenvalue of a Laplacian matrix to optimize the control system performance [106]. The fastest converging linear iteration was studied by using the semidefinite programming [107].

In contrast to the aforementioned literature, the purpose of this chapter is to study the optimal linear consensus algorithms for vehicles with single-integrator dynamics from an LQR perspective. Instead of studying locally optimal algorithms, this chapter focuses on the study of globally optimal algorithms.

5.1 Definitions

Definition 5.1.1 *We define* $Z^{n\times n} := \{B = [b_{ij}] \in \mathbb{R}^{n\times n} | b_{ij} \leq 0, i \neq j\}$, $\mathbf{0}_{m\times n} \in \mathbb{R}^{m\times n}$ *as an all-zero matrix, and* $I_n \in \mathbb{R}^{n\times n}$ *as an identity matrix.*

Definition 5.1.2 *A matrix $E \in \mathbb{R}^{m\times n}$ is said positive (nonnegative), i.e., $E > (\geq)0$, if each entry of E is positive (nonnegative). A square nonnegative matrix is (row) stochastic if all of its row sums are* 1.

Definition 5.1.3 [108] *A real matrix $B = [b_{ij}] \in \mathbb{R}^{n\times n}$ is called an M-matrix if it can be written as*

$$B = sI_n - C, \quad s > 0, C \geq 0$$

where $C \in \mathbb{R}^{n\times n}$ satisfies $\rho(C) \leq s$, where $\rho(C)$ is the spectral radius of matrix C. Matrix B is called a nonsingular M-matrix if $\rho(C) < s$.

Definition 5.1.4 [108] *A matrix $D \in \mathbb{R}^{n\times n}$ is called semiconvergent if $\lim_{i\to\infty} D^i$ exists.*

5.2 Global Cost Functions

5.2.1 Continuous-time Case

Consider vehicles with single-integrator dynamics given by

$$\dot{r}_i(t) = u_i(t) \tag{5.1}$$

where $r_i(t) \in \mathbb{R}$ and $u_i(t) \in \mathbb{R}$ are, respectively, the state and control input of the ith vehicle. A common linear consensus algorithm is studied as [36, 37, 39, 99]

$$u_i(t) = -\sum_{j=1}^{n} a_{ij}[r_i(t) - r_j(t)], \tag{5.2}$$

where a_{ij} is the (i, j)th entry of the weighted adjacency matrix $\mathcal{A}$ associated with graph $\mathcal{G}$. The objective of (6.2) is to guarantee consensus, i.e., for any $r_i(0)$, $r_i(t) \to r_j(t)$, $\forall i, j \in \{1, \cdots, n\}$, as $t \to \infty$. Substituting (6.2) into (5.1) and writing the closed-loop system in matrix form gives

$$\dot{X}(t) = -\mathcal{L}X(t), \tag{5.3}$$

where $X(t) = [r_1(t), r_2(t), \cdots, r_n(t)]^T$ and $\mathcal{L}$ is the (nonsymmetric) Laplacian matrix associated with $\mathcal{A}$. It can be noted that (5.3) is a linear differential equation. Consensus is reached for (5.3) if and only if $\mathcal{L}$ has a simple zero eigenvalue or equivalently the directed graph associated with $\mathcal{L}$ has a directed spanning tree [39].

Similar to the cost function used in optimal control problems for systems with linear differential equations, we propose the following two consensus cost functions for system (5.1) as

$$J_f = \int_0^\infty \left\{ \sum_{i=1}^{n} \sum_{j=1}^{i-1} c_{ij}[r_i(t) - r_j(t)]^2 + \sum_{i=1}^{n} \kappa_i u_i^2(t) \right\} dt, \tag{5.4}$$

$$J_r = \int_0^\infty \left\{ \sum_{i=1}^{n} \sum_{j=1}^{i-1} a_{ij}[r_i(t) - r_j(t)]^2 + \sum_{i=1}^{n} u_i^2(t) \right\} dt, \tag{5.5}$$

where $c_{ij} \geq 0$, $\kappa_i > 0$, and a_{ij} is defined in (6.2). In (5.4), both c_{ij} and κ_i can be chosen freely. Therefore J_f is called the *interaction-free cost function*. Because (5.5) depends on the weighted adjacency matrix $\mathcal{A}$, J_r is called the *interaction-related cost function*. The motivation of (5.4) and (5.5) is to weigh both the consensus errors and the control effort. The optimization problems can be written as

$$\min_{a_{ij}} \ J_f, \text{ subject to (5.1) and (6.2)}, \tag{5.6}$$

$$\min_{\beta} \ J_r, \text{ subject to (5.1) and } u_i(t) = -\sum_{j=1}^{n} \beta a_{ij}[r_i(t) - r_j(t)]. \tag{5.7}$$

5.2.2 Discrete-time Case

In the discrete-time case, continuous-time dynamics (5.1) can be written as

$$\frac{r_i[k+1] - r_i[k]}{T} = u_i[k], \tag{5.8}$$

where k is the discrete-time index, T is the sampling period, and $r_i[k]$ and $u_i[k]$ denote, respectively, the state and control input of the ith vehicle at $t = kT$. Sampling (6.2) gives

$$u_i[k] = -\sum_{j=1}^{n} a_{ij}\{r_i[k] - r_j[k]\}. \tag{5.9}$$

Substituting (5.9) into (5.8) and writing the closed-loop system in matrix form gives

$$X[k+1] = (I_n - T\mathcal{L})X[k], \tag{5.10}$$

where $X[k] = [r_1[k], r_2[k], \cdots, r_n[k]]^T$ and $\mathcal{L}$ is the (nonsymmetric) Laplacian matrix defined in (5.3). Consensus is reached for (5.10) if $\mathcal{L}$ has a simple zero eigenvalue and $T < \frac{1}{\max_i \ell_{ii}}$ [37].

Similar to the two cost functions proposed in the continuous-time case, we propose the discrete-time interaction-free and interaction-related cost functions as

$$J_f = \sum_{k=0}^{\infty}\sum_{i=1}^{n}\sum_{j=1}^{i-1} c_{ij}\{r_i[k] - r_j[k]\}^2 + \sum_{k=0}^{\infty}\sum_{i=1}^{n} \kappa_i u_i^2[k], \tag{5.11}$$

$$J_r = \sum_{k=0}^{\infty}\sum_{i=1}^{n}\sum_{j=1}^{i-1} a_{ij}\{r_i[k] - r_j[k]\}^2 + \sum_{k=0}^{\infty}\sum_{i=1}^{n} u_i^2[k], \tag{5.12}$$

where $c_{ij} \geq 0$, $r_i > 0$, and a_{ij} is defined in (6.2). The corresponding optimization problems can be written as

$$\min_{a_{ij}} \ J_f \text{ subject to (5.8) and (5.9)}, \tag{5.13}$$

$$\min_{\beta} \ J_r \text{ subject to (5.8) and } u_i[k] = -\sum_{j=1}^{n} \beta a_{ij}\{r_i[k] - r_j[k]\}. \tag{5.14}$$

5.3 LQR-based Optimal Linear Consensus Algorithms in a Continuous-time Setting

In this section, we derive the optimal linear consensus algorithms in a continuous-time setting from an LQR perspective. We first derive the optimal (nonsymmetric) Laplacian matrix using continuous-time interaction-free cost function (5.4). We will then find the optimal scaling factor

for a prespecified symmetric Laplacian matrix using continuous-time interaction-related cost function (5.5). Finally, illustrative examples will be provided.

5.3.1 Optimal Laplacian Matrix Using Interaction-free Cost Function

With interaction-free cost function (5.4), optimal control problem (5.6) can be written as

$$\min_{\mathcal{L}} J_f = \int_0^\infty [X^T(t)QX(t) + U^T(t)RU(t)]dt \tag{5.15}$$
$$\text{subject to: } \dot{X}(t) = U(t),\ U(t) = -\mathcal{L}X(t),$$

where $X(t)$ is defined in (5.3), $U(t) = [u_1(t), \cdots, u_n(t)]^T$, $Q \in \mathbb{R}^{n\times n}$ is symmetric with the (i,j)th entry (also the (j,i)th entry) given as $-c_{ij}$ for $i \neq j$ and the (i,i)th entry given as $\sum_{j=1,j\neq i}^n c_{ij}$, $R \in \mathbb{R}^{n\times n}$ is a positive definite (PD) diagonal matrix with r_i being the ith diagonal entry, and $\mathcal{L}$ is the (nonsymmetric) Laplacian matrix defined in (5.3). It can be noted that Q is a symmetric PSD Laplacian matrix.

The main result for optimal control problem (5.15) is given in the following theorem.

Theorem 5.3.1 *For optimal control problem* (5.15)*, where Q has a simple zero eigenvalue, the optimal consensus algorithm is $U(t) = -\sqrt{R^{-1}Q}X(t)$, that is, the optimal (nonsymmetric) Laplacian matrix is $\sqrt{R^{-1}Q}$. In addition, $\sqrt{R^{-1}Q}$ corresponds to a complete directed graph.*[1]

Before proving the theorem, we need the following lemmas.

Lemma 5.3.1 [108] *An M-matrix $B \in \mathbb{R}^{n\times n}$ has exactly one M-matrix as its square root if the characteristic polynomial of B has at most a simple zero root.*

If the characteristic polynomial of M-matrix B has at most a simple zero root, we use $\sqrt{B}$ hereafter to represent the M-matrix that is the square root of B.

Lemma 5.3.2 *An M-matrix that has a zero eigenvalue with a corresponding eigenvector $\mathbf{1}_n$ is a (nonsymmetric) Laplacian matrix.*

[1] Obviously, consensus is reached for (5.1) using $U(t) = -\sqrt{R^{-1}Q}X(t)$ since $\sqrt{R^{-1}Q}$ has a simple zero eigenvalue due to the fact that $\sqrt{R^{-1}Q}$ corresponds to a complete directed graph.

Proof: Follow Definition 5.1.3 and definition of a (nonsymmetric) Laplacian matrix. ■

Lemma 5.3.3 *Let Q and R be defined in* (5.15)*. Suppose that Q has a simple zero eigenvalue. There exists exactly one (nonsymmetric) Laplacian matrix W satisfying $W = \sqrt{R^{-1}Q}$ and W has a simple zero eigenvalue.*

Proof: The proof is divided into the following three steps:

Step 1*: $R^{-1}Q$ is a (nonsymmetric) Laplacian matrix with a simple zero eigenvalue.* We first note that $R^{-1}Q$ is a (nonsymmetric) Laplacian matrix because Q is a symmetric Laplacian matrix and R is a PD diagonal matrix. Because Q is a symmetric Laplacian matrix with a simple zero eigenvalue, it follows that the undirected graph associated with Q is connected, which implies that the directed graph associated with $R^{-1}Q$ is strongly connected. It thus follows that the (nonsymmetric) Laplacian matrix $R^{-1}Q$ also has a simple zero eigenvalue.

Step 2*: W has a simple zero eigenvalue with an associated eigenvector $\mathbf{1}_n$.* Let the ith eigenvalue of W be λ_i with an associated eigenvector ν_i. Noting that $W^2 = R^{-1}Q$, it follows that the ith eigenvalue of $R^{-1}Q$ is λ_i^2 with an associated eigenvector ν_i. Because $R^{-1}Q$ has a simple zero eigenvalue with an associated eigenvector $\mathbf{1}_n$, it follows that W has a simple zero eigenvalue with an associated eigenvector $\mathbf{1}_n$.

Step 3*: W is a (nonsymmetric) Laplacian matrix.* Note that a (nonsymmetric) Laplacian matrix is a special case of an M-matrix according to Definition 5.1.3. It follows from Lemma 5.3.1 and Step 1 that $R^{-1}Q$ has exactly one square root W that is also an M-matrix. Because W has a simple zero eigenvalue with an associated eigenvector $\mathbf{1}_n$ as shown in Step 2, it follows from Lemma 5.3.2 that W is a (nonsymmetric) Laplacian matrix. ■

We next show that the (nonsymmetric) Laplacian matrix W in Lemma 5.3.3 corresponds to a complete directed graph.

Lemma 5.3.4 *Let Q and R be defined in* (5.15)*. Suppose that Q has a simple zero eigenvalue. Then the (nonsymmetric) Laplacian matrix $\sqrt{R^{-1}Q}$ corresponds to a complete directed graph.*

Proof: We show that each entry of $\sqrt{R^{-1}Q}$ is nonzero, which implies that $\sqrt{R^{-1}Q}$ corresponds to a complete directed graph. Before moving on, we let q_{ij} denote the (i,j)th entry of Q. We also let

$W = \sqrt{R^{-1}Q}$ and denote w_{ij}, $w_{i,:}$, and $w_{:,i}$, respectively, as the (i,j)th entry, the ith row, and the ith column of W.

First, we will show that $w_{ij} \neq 0$ if $q_{ij} \neq 0$. We show this statement by contradiction. Assume that $w_{ij} = 0$. Because $R^{-1}Q = W^2$, it follows that $\frac{q_{ij}}{r_i} = w_{i,:}w_{:,j}$. When $i = j$, it follows from $w_{ii} = 0$ that $w_{i,:} = \mathbf{0}_{n\times 1}$ because W is a (nonsymmetric) Laplacian matrix, which then implies that $\frac{q_{ij}}{r_i} = w_{i,:}w_{:,j} = 0$. This contradicts the assumption that $q_{ij} \neq 0$. When $i \neq j$, because we assume that $w_{ij} = 0$, it follows that $\frac{q_{ij}}{r_i} = w_{i,:}w_{:,j} = \sum_{k=1,k\neq i,k\neq j}^{n} w_{ik}w_{kj} \geq 0$ due to the fact $w_{i,k} \leq 0, \forall i \neq k$, because W is a (nonsymmetric) Laplacian matrix. Because Q is a symmetric Laplacian matrix, it follows that $q_{ij} \leq 0, \forall i \neq j$. Therefore, $\frac{q_{ij}}{r_i} \geq 0, \forall i \neq j$, implies $q_{ij} = 0$, which also contradicts the assumption that $q_{ij} \neq 0$.

Second, we will show that $w_{ij} \neq 0$ if $q_{ij} = 0$. We also show this statement by contradiction. Assume that $w_{ij} = 0$. To ensure that $q_{ij} = 0$, it follows from $\frac{q_{ij}}{r_i} = w_{i,:}w_{:,j} = \sum_{k=1,k\neq i,k\neq j}^{n} w_{ik}w_{kj}$ that $w_{ik}w_{kj} = 0, \forall k \neq i, k \neq j, k = 1, \cdots, n$. Denote $\hat{k}_1$ as the node set such that $w_{im} \neq 0$ for each $m \in \hat{k}_1$. Then we have $w_{mj} = 0$ for each $m \in \hat{k}_1$ because $w_{ik}w_{kj} = 0$. Similarly, denote $\bar{k}_1$ as the node set such that $w_{mj} \neq 0$ for each $m \in \bar{k}_1$. Then we have $w_{im} = 0$ for each $m \in \bar{k}_1$ because $w_{ik}w_{kj} = 0$. From the discussion in the previous paragraph, when $w_{mj} = 0$, we have $q_{mj} = 0$, which implies that $w_{mp}w_{pj} = 0, \forall p \neq m, p \neq j, p = 1, \cdots, n$. By following a similar analysis, we can consequently define $\hat{k}_i$ and $\bar{k}_i, i = 2, \cdots, \kappa$, where $\hat{k}_i \cap \hat{k}_j = \emptyset, \bar{k}_i \cap \bar{k}_j = \emptyset, \forall j < i$. Noting that the undirected graph associated with Q is connected and the directed graph associated with W has a directed spanning tree because W has a simple zero eigenvalue, it follows that $\kappa \leq n$. Therefore, each entry of $w_{:,j}$ is equal to zero by following the previous analysis for at most n times. This implies that $q_{ij} = 0, \forall i \neq j$, because $\frac{q_{ij}}{r_i} = w_{i,:}w_{:,j}$. Considering the fact that Q is a symmetric Laplacian matrix, it follows that $q_{ii} = 0$, which also contradicts the fact that the undirected graph associated with Q is connected. ■

We next prove Theorem 5.3.1 based on the previous lemmas.

Proof of Theorem 5.3.1: Consider the following standard LQR problem

$$\min_{U(t)} J_f \quad \text{subject to:} \quad \dot{X}(t) = AX(t) + BU(t), \tag{5.16}$$

where J_f is defined by (5.15), $A = \mathbf{0}_{n\times n}$, and $B = I_n$. It can be noted that (A, B) is controllable, which implies that there exists a P satisfying the continuous-time algebraic Riccati equation (ARE)

$$A^T P + PA - PBR^{-1}B^T P + Q = \mathbf{0}_{n\times n}. \tag{5.17}$$

It follows from (5.17) that $PR^{-1}P = Q$, which implies $R^{-1}PR^{-1}P = R^{-1}Q$. It then follows from Lemma 5.3.3 that $R^{-1}P = \sqrt{R^{-1}Q}$ is also a (nonsymmetric) Laplacian matrix when Q has a simple zero eigenvalue. Therefore, the optimal control is $U(t) = -R^{-1}B^T PX(t) = -\sqrt{R^{-1}Q}X(t)$, which implies that $\sqrt{R^{-1}Q}$ is the optimal (nonsymmetric) Laplacian matrix. It also follows from Lemma 5.3.4 that $\sqrt{R^{-1}Q}$ corresponds to a complete directed graph. ■

Remark 5.3.2 *From Theorem 5.3.1, it can be noted that the interaction graph corresponding to $\sqrt{R^{-1}Q}$ is in general different from that corresponding to Q.*

Remark 5.3.3 *One may think that since the discussion in Theorem 5.3.1 (correspondingly, the discussion in Theorem 5.4.1) is a standard LQR problem, the solution can be solved using the standard Matlab command. However, it is not clear why the standard LQR solution is a (nonsymmetric) Laplacian matrix and the solution corresponds to a complete directed graph. The contribution of Section 5.3.1(correspondingly, Section 5.4.1) is that we mathematically derive the conditions under which the square root of a (nonsymmetric) Laplacian matrix is still a (nonsymmetric) Laplacian matrix, explicitly derive the (nonsymmetric) optimal Laplacian matrix for a given global cost function, and show that the optimal solution corresponds to a complete directed graph. Although it may be intuitively true that a global optimization problem in the context of consensus building normally requires that each agent have full knowledge of all other agents, it is nontrivial to theoretically prove this fact. We have provided a theoretical explanation. In addition, the results in this paper can also be used to interpret some phenomena in economy, management, and social science, to name a few. For example, each company in a country needs to (theoretically) have a complete and correct understanding of other companies' status and act on the available information in order to achieve a globally optimal objective. Unfortunately, an economic crisis might still happen because either*

the available information to each company is not complete or some companies do not act correctly on the available information.

Remark 5.3.4 *Note that $\sqrt{R^{-1}Q}$ is not necessarily symmetric in general. When R is a diagonal matrix with identical diagonal entries, i.e., $R = cI_n$ with $c > 0$, $\sqrt{R^{-1}Q}$ is symmetric.*

Remark 5.3.5 *Theorem 5.3.1 requires that Q be a symmetric PSD Laplacian matrix with a simple zero eigenvalue. When Q has more than one zero eigenvalue, $X^T(t)QX(t)$ can be written as the sum of at least two parts as*

$$X^T(t)QX(t) = X_1^T(t)Q_1X_1(t) + X_2^T(t)Q_2X_2(t) + \cdots,$$

where $X_i, i = 1, 2, \cdots$, are column vectors, $Q_i, i = 1, 2, \cdots$, are square positive semi-definite matrices with compatible sizes, and X_i and $X_j, \forall i \neq j$, are independent. This implies that optimal control problem (5.15) *can be decoupled into at least two independent optimal control problems. By solving the independent optimal control problems, the final states of $X_i, i = 1, 2, \cdots$, in general, are not equal. Therefore, the requirement that Q has a simple zero eigenvalue is necessary to ensure consensus.*

Theorem 5.3.6 *Any symmetric Laplacian matrix $\mathcal{L} \in \mathbb{R}^{n\times n}$ with a simple zero eigenvalue is the optimal symmetric Laplacian matrix for cost function $J = \int_0^\infty [X^T(t)\mathcal{L}^2X^T + U^T(t)U(t)]dt$.*

Proof: By letting $Q = \mathcal{L}^2$ and $R = I_n$, it follows directly from the proof of Theorem 5.3.1 that $\mathcal{L}$ is the optimal symmetric Laplacian matrix. ■

5.3.2 Optimal Scaling Factor Using Interaction-related Cost Function

With interaction-related cost function (5.5), optimal control problem (5.7) can be written as

$$\begin{aligned} \min_{\beta} J_r &= \int_0^\infty \left[X^T(t)\mathcal{L}X(t) + U^T(t)U(t)\right] dt \\ \text{subject to: } & \dot{X}(t) = U(t),\ U(t) = -\beta\mathcal{L}X(t), \end{aligned} \tag{5.18}$$

where $\mathcal{L}$ is a prespecified symmetric Laplacian matrix and β is the scaling factor.

Theorem 5.3.7 *For optimal control problem* (5.18)*, where the symmetric Laplacian matrix $\mathcal{L}$ has a simple zero eigenvalue, the optimal β is $\sqrt{\frac{X^T(0)X(0)-X^T(0)m_1m_1^TX(0)}{X^T(0)\mathcal{L}X(0)}}$, where $m_1 = \frac{\mathbf{1}_n}{\sqrt{n}}$.*

Proof: The cost function J_r can be written as

$$J_r = \int_0^\infty X^T(0)\left[e^{-\beta\mathcal{L}t}\mathcal{L}e^{-\beta\mathcal{L}t} + \beta^2 e^{-\beta\mathcal{L}t}\mathcal{L}^2e^{-\beta\mathcal{L}t}\right]X(0)dt.$$

Taking derivative of J_r with respect to β gives

$$\frac{dJ_r}{d\beta} = \int_0^\infty X^T(0)\left[-2\mathcal{L}te^{-\beta\mathcal{L}t}\mathcal{L}e^{-\beta\mathcal{L}t} + 2\beta e^{-\beta\mathcal{L}t}\mathcal{L}^2e^{-\beta\mathcal{L}t} - 2\beta^2\mathcal{L}te^{-\beta\mathcal{L}t}\mathcal{L}^2e^{-\beta\mathcal{L}t}\right]X(0)dt.$$

Setting $\frac{dJ_r}{d\beta} = 0$ gives

$$\begin{aligned}
&\beta^2X^T(0)\left[\int_0^\infty \mathcal{L}te^{-\beta\mathcal{L}t}\mathcal{L}^2e^{-\beta\mathcal{L}t}dt\right]X(0)\\
&\quad-\beta X^T(0)\left[\int_0^\infty e^{-\beta\mathcal{L}t}\mathcal{L}^2e^{-\beta\mathcal{L}t}dt\right]X(0)\\
&\quad+X^T(0)\left[\int_0^\infty \mathcal{L}te^{-\beta\mathcal{L}t}\mathcal{L}e^{-\beta\mathcal{L}t}dt\right]X(0) = 0,
\end{aligned} \tag{5.19}$$

where we have used the fact that $\mathcal{L}$ and $e^{-\beta\mathcal{L}t}$ commute. Because $\mathcal{L}$ is symmetric, $\mathcal{L}$ can be diagonalized as

$$\mathcal{L} = M\underbrace{\begin{bmatrix}\lambda_1 & 0 & \cdots & 0\\ 0 & \lambda_2 & \cdots & 0\\ \cdots & \cdots & & \\ 0 & 0 & \cdots & \lambda_n\end{bmatrix}}_{\Lambda}M^T, \tag{5.20}$$

where M is an orthogonal matrix and λ_i is the ith eigenvalue of $\mathcal{L}$. It follows that

$$\begin{aligned}
&\int_0^\infty \mathcal{L}te^{-\beta\mathcal{L}t}\mathcal{L}^2e^{-\beta\mathcal{L}t}dt \\
=&\int_0^\infty M\begin{bmatrix} 0 & 0 & \cdots & 0 \\ 0 & e^{-2\beta\lambda_2 t}\lambda_2^3 t & \cdots & 0 \\ \cdots & \cdots & & \\ 0 & 0 & \cdots & e^{-2\beta\lambda_n t}\lambda_n^3 t \end{bmatrix} M^T dt \\
=&\frac{1}{4\beta^2}M\begin{bmatrix} 0 & 0 & \cdots & 0 \\ 0 & \lambda_2 & \cdots & 0 \\ \cdots & \cdots & & \\ 0 & 0 & \cdots & \lambda_n \end{bmatrix} M^T = \frac{1}{4\beta^2}\mathcal{L}.
\end{aligned} \tag{5.21}$$

Similarly, it follows that

$$\int_0^\infty e^{-\beta\mathcal{L}t}\mathcal{L}^2e^{-\beta\mathcal{L}t}dt = \int_0^\infty M\begin{bmatrix} 0 & 0 & \cdots & 0 \\ 0 & e^{-2\beta\lambda_2 t}\lambda_2^2 & \cdots & 0 \\ \cdots & \cdots & & \\ 0 & 0 & \cdots & e^{-2\beta\lambda_n t}\lambda_n^2 \end{bmatrix} M^T dt = \frac{1}{2\beta}\mathcal{L}, \tag{5.22}$$

and

$$\begin{aligned}
&\int_0^\infty \mathcal{L}te^{-\beta\mathcal{L}t}\mathcal{L}e^{-\beta\mathcal{L}t}dt \\
=&\int_0^\infty M\begin{bmatrix} 0 & 0 & \cdots & 0 \\ 0 & e^{-2\beta\lambda_2 t}\lambda_2^2 t & \cdots & 0 \\ \cdots & \cdots & & \\ 0 & 0 & \cdots & e^{-2\beta\lambda_n t}\lambda_n^2 t \end{bmatrix} M^T dt \\
=&\frac{I_n - m_1 m_1^T}{4\beta^2},
\end{aligned} \tag{5.23}$$

where $m_1 = \frac{\mathbf{1}_n}{\sqrt{n}}$. By substituting (5.21), (5.22), and (5.23) into (5.19), it follows that the optimal gain satisfies $\beta = \sqrt{\frac{X^T(0)X(0) - X^T(0)m_1 m_1^T X(0)}{X^T(0)\mathcal{L}X(0)}}$. ■

Remark 5.3.8 *In Theorem 5.3.7, we considered a simple case when the coupling gain for each vehicle is the same and presented the explicit optimal coupling gain. It is also possible to consider the case when the coupling gain for each vehicle is different. However, it is, in general, hard to give the explicit optimal coupling gains. Instead, numerical solutions can be obtained accordingly.*

5.3.3 Illustrative Examples

In this subsection, we provide two illustrative examples about the optimal (nonsymmetric) Laplacian matrix and the optimal scaling factor derived in Section 5.3.1 and Section 5.3.2, respectively.

In (5.15), we randomly choose $Q = \begin{bmatrix} 2 & -1 & -1 & 0 \\ -1 & 2 & -1 & 0 \\ -1 & -1 & 3 & -1 \\ 0 & 0 & -1 & 1 \end{bmatrix}$ and $R = \begin{bmatrix} 1 & 0 & 0 & 0 \\ 0 & 2 & 0 & 0 \\ 0 & 0 & 3 & 0 \\ 0 & 0 & 0 & 4 \end{bmatrix}$. It then follows from Theorem 5.3.1 that the optimal (nonsymmetric) Laplacian matrix is given by $\begin{bmatrix} 1.3134 & -0.5459 & -0.5964 & -0.1711 \\ -0.2730 & 0.8491 & -0.4206 & -0.1556 \\ -0.1988 & -0.2804 & 0.8218 & -0.3426 \\ -0.0428 & -0.0778 & -0.2570 & 0.3775 \end{bmatrix}$. Note that the optimal (nonsymmetric) Laplacian matrix corresponds to a complete directed graph.

In (5.18), we randomly choose $\mathcal{L} = \begin{bmatrix} 2 & -1 & -1 & 0 \\ -1 & 2 & 1 & 0 \\ -1 & -1 & 3 & -1 \\ 0 & 0 & -1 & 1 \end{bmatrix}$ and initial state $X(0) = [1, 2, 3, 4]^T$. Figure 5.1 shows how cost function J_r evolves as scaling factor β increases. From Theorem 5.3.7, it can be computed that the optimal scaling factor is $\beta = 0.845$, which is consistent with the result shown in Fig. 5.1.

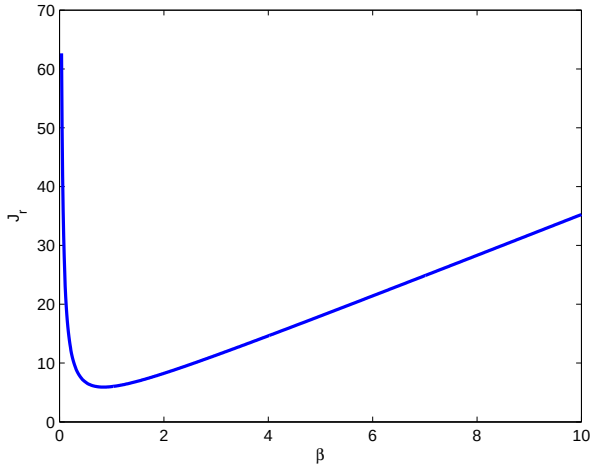

Fig. 5.1: Evolution of cost function J_r as a function of β.

5.4 LQR-based Optimal Linear Consensus Algorithms in a Discrete-time Setting

In this section, we study the optimal consensus algorithms in a discrete-time setting from an LQR perspective. As shown later, the analysis in the discrete-time case is more challenging than that in the continuous-time case. We will first derive the optimal (nonsymmetric) Laplacian matrix using discrete-time interaction-free cost function (5.11). We will then derive the optimal scaling factor for a prespecified symmetric Laplacian matrix using discrete-time interaction-related cost function (5.12). Finally, illustrative examples will be provided.

5.4.1 Optimal Laplacian Matrix Using Interaction-free Cost Function

With discrete-time interaction-free cost function (5.11), optimal control problem (5.13) can be written as

$$\min_{\mathcal{L}} J_f = \sum_{k=0}^{\infty} \{X[k]QX[k] + U[k]RU[k]\} \tag{5.24}$$

$$\text{subject to: } X[k+1] = X[k] + TU[k],\ U[k] = -\mathcal{L}X[k],$$

where Q, R, and $\mathcal{L}$ are defined as in (5.15).

The main result for optimal control problem (5.24) is given in the following theorem.

Theorem 5.4.1 *For optimal control problem* (5.24)*, where Q has a simple zero eigenvalue, the optimal consensus algorithm is*

$$U[k] = -\frac{T[\sqrt{(R^{-1}Q)^2 + 4R^{-1}Q/T^2} - R^{-1}Q]}{2}X[k], \tag{5.25}$$

that is, the optimal (nonsymmetric) Laplacian matrix is $\frac{T[\sqrt{(R^{-1}Q)^2+4R^{-1}Q/T^2}-R^{-1}Q]}{2}$. In addition, the optimal (nonsymmetric) Laplacian matrix corresponds to a complete directed graph.

Before proving the theorem, we need the following lemmas.

Lemma 5.4.1 [108] *Let there be an n by n nonnegative matrix $P = [p_{ij}]$, where $\rho(P) \leq 1$ and $p_{ii} > 0$. Let $\alpha \geq 1$. Then the following three statements hold:*

(a) There exists a nonnegative matrix $B \in \mathbb{R}^{n\times n}$, where $\rho(B) \leq \alpha$ and $I_n - P = (\alpha I_n - B)^2$, if and only if the iteration method

$$X_{i+1} = \frac{1}{2\alpha}[P + (\alpha^2 - 1)I_n + X_i^2], \quad X_0 = \mathbf{0}_{n\times n}, \tag{5.26}$$

is convergent. In this case, $B \geq X^\star = \lim_{i\to\infty} X_i$, $X^\star \geq 0$, $\rho(X^\star) \leq \alpha$, diag$_i(X^\star) > 0$,[2] $i = 1, \cdots, n$, and $(\alpha I_n - X^\star)^2 = I_n - P$.

(b) If (5.26) *is convergent, it follows that P and $\frac{X^\star}{\alpha}$ are semiconvergent.*

(c) If P is semiconvergent, then (5.26) *is convergent for all $\alpha \geq 1$. Denoting in this case the limit of the iteration method*

$$Y_{i+1} = \frac{1}{2}(P + Y_i^2), \quad Y_0 = \mathbf{0}_{n\times n},$$

by $Y^\star$, the equation $\alpha I_n - X^\star = I_n - Y^\star$ holds.

Lemma 5.4.2 [108] *$B \in Z^{n\times n}$, where $Z^{n\times n}$ is defined in Definition 5.1.1, is a nonsingular M-matrix if and only if B has a square root which is a nonsingular M-matrix.*

Lemma 5.4.3 [108] *$B \in Z^{n\times n}$, where $Z^{n\times n}$ is defined in Definition 5.1.1, is a nonsingular M-matrix if and only if B^{-1} exists and $B^{-1} \geq 0$.*

[2] Here, diag$_i(\cdot)$ denotes the ith diagonal entry of a square matrix.

Lemma 5.4.4 *Let P_1 and P_2 be two n by n nonnegative matrices satisfying $\rho(P_i) \leq 1$ and their diagonal entries are positive. Denote*

$$X_{i+1,j} = \frac{1}{2}[P_j + (X_{i,j})^2], \quad X_{0,j} = \mathbf{0}_{n\times n}, \tag{5.27}$$

for $j = 1, 2$. Also let $X_j^\star = \lim_{i\to\infty} X_{i,j}, j = 1, 2$. If P_1 and P_2 are commutable, the following statements hold:

1) $X_j^\star$ and P_k are commutable for $j, k \in \{1, 2\}$;

2) $X_1^\star$ and $X_2^\star$ are commutable.

Proof: We prove the lemma by induction. It can be computed from (5.27) that $X_{1,1} = \frac{1}{2}P_1$ and $X_{1,2} = \frac{1}{2}P_2$. Therefore, it is easy to verify that P_k and $X_{1,j}$ are commutable for $j, k \in \{1, 2\}$. Similarly, $X_{1,1}$ and $X_{1,2}$ are also commutable. Assume that P_k and $X_{n,j}$ are commutable for $j, k \in \{1, 2\}$ and $X_{n,1}$ and $X_{n,2}$ are commutable. It can be computed from (5.27) that $X_{n+1,j} = \frac{1}{2}[P_j + (X_{n,j})^2]$ for $j = 1, 2$. It can also be easily verified that $X_{n+1,j}$ and P_k are commutable for $j, k \in \{1, 2\}$. In addition, we also have

$$\begin{aligned}
&X_{n+1,1}X_{n+1,2}\\
=&\frac{1}{4}[P_1 + (X_{n,1})^2][P_2 + (X_{n,2})^2]\\
=&\frac{1}{4}[P_1P_2 + (X_{n,1})^2P_2 + P_1(X_{n,2})^2 + (X_{n,1})^2(X_{n,2})^2]\\
=&\frac{1}{4}[P_2P_1 + P_2(X_{n,1})^2 + (X_{n,2})^2P_1 + (X_{n,2})^2(X_{n,1})^2]\\
=&X_{n+1,2}X_{n+1,1},
\end{aligned}$$

where we have used the assumption that P_k and $X_{n,j}$ are commutable for $j, k \in \{1, 2\}$ and $X_{n,1}$ and $X_{n,2}$ are commutable to derive the final result. Therefore, $X_{n+1,1}$ and $X_{n+1,2}$ are also commutable. By induction, P_k and $\lim_{i\to\infty} X_{i,j}$ are commutable for $j, k \in \{1, 2\}$ and $\lim_{k\to\infty} X_{i,1}$ and $\lim_{k\to\infty} X_{i,2}$ are commutable. Because $X_j^\star = \lim_{i\to\infty} X_{i,j}, j = 1, 2$, the lemma holds apparently.

■

Lemma 5.4.5 *Let G be a (nonsymmetric) Laplacian matrix that has a simple zero eigenvalue with a corresponding eigenvector $\mathbf{1}_n$. When $\gamma \geq 0$, $\sqrt{G^2 + \gamma G}$ is a (nonsymmetric) Laplacian matrix with a simple zero eigenvalue.*

Proof: When $\gamma = 0$, the proof is trivial. When $\gamma \neq 0$, the proof follows three steps as follows:

Step 1: The off-diagonal entries of $\sqrt{G + \gamma I_n}\sqrt{G}$ are nonpositive. Because $G = [g_{ij}]$ is a (nonsymmetric) Laplacian matrix, G can be written as $G = s(I_n - P)$, where $s > 2\max_i g_{ii}$, and P is a row stochastic matrix with positive diagonal entries. According to part (a) in Lemma 5.4.1, $\sqrt{G} = \sqrt{s}(I_n - X^\star)$, where $X^\star$ is defined in (5.26) for $\alpha = 1$. Similarly, $G + \gamma I_n$ can be written as $G + \gamma I_n = (s+\gamma)(I_n - \frac{s}{s+\gamma}P)$. By following a similar analysis to that of G, it follows that $\sqrt{G + \gamma I_n} = \sqrt{s+\gamma}(I_n - \hat{X}^\star)$, where $\hat{X}^\star$ is defined in (5.26) by replacing P with $\frac{s}{s+\gamma}P$ for $\alpha = 1$. With P and $\frac{s}{s+\gamma}P$ playing the role of P_1 and P_2 in Lemma 5.4.4, it follows from parts (a) and (c) in Lemma 5.4.1 and Lemma 5.4.4 that $X^\star$ and $\hat{X}^\star$ are commutable because P and $\frac{s}{s+\gamma}P$ are commutable. Then we have

$$
\begin{aligned}
&\frac{1}{\sqrt{s(s+\gamma)}}\sqrt{G + \gamma I_n}\sqrt{G} \\
=&(I_n - X^\star - \hat{X}^\star + X^\star\hat{X}^\star) \\
=&I_n - \frac{1}{2}[P + (X^\star)^2] - \frac{1}{2}[\frac{s}{s+\gamma}P + (\hat{X}^\star)^2] + X^\star\hat{X}^\star \qquad (5.28)\\
=&I_n - \frac{1}{2}[P + \frac{s}{s+\gamma}P + (X^\star - \hat{X}^\star)^2], \qquad (5.29)
\end{aligned}
$$

where we have used the fact that $X^\star = \frac{1}{2}[P + (X^\star)^2]$ and $\hat{X}^\star = \frac{1}{2}[\frac{s}{s+\gamma}P + (\hat{X}^\star)^2]$ as shown in part (c) of Lemma 5.4.1 to derive (5.28) and the fact that $X^\star$ and $\hat{X}^\star$ are commutable to derive (5.29).

From (5.29), a sufficient condition to show that the off-diagonal entries of $\sqrt{G + \gamma I_n}\sqrt{G}$ are nonpositive is to show that $X^\star - \hat{X}^\star \geq 0$ because P is a row stochastic matrix. We next show that this condition can be satisfied. It follows from part (a) of Lemma 5.4.1 that $I - P = (I_n - X^\star)^2$

and $I - \frac{s}{s+\gamma}P = (I_n - \hat{X}^\star)^2$ when $\alpha = 1$. Therefore, we have

$$\begin{aligned}\frac{\gamma}{s+\gamma}P =&(I_n - \hat{X}^\star)^2 - (I_n - X^\star)^2\\ =&2(X^\star - \hat{X}^\star) - (X^\star - \hat{X}^\star)(X^\star + \hat{X}^\star)\\ =&(X^\star - \hat{X}^\star)(I_n - X^\star + I_n - \hat{X}^\star). \end{aligned} \tag{5.30}$$

We next show that $I_n - X^\star + I_n - \hat{X}^\star$ is a nonsingular M-matrix and then use Lemma 5.4.3 to show that $X^\star - \hat{X}^\star \geq 0$. Because $G + \gamma I_n$ is a nonsingular matrix from Definition 5.1.3, it follows from Lemma 5.4.2 that $\sqrt{G + \gamma I_n}$ is also a nonsingular M-matrix. Because $\sqrt{G + \gamma I_n} = \sqrt{s+\gamma}(I_n - \hat{X}^\star)$, it follows that $\rho(\hat{X}^\star) < 1$ according to Definition 5.1.3. Similarly, it follows from Lemma 5.3.1 that $\sqrt{G}$ is an M-matrix. Because $\sqrt{G} = \sqrt{s}(I_n - X^\star)$, it follows that $\rho(X^\star) \leq 1$ according to Definition 5.1.3. Because $\hat{X}^\star$ and $X^\star$ are commutable as shown in (5.29), it then follows that $\rho(\hat{X}^\star + X^\star) \leq \rho(\hat{X}^\star) + \rho(X^\star) < 2$ [109]. Therefore, $I_n - X^\star + I_n - \hat{X}^\star$ is a nonsingular M-matrix according to Definition 5.1.3. Because $I_n - X^\star + I_n - \hat{X}^\star$ is a nonsingular M-matrix, it follows from Lemma 5.4.3 that $(I_n - X^\star + I_n - \hat{X}^\star)^{-1} \geq 0$, which implies that $X^\star - \hat{X}^\star \geq 0$ because $X^\star - \hat{X}^\star = \frac{\gamma}{s+\gamma}P(I_n - X^\star + I_n - \hat{X}^\star)^{-1}$ and P is a row stochastic matrix. Therefore, it follows from (5.29) that the off-diagonal entries of $\sqrt{G + \gamma I_n}\sqrt{G}$ are nonpositive.

Step 2: $\sqrt{G + \gamma I_n}\sqrt{G} = \sqrt{G + \gamma I_n}\sqrt{G} = \sqrt{G^2 + \gamma G}$. From Step 1, we know that $\sqrt{G} = \sqrt{s}(I_n - X^\star)$, $\sqrt{G + \gamma I_n} = \sqrt{s+\gamma}(I_n - \hat{X}^\star)$, and $X^\star$ and $\hat{X}^\star$ are commutable. It follows that $\sqrt{G}$ and $\sqrt{G + \gamma I_n}$ are also commutable, which implies that $\sqrt{G + \gamma I_n}\sqrt{G} = \sqrt{G + \gamma I_n}\sqrt{G} = \sqrt{G^2 + \gamma G}$.

Step 3: *$\sqrt{G^2 + \gamma G}$ is a (nonsymmetric) Laplacian matrix with a simple zero eigenvalue.* Similar to the analysis in Step 2 in Lemma 5.3.3, $\sqrt{G}$ has a simple zero eigenvalue with a corresponding eigenvector $\mathbf{1}_n$. Then $\sqrt{G + \gamma I_n}\sqrt{G}$ also has a simple zero eigenvalue with a corresponding eigenvector $\mathbf{1}_n$ because $\sqrt{G + \gamma I_n}$ is a nonsingular M-matrix as shown in Step 1. Combining with Step 1 indicates that $\sqrt{G + \gamma I_n}\sqrt{G}$ is a (nonsymmetric) Laplacian matrix with a simple zero eigenvalue, which implies that $\sqrt{G^2 + \gamma G}$ is also a (nonsymmetric) Laplacian matrix with a simple zero eigenvalue according to Step 2. ■

Lemma 5.4.6 *Let G be a (nonsymmetric) Laplacian matrix that has a simple zero eigenvalue with a corresponding eigenvector $\mathbf{1}_n$. When $\gamma > 0$, $\sqrt{G^2 + \gamma G} - G$ is also a (nonsymmetric) Laplacian matrix with a simple zero eigenvalue.*

Proof: It can be computed that $P = \sqrt{G^2 + \gamma G} + G$ is the solution of the following matrix equation

$$P^2 - 2PG - \gamma G = \mathbf{0}_{n \times n}, \tag{5.31}$$

where we have used the fact that $\sqrt{G^2 + \gamma G}$ and G are commutable because $\sqrt{G + \gamma I_n}$ and $\sqrt{G}$ are commutable as shown in Step 2 of the proof in Lemma 5.4.5. From Lemma 5.4.5, we know that $\sqrt{G^2 + \gamma G}$ is a (nonsymmetric) Laplacian matrix, which implies that P is also a (nonsymmetric) Laplacian matrix because $P = \sqrt{G^2 + \gamma G} + G$. Therefore, $\gamma I_n + 2P$ is a nonsingular M-matrix according to Definition 5.1.3. From (5.31), we can get $G = (2P + \gamma I_n)^{-1} P^2 = \frac{1}{2}[I_n - \gamma(2P + \gamma I_n)^{-1}]P$, which implies

$$\frac{1}{2}\gamma(2P + \gamma I_n)^{-1} P = \frac{1}{2}P - G = \frac{1}{2}(\sqrt{G^2 + \gamma G} - G). \tag{5.32}$$

Note also that

$$\gamma(\gamma I_n + 2P)^{-1} P = \frac{1}{2}\gamma[I_n - \gamma(\gamma I_n + 2P)^{-1}]. \tag{5.33}$$

Combining (5.32) and (5.33) gives that

$$\sqrt{G^2 + \gamma G} - G = P - 2G = \gamma[I_n - \gamma(\gamma I_n + 2P)^{-1}]. \tag{5.34}$$

From Lemma 5.4.3, $(\gamma I_n + 2P)^{-1} \geq 0$ because $\gamma I_n + 2P$ is a nonsingular M-matrix. It then follows from (5.34) that the off-diagonal entries of $\sqrt{G^2 + \gamma G} - G$ are nonpositive.

Because the off-diagonal entries of $\sqrt{G^2 + \gamma G} - G$ are nonpositive, to show that $\sqrt{G^2 + \gamma G} - G$ is a (nonsymmetric) Laplacian matrix with a simple zero eigenvalue, it is sufficient to show that $\sqrt{G^2 + \gamma G} - G$ has a simple zero eigenvalue with an associated eigenvector $\mathbf{1}_n$. Because $\sqrt{G^2 + \gamma G}$ is a (nonsymmetric) Laplacian matrix with a simple zero eigenvalue as shown in

Lemma 5.4.5 and G is also a (nonsymmetric) Laplacian matrix with a simple zero eigenvalue, it follows that the interaction graphs associated with both $\sqrt{G^2+\gamma G}$ and G have a directed spanning tree. Because $P=\sqrt{G^2+\gamma G}+G$, it follows that P is a (nonsymmetric) Laplacian matrix and the interaction graph associated with P also has a directed spanning tree, which implies that P has a simple zero eigenvalue and the associated eigenvector is $\mathbf{1}_n$. Therefore, $\sqrt{G^2+\gamma G}-G$ also has the same property according to (5.34). Therefore, $\sqrt{G^2+\gamma G}-G$ is a (nonsymmetric) Laplacian matrix with a simple zero eigenvalue. ■

Lemma 5.4.7 *For any nonsingular M-matrix $B=[b_{ij}]\in\mathbb{R}^{n\times n}$ with each off-diagonal entry not equal to zero, each entry of B^{-1} is positive.*

Proof: From Definition 5.1.3, $B=sI_n-C$. By choosing $s>\max_i b_{ii}$, it follows that $C>0$. Because B is a nonsingular M-matrix, it follows from Definition 5.1.3 that $\rho(C)<s$. Therefore, $B^{-1}=s^{-1}(I_n-\frac{C}{s})^{-1}=s^{-1}[I_n+\frac{C}{s}+(\frac{C}{s})^2+\cdots]$ because $\lim_{k\to\infty}(\frac{C}{s})^k=\mathbf{0}_{n\times n}$ due to the fact that $\rho(C)<s$. Because $C>0$, it follows directly that each entry of B^{-1} is positive. ■

Lemma 5.4.8 *Let Q and R be defined in* (5.24)*. Suppose Q has a simple zero eigenvalue. The (nonsymmetric) Laplacian matrix $\sqrt{(R^{-1}Q)^2+\gamma R^{-1}Q}-R^{-1}Q$ corresponds to a complete directed graph for any $\gamma>0$.*

Proof: We study how $\sqrt{(R^{-1}Q)^2+\gamma R^{-1}Q}-R^{-1}Q$ evolves when γ increases. Taking the derivative of $R^{-1}Q+\gamma I_n$ with respect to γ gives

$$\frac{d(R^{-1}Q+\gamma I_n)}{d\gamma}=I_n. \tag{5.35}$$

We also have

$$\frac{d(\sqrt{R^{-1}Q+\gamma I_n})^2}{d\gamma}=2\sqrt{R^{-1}Q+\gamma I_n}\frac{d\sqrt{R^{-1}Q+\gamma I_n}}{d\gamma}. \tag{5.36}$$

Therefore, we have $\frac{d\sqrt{R^{-1}Q+\gamma I_n}}{d\gamma} = \frac{1}{2}(\sqrt{R^{-1}Q+\gamma I_n})^{-1}$ from (5.35) and (5.36). It then follows that

$$\begin{aligned}
&\frac{d\sqrt{(R^{-1}Q)^2+\gamma R^{-1}Q}}{d\gamma} \\
=&\sqrt{R^{-1}Q}\frac{d\sqrt{R^{-1}Q+\gamma I_n}}{d\gamma} \qquad (5.37)\\
=&\frac{1}{2}\sqrt{R^{-1}Q}(\sqrt{R^{-1}Q+\gamma I_n})^{-1} \\
=&\frac{1}{2}I_n-\frac{1}{2\gamma}(\sqrt{R^{-1}Q+\gamma I_n}+\sqrt{R^{-1}Q})^{-1}(\sqrt{R^{-1}Q+\gamma I_n})^{-1}, \qquad (5.38)
\end{aligned}$$

where we have used Step 2 in the proof of Lemma 5.4.5 to derive (5.37). Because $R^{-1}Q+\gamma I_n$ is a nonsingular M-matrix, it follows from Lemma 5.4.2 that $\sqrt{R^{-1}Q+\gamma I_n}$ is also a nonsingular M-matrix. Meanwhile, by following a similar analysis to that of Lemma 5.3.4, each entry of $\sqrt{R^{-1}Q+\gamma I_n}$ is not equal to zero. It follows from Lemma 5.4.7 that each entry of $(\sqrt{R^{-1}Q+\gamma I_n})^{-1}$ is positive. Similarly, each entry of $(\sqrt{R^{-1}Q+\gamma I_n}+\sqrt{R^{-1}Q})^{-1}$ is also positive. It then follows from (5.38) that each off-diagonal entry of $\frac{d\sqrt{R^{-1}Q^2+\gamma R^{-1}Q}}{d\gamma}$ is negative, which implies that the off-diagonal entries of $\sqrt{(R^{-1}Q)^2+\gamma R^{-1}Q}-R^{-1}Q$ will decrease. Noting that $\sqrt{(R^{-1}Q)^2+\gamma R^{-1}Q}-R^{-1}Q=\mathbf{0}_{n\times n}$ when $\gamma=0$, it follows that the off-diagonal entries are less than zero for any $\gamma>0$. Because $\sqrt{(R^{-1}Q)^2+\gamma R^{-1}Q}-R^{-1}Q$ is a (nonsymmetric) Laplacian matrix from Lemma 5.4.6 by considering $R^{-1}Q$ as G, it follows that the diagonal entries of $\sqrt{(R^{-1}Q)^2+\gamma R^{-1}Q}-R^{-1}Q$ are also not equal to zero. Combining the previous arguments shows that each entry of $\sqrt{(R^{-1}Q)^2+\gamma R^{-1}Q}-R^{-1}Q$ is not equal to zero, which implies that the (nonsymmetric) Laplacian matrix $\sqrt{(R^{-1}Q)^2+\gamma R^{-1}Q}-R^{-1}Q$ corresponds to a complete directed graph. ■

We next prove Theorem 5.4.1 based on the previous lemmas.

Proof of Theorem 5.4.1: We first show that (5.25) can always guarantee consensus. When using (5.25) for (5.8), we have

$$X[k+1]=\left(I_n-\frac{T^2[\sqrt{(R^{-1}Q)^2+4R^{-1}Q/T^2}-R^{-1}Q]}{2}\right)X[k]. \qquad (5.39)$$

Because $\sqrt{(R^{-1}Q)^2+4R^{-1}Q/T^2}-R^{-1}Q$ is a (nonsymmetric) Laplacian matrix with a simple zero eigenvalue when considering $R^{-1}Q$ and $\frac{4}{T^2}$ as, respectively, G and γ in Lemma 5.4.6, a sufficient condition to ensure consensus is that all diagonal entries of $I_n-\frac{T^2[\sqrt{(R^{-1}Q)^2+4R^{-1}Q/T^2}-R^{-1}Q]}{2}$ are positive according to Lemmas 3.4 and 3.7 [39]. Next, we show that this condition can be satisfied. By considering $\frac{T^2}{4}R^{-1}Q$ as G and $\gamma=1$, it follows from Step 2 in the proof of Lemma 5.4.5 that $\sqrt{I_n+\frac{T^2}{4}R^{-1}Q}$ and $\sqrt{\frac{T^2}{4}R^{-1}Q}$ are commutable. After some manipulations, we have

$$I_n-\frac{T^2[\sqrt{(R^{-1}Q)^2+4R^{-1}Q/T^2}-R^{-1}Q]}{2}=\left(\sqrt{I_n+\frac{T^2}{4}R^{-1}Q}-\sqrt{\frac{T^2}{4}R^{-1}Q}\right)^2.$$

By following a similar proof to that of Lemma 5.4.8, we have that $\sqrt{\gamma I_n+\frac{T^2}{4}R^{-1}Q}-\sqrt{\frac{T^2}{4}R^{-1}Q}$ is an M-matrix with each entry not equal to zero for any $\gamma>0$, which implies that each entry of $\sqrt{I_n+\frac{T^2}{4}R^{-1}Q}-\sqrt{\frac{T^2}{4}R^{-1}Q}$ is not equal to zero. Combining with Definition 5.1.3 shows that all diagonal entries of $(\sqrt{I_n+\frac{T^2}{4}R^{-1}Q}-\sqrt{\frac{T^2}{4}R^{-1}Q})^2$ are positive. Therefore, consensus can always be achieved when using (5.25).

We next show that (5.25) is the optimal consensus algorithm. Consider the following LQR problem

$$\min_{U[k]} J_f=\sum_{k=0}^{\infty}\{X[k]QX[k]+U[k]RU[k]\} \tag{5.40}$$
$$\text{subject to: } X[k+1]=AX[k]+BU[k],$$

where Q and R are defined in (5.24), $A=I_n$, and $B=TI_n$. It can be noted that (A,B) is controllable in (5.40), which implies that there exists a matrix P satisfying the following discrete-time algebraic Riccati equation (ARE)

$$P=Q+A^T[P-PB(R+B^TPB)^{-1}B^TP]A. \tag{5.41}$$

Noting that $A=I_n$ and $B=TI_n$, (5.41) can be simplified as

$$Q=PT(R+T^2P)^{-1}TP. \tag{5.42}$$

By multiplying R^{-1} on both sides of (5.42) and some manipulations, we can get $R^{-1}Q = R^{-1}PT(I_n + T^2R^{-1}P)^{-1}TR^{-1}P$. It then follow from the fact $(I_n+T^2R^{-1}P)^{-1} = I_n-(I+T^2R^{-1}P)^{-1}T^2R^{-1}P$ that

$$R^{-1}Q = [I_n - (I_n + T^2R^{-1}P)^{-1}]R^{-1}P, \tag{5.43}$$

which can be simplified as

$$(R^{-1}P)^2 - R^{-1}Q(R^{-1}P) - \frac{1}{T^2}R^{-1}Q = \mathbf{0}_{n\times n}. \tag{5.44}$$

It can be computed that (5.44) holds when $R^{-1}P = \frac{R^{-1}Q+\sqrt{(R^{-1}Q)^2+4(R^{-1}Q)/T^2}}{2}$. The optimal control strategy of (5.40) is given by $U[k] = -FX[k]$ with

$$\begin{aligned} F =&(I_n + T^2R^{-1}P)^{-1}TR^{-1}P \\ =&T(R^{-1}P - R^{-1}Q) \\ =&\frac{T(\sqrt{(R^{-1}Q)^2 + 4R^{-1}Q/T^2} - R^{-1}Q)}{2}, \end{aligned}$$

where we used (5.43) to derive from the second to the last equality. Because $\sqrt{(R^{-1}Q)^2 + 4R^{-1}Q/T^2}-R^{-1}Q$ is a (nonsymmetric) Laplacian matrix and corresponds to a complete directed graph by considering $\frac{4}{T^2}$ as γ in Lemma 5.4.8, it follows that $\frac{T(\sqrt{(R^{-1}Q)^2+4R^{-1}Q/T^2}-R^{-1}Q)}{2}$ is the optimal (nonsymmetric) Laplacian matrix and also corresponds to a complete directed graph. ■

Remark 5.4.2 *From Theorem 5.4.1, it is easy to verify that when $T \to 0$, the optimal (nonsymmetric) Laplacian matrix is the same as that in the continuous-time case in Theorem 5.3.1. In addition, matrix $\frac{T(\sqrt{(R^{-1}Q)^2+4R^{-1}Q/T^2}-R^{-1}Q)}{2}$ is not necessarily symmetric. When R is a diagonal matrix with identical diagonal entries, i.e., $R = cI_n$ with $c > 0$, $\frac{T(\sqrt{(R^{-1}Q)^2+4R^{-1}Q/T^2}-R^{-1}Q)}{2}$ is symmetric.*

Remark 5.4.3 *It can be noted from Theorem 5.4.1 that there is no constraint on the sampling period T. For any positive sampling period T, $\frac{T[\sqrt{(R^{-1}Q)^2+4R^{-1}Q/T^2}-R^{-1}Q]}{2}$ is the optimal Laplacian matrix that can always guarantee consensus.*

Similar to the discussion in Section 5.3, we next show that any symmetric Laplacian matrix $\mathcal{L}$ that has a simple zero eigenvalue is the optimal symmetric Laplacian matrix for some given cost function.

Theorem 5.4.4 *Any symmetric Laplacian matrix $\mathcal{L} = [\ell_{ij}] \in \mathbb{R}^{n\times n}$ that has a simple zero eigenvalue is the optimal symmetric Laplacian matrix for cost function $J = \sum_{k=0}^{\infty} \{X[k]QX[k] + U[k]U[k]\}$, where $Q = (I_n - T\mathcal{L})^{-1}\mathcal{L}^2$ and $T < \min_i \frac{1}{\ell_{ii}}$.*

Proof: When $T < \min_i \frac{1}{\ell_{ii}}$, it follows from the Gershgorin disc theorem [86] that $T\mathcal{L}$ has all eigenvalues within the unit circle and $I_n - T\mathcal{L}$ has all eigenvalues not equal to zero. It then follows that $\lim_{k\to\infty}[T\mathcal{L}]^k = \mathbf{0}_{n\times n}$. This implies $(I_n - T\mathcal{L})[I_n + T\mathcal{L} + (T\mathcal{L})^2 + \cdots] = I_n$, i.e., $(I_n - T\mathcal{L})^{-1} = I_n + T\mathcal{L} + (T\mathcal{L})^2 + \cdots$. It then follows that Q is PSD because both $(I_n - T\mathcal{L})^{-1}$ and $\mathcal{L}^2$ are PSD.

Note that $Q = (I_n - T\mathcal{L})^{-1}\mathcal{L}^2$ implies that $(I_n - T\mathcal{L})Q = \mathcal{L}^2$, i.e., $Q = \mathcal{L}^2 + T\mathcal{L}Q$, which implies

$$(TQ)^2 + 4Q = (2\mathcal{L} + TQ)^2. \tag{5.45}$$

By taking square root of both sides of (5.45) and some simplifications, we can get $\frac{T(\sqrt{Q^2+4Q/T^2}-Q)}{2} = \mathcal{L}$. Applying Theorem 5.4.1 finishes the proof. ■

5.4.2 Optimal Scaling Factor Using Interaction-related Cost Function

With interaction-related cost function (5.12), optimal control problem (5.14) can be written as

$$\begin{aligned} \min_{\beta} J_r &= \sum_{k=0}^{\infty} \left\{X^T[k]\mathcal{L}X[k] + U^T[k]U[k]\right\}, \\ \text{subject to: } & X[k+1] = X[k] + TU[k], \\ & U[k] = -\beta\mathcal{L}X[k], \end{aligned} \tag{5.46}$$

where $\mathcal{L}$ is a prespecified symmetric Laplacian matrix and β is the scaling factor. Because $\mathcal{L}$ is a symmetric Laplacian matrix, it thus can be written in a diagonal form as in (5.20) with λ_i being the ith eigenvalue of $\mathcal{L}$. Without loss of generality, let λ_i satisfy $0 = \lambda_1 \le \lambda_2 \le \cdots \le \lambda_n$.

Theorem 5.4.5 *For optimal control problem* (5.46)*, where symmetric Laplacian matrix $\mathcal{L}$ has a simple zero eigenvalue, the optimal scaling factor β_{opt} satisfies* $\frac{-T+\sqrt{T^2+\frac{4}{\lambda_n}}}{2} \leq \beta_{opt} \leq \frac{-T+\sqrt{T^2+\frac{4}{\lambda_2}}}{2}$.[3]

Proof: By rewriting $\mathcal{L}$ in a diagonal form as shown in (5.20), (5.46) can be written as

$$J_r = \sum_{k=0}^{\infty} X^T[0]M\{(I_n - \beta T\Lambda)^k \Lambda (I_n - \beta T\Lambda)^k + (I_n - \beta T\Lambda)^k (\beta\Lambda)^2 (I_n - \beta T\Lambda)^k\} M^T X[0].$$

Because $\mathcal{L}$ has a simple zero eigenvalue, it follows that $\lambda_i > 0, i = 2, \cdots, n$. After some manipulations, we have $J_r = X^T[0]M \begin{bmatrix} 0 & 0 & \cdot & 0 \\ 0 & \frac{\frac{1}{T}}{\frac{2\beta+T}{1+\beta^2\lambda_2}-T} & \cdot & 0 \\ \cdots & \cdots & & \\ 0 & 0 & \cdot & \frac{\frac{1}{T}}{\frac{2\beta+T}{1+\beta^2\lambda_n}-T} \end{bmatrix} M^T X[0]$. For $i = 2, \cdots, n$, taking derivative of $\frac{2\beta+T}{1+\beta^2\lambda_i} - T$ with respect to β and setting the derivative to zero gives

$$\frac{2(1+\beta^2\lambda_i) - 2\beta\lambda_i(2\beta+T)}{(1+\beta^2\lambda_i)^2} = 0.$$

It can be computed that $\beta = \frac{-T+\sqrt{T^2+\frac{4}{\lambda_i}}}{2}$. Note that for $\beta < \frac{-T+\sqrt{T^2+\frac{4}{\lambda_n}}}{2}$, the cost function J_r will decrease when β increases because $\frac{\frac{1}{T}}{\frac{2\beta+T}{1+\beta^2\lambda_i}-T}$ increases when β increases, $i = 2, \cdots, n$. Similarly, for $\beta > \frac{-T+\sqrt{T^2+\frac{4}{\lambda_2}}}{2}$, the cost function J_r will increase when β increases because $\frac{\frac{1}{T}}{\frac{2\beta+T}{1+\beta^2\lambda_i}-T}$ decreases when β increases, $i = 2, \cdots, n$. Combining the previous arguments shows that $\frac{-T+\sqrt{T^2+\frac{4}{\lambda_n}}}{2} \leq \beta_{opt} \leq \frac{-T+\sqrt{T^2+\frac{4}{\lambda_2}}}{2}$. ■

Remark 5.4.6 *The optimal control problem in Theorem 5.4.5 is essentially a polynomial optimization problem. Numerical optimization methods can be used to solve this problem* [110].

5.4.3 Illustrative Examples

In this subsection, we provide two illustrative examples about the optimal (nonsymmetric)

[3] Note that there always exists β such that consensus can be achieved. In this case, J_r is finite. Therefore, the optimal β_{opt} can always guarantee consensus because otherwise J_r will go to infinity, which will then result in a contradiction.

Laplacian matrix and the optimal scaling factor derived in Section 5.4.1 and Section 5.4.2, respectively.

In (5.24), let Q and R be defined as in Section 5.3.3 and sampling period $T = 0.1$ s. From Theorem 5.4.1, it can be computed that the optimal (nonsymmetric) Laplacian matrix is give by $\begin{bmatrix} 1.2173 & -0.498 & -0.5484 & -0.1709 \\ -0.249 & 0.8007 & -0.3963 & -0.1554 \\ -0.1828 & -0.2642 & 0.7734 & -0.3264 \\ -0.0427 & -0.0777 & -0.2448 & 0.3653 \end{bmatrix}$. Note that this matrix corresponds to a complete directed graph.

In (5.46), let $\mathcal{L}$ and initial state $X[0]$ be defined as in Section 5.3.3. Figure 5.2 shows how cost function J_r evolves as scaling factor β increases. From Theorem 5.4.5, it can be computed that the optimal scaling factor β satisfies $0.45 \leq \beta \leq 0.95$, which is consistent with the result shown in Fig. 5.2.

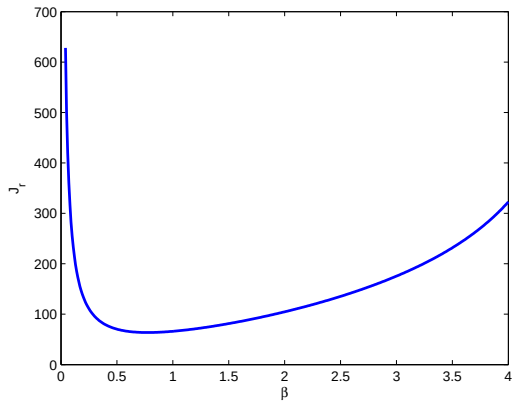

Fig. 5.2: Evolution of cost function J_r as a function of β.

Chapter 6

Decentralized Coordination Algorithms of Networked Fractional-order Systems

In the previous several chapters, we focus on the study of decentralized coordination algorithms for integer-order systems. In practice, the vehicle dynamics are sometimes better to be represented in a fractional-order form instead of a integer-order form, especially when the vehicles are working in complicated environments. Motivated by the broad application of coordination algorithms in multi-vehicle systems and the fact that many practical vehicles demonstrate fractional dynamics, we study coordination algorithms for networked fractional-order systems in this chapter. We study both fixed and switching network topology cases. Some background information is given in Appendix B.

6.1 Fractional Calculus

Fractional calculus can be dated back to the 17th century [111]. Fractional calculus studies fractional derivatives, fractional integrals, and their properties. Different from the integer orders of derivatives and integrals in conventional calculus, the orders of derivatives and integrals in fractional calculus are real numbers. The foundations of fractional calculus were laid on some pioneer work [112–114]. With the development of fractional calculus, its applications were also studied by researchers from different disciplines [115, 116]. Examples include study of formation of particulate aggregates [117] and study of motion of objects in viscoelastic materials [118–120]. In particular, fractional calculus was also introduced into the engineering community to design the CRONE controller [121] and synthesize control systems [122], to name a few.

In addition, fractional dynamics were also presented and studied from different perspectives. The dynamics of self-similar protein was modeled in a fractional-order sense because the relaxation processes and reaction kinematics of proteins deviated from exponential behavior [123]. The

fractional-order dynamics of international commodity prices were demonstrated from the commodity price series [124]. The fractional-order PID controllers were shown to demonstrate better performance when used for the control of fractional-order systems than the classical PID controllers [125, 126]. Fractional equations have become a complementary tool in the description of anomalous transport processes in complex systems [127].

6.2 Mathematical Model

In this section, we introduce a general mathematical model of coordination for fractional-order systems by summarizing the following three different cases:

Case 1: Fractional-order agent dynamics with an integer-order coordination algorithm

Assume that the agent dynamics are

$$r_i^{(\alpha)}(t) = u_i(t), \tag{6.1}$$

where $r_i(t)$ and $u_i(t)$ represent, respectively, the state and control input for the ith agent, and $r_i^{(\alpha)}(t)$ is the αth derivative of $r_i(t)$ with $\alpha \in \mathbb{R}^+$.[1] An integer-order coordination algorithm is given by

$$u_i(t) = \sum_{j \in N_i} a_{ij}\{[r_j(t) - \delta_j] - [r_i(t) - \delta_i]\}, \tag{6.2}$$

where a_{ij} is the (i, j)th entry of the adjacency matrix $\mathcal{A}$, N_i denotes the neighbor set of agent i, and δ_i is constant.

Case 2: Integer-order agent dynamics with a fractional-order coordination algorithm

Assume that the agent dynamics are given by $\dot{r}_i(t) = u_i(t)$, where $r_i(t)$ and $u_i(t)$ are defined as in (6.1). A fractional-order coordination algorithm is given by

$$u_i(t) = \sum_{j \in N_i} a_{ij}\{[r_j(t) - \delta_j]^{(\beta)} - [r_i(t) - \delta_i]^{(\beta)}\}, \tag{6.3}$$

where $\beta \in \mathbb{R}^+$, and a_{ij}, N_i, and δ_i are defined as in (6.2).

Case 3: Fractional-order agent dynamics with a fractional-order coordination algorithm

[1] For a given system, α is fixed.

Assume that the agent dynamics are given by (6.1). A fractional-order coordination algorithm is given by (6.3).

Define $\delta_{ij} \triangleq \delta_i - \delta_j$. The objective of the algorithm in each case is to guarantee coordination, i.e., $r_i(t) - r_j(t) \to \delta_{ij}$ as $t \to \infty$ for any initial $r_i(0)$ and $r_j(0)$. Note that integer-order dynamics, i.e., α is an integer in (6.1), is a special case of fractional-order dynamics. The existing consensus algorithm for single-integrator dynamics (e.g., [36, 37, 39]) corresponds to a special case of Case 1 when $\alpha = 1$ in (6.1) and $\delta_{ij} = 0$ in (6.2).

When applying Caputo derivative to (6.1) and (6.3), it follows that Cases 2 and 3 can be written as Case 1 by applying the fractional operator ${}_a^C D_t^{-\beta}$ on both sides of the corresponding system. Therefore, the model in Case 1 can be considered a general model. In the following, we focus on Case 1. For an n-agent system, using (6.2), (6.1) can be written in matrix form as

$$\tilde{X}^{(\alpha)}(t) = -\mathcal{L}\tilde{X}(t), \tag{6.4}$$

where $\tilde{X}(t) = [\tilde{r}_1(t), \tilde{r}_2(t), \ldots, \tilde{r}_n(t)]^T \in \mathbb{R}^n$ with $\tilde{r}_i(t) = r_i(t) - \delta_i$ and $\mathcal{L}$ is the (nonsymmetric) Laplacian matrix. Although the dynamics for a given system are fixed, α in the general model (6.4) can be changed by choosing coordination algorithms with different fractional orders.

6.3 Coordination Algorithms for Fractional-order Systems Without Damping Terms

In this section, we study the coordination algorithms in the absence of damping terms, that is, the control algorithms only depends on the states.

6.3.1 Convergence Analysis

We first investigate the conditions on the network topology and the fractional order such that convergence can be achieved. In particular, we study both fixed network topology and switching network topology cases.

Fixed Network Topology

We first study the case when the network topology is fixed, i.e., $\mathcal{L}$ is fixed in (6.4). We focus

on deriving the conditions on the network topology and the fractional order such that coordination can be achieved.

Note that $\mathcal{L}$ can be written in Jordan canonical form as $\mathcal{L} = P \underbrace{\begin{bmatrix} \Lambda_1 & 0 & \cdots & 0 \\ 0 & \Lambda_2 & \cdots & 0 \\ \cdots & \cdots & & \\ 0 & 0 & \cdots & \Lambda_k \end{bmatrix}}_{\Lambda} P^{-1}$, where $\Lambda_m,\ m = 1, 2, \ldots, k$, are standard Jordan blocks. Without loss of generality, let the initial time $a = 0$. By defining $Y(t) \triangleq P^{-1}\tilde{X}(t)$, (6.4) can be written as

$$Y^{(\alpha)}(t) = -\Lambda Y(t). \tag{6.5}$$

Suppose that the diagonal entry of Λ_i is λ_i, i.e., an eigenvalue of $\mathcal{L}$. Noting that the standard Jordan block $\Lambda_i = \begin{bmatrix} \lambda_i & 1 & \cdots & 0 \\ 0 & \lambda_i & \cdots & 0 \\ \cdots & \cdots & & \\ 0 & 0 & \cdots & \lambda_i \end{bmatrix}$, it follows that (6.25) can be decoupled into n one-dimensional equations represented by either

$$y_i^{(\alpha)}(t) = -\lambda_i y_i(t) \tag{6.6}$$

for the equation corresponding to Λ_i which has dimension equal to one or the last equation corresponding to Λ_i which has dimension larger than one, or

$$y_i^{(\alpha)}(t) = -\lambda_i y_i(t) - y_{i+1}(t), \tag{6.7}$$

otherwise, where $y_i(t)$ is the ith component of $Y(t)$.

Before deriving the main result, we need the following two lemmas.

Lemma 6.3.1 *When* $\mathrm{Re}(\lambda_i) \geq 0$, *where* $\mathrm{Re}(\cdot)$ *denotes the real part of a complex number, the solution of* (6.26) *has the following properties:*

1) When $\alpha \in (0, \frac{2\theta_i}{\pi})$ *and* $\mathrm{Re}(\lambda_i) > 0$, $\lim_{t\to\infty} y_i(t) \to 0$ *as* $t \to \infty$, *where* $\theta_i = \pi - \arg\{\lambda_i\}$ *with*

$\arg\{\lambda_i\}$ *denoting the phase of* λ_i.[2]

2) When $\alpha \in (0, 1]$ *and* $\lambda_i = 0$, $y_i(t) \equiv y_i(0),\ \forall t$.

3) When $\alpha \in (1, 2)$ *and* $\lambda_i = 0$, $y_i(t) = y_i(0) + \dot{y}_i(0)t$.

4) When $\alpha \in (2, \infty)$, *the system is not stable.*

Proof: (Proof of Property 1) By taking the Laplace transform of (6.26), it can be computed from the Laplace transform of $L\{f^{(\alpha)}(t)\}$ in Appendix B that

$$L\{y_i(t)\} = \frac{y_i(0^-)s^{\alpha-1}}{s^\alpha + \lambda_i},\ \alpha \in (0, 1] \tag{6.8}$$

and

$$L\{y_i(t)\} = \frac{y_i(0^-)s^{\alpha-1} + \dot{y}_i(0^-)s^{\alpha-2}}{s^\alpha + \lambda_i},\ \alpha \in (1, 2). \tag{6.9}$$

From (6.8) and (6.9), it can be seen that the denominator of $L\{y_i(t)\}$ is $s^\alpha + \lambda_i$ when $\alpha \in (0, 2)$. To ensure that all poles of $L\{y_i(t)\}$ are in the open left half plane (LHP), it follows that $\alpha \in (0, \frac{2(\pi - \arg\{\lambda_i\})}{\pi})$ [128], that is, $\alpha \in (0, \frac{2\theta_i}{\pi})$, where $\frac{2\theta_i}{\pi} > 1$ because $\mathrm{Re}(\lambda_i) > 0$, i.e., $\arg\{\lambda_i\} \in (-\frac{\pi}{2}, \frac{\pi}{2})$. In particular, when $\lambda_i \in \mathbb{R}^+$, $\alpha \in (0, 2)$ because $\arg\{\lambda_i\} = 0$.

(Proof of Properties 2 and 3) The proofs of Properties 2 and 3 follow from Podlubny [116].

(Proof of Property 4) See Gorenflo and Mainardi [129]. ■

Lemma 6.3.2 *Assume that continuous function* $y_{i+1}(t)$ *satisfies* $\lim_{t\to\infty} y_{i+1}(t) = 0$. *When* $\mathrm{Re}(\lambda_i) > 0$, *i.e.,* $\arg\{\lambda_i\} \in (-\frac{\pi}{2}, \frac{\pi}{2})$, *and* $\alpha \in (0, \frac{2\theta_i}{\pi})$, *where* $\theta_i = \pi - \arg\{\lambda_i\}$, *the solution of* (6.27) *satisfies* $\lim_{t\to\infty} y_i(t) = 0$.

Proof: When $\alpha \in (0, 1]$, by taking the Laplace transform of (6.27), it can be computed from the Laplace transform of $L\{f^{(\alpha)}(t)\}$ that

$$L\{y_i(t)\} = \frac{s^{\alpha-1}y_i(0^-) - L\{y_{i+1}(t)\}}{s^\alpha + \lambda_i}. \tag{6.10}$$

[2]We follow the convention that $\arg\{x\} \in (-\pi, \pi]$ for $x \in \mathbb{C}$.

It follows from the proof of Property 1 in Lemma 6.3.1 that the poles of (6.10) are in the open LHP when $\alpha \in (0, 1]$. By applying the final value theorem of the Laplace transform,

$$\lim_{t\to\infty} y_i(t) = \lim_{s\to 0} sL\{y_i(t)\} = \lim_{s\to 0} \frac{s^\alpha y_i(0^-) - sL\{y_{i+1}(t)\}}{s^\alpha + \lambda_i} = 0,$$

where we have used the fact $sL\{y_{i+1}(t)\} = 0$ to derive the last equality because $\lim_{t\to\infty} y_{i+1}(t) = 0$.

When $\alpha \in (1, \frac{2\theta_i}{\pi})$, it follows from the proof of Property 1 in Lemma 6.3.1 that the poles of (6.10) are also in the open LHP. By taking the Laplace transform of (6.27), it can be computed from the Laplace transform of $L\{f^{(\alpha)}(t)\}$ that

$$L\{y_i(t)\} = \frac{s^{\alpha-1} y_i(0^-) + s^{\alpha-2}\dot{y}_i(0^-) - L\{y_{i+1}(t)\}}{s^\alpha + \lambda_i}. \tag{6.11}$$

Following a similar discussion for $\alpha \in (0, 1]$ gives $\lim_{t\to\infty} y_i(t) = 0$.

Combining the above arguments proves the lemma. ■

Based on Lemmas 6.3.1 and 6.3.2, we next study the conditions on the fractional order α and the interaction graph such that coordination can be achieved.

Theorem 6.3.1 *Let λ_i be the ith eigenvalue of L and $\theta = \min_{\lambda_i\neq 0, i=1,2,\cdots,n} \theta_i$, where $\theta_i = \pi - \arg\{\lambda_i\}$. For fractional-order system* (6.4)*, coordination is achieved if the fixed interaction graph has a directed spanning tree and $\alpha \in (0, \frac{2\theta}{\pi})$. When $\alpha \in (0, 1]$, the solution of* (6.4) *satisfies $\tilde{r}_i(t) \to \tilde{r}_j(t) \to \mathbf{p}^T\tilde{X}(0)$, i.e., $r_i(t) - r_j(t) \to \delta_{ij}$ as $t \to \infty$, where $\mathbf{p}$ is the left eigenvector of L associated with the zero eigenvalue satisfying $\mathbf{p}^T\mathbf{1} = 1$. When $\alpha \in (1, \frac{2\theta}{\pi})$, the solution of* (6.4) *satisfies $\tilde{r}_i(t) \to \tilde{r}_j(t) \to \mathbf{p}^T\tilde{X}(0) + \mathbf{p}^T\dot{\tilde{X}}(0)t$ and $\dot{\tilde{r}}_i(t) \to \dot{\tilde{r}}_j(t) \to \mathbf{p}^T\dot{\tilde{X}}(0)$, i.e., $r_i(t) - r_j(t) \to \delta_{ij}$, as $t \to \infty$.*

Proof: Noting that the interaction graph has a directed spanning tree, it follows that $\mathcal{L}$ has a simple zero eigenvalue and all other eigenvalues have positive real parts [39]. Without loss of generality, let $\lambda_1 = 0$ and $\mathrm{Re}(\lambda_i) > 0,\ i \neq 1$. When $\alpha \in (0, 1]$, because $\lambda_1 = 0$ is a simple zero eigenvalue, λ_1 satisfies (6.26). It follows from Property 2 in Lemma 6.3.1 that $y_1(t) \equiv y_1(0)$. When $\lambda_i,\ i \neq 1$, satisfies (6.26), it follows from Property 1 in Lemma 6.3.1 that $\lim_{t\to\infty} y_i(t) = 0,\ i \neq 1$. When $\lambda_i,\ i \neq 1$, satisfies (6.27), it follows from Lemma 6.3.2 that $\lim_{t\to\infty} y_i(t) = 0,\ i \neq 1$, as well because

$y_{i+1}(t)$ also satisfies either (6.26) or (6.27), which implies $\lim_{t\to\infty} y_{i+1}(t) = 0$. Combining the above arguments gives $\lim_{t\to\infty} Y(t) = [y_1(0), 0, \cdots, 0]^T,\ i \neq 1$, which implies $\lim_{t\to\infty} \tilde{X}(t) = \lim_{t\to\infty} PY(t) = PSY(0) = PSP^{-1}\tilde{X}(0)$, where $S = [s_{ij}] \in \mathbb{R}^{n\times n}$ has only one nonzero entry $s_{11} = 1$. Note that the first column of P can be chosen as $\mathbf{1}$ while the first row of P^{-1} can be chosen as $\mathbf{p}$ by noting that $\mathbf{1}$ and $\mathbf{p}$ are, respectively, a right and left eigenvector of L associated with $\lambda_1 = 0$ and $\mathbf{p}^T\mathbf{1} = 1$. Therefore, $\lim_{t\to\infty} \tilde{X}(t) = PSP^{-1}\tilde{X}(0) = \mathbf{1}\mathbf{p}^T\tilde{X}(0)$, that is, $\lim_{t\to\infty} \tilde{r}_i(t) = \mathbf{p}^T\tilde{X}(0)$. This implies that $r_i(t) - r_j(t) \to \delta_{ij}$ as $t \to \infty$.

When $\alpha \in (1, \frac{2\theta}{\pi})$, similar to the previous discussion for $\alpha \in (0, 1]$, λ_1 satisfies (6.26). It follows from Property 3 in Lemma 6.3.1 that $y_1(t) = y_1(0) + \dot{y}_1(0)t$. Because $\mathrm{Re}(\lambda_i) > 0,\ i \neq 1$, similar to the previous discussion for $\alpha \in (0, 1]$, it follows from Property 1 in Lemma 6.3.1 and Lemma 6.3.2 that $\lim_{t\to\infty} y_i(t) = 0,\ i \neq 1$. Therefore, it follows that $\lim_{t\to\infty} Y(t) = [y_1(0) + \dot{y}_1(0)t, 0, \cdots, 0]^T$, which implies that $\lim_{t\to\infty} \dot{Y}(t) = [\dot{y}_1(0), 0, \cdots, 0]^T$. Similar to the proof for $\alpha \in (0, 1]$, it follows directly that $\lim_{t\to\infty} \tilde{r}_i(t) = \mathbf{p}^T\tilde{X}(0) + \mathbf{p}^T\dot{\tilde{X}}(0)t$ and $\lim_{t\to\infty} \dot{\tilde{r}}_i(t) = \mathbf{p}^T\dot{\tilde{X}}(0)$. This implies that $r_i(t) - r_j(t) \to \delta_{ij}$ as $t \to \infty$.

Combining the previous arguments for $\alpha \in (0, 1]$ and $\alpha \in (1, \frac{2\theta}{\pi})$ proves the theorem. ■

As a special case, when the fixed interaction graph is undirected, we can obtain the following result.

Corollary 6.3.2 *Assume that the fixed interaction graph is undirected. For fractional-order system* (6.4)*, coordination is achieved if the interaction graph is connected and* $\alpha \in (0, 2)$*. The coordination equilibria when* $\alpha \in (0, 1]$ *and* $\alpha \in (1, \frac{2\theta}{\pi})$ *are the same as those in Theorem 6.3.1.*

Proof: When the undirected interaction graph is connected, it follows that there is a simple zero eigenvalue and all other eigenvalues are positive, which implies that $\theta = \pi$. The statements then follow from the proof in Theorem 6.3.1. ■

From Theorem 6.3.1, it can be seen that the range of the fractional order α is determined by θ. Note that θ is closely related to the eigenvalues of $\mathcal{L}$, which are also related to the number of agents. In the following, we characterize the relationship between α and the number of agents to ensure coordination.

Theorem 6.3.3 *Assume that there are n agents with $n \geq 2$. For fractional-order system* (6.4)*, coordination can be achieved if the fixed interaction graph has a directed spanning tree and $\alpha \in (0, 1 + \frac{2}{n})$.*

Proof: Letting λ_i be the ith eigenvalue of $\mathcal{L}$, it follows that $\arg\{\lambda_i\} \in [-\frac{\pi}{2} + \frac{\pi}{n}, \frac{\pi}{2} - \frac{\pi}{n}]$ for all $\lambda_i \neq 0$ [130], which implies $\frac{2\theta}{\pi} \geq 1 + \frac{2}{n}$. Therefore, the statement holds apparently from Theorem 6.3.1. ■

Remark 6.3.4 *From Theorem 6.3.1, it can be seen that the final coordination equilibrium of* (6.4) *for $\alpha \in (0, 1]$ is the same as that of*

$$\dot{\tilde{X}}(t) = -\mathcal{L}\tilde{X}(t), \tag{6.12}$$

under the same $\mathcal{L}$.

Remark 6.3.5 *From Theorem 6.3.3, when there exist more agents in a team, i.e., n becomes larger, α has to be chosen smaller to ensure coordination. As $n \to \infty$, $\frac{2\theta}{\pi} \to 1$, i.e., $\alpha \in (0, 1]$, which implies that the coordination property for systems with single-integrator dynamics does not depend on n.*

Switching Network Topology

In this section, we derive the conditions on the network topology and the fractional orders such that coordination will be achieved for fractional-order system (6.4) under a directed dynamic network topology. We assume that the interaction is constant over time interval $[\sum_{j=1}^{k} \Delta_j, \sum_{j=1}^{k+1} \Delta_j)$ and switches at time $t = \sum_{j=1}^{k} \Delta_j$ with $k = 0, 1, \cdots$,[3] where $\Delta_j > 0, j = 1, \cdots$. Let $\mathcal{G}_k$ and A_k denote, respectively, the directed graph and the adjacency matrix for $t \in [\sum_{j=1}^{k} \Delta_j, \sum_{j=1}^{k+1} \Delta_j)$. We also assume that each nonzero entry of A_k has a lower bound $\underline{a}$ and an upper bound $\overline{a}$, where $\underline{a}$ and $\overline{a}$ are positive constants with $\overline{a} \geq \underline{a}$. Then (6.4) becomes

$$\tilde{X}^{(\alpha)}[k+1] = -\mathcal{L}_k \tilde{X}[k], \tag{6.13}$$

where $\mathcal{L}_k \in \mathbb{R}^{n \times n}$ represents the Laplacian matrix associated with $\mathcal{A}_k$.

[3] We define $\sum_{j=1}^{k} \Delta_j \triangleq 0$ when $k = 0$.

We first focus on the case where $0 < \alpha < 1$. We have the following result.

Theorem 6.3.6 *Assume that $\alpha \in (0, 1)$. Using* (6.2) *for* (6.1)*, a necessary condition to guarantee coordination is that there exists a finite constant N such that the union of $\mathcal{G}_j$, $j = k, k+1, \cdots, k+N$, has a directed spanning tree for any finite k. Furthermore, if $\mathcal{G}_j, j = 0, 1, \cdots$, has a directed spanning tree at each time interval, there exists positive $\overline{\Delta}_i$ such that coordination will be achieved globally when $\Delta_i > \overline{\Delta}_i$.*[4]

Proof: For the first statement, when there does not exist a finite constant N such that the union of $\mathcal{G}_j, j = k, \cdots, k+N$, has a directed spanning tree for some k, it follows that at least one system, labeled as i, is separated from the other systems for $t \in [\sum_{j=1}^{k} \Delta_j, \infty)$. It follows that the state of system i is independent of the states of the other systems for $t \geq \sum_{j=1}^{k} \Delta_j$, which implies that all systems cannot always achieve coordination for arbitrary initial conditions.

For the second statement, it follows from Theorem 3.9 [131] that

$$\tilde{X}(t) = E_\alpha(-\mathcal{L}t^\alpha)\tilde{X}(0).$$

Therefore, the solution to (6.13) is given by

$$\tilde{X}(\sum_{j=1}^{k} \Delta_j) = \prod_{i=1}^{k} E_\alpha(-\mathcal{L}_k(\sum_{j=1}^{k+1} \Delta_j)^\alpha)[E_\alpha(-\mathcal{L}_k(\sum_{j=1}^{k} \Delta_j)^\alpha)]^{-1} E_\alpha(-\mathcal{L}_0\Delta_1)^\alpha)\tilde{X}(0). \quad (6.14)$$

Define $\overline{x} \stackrel{\triangle}{=} \max_i \tilde{x}_i$, $\underline{x} \stackrel{\triangle}{=} \min_i \tilde{x}_i$, and $V \stackrel{\triangle}{=} \max_i \tilde{x}_i - \min_i \tilde{x}_i$. It follows from Theorem 3.1 [132] that $\tilde{x}_i$ converges to $\tilde{x}_j$ as $t \to \infty$ if the network topology has a directed spanning tree. That is, there exists positive $\overline{\Delta}_1$ such that $V(t) < V(0)$ for any $t \geq \overline{\Delta}_1$. Similarly, by considering $[E_\alpha(-\mathcal{L}_1(\Delta_1)^\alpha)]^{-1} E_\alpha(-\mathcal{L}_0\Delta_1)^\alpha)\tilde{X}(0)$ as the new initial state, it follows that there exists $\overline{\Delta}_2$ such that $V(t + \Delta_1) < V(\Delta_1)$ for any $t > \overline{\Delta}_2$. By following a similar analysis, there also exist $\overline{\Delta}_3, \cdots$. When $\Delta_i \geq \overline{\Delta}_i$, $V(\sum_{j=1}^{i+1} \Delta_k) < V(\sum_{j=1}^{i} \Delta_k)$. Therefore, $V(\sum_{j=1}^{i} \Delta_k) \to 0$ as $i \to \infty$. Therefore, $\tilde{x}_i[k] \to \tilde{x}_j[k]$, i.e., $x_i[k] - x_j[k] \to \delta_{ij}$ as $k \to \infty$ under the condition of the theorem. ■

[4] Here the values of $\overline{\Delta}_i, i = 1, \cdots$, depend on the initial states, the fractional-order α, and $\mathcal{G}_k$.

Remark 6.3.7 *For system $\dot{x}_i(t) = u_i(t)$, $x_i(t)$ will decrease if $u_i(t) < 0$ and $x_i(t)$ will increase if $u_i(t) > 0$. However, for system $x_i^{(\alpha)}(t) = u_i(t)$ with $\alpha \in (0, 1)$, due to the long memory process of fractional calculus, the aforementioned properties do not necessarily hold. Therefore, even if the switching network topology has a directed spanning tree at each time interval, coordination might not be achieved ultimately because the switching sequence also plays an important role.*

We next study the case where $1 < \alpha < 1 + \frac{2}{n}$, where $n \geq 2$. When the directed network topology is fixed, we have the following lemma regarding the solution of (6.4).

Lemma 6.3.3 *When $\alpha \in (1, 2)$, the solution of* (6.4) *is*

$$\tilde{X}(t) = E_\alpha(-\mathcal{L}t^\alpha)\tilde{X}(0) + tE_{\alpha,2}(-\mathcal{L}t^\alpha)\dot{\tilde{X}}(0). \tag{6.15}$$

Proof: Consider the fractional-order system given by (6.4). By applying the Laplace transform to both sides of (6.4), it follows that

$$s^{-(2-\alpha)}[L\{\ddot{\tilde{X}}(t)\}] = -\mathcal{L}\tilde{X}(s). \tag{6.16}$$

Eq. (6.16) can be written as

$$s^{-(2-\alpha)}[s^2\tilde{X}(s) - s\tilde{X}(0) - \dot{\tilde{X}}(0)] = -\mathcal{L}\tilde{X}(s). \tag{6.17}$$

After some manipulation, (6.17) can be written as

$$\tilde{X}(s) = (s^\alpha I_n + \mathcal{L})^{-1}s^{\alpha-1}\tilde{X}(0) + (s^\alpha I_n + \mathcal{L})^{-1}s^{\alpha-2}\dot{\tilde{X}}(0). \tag{6.18}$$

By applying the inverse Laplace transform to (6.18), it follows from Theorem 3.2 [131] that (6.15) is a solution of (6.4). Noting also that $\mathcal{L}$ is a constant matrix, it follows from the uniqueness and existence theorem of fractional equations [116] that (6.15) is the unique solution of (6.4). ■

Taking derivative of (6.15) with respect to t gives that

$$\dot{\tilde{X}}(t) = \frac{1}{t}E_{\alpha,0}(-\mathcal{L}t^\alpha)\tilde{X}(0) + E_\alpha(-\mathcal{L}t^\alpha)\dot{\tilde{X}}(0). \tag{6.19}$$

Combining (6.15) and (6.19) leads to the following matrix form

$$\begin{bmatrix} \tilde{X}(t) \\ \dot{\tilde{X}}(t) \end{bmatrix} = \begin{bmatrix} E_\alpha(-\mathcal{L}t^\alpha) & tE_{\alpha,2}(-\mathcal{L}t^\alpha) \\ \frac{1}{t}E_{\alpha,0}(-\mathcal{L}t^\alpha) & E_\alpha(-\mathcal{L}t^\alpha) \end{bmatrix} \begin{bmatrix} \tilde{X}(0) \\ \dot{\tilde{X}}(0) \end{bmatrix}. \tag{6.20}$$

Therefore, we can get that

$$\begin{bmatrix} \tilde{X}(\Delta_1) \\ \dot{\tilde{X}}(\Delta_1) \end{bmatrix} = \begin{bmatrix} E_\alpha(-\mathcal{L}_0\Delta_1^\alpha) & \Delta_1 E_{\alpha,2}(-\mathcal{L}_0\Delta_1^\alpha) \\ \frac{1}{\Delta_1}E_{\alpha,0}(-\mathcal{L}_0\Delta_1^\alpha) & E_\alpha(-\mathcal{L}_0\Delta_1^\alpha) \end{bmatrix} \begin{bmatrix} \tilde{X}(0) \\ \dot{\tilde{X}}(0) \end{bmatrix}.$$

Similarly, we can also get that

$$\begin{bmatrix} \tilde{X}(\Delta_k) \\ \dot{\tilde{X}}(\Delta_k) \end{bmatrix} = \prod_{i=1}^{k} C_{k-i}B_{0,0} \begin{bmatrix} \tilde{X}(0) \\ \dot{\tilde{X}}(0) \end{bmatrix}, \tag{6.21}$$

where $C_k = B_{k+1,k+1}B_{k+1,k}^{-1}$ with

$$B_{m,n} = \begin{bmatrix} E_\alpha(-\mathcal{L}_m(\sum_{i=1}^{n+1}\Delta_i)^\alpha) & \sum_{i=1}^{n+1}\Delta_i E_{\alpha,2}(-\mathcal{L}_m(\sum_{i=1}^{n+1}\Delta_i)^\alpha) \\ \frac{E_{\alpha,0}(-\mathcal{L}_m(\sum_{i=1}^{n+1}\Delta_i)^\alpha)}{\sum_{i=1}^{n+1}\Delta_i} & E_\alpha(-\mathcal{L}_m(\sum_{i=1}^{n+1}\Delta_i)^\alpha) \end{bmatrix},$$

where $C_0 \triangleq I_{2n}$ is the $2n$ by $2n$ identity matrix. Note that unlike the integer-order systems, there does not exist a transition matrix for fractional-order systems. Therefore, the analysis for fractional-order systems is more challenging than that for integer-order systems. Next we show the sufficient conditions on the directed dynamic network topology such that coordination will be achieved.

Theorem 6.3.8 *Assume that $\alpha \in (1, 1+\frac{2}{n})$ and $\mathcal{G}_k$ has a directed spanning tree. Define $V(t) \triangleq \max_j \tilde{x}_j(t) - \min_j \tilde{x}_j(t)$. For* (6.21)*, there exists positive $\bar{\Delta}_i$ such that $V(t) < V(\sum_{j=1}^{i-1}\Delta_j)$ for any $\Delta_i \geq \bar{\Delta}_i$ when $t \geq \sum_{j=1}^{i}\Delta_j$, $i = 1, \cdots$.*[5] *In addition, if $\Delta_i \geq \bar{\Delta}_i$, coordination will be achieved globally.*

[5]Here the values of $\bar{\Delta}_i, i = 1, \cdots$, depend on the initial states, the fractional-order α, and $\mathcal{G}_k$.

Proof: For the first statement, when the directed fixed network topology has a directed spanning tree, it follows from Theorem 3.3 [132] that coordination will be achieved for $\alpha \in (1, 1+\frac{2}{n})$. It then follows that there exists a positive $\bar{\Delta}_1$ such that $V(t) < V(0)$ for any $t > \bar{\Delta}_1$. Similarly, by considering $B_{1,0}^{-1} B_{0,0} \begin{bmatrix} X(0) \\ \dot{X}(0) \end{bmatrix}$ the new initial state, it follows that there exists a positive $\bar{\Delta}_2$ such that $V(\Delta_1 + t) < V(\Delta_1)$ for any $t > \bar{\Delta}_2 + \Delta_1$. Similarly, we can also show the existence of $\Delta_i, i = 3, \cdots$.

For the second statement, because $V(\sum_{j=1}^{i+1} \Delta_k) < V(\sum_{j=1}^{i} \Delta_j)$, it follows that $V(\sum_{j=1}^{i} \Delta_j) \to 0$ as $i \to \infty$. Therefore, we can get that $\tilde{x}_i[k] \to \tilde{x}_j[k]$, i.e., $x_i[k] - x_j[k] \to \delta_{ij}$ as $k \to \infty$ under the condition of the theorem. ■

Remark 6.3.9 *Theorems 6.3.6 and 6.3.8 can be extended to the case when the fractional order $\alpha \in (1, 1+\frac{2}{n})$ is constant for $t \in [\sum_{j=1}^{k} \Delta_j, \sum_{j=1}^{k+1} \Delta_j)$ and switches at $t = \sum_{j=1}^{k} \Delta_j$.*

6.3.2 Comparison Between Coordination for Fractional-order Systems and Integer-order Systems

In this section, we compare coordination for fractional-order systems with that for integer-order systems. Based on the comparison, we propose a varying-order fractional-order coordination strategy to achieve higher convergence speed. Before moving on, we first derive the solutions of (6.26) and (6.27).

For $\alpha \in (0, 1]$, the Laplace transform of (6.26) is (6.8). Taking the inverse Laplace transform of (6.8) gives

$$y_i(t) = y_i(0^-) E_\alpha(-\lambda_i t^\alpha),$$

where $E_\alpha(\cdot)$ is the Mittag-Leffler function defined in (B.3). Similarly, for $\alpha \in (1, 2)$, the Laplace transform of (6.26) is (6.9). Taking the inverse Laplace transform of (6.9) gives

$$y_i(t) = y_i(0^-) E_\alpha(-\lambda_i t^\alpha) + \dot{y}_i(0^-) t E_{\alpha,2}(-\lambda_i t^\alpha),$$

where $E_{\alpha,2}(\cdot)$ is the Mittag-Leffler function defined in (B.2).

For $\alpha \in (0, 1]$, the Laplace transform of (6.27) is (6.10). Taking the inverse Laplace transform of (6.10) gives

$$y_i(t) = y_i(0^-)E_\alpha(-\lambda_i t^\alpha) - y_{i+1}(t) * [t^{\alpha-1}E_{\alpha,\alpha}(-\lambda_i t^\alpha)],$$

where $*$ denotes the convolution operation. Similarly, for $\alpha \in (1, 2)$, the Laplace transform of (6.27) is (6.11). Taking the inverse Laplace transform of (6.11) gives

$$y_i(t) = y_i(0^-)E_\alpha(-\lambda_i t^\alpha) + \dot{y}_i(0^-)tE_{\alpha,2}(-\lambda_i t^\alpha) - y_{i+1}(t) * [t^{\alpha-1}E_{\alpha,\alpha}(-\lambda_i t^\alpha)].$$

It can be observed from these solutions that the decaying speeds of Mittag-Leffler functions determine the speed at which $y_i(t)$, where $\mathrm{Re}(\lambda_i) < 0$, approaches zero. As a result, it follows that the convergence speed of (6.4) is also determined by the decaying speeds of Mittag-Leffler functions due to the fact shown in the proof of Theorem 6.3.1 that coordination is achieved if $y_i(t) = 0$ for all $\lambda_i \neq 0$. As a special case, for single integer-order systems, i.e., $\alpha = 1$, (6.4) becomes (6.12) and the corresponding solution is $\tilde{X}(t) = e^{-\mathcal{L}t}\tilde{X}(0)$. Similarly, the solution for high integer-order systems, i.e., $\alpha = 2, 3, \cdots$, can also be written in the form of exponential functions. Therefore, it is worthwhile to study the difference between Mittag-Leffler functions and exponential functions in order to compare coordination for fractional-order dynamics and that for integer-order dynamics. As an example, we next study the decaying speeds of the Mittag-Leffler function $E_\alpha(-\lambda t^\alpha)$ and the exponential function $e^{-\lambda t}$.

Theorem 6.3.10 *There exists a positive scalar T such that $E_\alpha(-\lambda t^\alpha)$ decreases faster than $e^{-\lambda t}$ for $t \in (0, T)$, where $\lambda \in \mathbb{R}^+$ and $\alpha \in \mathbb{R}^+$.*

Proof: Note that both $e^{-\lambda t}$ and $E_\alpha(-\lambda t^\alpha)$ equal to 1 when $t = 0$. Taking derivatives of both functions gives $\frac{d}{dt}[e^{-\lambda t}]|_{t=0} = -\lambda e^{-\lambda t}|_{t=0} = -\lambda$ and $\frac{d}{dt}[E_\alpha(-\lambda t^\alpha)]|_{t=0} = -\infty$. Because $\frac{d}{dt}[e^{-\lambda t}]$ and $\frac{d}{dt}[E_\alpha(-\lambda t^\alpha)]$ are continuous with respect to t, there exists a positive scalar T such that $E_\alpha(-\lambda t^\alpha)$ decreases faster than $e^{-\lambda t}$ for $t \in (0, T)$ by using the comparison principle. ■

To illustrate, Figs. 6.1(a) and 6.1(b) show, respectively, Mittag-Leffler functions and their derivatives with different orders for $\lambda = 1$. Figure 6.1(a) shows Mittag-Leffler functions when

$\alpha = 0.2i, i = 1, 2, 3, 4, 5$.[6] A noticeable phenomenon in Fig. 6.1(a) is that the smaller α is, the faster the decaying speed will be when the time is close to zero. Figure 6.1(b) shows the derivatives of Mittag-Leffler functions for $\alpha = 0.2i, i = 1, 2, 3, 4, 5$. Note that Figs. 6.1(a) and 6.1(b) verified Theorem 6.3.10. Because the decaying speeds of Mittag-Leffler functions with different fractional orders are different as shown in Fig. 6.1, we are motivated to adopt a varying-order fractional-order coordination strategy to increase the convergence speed.

Remark 6.3.11 *In order to achieve higher convergence speed, a varying-order fractional-order coordination strategy can be adopted. The strategy can be described as follows: Let* $\alpha_1 < \cdots < \alpha_m < 1$ *and choose* α *in* (6.4) *as* $\alpha = \begin{cases} \alpha_1, & t < t_1; \\ \alpha_i, & t_{i-1} \leq t < t_i,\ i = 2, \cdots, m; \\ 1, & t \geq t_m. \end{cases}$ *Here* t_1 *is chosen such that the convergence speed with order* α_1 *is the highest when* $t < t_1$. *Similarly,* $t_i,\ i = 2, \cdots, m$, *is chosen such that the convergence speed with order* α_i *is highest for* $t \in [t_{i-1}, t_i)$, *and* $\alpha = 1$ *if* $t \geq t_m$. *Given the same* L, *the convergence speed of this varying-order fractional-order coordination strategy is higher than that of the single-integrator coordination strategy because the convergence speed of the proposed strategy is higher than that of the single-integrator coordination strategy when* $t < t_m$ *and equal to that of the single-integrator coordination strategy when* $t \geq t_m$.

Remark 6.3.12 *The convergence speed for fractional-order systems can be increased by applying a varying-order fractional-order coordination strategy. Similarly, the convergence speed can also be increased by separating the time interval into more pieces* $[t_i,\ t_{i+1})$.

Remark 6.3.13 *There should exist an optimal varying-order fractional-order coordination strategy to maximize the convergence speed and the order of the corresponding fractional-order coordination strategy may be continuous with respect to* t. *This optimal strategy might be related to the sensitivity function of* $E_\alpha(-\lambda t^\alpha)$ *with respect to* α, *i.e.,* $\frac{d}{d\alpha}[E_\alpha(-\lambda t^\alpha)]$.

[6] When $\alpha = 1$, the corresponding Mittag-Leffler function becomes the exponential function.

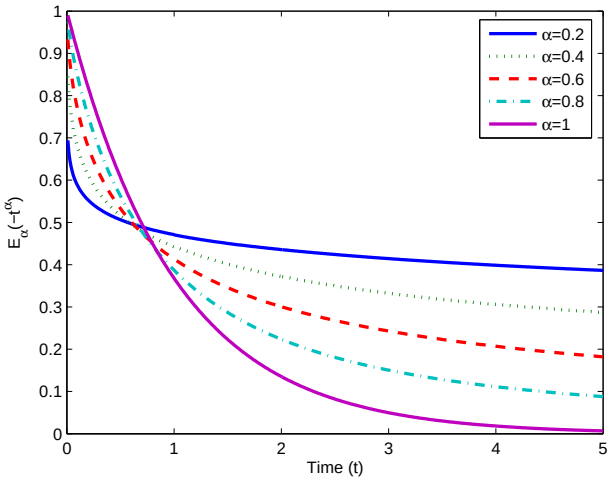

(a) Mittag-Leffler functions with different orders.

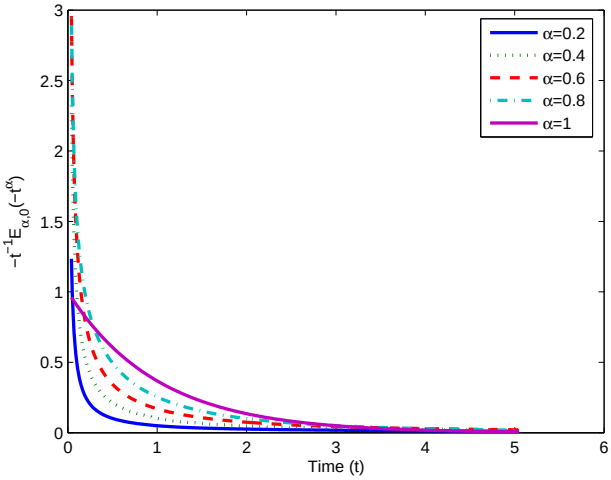

(b) Derivatives of Mittag-Leffler functions with different orders.

Fig. 6.1: Mittag-Leffler functions and the derivatives.

6.3.3 Simulation Illustrations and Discussions

In this section, several simulation results are presented to illustrate the fractional-order coordination algorithm proposed in Section 6.2 and the varying-order coordination strategy in Section 6.3.2. We consider a group of twelve agents with an interaction graph given by Fig. 6.2. Note that the interaction graph in Fig. 6.2 has a directed spanning tree with node 1 being the root. Although we only consider twelve agents in our simulation, similar results can be obtained for a large number of agents if the conditions in Theorem 6.3.1 are satisfied. Here for simplicity we have chosen $\delta_i = 0, i = 1, \cdots, 12$, i.e., $\tilde{X}(t) = X(t)$, where $X(t) = [r_1(t), \cdots, r_{12}(t)]^T$. The corresponding (nonsymmetric) Laplacian matrix is chosen such that $a_{ij} = 1$ if $(v_j, v_i) \in \mathcal{W}$ and $a_{ij} = 0$ otherwise. It can be computed that $\mathbf{p} = [\frac{1}{11}, \frac{1}{11}, \frac{1}{11}, \frac{1}{11}, 0, \frac{1}{11}, \frac{1}{11}, \frac{1}{11}, \frac{1}{11}, \frac{1}{11}, \frac{1}{11}, \frac{1}{11}]^T$ and the eigenvalues of $\mathcal{L}$ are $0, 1, 1.9595 \pm 0.2817\mathbf{j}, 1.6549 \pm 0.7557\mathbf{j}, 1.1423 \pm 0.9898\mathbf{j}, 0.5846 \pm 0.9096\mathbf{j}$, and $0.1587 \pm 0.5406\mathbf{j}$, where $\mathbf{j}$ is the imaginary unit.

For $\alpha \in (0, 1]$, let the initial states be $X(0) = [6, 3, 1, -3, 4, 2, 0, -5, -2, -5, 2, 7]^T$. When the fractional order is $\alpha = 0.8$, the states using (6.4) are shown in Fig. 6.3(a). It can be seen that coordination is achieved with the final coordination equilibrium for $r_i(t)$ being 0.5455, which is equal to $\mathbf{p}^T X(0)$. When $\alpha = 1$, i.e., the system takes in the form of single-integrator dynamics, the states using (6.4) are shown in Fig. 6.3(b). From these two figures, it can be seen that the equilibrium states for both cases are the same. In addition, it can also be observed that the convergence speed of the fractional-order case is higher than that of the single-integrator case when t is close to the origin.

For $\alpha \in (1, \frac{2\theta}{\pi})$, we let the initial states be $X(0) = [6, 3, 1, -3, 4, 2, 0, -5, -2, -5, 2, 7]^T$ and

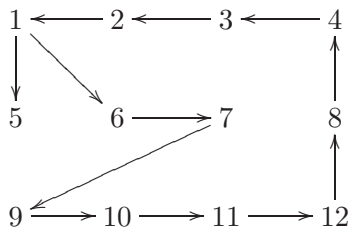

Fig. 6.2: Interaction graph for twelve agents. An arrow from j to i denotes that agent i can receive information from agent j.

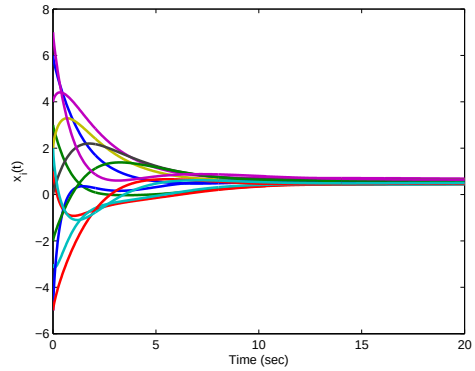

(a) $\alpha = 0.8$.

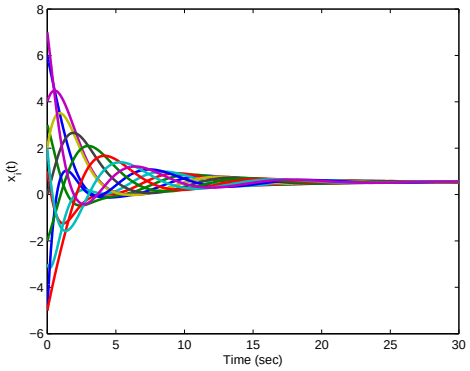

(b) $\alpha = 1$. ($|r_i(t) - r_j(t)| < 0.1$ for any $t > 22.22$ s.)

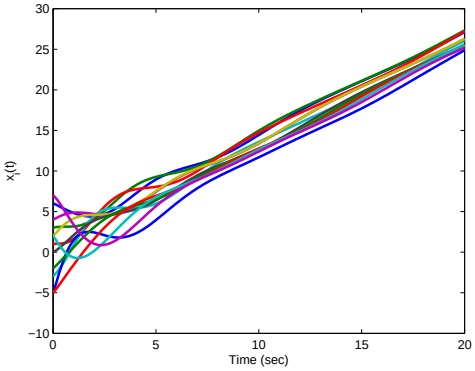

(c) $\alpha = 1.15$.

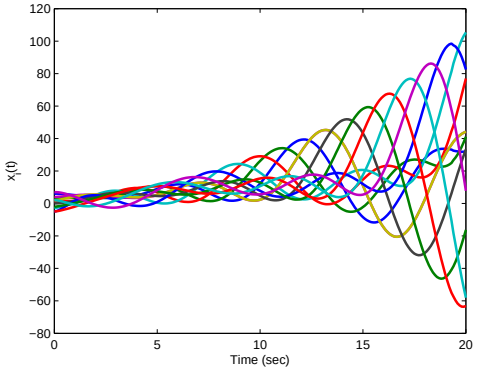

(d) $\alpha = 1.5$.

Fig. 6.3: Simulation results using (6.4) with different orders.

$\dot{X}(0) = [1, 2, 3, 4, 0, 0, 0, 0, 1, 1, 1, 1]^T$. It follows from the definition of θ in Theorem 6.3.1 that $\theta = 1.8563$, which implies $\alpha \in (0, 1.182)$. Figures. 6.3(c) and 6.3(d) show the states using (6.4) for $\alpha = 1.15$ and $\alpha = 1.5$, respectively. From Fig. 6.3(c), it can be observed that coordination can be achieved. From Fig. 6.3(d), it can be observed that coordination cannot be achieved. The four subfigures in Fig. 6.3 validate Theorem 6.3.1.

We next present the simulation results using the varying-order coordination strategy described in Remark 6.3.11 and compare the simulation results with those using the integer-order coordination strategy in Fig. 6.3(b). Let the initial states be $X(0) = [6, 3, 1, -3, 4, 2, 0, -5, -2, -5, 2, 7]^T$. Figure 6.4 shows the states using the varying-order coordination strategy when the parameters in Remark 6.3.11 are arbitrarily chosen as $\alpha_i = 0.4 + 0.1i$ and $t_i = 0.1 + 0.04i$ for $i = 1, 2, 3, 4$. Note that $|r_i(t) - r_j(t)| < 0.1$ for all $t > 21.73$ s in Fig. 6.4 while $|r_i(t) - r_j(t)| < 0.1$ for all $t > 22.22$ s in Fig. 6.3(b). Therefore, we can see that the convergence speed using the varying-order coordination strategy is higher than that using the single integer-order coordination strategy. The comparison shows the effectiveness of the proposed varying-order coordination strategy. Of course, when we choose different parameters (α_i, t_i) carefully as described in Remark 6.3.11, the convergence speed can be further improved.

6.4 Convergence Analysis of Fractional-order Coordination Algorithms with Absolute/ Relative Damping

In this section, we propose fractional-order coordination algorithms with absolute/relative damping and then study the conditions on the network topology and the fractional orders such that coordination will be achieved when using these algorithms for fractional-order systems under a directed fixed network topology.

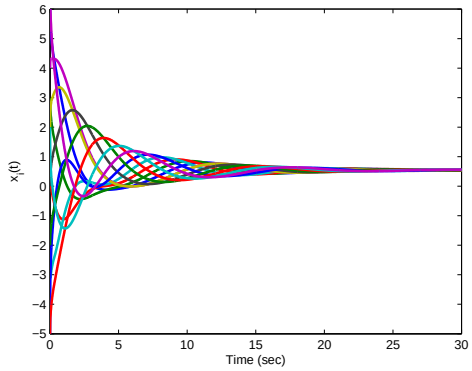

Fig. 6.4: Simulation result using (6.4) with varying orders. ($|r_i(t) - r_j(t)| < 0.1$ for any $t > 21.73$ s.).

6.4.1 Absolute Damping

For n ($n \geq 2$) systems with dynamics given by (6.1), we propose the following fractional-order coordination algorithm with absolute damping as

$$u_i(t) = -\sum_{j=1}^{n} a_{ij}[x_i(t) - x_j(t) - (\delta_i - \delta_j)] - \beta x_i^{(\alpha/2)}(t), \tag{6.22}$$

where $\beta \in \mathbb{R}^+$ and $\delta_i \in \mathbb{R}$ is constant. Using (6.22), (6.1) can be written in matrix form as

$$\tilde{X}^{(\alpha)}(t) + \beta \tilde{X}^{(\alpha/2)}(t) + \mathcal{L}\tilde{X}(t) = 0, \tag{6.23}$$

where $\tilde{X}(t)$ and $\mathcal{L}$ are defined in (6.4). It then follows that (6.23) can be written as

$$\begin{bmatrix} \tilde{X}(t) \\ \tilde{X}^{(\alpha/2)}(t) \end{bmatrix}^{(\alpha/2)} = \underbrace{\begin{bmatrix} \mathbf{0}_{n\times n} & I_n \\ -\mathcal{L} & -\beta I_n \end{bmatrix}}_{F} \begin{bmatrix} \tilde{X}(t) \\ \tilde{X}^{(\alpha/2)}(t) \end{bmatrix}, \tag{6.24}$$

where $\mathbf{0}_{n\times n}$ is the n by n all-zero matrix. Note that each eigenvalue of $\mathcal{L}$, λ_i, corresponds to two eigenvalues of F, denoted by $\mu_{2i-1} = \frac{-\beta+\sqrt{\beta^2-4\lambda_i}}{2}$ and $\mu_{2i} = \frac{-\beta-\sqrt{\beta^2-4\lambda_i}}{2}$ [71].

Note that F can be written in Jordan canonical form as

$$F = P \underbrace{\begin{bmatrix} \Lambda_1 & 0 & \cdots & 0 \\ 0 & \Lambda_2 & \cdots & 0 \\ \cdots & \cdots & & \\ 0 & 0 & \cdots & \Lambda_k \end{bmatrix}}_{\Lambda} P^{-1},$$

where $\Lambda_m,\ m = 1, 2, \ldots, k$, are standard Jordan blocks. By defining $Z(t) = [z_1(t), \cdots, z_n(t)]^T \triangleq P^{-1} \begin{bmatrix} \tilde{X}(t) \\ \tilde{X}^{(\alpha/2)}(t) \end{bmatrix}$, (6.24) can be written as

$$Z^{(\alpha/2)}(t) = \Lambda Z(t). \tag{6.25}$$

Suppose that each diagonal entry of Λ_i is μ_i, i.e., an eigenvalue of F. Similarly, (6.25) can be decoupled into n one-dimensional equations represented by either

$$z_i^{(\alpha/2)}(t) = \mu_i z_i(t), \tag{6.26}$$

or

$$z_i^{(\alpha/2)}(t) = \mu_i z_i(t) + z_{i+1}(t). \tag{6.27}$$

Lemma 6.4.1 [133] *Let λ_i be the ith eigenvalue of $\mathcal{L}$, μ_{2i-1} and μ_{2i} are the two eigenvalues of F corresponding to λ_i, and $\mathrm{Im}(\cdot)$ denotes the imaginary part of a complex number. When $\mathrm{Re}(\lambda_i) > 0$, $\mathrm{Re}(\mu_{2i-1}) < 0$ and $\mathrm{Re}(\mu_{2i}) < 0$ if and only if $\beta > \sqrt{\frac{[\mathrm{Im}(\lambda_i)]^2}{\mathrm{Re}(\lambda_i)}}$.*

Theorem 6.4.1 *Let λ_i be the ith eigenvalue of $\mathcal{L}$, and μ_{2i-1} and μ_{2i} be the two eigenvalues of F corresponding to λ_i. Define $\theta \triangleq \min_{\mu_i \neq 0, i=1,2,\cdots,2n} \theta_i$, where $\theta_i = \pi - |\arg\{-\mu_i\}|$. Using* (6.22) *for* (6.1)*, coordination will be achieved if the directed fixed network topology has a directed spanning tree and $\alpha \in (0, \frac{4\theta}{\pi})$. In particular, the following properties hold.*

Case 1: $\beta > \max_{\lambda_i \neq 0} \sqrt{\frac{[\mathrm{Im}(\lambda_i)]^2}{\mathrm{Re}(\lambda_i)}}$. When $\alpha \in (0, 2]$, $\tilde{x}_i(t)$ and $\tilde{x}_j(t)$ converge to $\mathbf{p}^T \tilde{X}(0) + \frac{1}{\beta} \mathbf{p}^T \tilde{X}^{(\alpha/2)}(0)$ as $t \to \infty$, where $\mathbf{p}$ is the left eigenvector of L associated with the zero eigenvalue

satisfying $\mathbf{p}^T\mathbf{1} = 1$. *When* $\alpha \in (2, \frac{4\theta}{\pi})$,[7] $\tilde{x}_i(t)$ *and* $\tilde{x}_j(t)$ *converge to* $\mathbf{p}^T\tilde{X}(0) + \frac{1}{\beta}\mathbf{p}^T\tilde{X}^{(\alpha/2)}(0) + [\mathbf{p}^T\dot{\tilde{X}}(0) + \frac{1}{\beta}\mathbf{p}^T\tilde{X}^{(1+\alpha/2)}(0)]t$, *and* $\dot{\tilde{x}}_i(t)$ *and* $\dot{\tilde{x}}_j(t)$ *converge to* $\mathbf{p}^T\dot{\tilde{X}}(0) + \frac{1}{\beta}\mathbf{p}^T\tilde{X}^{(1+\alpha/2)}(0)$ *as* $t \to \infty$.

Case 2: $0 < \beta \leq \max_{\lambda_i \neq 0} \sqrt{\frac{[\mathrm{Im}(\lambda_i)]^2}{\mathrm{Re}(\lambda_i)}}$. *Then we have that* $\tilde{x}_i(t)$ *and* $\tilde{x}_j(t)$ *and* $\mathbf{p}^T\tilde{X}(0) + \frac{1}{\beta}\mathbf{p}^T\tilde{X}^{(\alpha/2)}(0)$ *as* $t \to \infty$.

Proof: (Proof of Case 1) When the directed fixed network topology has a directed spanning tree, $\mathcal{L}$ has a simple zero eigenvalue and all other eigenvalues have positive real parts [39,101]. Without loss of generality, let $\lambda_1 = 0$ and $\mathrm{Re}(\lambda_i) > 0,\ i \neq 1$. For $\lambda_1 = 0$, it follows that $\mu_1 = 0$ and $\mu_2 = -\beta$. Because $-\beta < 0$, it follows from Property 1 of Lemma 6.3.1 that $z_2(t) \to 0$ as $t \to \infty$. When $\alpha \in (0, 2]$, because $\mu_1 = 0$ is a simple zero eigenvalue, μ_1 satisfies (6.26). It follows from Property 2 in Lemma 6.3.1 that $z_1(t) \equiv z_1(0)$. When $\beta > \max_{\lambda_i \neq 0} \sqrt{\frac{[\mathrm{Im}(\lambda_i)]^2}{\mathrm{Re}(\lambda_i)}}$, it follows from Lemma 6.4.1 that $\mathrm{Re}(\mu_{2i-1}) < 0$ and $\mathrm{Re}(\mu_{2i}) < 0,\ i \neq 1$. When μ_{2i-1} and μ_{2i} satisfy (6.26), it then follows from Property 1 of Lemma 6.3.1 that $z_{2i-1}(t) \to 0$ and $z_{2i}(t) \to 0$ as $t \to \infty$. When μ_{2i-1} satisfies (6.26) and μ_{2i} satisfies (6.27), it then follows from Lemma 6.3.1 and Lemma 6.3.2 that $z_{2i-1}(t) \to 0$ and $z_{2i}(t) \to 0$ as $t \to \infty$ as well. Recalling the structure of the standard Jordan block, by following the previous analysis, it can be shown that $z_{2i-1}(t) \to 0$ and $z_{2i}(t) \to 0$ as $t \to \infty$ when μ_{2i-1} and μ_{2i} satisfy (6.27). Combining the above arguments gives $\lim_{t\to\infty} Z(t) = [z_1(0), 0, \cdots, 0]^T$, which implies $\lim_{t\to\infty} \begin{bmatrix} \tilde{X}(t) \\ \tilde{X}^{(\alpha/2)}(t) \end{bmatrix} = \lim_{t\to\infty} PZ(t) = PSZ(0) = PSP^{-1} \begin{bmatrix} \tilde{X}(0) \\ \tilde{X}^{(\alpha/2)}(0) \end{bmatrix}$, where $S = [s_{ij}] \in \mathbb{R}^{n\times n}$ has only one nonzero entry $s_{11} = 1$. Note that the first column of P can be chosen as $[\mathbf{1}^T, \mathbf{0}^T]^T$ while the first row of P^{-1} can be chosen as $[\mathbf{p}^T, \frac{1}{\beta}\mathbf{p}^T]^T$ by noting that $[\mathbf{1}^T, \mathbf{0}^T]^T$ and $[\mathbf{p}^T, \frac{1}{\beta}\mathbf{p}^T]^T$ are, respectively, a right and left eigenvector of F associated with $\mu_1 = 0$ and $[\mathbf{p}^T, \frac{1}{\beta}\mathbf{p}^T][\mathbf{1}^T, \mathbf{0}^T]^T = 1$, where $\mathbf{0}$ is an all-zero column vector with a compatible size. Therefore, $\lim_{t\to\infty} \begin{bmatrix} \tilde{X}(t) \\ \tilde{X}^{(\alpha/2)}(t) \end{bmatrix} = PSP^{-1} \begin{bmatrix} \tilde{X}(0) \\ \tilde{X}^{(\alpha/2)}(0) \end{bmatrix} = [\mathbf{1}^T, \mathbf{0}^T][\mathbf{p}^T, \frac{1}{\beta}\mathbf{p}^T]^T \begin{bmatrix} \tilde{X}(0) \\ \tilde{X}^{(\alpha/2)}(0) \end{bmatrix}$, that is, $\lim_{t\to\infty} \tilde{x}_i(t) = \mathbf{p}^T\tilde{X}(0) + \frac{1}{\beta}\mathbf{p}^T\tilde{X}^{(\alpha/2)}(0)$.

[7] Note that $\frac{4\theta}{\pi} > 2$ because $\theta > \frac{\pi}{2}$ according to Lemma 6.3.1.

When $\alpha \in (2, \frac{4\theta}{\pi})$, it follows from Property 3 of Lemma 6.3.1 that $z_1(t) = z_1(0) + \dot{z}_1(0)t$. A similar discussion to that for $\alpha \in (0, 2]$ shows that $z_i(t) \to 0$ as $t \to \infty$ for $i = 3, \cdots, 2n$. Therefore, it follows that $\lim_{t\to\infty} Z(t) = [z_1(0) + \dot{z}_1(0)t, 0, \cdots, 0]^T$, which implies that $\lim_{t\to\infty} \dot{Z}(t) = [\dot{z}_1(0), 0, \cdots, 0]^T$. Similar to the proof for $\alpha \in (0, 2]$, we can get that $\lim_{t\to\infty} \tilde{x}_i(t) = \mathbf{p}^T\tilde{X}(0) + \frac{1}{\beta}\mathbf{p}^T\tilde{X}^{(\alpha/2)}(0) + [\mathbf{p}^T\dot{\tilde{X}}(0) + \frac{1}{\beta}\mathbf{p}^T\tilde{X}^{(1+\alpha/2)}(0)]t$ and $\lim_{t\to\infty} \dot{\tilde{x}}_i(t) = \mathbf{p}^T\dot{\tilde{X}}(0) + \frac{1}{\beta}\mathbf{p}^T\tilde{X}^{(1+\alpha/2)}(0)$.

(Proof of Case 2) When $0 < \beta \leq \max_{\lambda_i \neq 0} \sqrt{\frac{[\mathrm{Im}(\lambda_i)]^2}{\mathrm{Re}(\lambda_i)}}$, it follows from Lemma (6.4.1) that $\mathrm{Re}(\mu_{2i-1}) \geq 0$ for some i, which implies that $\frac{4\theta}{\pi} \leq 2$. Therefore, we can get that $\alpha \in (0, 2)$. The proof then follows a similar analysis to that of Case 1 when $\alpha \in (0, 2]$. ■

Remark 6.4.2 *From Theorem 6.4.1, it can be noted that the control gain β can be chosen as any positive number. In particular, the possible range of α to ensure coordination will be different depending on β. In addition, when there exists absolute damping, the final velocity may not be zero as shown in Theorem 6.3.6, which is different from some existing results* [61, 71]. *The existing coordination algorithms for double-integrator dynamics with absolute damping* [61, 71] *can be viewed as a special case of Theorem 6.4.1 when $\alpha = 2$.*

6.4.2 Relative Damping

For n ($n \geq 2$) systems with dynamics given by (6.1), we propose the following fractional-order coordination algorithm with relative damping as

$$u_i(t) = -\sum_{j=1}^{n} a_{ij}\{x_i(t) - x_j(t) - (\delta_i - \delta_j) + \gamma[x_i^{(\alpha/2)}(t) - x_j^{(\alpha/2)}(t)]\}, \tag{6.28}$$

where $\gamma \in \mathbb{R}^+$ and $\delta_i \in \mathbb{R}$ is constant. Using (6.28), (6.1) can be written in matrix form as

$$\tilde{X}^{(\alpha)}(t) + \gamma\mathcal{L}\tilde{X}^{(\alpha/2)}(t) + \mathcal{L}\tilde{X}(t) = 0, \tag{6.29}$$

where $\tilde{X}(t)$ and $\mathcal{L}$ are defined in (6.4). It follows that (6.29) can be written as

$$\begin{bmatrix} \tilde{X}(t) \\ \tilde{X}^{(\alpha/2)}(t) \end{bmatrix}^{(\alpha/2)} = \underbrace{\begin{bmatrix} \mathbf{0}_{n\times n} & I_n \\ -\mathcal{L} & -\gamma\mathcal{L} \end{bmatrix}}_{G} \begin{bmatrix} \tilde{X}(t) \\ \tilde{X}^{(\alpha/2)}(t) \end{bmatrix}. \tag{6.30}$$

Note that each eigenvalue of $\mathcal{L}$, λ_i, also corresponds to two eigenvalues of G, denoted by $\mu_{2i-1} = \frac{-\gamma\lambda_i+\sqrt{\gamma^2\lambda_i^2-4\lambda_i}}{2}$ and $\mu_{2i} = \frac{-\gamma\lambda_i-\sqrt{\gamma^2\lambda_i^2-4\lambda_i}}{2}$ [60].

Note that G can also be written in Jordan canonical form as

$$G = Q \underbrace{\begin{bmatrix} \Sigma_1 & 0 & \cdots & 0 \\ 0 & \Sigma_2 & \cdots & 0 \\ \cdots & \cdots & & \\ 0 & 0 & \cdots & \Sigma_k \end{bmatrix}}_{\Sigma} Q^{-1},$$

where $\Sigma_m,\ m = 1, 2, \ldots, k$, are standard Jordan blocks. By defining $Z(t) = [z_1(t), \cdots, z_n(t)]^T \triangleq Q^{-1} \begin{bmatrix} \tilde{X}(t) \\ \tilde{X}^{(\alpha/2)}(t) \end{bmatrix}$, (6.30) can be written as

$$Z^{(\alpha/2)}(t) = \Sigma Z(t). \tag{6.31}$$

Suppose that each diagonal entry of Σ_i is μ_i, i.e., an eigenvalue of G. Similar to the analysis of (6.25), (6.31) can be decoupled into n one-dimensional equations represented by either (6.26) or (6.27). Before moving on, we need the following lemma.

Lemma 6.4.2 *Let λ_i be the ith eigenvalue of $\mathcal{L}$, and μ_{2i-1} and μ_{2i} be the two eigenvalues of G corresponding to λ_i. Suppose that $\mathrm{Re}(\lambda_i) > 0$. Then $\mathrm{Re}(\mu_{2i-1}) < 0$ and $\mathrm{Re}(\mu_{2i}) < 0$ if and only if $\gamma > \bar{\gamma}_i$, where $\bar{\gamma}_i \triangleq \sqrt{\frac{\mathrm{Im}(\lambda_i)^2}{\mathrm{Re}(\lambda_i)|\lambda_i|^2}}$.*

Proof: The characteristic polynomial of G is given by

$$s(s + \gamma\lambda_i) + \lambda_i = 0. \tag{6.32}$$

Letting s_1 and s_2 be the two roots of (6.32), it follows from (6.32) that $s_1 + s_2 = -\gamma\lambda_i$. Because $\mathrm{Re}(\lambda_i) > 0$, at least one of the two roots are in the open left half plane if $\gamma > 0$. Note that the bound of γ, $\bar{\gamma}_i$, can be obtained when one of the two roots are on the imaginary axis. Without loss of generality, we let $s_1 = z\mathbf{j}$, where z is a real constant and $\mathbf{j}$ is the imaginary unit. Substituting $s_1 = z\mathbf{j}$ into (6.32) gives that $-z^2 + \bar{\gamma}_i\lambda_i z\mathbf{j} + \lambda_i = 0$. After some manipulation, we can get that $\bar{\gamma}_i$ satisfies $-\mathrm{Im}(\lambda_i)^2 + \bar{\gamma}_i^2\mathrm{Im}(\lambda_i)^2\mathrm{Re}(\lambda_i) + \bar{\gamma}_i^2\mathrm{Re}(\lambda_i)^3 = 0$, which can be simplified as $\bar{\gamma}_i = \sqrt{\frac{\mathrm{Im}(\lambda_i)^2}{\mathrm{Re}(\lambda_i)|\lambda_i|^2}}$. ■

Theorem 6.4.3 *Let λ_i be the ith eigenvalue of $\mathcal{L}$, and μ_{2i-1} and μ_{2i} be the two eigenvalues of G corresponding to λ_i. Define $\bar{\gamma} \triangleq \max_{\lambda_i \neq 0} \bar{\gamma}_i$ with $\bar{\gamma}_i$ being defined in Lemma 6.4.2, and $\theta = \min_{\mu_i \neq 0, i=1,2,\cdots,2n} \theta_i$, where $\theta_i = \pi - |\arg\{-\mu_i\}|$. Using* (6.29) *for* (6.1)*, coordination will be achieved if the directed fixed network topology has a directed spanning tree and $\alpha \in (0, \frac{4\theta}{\pi})$. In addition, the following properties hold.*

Case 1*: $\gamma > \bar{\gamma}$. When $\alpha \in (0, 2]$, $\tilde{x}_i(t)$ and $\tilde{x}_j(t)$ converge to $\mathbf{p}^T\tilde{X}(0) + \frac{t^{\alpha/2}}{\Gamma(1+\alpha/2)}\mathbf{p}^T\tilde{X}^{(\alpha/2)}(0)$ as $t \to \infty$, where $\mathbf{p}$ is defined in Theorem 6.4.1. When $\alpha \in (2, \frac{4\theta}{\pi})$,*[8] *$\tilde{x}_i(t)$ and $\tilde{x}_j(t)$ converge to $\mathbf{p}^T\tilde{X}(0) + \frac{t^{\alpha/2}}{\Gamma(1+\alpha/2)}\mathbf{p}^T\tilde{X}^{(\alpha/2)}(0) + \frac{t^{1+\alpha/2}}{\Gamma(\alpha/2+2)}\tilde{X}^{(\alpha/2+1)}(0)$ as $t \to \infty$.*

Case 2*: $\gamma \leq \bar{\gamma}$. Then we have that $\tilde{x}_i(t)$ and $\tilde{x}_j(t)$ converge to $\mathbf{p}^T\tilde{X}(0) + \frac{t^{\alpha/2}}{\Gamma(1+\alpha/2)}\mathbf{p}^T\tilde{X}^{(\alpha/2)}(0)$ as $t \to \infty$.*

Proof: (Proof of Case 1) When the directed fixed network topology has a directed spanning tree, $\mathcal{L}$ has a simple zero eigenvalue and all other eigenvalues have positive real parts [39, 101]. Without loss of generality, let $\lambda_1 = 0$ and $\mathrm{Re}(\lambda_i) > 0,\ i \neq 1$. For $\lambda_1 = 0$, it follows from (6.32) that $\mu_1 = 0$ and $\mu_2 = 0$. Because G has two zero eigenvalues whose geometric multiplicity is 1, it follows that $\mu_2 = 0$ satisfies (6.26) and $\mu_1 = 0$ satisfies (6.27). When $\alpha \in (0, 2]$, it follows from Property 2 in Lemma 6.3.1 that $z_2(t) \equiv z_2(0)$. By substituting $z_2(t) = z_2(0)$ into (6.27), it follows that

$$z_1(t) = z_2(0)\frac{t^{\alpha/2}}{\Gamma(1+\alpha/2)} + z_1(0). \tag{6.33}$$

We next study the case of $\lambda_i, i \neq 1$. Because $\mathrm{Re}(\lambda_i) > 0, i \neq 1$, it follows from Lemma 6.4.1 that $\mathrm{Re}(\mu_{2i-1}) < 0$ and $\mathrm{Re}(\mu_{2i}) < 0$ when $\gamma > \bar{\gamma}$. By following a similar analysis to that in the

[8] Note that $\frac{4\theta}{\pi} > 2$ because $\theta > \frac{\pi}{2}$ according to Lemma 6.4.2.

proof of Theorem 6.4.1, it can be shown that $z_{2i-1}(t) \to 0$ and $z_{2i}(t) \to 0$ as $t \to \infty$ as well. Similar to the analysis in the proof of Theorem 6.4.1, it can also be computed that $w_1 = [\mathbf{1}^T, \mathbf{0}^T]^T$ and $v_1 = [\mathbf{0}^T, \mathbf{p}^T]^T$ are the right and left eigenvectors corresponding to $\mu_1 = 0$. Meanwhile, $w_2 = [\mathbf{0}^T, \mathbf{1}^T]^T$ and $v_2 = [\mathbf{p}^T, \mathbf{0}^T]^T$ are the generalized right and left eigenvectors corresponding to $\mu_2 = 0$, where $v_1^T w_2 = 1$ and $v_2^T w_1 = 1$. Therefore, the first and second columns of Q can be chosen as $[\mathbf{1}^T, \mathbf{0}^T]^T$ and $[\mathbf{0}^T, \mathbf{1}^T]^T$ while the first and second rows of Q^{-1} can be chosen as $[\mathbf{p}^T, \mathbf{0}^T]^T$ and $[\mathbf{0}^T, \mathbf{p}^T]^T$. Therefore, $\lim_{t\to\infty} \begin{bmatrix} \tilde{X}(t) \\ \tilde{X}^{(\alpha/2)}(t) \end{bmatrix} = \lim_{t\to\infty} QZ(t) = \lim_{t\to\infty} QSZ(0) = \lim_{t\to\infty} QSQ^{-1} \begin{bmatrix} \tilde{X}(0) \\ \tilde{X}^{(\alpha/2)}(0) \end{bmatrix}$, where $S = [s_{ij}] \in \mathbb{R}^{n\times n}$ has three entries which are not equal to zero, $s_{11} = 1$, $s_{12} = \frac{t^{\alpha/2}}{\Gamma(1+\alpha/2)}$ and $s_{22} = 1$, where s_{12} is derived from (6.33). After some manipulation, we can get that $\lim_{t\to\infty} \begin{bmatrix} \tilde{X}(t) \\ \tilde{X}^{(\alpha/2)}(t) \end{bmatrix} = \begin{bmatrix} \mathbf{1}\mathbf{p}^T\tilde{X}(0) + \frac{t^{\alpha/2}}{\Gamma(1+\alpha/2)}\mathbf{1}\mathbf{p}^T\tilde{X}^{(\alpha/2)}(0) \\ \mathbf{1}\mathbf{p}^T\tilde{X}^{(\alpha/2)}(0) \end{bmatrix}$, that is, $\lim_{t\to\infty} \tilde{x}_i(t) = \mathbf{p}^T\tilde{X}(0) + \frac{t^{\alpha/2}}{\Gamma(1+\alpha/2)}\mathbf{p}^T\tilde{X}^{(\alpha/2)}(0)$.

When $\alpha \in (2, \frac{4\theta}{\pi})$, it follows from Property 3 of Lemma 6.3.1 that $z_2(t) = z_2(0) + \dot{z}_2(0)t$. Because $z_1(t)$ satisfies (6.27), we can get that $z_1(t) = z_1(0) + z_2(0)\frac{t^{\alpha/2}}{\Gamma(\alpha/2+1)} + \dot{z}_2(0)\frac{t^{1+\alpha/2}}{\Gamma(\alpha/2+2)}$. A similar discussion to that for $\alpha \in (0, 2]$ shows that $z_i(t) \to 0$ as $t \to \infty$ for $i = 3, \cdots, 2n$. Therefore, it follows that $\lim_{t\to\infty} Z(t) = [z_1(0)+z_2(0)\frac{t^{\alpha/2}}{\Gamma(\alpha/2+1)}+\dot{z}_2(0)\frac{t^{1+\alpha/2}}{\Gamma(\alpha/2+2)}, z_2(0)+\dot{z}_2(0)t, 0, \cdots, 0]^T$. Similar to the proof for $\alpha \in (0, 2]$, we can get that $\lim_{t\to\infty} \tilde{x}_i(t) = \mathbf{p}^T\tilde{X}(0)+\frac{t^{\alpha/2}}{\Gamma(1+\alpha/2)}\mathbf{p}^T\tilde{X}^{(\alpha/2)}(0)+\frac{t^{1+\alpha/2}}{\Gamma(\alpha/2+2)}\tilde{X}^{(\alpha/2+1)}(0)$.

(Proof of Case 2) When $\gamma \le \bar{\gamma}$, it follows from Lemma 6.4.2 that $\mathrm{Re}(\mu_{2i-1}) \ge 0$ for some i, which implies that $\frac{4\theta}{\pi} \le 2$. Therefore, we can get that $\alpha \in (0, 2)$. The proof then follows a similar analysis to that of Case 1 when $\alpha \in (0, 2]$. ■

Remark 6.4.4 *From Theorem 6.4.3, it can be noted that the control gain γ can also be chosen as any positive number. In particular, the range of α will be different depending on γ. In addition, when there exists relative damping, the final velocity may not be constant as shown in Theorem 6.4.3, which is different from some existing results* [60]*. The existing coordination algorithms for double-integrator dynamics with relative damping* [60] *can be viewed as a special case of Theorem 6.4.3*

when $\alpha = 2$.

6.4.3 Simulation

In this section, we present several simulation results to illustrate the theoretical results in Section 6.4. We consider a network of four systems.

To illustrate the results in Section 6.4, we consider the case of a directed fixed network topology shown by Fig. 6.5 which has a directed spanning tree. The simulation result using (6.22) is shown in Fig. 6.6 when $\alpha = 1.6$ and $\beta = 1$. The simulation result using (6.28) is shown in Fig. 6.7 when $\alpha = 1.2$ and $\gamma = 1$. Here for simplicity we have again chosen $\delta_i = 0$. It can be noted from Figs. 6.6 and 6.7 that coordination is achieved. In particular, it can be seen from the bottom subplot of Fig. 6.7 that using (6.28) the final velocity $\dot{x}_i(t)$ is no longer constant when $\alpha = 1.2$ and $\gamma = 1$.

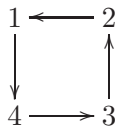

Fig. 6.5: Directed network topology for four systems. An arrow from j to i denotes that system i can receive information from system j.

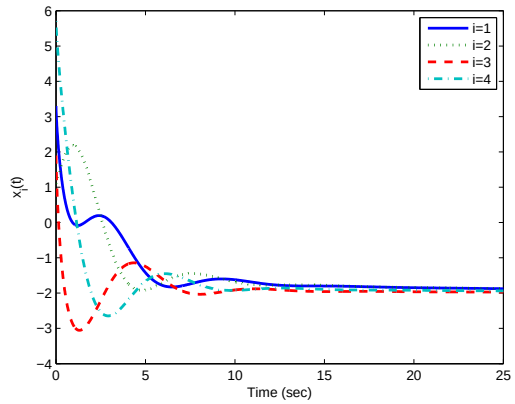

Fig. 6.6: States of the four systems using (6.22) with $\alpha = 1.6$ and $\beta = 1$ with the directed fixed network topology given by Fig. 6.5.

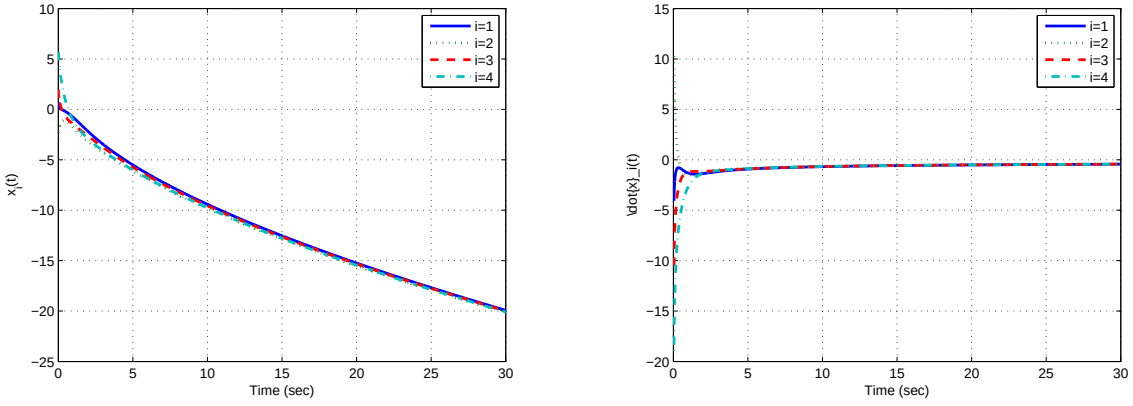

(a) $x_i(t)$. (b) $\dot{x}_i(t)$.

Fig. 6.7: States of the four systems using (6.28) with $\alpha = 1.2$ and $\gamma = 1$ with the directed fixed network topology given by Fig. 6.5.

Chapter 7

Conclusion and Future Research

7.1 Summary of Contributions

The dissertation studied decentralized coordination algorithms under several different cases. First, we investigated decentralized coordination algorithms when there exist none, one, multiple group reference states. When there exists no group reference state, decentralized coordination algorithms for double-integrator dynamics were proposed and studied in the sampled-data setting. In the presence of absolute damping, all vehicles will reach the desired configuration with a zero final velocity. In the presence of relative damping, all vehicles will reach the desired configuration with a (general) nonzero final velocity.

When there exists one group reference state, we studied both consensus tracking and swarm tracking scenarios. We first investigated decentralized coordinated tracking in the continuous-time setting by using a variable structure approach. Compared with other approaches, the proposed approach requires less state information and only local interaction. Then we studied a PD-like discrete-time consensus algorithm and showed the upper bound of the final tracking errors.

When there exist multiple group reference states, we proposed containment control algorithms to guarantee that all followers will move into the convex hull formed by the references. Both single-integrator kinematics and double-integrator dynamics were studied. We also presented experimental results on a multi-robot platform to validate the theoretical results.

Finally, we studied two other problems: optimality problem and the study of coordination algorithms for fractional-order systems. The optimality problem is motivated by the fact that a number of different consensus algorithms can be used to achieve consensus. In particular, the optimality problems, including optimal Laplacian matrix and optimal coupling factor, are studied in the presence of global cost functions. The study of coordination algorithms for fractional-order systems is motivated by the application of fractional calculus in real systems, especially those work-

ing in complicated environments. We proposed and studied decentralized coordination algorithms with/without damping terms.

7.2 Ongoing and Future Research

Currently, there are still a number of open questions which deserve further consideration. First, the current decentralized algorithms are studied mostly under the assumption that no constraint exists. However, each vehicle may have its own constraints as well as the constraint from where the vehicle is involved in. Therefore, it is worthwhile to investigate the decentralized coordination algorithms with constraints. Second, the optimization problems in decentralized coordination algorithms. The current stage mainly focuses on the study of decentralized algorithms without optimization mechanism involved. In real applications, decentralized coordination is not the unique objective. One important problem is to achieve coordination in a better way. Third, the application in economy, social science, engineering, etc. It is worthwhile to mention that the purpose of research is to find the applications in real world. It will be interesting to explain the phenomena in various disciplines and even find ways to solve the problems as well. For example, it might be interesting to study the relationship between centralization and decentralization to avoid the economic crisis. We hope that our research can motivate further research in this field.

References

[1] J. Lin, A. S. Morse, and B. D. O. Anderson, "The multi-agent rendezvous problem," in *Proceedings of the IEEE Conference on Decision and Control*, pp. 1508–1513, Dec. 2003.

[2] J. Lin, A. S. Morse, and B. D. O. Anderson, "The multi-agent rendezvous problem - the asynchronous case," in *Proceedings of the IEEE Conference on Decision and Control*, pp. 1926–1931, Dec. 2004.

[3] S. Martinez, J. Cortes, and F. Bullo, "On robust rendezvous for mobile autonomous agents," in *International Federation of Automatic Control World Congress*, 2005.

[4] R. Olfati-Saber, "Flocking for multi-agent dynamic systems: Algorithms and theory," *IEEE Transactions on Automatic Control*, vol. 51, no. 3, pp. 401–420, Mar. 2006.

[5] H. G. Tanner, A. Jadbabaie, and G. J. Pappas, "Flocking in fixed and switching networks," *IEEE Transactions on Automatic Control*, vol. 52, no. 5, pp. 863–868, May 2007.

[6] N. Moshtagh and A. Jadbabaie, "Distributed geodesic control laws for flocking of nonholonomic agents," *IEEE Transactions on Automatic Control*, vol. 52, no. 4, pp. 681–686, Apr. 2007.

[7] J. R. Lawton, R. W. Beard, and B. Young, "A decentralized approach to formation maneuvers," *IEEE Transactions on Robotics and Automation*, vol. 19, no. 6, pp. 933–941, Dec. 2003.

[8] W. Ren, "Consensus strategies for cooperative control of vehicle formations," *IET Control Theory & Applications: Special Issue on Cooperative Control of Multiple Spacecraft Flying in Formation*, vol. 1, no. 2, pp. 505–512, Mar. 2007.

[9] R. Olfati-Saber and J. S. Shamma, "Consensus filters for sensor networks and distributed sensor fusion," in *Proceedings of the IEEE Conference on Decision and Control*, pp. 6698–6703, Dec. 2005.

[10] D. P. Spanos and R. M. Murray, "Distributed sensor fusion using dynamic consensus," in *International Federation of Automatic Control World Congress*, 2005.

[11] R. A. Freeman, P. Yang, and K. M. Lynch, "Distributed estimation and control of swarm formation statistics," in *Proceedings of the American Control Conference*, pp. 749–755, June 2006.

[12] R. W. Beard, J. R. Lawton, and F. Y. Hadaegh, "A coordination architecture for spacecraft formation control," *IEEE Transactions on Control Systems Technology*, vol. 9, no. 6, pp. 777–790, Nov. 2001.

[13] R. M. Murray, "Recent research in cooperative control of multivehicle systems," *Journal of Dynamic Systems, Measurement, and Control*, vol. 129, no. 5, pp. 571–583, Sept. 2007.

[14] M. S. de Queiroz, V. Kapila, and Q. Yan, "Adaptive nonlinear control of multiple spacecraft formation flying," *Journal of Guidance, Control, and Dynamics*, vol. 23, no. 3, pp. 385–390, May–June 2000.

[15] J. P. Desai, J. Ostrowski, and V. Kumar, "Modeling and control of formations of nonholonomic mobile robots," *IEEE Transactions on Robotics and Automation*, vol. 17, no. 6, pp. 905–908, Dec. 2001.

[16] F. Fahimi, "Sliding-mode formation control for underactuated surface vessels," *IEEE Transactions on Robotics*, vol. 23, no. 3, pp. 617–622, June 2007.

[17] O. A. A. Orqueda, X. T. Zhang, and R. Fierro, "An output feedback nonlinear decentralized controller for unmanned vehicle co-ordination," *International Journal of Robust and Nonlinear Control*, vol. 17, no. 12, pp. 1106–1128, Aug. 2007.

[18] L. Consolini, F. Morbidi, D. Prattichizzo, and M. Tosques, "Leaderfollower formation control of nonholonomic mobile robots with input constraints," *Automatica*, vol. 44, no. 5, pp. 1343–1349, 2008.

[19] T. Balch and R. C. Arkin, "Behavior-based formation control for multirobot teams," *IEEE Transactions on Robotics and Automation*, vol. 14, no. 6, pp. 926–939, Dec. 1998.

[20] M. C. VanDyke and C. D. Hall, "Decentralized coordinated attitude control within a formation of spacecraft," *Journal of Guidance, Control, and Dynamics*, vol. 29, no. 5, pp. 1101–1109, Sept.-Oct. 2006.

[21] V. Gazi, "Swarm aggregations using artificial potentials and sliding-mode control," *IEEE Transactions on Robotics*, vol. 21, no. 6, pp. 1208–1214, Dec. 2005.

[22] W. Xi, X. Tan, and J. S. Baras, "Gibbs sampler-based coordination of autonomous swarms," *Automatica*, vol. 42, pp. 1107–1119, 2006.

[23] J. Yao, R. Ordonez, and V. Gazi, "Swarm tracking using artificial potentials and sliding mode control," *Journal of Dynamic Systems, Measurement, and Control*, vol. 129, no. 5, pp. 749–754, Sept. 2007.

[24] M. A. Lewis and K.-H. Tan, "High precision formation control of mobile robots using virtual structures," *Autonomous Robots*, vol. 4, pp. 387–403, 1997.

[25] N. E. Leonard and E. Fiorelli, "Virtual leaders, artificial potentials and coordinated control of groups," in *Proceedings of the IEEE Conference on Decision and Control*, pp. 2968–2973, Dec. 2001.

[26] C. Belta and V. Kumar, "Abstraction and control for groups of robots," *IEEE Transactions on Robotics and Automation*, vol. 20, no. 5, pp. 865–875, Oct. 2004.

[27] W. Ren and R. W. Beard, "Decentralized scheme for spacecraft formation flying via the virtual structure approach," *Journal of Guidance, Control, and Dynamics*, vol. 27, no. 1, pp. 73–82, Jan.–Feb. 2004.

[28] W. Ren and R. W. Beard, "Formation feedback control for multiple spacecraft via virtual structures," *IEE Proceedings - Control Theory and Applications*, vol. 151, no. 3, pp. 357–368, May 2004.

[29] M. Porfiri, D. G. Roberson, and D. J. Stilwell, "Tracking and formation control of multiple autonomous agents: A two-level consensus approach," *Automatica*, vol. 43, pp. 1318–1328, 2007.

[30] L. Krick, M. E. Broucke, and B. A. Francis, "Stabilisation of infinitesimally rigid formations of multi-robot networks," *International Journal of Control*, vol. 82, no. 3, pp. 423–439, Mar. 2009.

[31] R. Olfati-Saber and R. M. Murray, "Distributed cooperative control of multiple vehicle formations using structural potential functions," in *International Federation of Automatic Control World Congress*, July 2002.

[32] T. Eren, P. N. Belhumeur, and A. S. Morse, "Closing ranks in vehicle formations based on rigidity," in *Proceedings of the IEEE Conference on Decision and Control*, pp. 2959–2964, Dec. 2002.

[33] P. Ogren, E. Fiorelli, and N. E. Leonard, "Cooperative control of mobile sensor networks: Adaptive gradient climbing in a distributed environment," *IEEE Transactions on Automatic Control*, vol. 49, no. 8, pp. 1292–1302, Aug. 2004.

[34] J. M. Hendrickx, B. D. O. Anderson, J.-C. Delvenne, and V. D. Blondel, "Directed graphs for the analysis of rigidity and persistence in autonomous agent systems," *International Journal of Robust and Nonlinear Control*, vol. 17, no. 11, pp. 960–981, July 2007.

[35] C. Yu, J. M. Hendrickx, B. Fidan, B. D. Anderson, and V. D. Blondel, "Three and higher dimensional autonomous formations: rigidity, persistence and structural persistence," *Automatica*, vol. 43, pp. 387–402, 2007.

[36] A. Jadbabaie, J. Lin, and A. S. Morse, "Coordination of groups of mobile autonomous agents using nearest neighbor rules," *IEEE Transactions on Automatic Control*, vol. 48, no. 6, pp. 988–1001, June 2003.

[37] R. Olfati-Saber and R. M. Murray, "Consensus problems in networks of agents with switching topology and time-delays," *IEEE Transactions on Automatic Control*, vol. 49, no. 9, pp. 1520–1533, Sept. 2004.

[38] L. Moreau, "Stability of multi-agent systems with time-dependent communication links," *IEEE Transactions on Automatic Control*, vol. 50, no. 2, pp. 169–182, Feb. 2005.

[39] W. Ren and R. W. Beard, "Consensus seeking in multiagent systems under dynamically changing interaction topologies," *IEEE Transactions on Automatic Control*, vol. 50, no. 5, pp. 655–661, May 2005.

[40] F. Xiao and L. Wang, "Asynchronous consensus in continuous-time multi-agent systems with switching topology and time-varying delays," *IEEE Transactions on Automatic Control*, vol. 53, no. 8, pp. 1804–1816, Sept. 2008.

[41] M. Cao, A. S. Morse, and B. D. O. Anderson, "Agreeing asynchronously," *IEEE Transactions on Automatic Control*, vol. 53, no. 8, pp. 1826–1838, Sept. 2008.

[42] J. A. Fax and R. M. Murray, "Information flow and cooperative control of vehicle formations," *IEEE Transactions on Automatic Control*, vol. 49, no. 9, pp. 1465–1476, Sept. 2004.

[43] Z. Lin, B. Francis, and M. Maggiore, "Necessary and sufficient graphical conditions for formation control of unicycles," *IEEE Transactions on Automatic Control*, vol. 50, no. 1, pp. 121–127, Jan. 2005.

[44] J. A. Marshall, M. E. Broucke, and B. A. Francis, "Formations of vehicles in cyclic pursuit," *IEEE Transactions on Automatic Control*, vol. 49, no. 11, pp. 1963–1974, 2004.

[45] G. Lafferriere, A. Williams, J. Caughman, and J. J. P. Veerman, "Decentralized control of vehicle formations," *Systems and Control Letters*, vol. 54, no. 9, pp. 899–910, 2005.

[46] R. Olfati-Saber, J. A. Fax, and R. M. Murray, "Consensus and cooperation in networked multi-agent systems," *Proceedings of the IEEE*, vol. 95, no. 1, pp. 215–233, Jan. 2007.

[47] D. V. Dimarogonas, S. G. Loizou, K. J. Kyriakopoulos, and M. M. Zavlanos, "A feedback stabilization and collision avoidance scheme for multiple independent non-point agents," *Automatica*, vol. 42, no. 2, pp. 229–243, 2006.

[48] D. Lee and M. W. Spong, "Stable flocking of multiple inertial agents on balanced graphs," *IEEE Transactions on Automatic Control*, vol. 52, no. 8, pp. 1469–1475, 2007.

[49] F. Cucker and S. Smale, "Emergent behavior in flocks," *IEEE Transactions on Automatic Control*, vol. 52, no. 5, pp. 852–862, May 2007.

[50] R. L. Winkler, "The consensus of subjective probability distributions," *Manage Science*, vol. 15, no. 2, pp. B61–B75, 1968.

[51] M. H. DeGroot, "Reaching a consensus," *Journal of American Statistical Association*, vol. 69, no. 345, pp. 118–121, 1974.

[52] T. Vicsek, A. Czirok, E. B. Jacob, I. Cohen, and O. Schochet, "Novel type of phase transitions in a system of self-driven particles," *Physical Review Letters*, vol. 75, no. 6, pp. 1226–1229, 1995.

[53] L. Fang and P. J. Antsaklis, "Information consensus of asynchronous discrete-time multi-agent systems," in *Proceedings of the American Control Conference*, pp. 1883–1888, June 2005.

[54] Y. Hatano and M. Mesbahi, "Agreement over random networks," *IEEE Transactions on Automatic Control*, vol. 50, no. 11, pp. 1867–1872, 2005.

[55] C. W. Wu, "Synchronization and convergence of linear dynamics in random directed networks," *IEEE Transactions on Automatic Control*, vol. 51, no. 7, pp. 1207–1210, July 2006.

[56] M. Porfiri and D. J. Stilwell, "Consensus seeking over random weighted directed graphs," *IEEE Transactions on Automatic Control*, vol. 52, no. 9, pp. 1767–1773, 2007.

[57] A. Tahbaz-Salehi and A. Jadbabaie, "A necessary and sufficient condition for consensus over random networks," *IEEE Transactions on Automatic Control*, vol. 53, no. 3, pp. 791–795, 2008.

[58] F. Xiao and L. Wang, "Consensus protocols for discrete-time multi-agent systems with time-varying delays," *Automatica*, vol. 44, no. 10, pp. 2577–2582, 2008.

[59] L. Fang and P. J. Antsaklis, "Asynchronous consensus protocols using nonlinear paracontractions theory," *IEEE Transactions on Automatic Control*, vol. 53, no. 10, pp. 2351–2355, 2008.

[60] W. Ren and E. M. Atkins, "Distributed multi-vehicle coordinated control via local information exchange," *International Journal of Robust and Nonlinear Control*, vol. 17, no. 10–11, pp. 1002–1033, July 2007.

[61] G. Xie and L. Wang, "Consensus control for a class of networks of dynamic agents," *International Journal of Robust and Nonlinear Control*, vol. 17, no. 10-11, pp. 941–959, July 2007.

[62] T. Hayakawa, T. Matsuzawa, and S. Hara, "Formation control of multi-agent systems with sampled information," in *Proceedings of the IEEE Conference on Decision and Control*, Dec. 2006.

[63] Y. Cao and W. Ren, "Multivehicle coordination for double-integrator dynamics in a sampled-data setting," *International Journal of Robust and Nonlinear Control*, vol. 20, pp. 987–1000, 2009.

[64] Y. Cao and W. Ren, "Sampled-data discrete-time consensus algorithms for double-integrator dynamics under dynamic directed interaction," *International Journal of Control*, vol. 83, pp. 506–515, 2010.

[65] Y. Cao, Y. Li, W. Ren, and Y. Chen, "Distributed coordination of networked fractional-order systems," *IEEE Transactions on Systems, Man, and Cybernetics, part B: Cybernetics*, vol. 40, pp. 362–370, 2009.

[66] W. Ren, R. W. Beard, and E. M. Atkins, "Information consensus in multivehicle cooperative control: Collective group behavior through local interaction," *IEEE Control Systems Magazine*, vol. 27, no. 2, pp. 71–82, 2007.

[67] Y. Hong, J. Hu, and L. Gao, "Tracking control for multi-agent consensus with an active leader and variable topology," *Automatica*, vol. 42, no. 7, pp. 1177–1182, July 2006.

[68] Y. Hong, G. Chen, and L. Bushnell, "Distributed observers design for leader-following control of multi-agent networks," *Automatica*, vol. 44, no. 3, pp. 846–850, 2008.

[69] W. Ren, "Multi-vehicle consensus with a time-varying reference state," *Systems & Control Letters*, vol. 56, no. 7–8, pp. 474–483, July 2007.

[70] Y. Cao, W. Ren, and Y. Li, "Distributed discrete-time coordinated tracking with a time-varying reference state and limited communication," *Automatica*, vol. 45, no. 5, pp. 1299–1305, 2009.

[71] W. Ren, "On consensus algorithms for double-integrator dynamics," *IEEE Transactions on Automatic Control*, vol. 53, no. 6, pp. 1503–1509, July 2008.

[72] K. Peng and Y. Yang, "Leader-following consensus problem with a varying-velocity leader and time-varying delays," *Physica A*, vol. 388, no. 2–3, pp. 193–208, 2009.

[73] H. Su, X. Wang, and Z. Lin, "Flocking of multi-agents with a virtual leader," *IEEE Transactions on Automatic Control*, vol. 54, no. 2, pp. 293–307, Feb. 2009.

[74] H. Shi, L. Wang, and T. Chu, "Flocking of multi-agent systems with a dynamic virtual leader," *International Journal of Control*, vol. 82, no. 1, pp. 43–58, Jan. 2009.

[75] Y. Cao and W. Ren, "Distributed coordinated tracking with reduced interaction via a variable structure approach," *IEEE Transactions on Automatic Control*, 2010, in press.

[76] M. Ji, G. Ferrari-Trecate, M. Egerstedt, and A. Buffa, "Containment control in mobile networks," *IEEE Transactions on Automatic Control*, vol. 53, no. 8, pp. 1972–1975, Sept. 2008.

[77] Y. Cao and W. Ren, "Distributed consensus for fractional-order systems: Dynamic interaction and absolute/relative damping," in *Proceedings of the IEEE Conference on Decision and Control*, Dec. 2009.

[78] Y. Cao and W. Ren, "Optimal linear consensus algorithms: An LQR perspective," *IEEE Transactions on Systems, Man, and Cybernetics, part B: Cybernetics*, 2009, accepted.

[79] Y. Cao, W. Ren, and Y. Li, "Distributed pd-like discrete-time consensus algorithm with a time-varying reference state," *Automatica*, vol. 45, pp. 1299–1305, May 2009.

[80] Y. Cao and W. Ren, "Sampled-data formation control under dynamic directed interaction," in *Proceedings of the American Control Conference*, pp. 5186–5191, June 2009.

[81] Y. Cao and W. Ren, "LQR-based optimal linear consensus algorithms," in *Proceedings of the American Control Conference*, pp. 5204–5209, June 2009.

[82] Y. Cao and W. Ren, "Distributed containment control with multiple stationary or dynamic leaders in fixed and switching directed networks," in *Proceedings of the IEEE Conference on Decision and Control*, Dec. 2009.

[83] G. F. Franklin, J. D. Powell, and M. Workman, *Digital Control of Dynamic Systems*. Boston, MA: Addison Wesley, 2006.

[84] I. Kovacs, D. S. Silver, and S. G. Williams, "Determinants of block matrices and schur's formula," 1999 [Online]. Available: `http://citeseer.ist.psu.edu/497635.html`.

[85] R. Merris, "Laplacian matrices of graphs: A survey," *Linear Algebra and its Applications*, vol. 197-198, pp. 143–176, 1994.

[86] R. A. Horn and C. R. Johnson, *Matrix Analysis*. Cambridge, England: Cambridge University Press, 1985.

[87] Z. Jovanovic and B. Dankovic, "On the probability stability of discrete-time control systems," *Series: Electronics and Energetics*, vol. 17, pp. 11–20, Apr. 2004.

[88] A.-L. Cauchy, "Exercices de mathematiques, iv annee," de Bure Freres, Paris, 1829.

[89] R. C. Riddell, "Upper bounds on the moduli of the zeros of a polynomial," *Mathematics Magazine*, vol. 47, no. 5, pp. 267–273, Nov. 1974.

[90] J. Wolfowitz, "Products of indecomposable, aperiodic, stochastic matrices," *Proceedings of the American Mathematical Society*, vol. 15, pp. 733–736, 1963.

[91] A. F. Filippov, *Differential Equations with Discontinuous Righthand Sides*. Norwell, MA: Kluwer Academic Publishers, 1988.

[92] B. Paden and S. Sastry, "A calculus for computing Filippov's differential inclusion with application to the variable structure control of robot manipulators," *IEEE Transactions on Circuits and Systems*, vol. CAS-34, no. 1, pp. 73–82, 1987.

[93] F. H. Clarke, *Optimization and Nonsmooth Analysis*. Philadelphia, PA: SIAM, 1990.

[94] J. Cortes, "Discontinuous dynamical systems - A tutorial on solutions, nonsmooth analysis, and stability," *IEEE Control Systems Magzine*, vol. 28, no. 3, pp. 36–73, 2008.

[95] M. M. Zavlanos, A. Jadbabaie, and G. J. Pappas, "Flocking while preserving network connectivity," in *Proceedings of the IEEE Conference on Decision and Control*, pp. 2919–2924, Dec. 2007.

[96] T. K. Moon and W. C. Stirling, *Mathematical Methods and Algorithms*. Englewood Cliffs, NJ: Prentice Hall, 2000.

[97] G. Ferrari-Trecate, M. Egerstedt, A. Buffa, and M. Ji, "Laplacian sheep: Hybrid, stop-go policy for leader-based containment control," in *Hybrid Systems: Computation and Control*, pp. 212–226. Springer-Verlag, 2006.

[98] L. Moreau, "Stability of continuous-time distributed consensus algorithms," in *Proceedings of the IEEE Conference on Decision and Control*, pp. 3998–4003, Dec. 2004.

[99] Z. Lin, M. Broucke, and B. Francis, "Local control strategies for groups of mobile autonomous agents," *IEEE Transactions on Automatic Control*, vol. 49, no. 4, pp. 622–629, 2004.

[100] J. S. Caughman and J. J. P. Veerman, "Kernels of directed graph laplacians," *The Electronic Journal of Combinatorics*, vol. 1, no. R39, Apr. 2006.

[101] R. Agaev and P. Chebotarev, "The matrix of maximum out forests of a digraph and its applications," *Automation and Remote Control*, vol. 61, no. 9, pp. 1424–1450, 2000.

[102] S. P. Bhat and D. S. Bernstein, "Continuous finite-time stabilization of the translational and rotational double integrators," *IEEE Transactions on Automatic Control*, vol. 43, no. 5, pp. 678–682, May 1998.

[103] D. Bauso, L. Giarre, and R. Pesenti, "Nonlinear protocols for optimal distributed consensus in networks of dynamic agents," *Systems & Control Letters*, vol. 55, no. 11, pp. 918–928, 2006.

[104] J.-C. Delvenne, R. Carli, and S. Zampieri, "Optimal strategies in the average consensus problem," in *Proceedings of the IEEE Conference on Decision and Control*, pp. 2498–2503, Dec. 2007.

[105] E. Semsar and K. Khorasani, "Optimal control and game theoretic approaches to cooperative control of a team of multi-vehicle unmanned systems," in *Proceedings of the IEEE International Conference on Networking, Sensing and Control*, pp. 628–633, Apr. 2007.

[106] Y. Kim and M. Mesbahi, "On maximizing the second smallest eigenvalue of a state-dependent graph Laplacian," *IEEE Transactions on Automatic Control*, vol. 51, no. 1, pp. 116–120, 2006.

[107] L. Xiao and S. Boyd, "Fast linear iterations for distributed averaging," *Systems and Control Letters*, vol. 53, no. 1, pp. 65–78, 2004.

[108] G. Alefeld and N. Schneider, "On square roots of M-matrices," *Linear Algebra and Its Applications*, vol. 42, pp. 119–132, Feb. 1982.

[109] F. Kittaneh, "Spectral radius inequalities for hilbert space operators," *Proceedings of the American Mathematical Society*, vol. 134, pp. 385–390, 2005.

[110] J. B. Lasserre, "Global optimization with polynomials and the problem of moments," *SIAM Journal on Optimization*, vol. 11, no. 3, pp. 796–817, 2001.

[111] B. Ross, "Fractional calculus," *Mathematics Magazine*, vol. 50, no. 3, pp. 115–122, May 1977.

[112] J. Liouville, "Mémoire sur le calcul des différentielles à indices quelconques," *Journal de l'Elole Polytechnique*, vol. 13, no. 21, pp. 71–162, 1832.

[113] B. Riemann, "Versuch einer allgemeinen auffasung der integration und differentiation," in *The Collected Works of Bernhard Riemann*, H. Weber, Ed., pp. 353–366, Dover, NY: Springer, 1953.

[114] H. Laurent, "Sur le calcul des dérivées à indices quelconques," *Nouvelles Annales de Mathmatiques*, vol. 3, no. 3, pp. 240–252, 1884.

[115] R. Orbach, "Fractal phenomena in disordered systems," *Annual Review of Materials Science*, vol. 19, pp. 497–525, 1989.

[116] I. Podlubny, *Fractional Differential Equations*. San Diego, CA: Academic Press, 1999.

[117] T. A. Witten and L. M. Sander, "Diffusion-limited aggregation, a kinetic critical phenomenon," *Physical Review Letters*, vol. 47, no. 19, pp. 1400–1403, Nov. 1981.

[118] R. L. Bagley and P. J. Torvik, "Fractional calculus - a different approach to the analysis of viscoelastically damped structures," *American Institute of Aeronautics and Astronautics Journal*, vol. 21, no. 5, pp. 741–748, 1983.

[119] R. L. Bagley and P. J. Torvik, "A theoretical basis for the application of fractional calculus to viscoelasticity," *Journal of Theology*, vol. 27, no. 3, pp. 201–210, 1983.

[120] R. L. Bagley and P. J. Torvik, "On the fractional calculus model of viscoelastic behavior," *Journal of Theology*, vol. 30, no. 1, pp. 133–155, 1986.

[121] A. Oustaloup, J. Sabatier, and P. Lanusse, "From fractal robustness to crone control," *Fractional Calculus and Applied Analysis*, vol. 2, no. 1, pp. 1–30, 1999.

[122] M. Axtell and M. E. Bise, "Fractional calculus applications in control systems," in *Proceedings of the IEEE National Aerospace and Electronics Conference*, pp. 563–566, 1990.

[123] W. G. Glöckle and T. F. Nonnenmacher, "A fractional calculus approach to self-similar protein dynamics," *Biophysical Joumal*, vol. 68, no. 1, pp. 46–53, Jan. 1995.

[124] J. Barkoulas, W. C. Labys, and J. Onochie, "Fractional dynamics in international commodity prices," *Journal of Futures Markets*, vol. 17, no. 2, pp. 161–189, 1997.

[125] I. Podlubny, L. Dorcak, and I. Kostial, "On fractional derivatives, fractional-orlder dynamic systems and $PI^{\lambda}D^{\mu}$-controllers," in *Proceedings of the IEEE Conference on Decision and Control*, pp. 4985–4990, Dec. 1997.

[126] I. Podlubny, "Fractional-order systems and $PI^{\lambda}D^{\mu}$-controllers," *IEEE Transactions on Automatic Control*, vol. 44, no. 1, pp. 208–213, Jan. 1999.

[127] R. Metzler and J. Klafter, "The random walk's guide to anomalous diffusion: a fractional dynamic approach," *Physics Reports*, vol. 339, no. 1, pp. 1–77, Dec. 2000.

[128] Y. Chen, H.-S. Ahn, and I. Podlubny, "Robust stability check of fractional order linear time invariant systems with interval uncertainties," *(Elsevier) Signal Processing*, vol. 86, pp. 2611–2618, Mar. 2006.

[129] R. Gorenflo and F. Mainardi, "Fractional oscillations and mittag-leffler functions," 1996 [Online]. Available: `citeseer.ist.psu.edu/gorenflo96fractional.html`.

[130] N. Dmitriev and E. Dynkin, "On the characteristic numbers of a stochastic matrix," *C.R. (Doklady) Academy Science URSS*, vol. 49, no. 3, pp. 159–162, 1946.

[131] Y. Li and Y. Chen, "Fractional order linear quadratic regulator," in *IEEE/ASME International Conference on Mechtronic and Embedded Systems and Applications*, pp. 363–368, Oct. 2008.

[132] Y. Cao, Y. Li, W. Ren, and Y. Chen, "Distributed consensus seeking over fractional order systems," in *Proceedings of the IEEE Conference on Decision and Control*, pp. 2920–2925, Dec. 2008.

[133] W. Ren, "Collective motion from consensus with Cartesian coordinate coupling - Part II: double-integrator dynamics," in *Proceedings of the IEEE Conference on Decision and Control*, pp. 1012–1017, Dec. 2008.

[134] R. Agaev and P. Chebotarev, "On the spectra of nonsymmetric laplacian matrices," *Linear Algebra and its Applications*, vol. 399, pp. 157–178, 2005.

Appendices

Appendix A

Graph Theory Notions

It is natural to model interaction among vehicles by directed graphs. Suppose that a team consists of n vehicles. A directed graph $\mathcal{G} = (\mathcal{V}, \mathcal{E})$ consists of a node set $\mathcal{V} = \{1, \ldots, n\}$ and an edge set $\mathcal{E} \subseteq \mathcal{V} \times \mathcal{V}$. An edge (i, j) in a directed graph denotes that vehicle j can obtain information from vehicle i, but not necessarily vice versa. Accordingly, vehicle j is called a neighbor of i. All neighbors of vehicle i is denoted by N_i. Adjacency matrix $\mathcal{A}$ of directed graph $\mathcal{G}$ is defined such that a_{ij} is a positive weight if $(j, i) \in \mathcal{E}$, while $a_{ij} = 0$ if $(j, i) \notin \mathcal{E}$. In particular, we assume that $a_{ii} = 0, i = 1, \cdots, n$ (i.e., no self edge allowed). A subgraph $\mathcal{G}_1 = (\mathcal{V}_1, \mathcal{E}_1)$ of $\mathcal{G}$ is a directed graph such that $\mathcal{V}_1 \in \mathcal{V}$ and $\mathcal{E}_1 \in \mathcal{E} \bigcap (\mathcal{V}_1 \times \mathcal{V}_1)$. The union of a collection of directed graphs is a directed graph whose node and edge sets are the unions of the node and edge sets of the directed graphs in the collection.

A directed path is a sequence of edges in a directed graph of the form $(i_1, i_2), (i_2, i_3), \ldots$, where $i_j \in \mathcal{V}$. A directed graph has a directed spanning tree if there exists at least one node having a directed path to all other nodes. A complete graph is a graph in which each pair of distinct nodes is connected by an edge. A complete graph in which each edge is bidirectional is called a complete directed graph. A complete undirected graph is an undirected graph in which each pair of distinct nodes is connected by an edge.

Let the (nonsymmetric) Laplacian matrix $\mathcal{L} = [\ell_{ij}] \in \mathbb{R}^{n \times n}$ associated with $\mathcal{A}$ be defined as [134] $\ell_{ii} = \sum_{j=1, j \neq i}^{n} a_{ij}$ and $\ell_{ij} = -a_{ij},\ i \neq j$. Zero is an eigenvalue of $\mathcal{L}$ with an associated eigenvector $\mathbf{1}_n$, where $\mathbf{1}_n$ is the $n \times 1$ column vector of all ones.

Given a matrix $S = [s_{ij}] \in \mathbb{R}^{n \times n}$, the directed graph of S, denoted by $\Gamma(S)$, is the directed graph with node set $\mathcal{V} = \{1, \cdots, n\}$ such that there is an edge in $\Gamma(S)$ from j to i if and only if $s_{ij} \neq 0$.

Appendix B

Caputo Fractional Operator

There are mainly two widely used fractional operators: Caputo and Riemann-Liouville (R-L) fractional operators [116]. In physical systems, Caputo fractional operator is more practical than R-L fractional operator because R-L fractional operator has initial value problems. Therefore, we will use Caputo fractional operator in this paper to model the system dynamics and analyze the stability of the proposed fractional-order algorithms. In the following of the subsection, we will review Caputo fractional operator. Generally, Caputo fractional operator includes Caputo integral and Caputo derivative. Caputo derivative is defined based on the following Caputo integral

$$ {}_a^C D_t^{-\alpha} f(t) = \frac{1}{\Gamma(\alpha)} \int_a^t \frac{f(\tau)}{(t-\tau)^{1-\alpha}} \mathrm{d}\tau, $$

where ${}_a^C D_t^{-\alpha}$ denotes the Caputo integral with order $\alpha \in (0,\ 1]$, $\Gamma(\cdot)$ is the Gamma function, and a is an arbitrary real number. For any real number p, Caputo derivative is defined as

$$ {}_a^C D_t^{p} f(t) = {}_a^C D_t^{-\alpha} [\frac{d^{[p]+1}}{dt^{[p]+1}} f(t)], \tag{B.1} $$

where $\alpha = [p] + 1 - p \in (0,\ 1]$ and $[p]$ is the integer part of p. If p is an integer, then $\alpha = 1$ and (B.1) is equivalent to the integer-order derivative. Because only Caputo fractional operator is used in the following of this paper, a simple notation $f^{(\alpha)}(t)$ is used to replace ${}_a^C D_t^{\alpha} f(t)$.

In the following, we will introduce the Laplace transform of Caputo derivative and the Mittag-Leffler function [129]. We first introduce the Laplace transform of Caputo derivative. Let $L\{\cdot\}$ denote the Laplace transform of a function. It follows from the formal definition of the Laplace

transform $F(s) = L\{f(t)\} = \int_{0^-}^{\infty} e^{-st} f(t)dt$ that

$$L\{f^{(\alpha)}(t)\} = \begin{cases} s^{\alpha}F(s) + s^{\alpha-1}f(0^-), & \alpha \in (0,1] \\ s^{\alpha}F(s) + s^{\alpha-1}f(0^-) + s^{\alpha-2}\dot{f}(0^-), & \alpha \in (1,2], \end{cases}$$

where $f(0^-) = \lim_{\epsilon \to 0^-} f(\epsilon)$ and $\dot{f}(0^-) = \lim_{\epsilon \to 0^-} \dot{f}(\epsilon)$. For $\alpha, \beta \in \mathbb{C}$, the Mittag-Leffler function in two parameters is defined as

$$E_{\alpha,\beta}(z) = \sum_{k=0}^{\infty} \frac{z^k}{\Gamma(k\alpha + \beta)}, \tag{B.2}$$

When $\beta = 1$ and $\alpha > 0$, (B.2) can be written in a special case as

$$E_{\alpha}(z) = \sum_{k=0}^{\infty} \frac{z^k}{\Gamma(k\alpha + 1)}. \tag{B.3}$$

Vita

Yongcan Cao

Published/Accepted Journal Articles

- Distributed Coordinated Tracking with Reduced Interaction via a Variable Structure Approach, Yongcan Cao and Wei Ren, *IEEE Transactions on Automatic Control*, *Accepted*.
- Distributed Coordination for Fractional-order Systems: Dynamic Interaction and Absolute/Relative Damping, Yongcan Cao and Wei Ren, *Systems and Control Letters*, Vol. 43, No. 3-4, pp. 233-240, 2010.
- Distributed Discrete-time Coordinated Tracking with a Time-varying Reference State and Limited Communication, Yongcan Cao, Wei Ren, and Yan Li, *Automatica*, vol. 45, no. 5, pp. 1299-1305, 2009.
- Optimal Linear Consensus Algorithms: An LQR perspective, Yongcan Cao and Wei Ren *IEEE Transactions on Systems, Man, and Cybernetics, part B: Cybernetics*, *Accepted*.
- Distributed coordination of networked fractional-order systems, Yongcan Cao, Yan Li, Wei Ren, and YangQuan Chen, *IEEE Transactions on Systems, Man, and Cybernetics, part B: Cybernetics*, Vol. 40, No. 2, pp. 362-370, 2010.
- Multivehicle Coordination for Double-integrator Dynamics under Fixed Undirected/Directed Interaction in a Sampled-data Setting, Yongcan Cao and Wei Ren, *International Journal of Robust and Nonlinear Control*, *Accepted.*
- Multivehicle Sampled-Data Discrete-time Consensus Algorithms for Double-Integrator Dynamics under Dynamic Directed Interaction, Yongcan Cao and Wei Ren, *International Journal of Control*, Vol. 83, No. 3, pp. 506-515, 2010.

- Multivehicle Distributed Discrete-time Coupled Harmonic Oscillators with Application to Synchronized Motion Coordination, Larry Ballard, Yongcan Cao, and Wei Ren, *IET Control Theory & Applications, Accepted.*

- Multi-agent Consensus Using Both Current and Outdated States, Yongcan Cao and Wei Ren, *Journal of Intelligent and Robotic Systems*, Vol. 58, No. 1, pp. 95-106.

- Autopilots for Small Fixed-Wing Unmanned Air Vehicles: A Survey, Haiyang Chao, Yongcan Cao, and YangQuan Chen, *International Journal of Control, Automation, and Systems*, Vol. 8, No. 1, pp. 36-44, 2010.

- Simulation and Experimental Study of Consensus Algorithm for Multiple Mobile Robots with Information Feedback, Wei Ren and Yongcan Cao, *Intelligent Automation and Soft Computing*, vol. 14, no. 1, pp. 73-87, 2008.

Published/Accepted Conference Papers

- Decentralized Finite-time Sliding Mode Estimators with Applications to Formation Tracking, Yongcan Cao, Wei Ren and Ziyang Meng, *IEEE American Control Conference*, Baltimore, July 2010. *Accepted.*

- Distributed Containment Control for Double-Integrator Dynamics: Algorithms and Experiments, Yongcan Cao, Daniel Stuart, Wei Ren and Ziyang Meng, *IEEE American Control Conference*, Baltimore, July 2010. *Accepted.*

- Some Stability and Boundedness Conditions for Second-order Leaderless and Leader-following Consensus with Communication and Input Delays, Ziyang Meng, Wei Ren, Yongcan Cao and Zhen You, *IEEE American Control Conference*, Baltimore, July 2010. *Accepted.*

- Distributed Coordinated Tracking via a Variable Structure Approach - Part I: Consensus Tracking, Yongcan Cao and Wei Ren, *IEEE American Control Conference*, Baltimore, July 2010. *Accepted.*

- Distributed Coordinated Tracking via a Variable Structure Approach - Part II: Swarm Tracking, Yongcan Cao and Wei Ren, *IEEE American Control Conference*, Baltimore, July 2010. *Accepted.*
- Distributed Containment Control with Multiple Stationary or Dynamic Leaders in Fixed and Switching Directed Networks, Yongcan Cao and Wei Ren, *IEEE Conference on Decision and Control*, Shanghai, China, 2009.
- Distributed Consensus for Fractional-order Systems: Dynamic Interaction and Absolute/Relative Damping, Yongcan Cao and Wei Ren, *IEEE Conference on Decision and Control*, Shanghai, China, 2009.
- Sample-data Formation Control under Dynamic Directed Interaction, Yongcan Cao and Wei Ren, *IEEE American Control Conference*, St. Louis, Mo, June 2009.
- LQR-based Optimal Linear Consensus Algorithms, Yongcan Cao and Wei Ren, *IEEE American Control Conference*, St. Louis, Mo, June 2009.
- Distributed Coordination Algorithms for Multiple Fractional-Order Systems, Yongcan Cao, Yan Li, Wei Ren, and YangQuan Chen, *IEEE Conference on Decision and Control*, Cancun, Mexico, December 2008.
- Convergence of Sampled-data Consensus Algorithms for Double-integrator Dynamics, Wei Ren and Yongcan Cao, *IEEE Conference on Decision and Control*, Cancun, Mexico, December 2008.
- Distributed PD-like Discrete-time Consensus Algorithm with a Time-varying Reference State, Yongcan Cao, Wei Ren, and Yan Li, *AIAA Guidance, Navigation and Control Conference*, Honolulu, HI, August 2008.
- Multi-Agent Consensus Using Both Current and Outdated States, Yongcan Cao, Wei Ren, and YangQuan Chen, *IFAC World Congress*, Seoul, Korea, July 2008.
- Band-reconfigurable Multi-UAV-based Cooperative Remote Sensing for Real-time Water Management and Distributed Irrigation Control, Haiyang Chao, Marc Baumann, Austin Jensen,

YangQuan Chen, Yongcan Cao, Wei Ren and Mac Mckee, *IFAC world congress*, Seoul, Korea, July 2008.

- Experiments in Consensus-based Cooperative Control of Multiple Mobile Robots, Yongcan Cao, Wei Ren, Nathan Sorensen, Larry Ballard, Andrew Reiter and Jonathan Kennedy *IEEE Int. Conf. on Mechatronics and Automation (ICMA)*, Harbin, China, August 2007.

- Autopilots for Small Fixed-Wing Unmanned Air Vehicles: A Survey, Haiyang Chao, Yongcan Cao, and YangQuan Chen *IEEE Int. Conf. on Mechatronics and Automation (ICMA)*, Harbin, China, August 2007.